technische universität
dortmund

PhD Thesis-

"Involvement of the WNT pathway in endometriosis."

In Zusammenarbeit mit

DISSERTATION

ZUR ERLAGNUNG DES AKADEMISCHEN GRADES DES DOKTORS DER
NATURWISSENSCHAFTEN (DR. RER. NAT)
DER FAKULTÄT FÜR CHEMIE UND CHEMISCHER BIOLOGIE
DER TECHNISCHEN UNIVERSITÄT DORTMUND

VORGELEGT VON

JULIANE HUNDT

DORTMUND, 2016

VERÖFFENTLICHUNG ALS DISSERTATION IN DER FAKULTÄT
CHEMIE UND BIOLOGISCHE CHEMIE

DER TECHNISCHEN UNIVERSITÄT DORTMUND

DORTMUND, 25.11.2016

Erstgutachter: Prof. Dr. Med. Jan Hengstler
Leibniz-Institut für Arbeitsforschung
Technische Universität Dortmund
Ardeystraße 67
44139 Dortmund
hengstler@ifado.de

Zweitgutachter: Prof. Dr. Frank Wehner
Fakultät für Chemie und Chemische Biologie
Technische Universität Dortmund &
Max-Planck-Institut für molekulare Physiologie
Otto-Hahn-Staße 11
44227 Dortmund
frank.wehner@mpi-dortmund.mpg.de

Tag der Disputation: 25.11.2016

Hereby I attest that this thesis has been prepared and written solely by me, Juliane Hundt. No other references and materials than what is cited in the paper were used or consulted.

Juliane Hundt

Dortmund, 01.09.2016

ACKNOWLEDGEMENTS

SUMMARY

Endometriosis is a common gynecological disorder defined by the presence of endometrial tissue outside the uterus causing among others chronic pelvic pain and infertility. The definite pathogenesis of endometriosis is still unknown but the most accepted theory is the retrograde menstruation. Due to the lack of reliable biomarkers, the gold standard for diagnose and treatment is still the removal of lesions via surgery. The WNT (wingless-type MMTV integration site family) pathway is essentially implicated in embryogenesis and in stem cell self-renewal of various different adult stem cell types. It has been already implicated in various diseases such as cancer. Several studies have also demonstrated a potential role of dysregulated WNT signaling in endometriosis. This study aimed to systematically investigate the impact of the WNT pathway in the pathogenesis of endometriosis.

Based on a previous clinical study (EMMA – Endometriosis Marker Austria), that revealed dysregulated WNT signaling in endometriosis, several particularly noticeable WNT pathway members were selected and further examined. TaqMan analyses with the same patient cohort confirmed elevated WNT2B, WNT7A, LGR5, RSPO1, and FZD7 mRNA levels in lesions. Manipulations of mRNA or protein levels of these WNT candidate genes in endometrial stromal cells (ESCs) already indicated a functional relevance of the WNT pathway in endometriosis. Increased levels of LGR5 led to increased WNT activity, viability, and migration activity and decreased cell death rate and caspase activity. Reduced mRNA levels exhibited reverse results suggesting that changes of LGR5 essentially influence WNT activity which consequently affects several cellular functions. Finally, when the WNT inhibitor LGK974 was applied in a retrograde menstruation model for endometriosis in mice, a significant reduction of disease burden in terms of lesion size and number was observed. Moreover, many WNT pathway genes that do also play a role in migration, proliferation, and vascularization were downregulated upon WNT inhibition.

All these data suggest that the WNT pathway is implicated in the pathogenesis of endometriosis. Herein, LGR5 seems to play a particular role. It has also been described as an adult endometrial stem cell marker. So possibly, endometrial stem cells reach the peritoneal cavity through retrograde menstruation, where they differentiate and form lesions. However, pharmaceutical targeting of the WNT pathway most likely would have pleiotropic effects, thereby limiting the therapeutic potential of WNT inhibitors in endometriosis. But eventually, several WNT pathway members, especially LGR5, might serve as a potential biomarkers that would allow non-invasive early stage diagnosis, helping to improve patient's quality of life.

ZUSAMMENFASSUNG

Endometriose ist eine häufige gynäkologische Erkrankung, die definiert ist durch die Präsenz von endometrialen Zellen außerhalb der Uterushöhle, was unter anderem starke Unterleibsschmerzen und Infertilität verursacht. Die Pathogenese ist noch nicht vollkommen geklärt, wobei die Theorie der retrograden Menstruation am meisten akzeptiert wird. Da noch keine zuverlässigen Biomarker gefunden wurden, ist der Goldstandard für die Therapie und Diagnose immer noch das Entfernen der Läsionen durch eine Operation. Der WNT Signalweg (*wingless-type MMTV integration site family*) ist essentiell für die Embryogenese und Stammzellselbsterneuerung von verschiedensten adulten Stammzellen. Er wurde auch schon mit vielen verschiedenen Erkrankungen in Verbindung gebracht. Verschiedene Studien haben auch demonstriert, dass WNT-Proteine ebenfalls bei der Pathogenese von Endometriose eine Rolle spielen könnten. Die vorliegende Studie adressierte die genauere Untersuchung dieser Hypothese.

Basierend auf einer vorherigen klinischen Studie (EMMA – *Endometriosis Marker Austria*), die ergab, dass der WNT Siganlweg tatsächlich in Endometriose dereguliert sein könnte, wurden einige besonders auffällige Mitglieder des WNT-Signalwegs ausgewählt und näher untersucht. TaqMan-Analysen derselben Patientenkohorte bestätigten, dass WNT2B, WNT7A, LGR5, RSPO1 und FZD7 in Läsionen hochreguliert sind. Manipulationen von mRNA-Leveln dieser WNT-Kandidatengene lieferten erste Hinweise auf einen Einfluss des WNT-Signalwegs in pathologisch relevante Mechanismen. Insbesondere erhöhte mRNA-Level von LGR5 steigerten die WNT-Aktivität, Viabilität und Migrationsaktivität und verringerten die Zelltodrate und Caspaseaktivität in endometrialen Stromazellen (ESCs). Reduzierte mRNA-Level führten zu umgekehrten Effekten, was darauf hinweist, dass Veränderungen von LGR5 direkt die WNT-Aktivität und somit auch dadurch regulierte zelluläre Funktionen beeinflusst. Schließlich wurde noch der WNT-Inhibitor LGK974 in einem retrograden Menstruationsmodell für Endometriose in Mäusen angewandt. Hier konnte eine signifikante Reduktion der Krankheitslast in Bezug auf Läsionsgröße und –anzahl beobachtet werden. Außerdem wurden viele WNT-Signalweggene, die auch eine Rolle bei Migration, Proliferation oder Vaskularisierung spielen, durch die WNT-Inhibition runterreguliert.

All diese Daten weisen darauf hin, dass der WNT Signalweg essentiell in die Pathogenese von Endometriose impliziert ist. Dabei spielt LGR5 wohl eine besondere Rolle. Es wurde bereits als adulter endometrialer Stammzellmarker beschrieben. Demzufolge ist es wahrscheinlich, dass adulte endometriale Stammzellen durch die retrograde Menstruation in das Peritoneum gelangen, wo sie ausdifferenzieren und Läsionen bilden. Allerdings hätte das pharmakologische Beeinflussen des WNT Signalweges pleiotrope Effekte, weshalb

dessen therapeutische Adressierung bei Endometriose wohl limitiert ist. Allerdings könnten möglicherweise einige WNT Signalwegmitglieder und vor allem LGR5 als Biomarker dienen, um eine frühzeitige, nicht-invasive Diagnose zu ermöglichen und somit durch eine zielgerichtete Therapie die Lebensqualität der Patientinnen zu verbessern.

CONTENT

1   INTRODUCTION

1.1   The menstrual cycle

The menstrual cycle is the development of a follicle from the ovary to establish a fertile oocyte in women. The entire process takes about 28 days and recurs every month between the menarche and menopause marking the fertile years of women. Each menstrual cycle starts with the menses, where low levels of estrogen (E2) and progesterone cause the endometrium (lining of the uterus) to break down and to shed as menstrual blood and cellular debris when an oocyte was not fertilized (figure 1). Now, the proliferative (follicular) phase begins and the pituitary gland in the hypothalamus produces increasing amounts of follicle stimulating hormone (FSH). It in turn promotes the development of several follicles containing one oocyte each from which only one will reach maturity. Rising levels of E2 secreted from the ovaries cause thickening of the endometrium. At approximately day 14 the proliferative phase ends with the ovulation which is provoked by the surge of lutenizing hormone (LH) from the pituitary. This facilitates the mature follicle to bulge out from the surface of the ovary and to burst. Thereby it releases the oocyte which travels through the fallopian tube into the uterus. This marks the beginning of the secretory or luteal phase, where the ruptured follicle develops into the corpus luteum. From then on it secretes increasing amounts of progesterone in large quantities. This hormone causes further thickening and decidualization of the endometrium as a preparation for the potential implantation of the fertilized oocyte after 6 or 7 days of ovulation. After successful implantation, the corpus luteum starts to produce chorionic gonadotropin (HCG) pregnancy hormone which maintains progesterone secretion by the corpus luteum to obtain pregnancy. If the oocyte was not fertilized, the corpus luteum degenerates about 14 days after ovulation causing the levels of progesterone and E2 to drop. Consequently, the endometrium breaks down and sheds, marking the start of the next menstrual cycle [1].
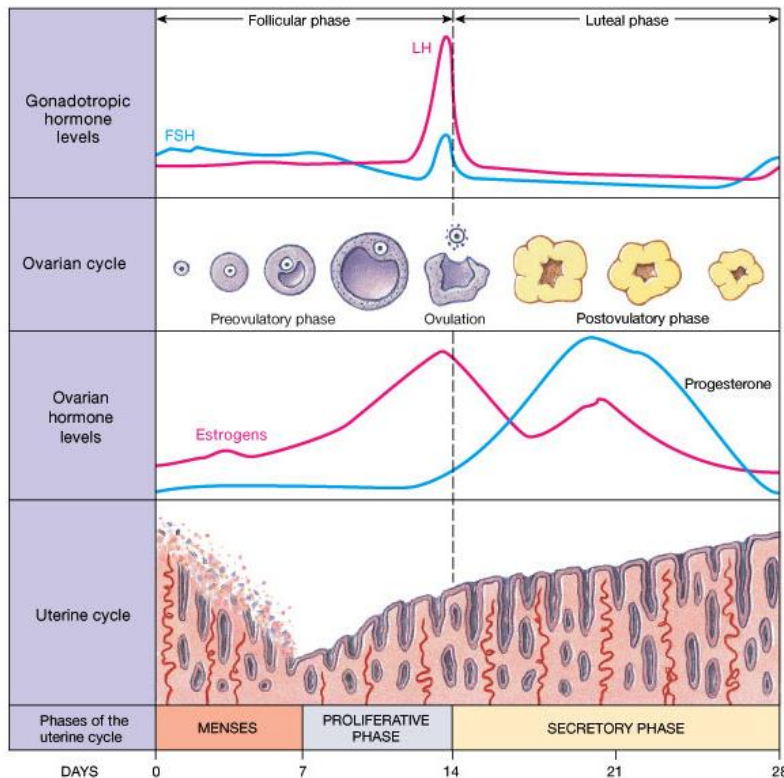
Figure 1: The menstrual cycle. The menstrual cycle starts with the shedding of the endometrium (uterine lining) as menstrual blood marking the beginning of the proliferative phase. The pituitary gland secretes rising amounts of follicle stimulating hormone (FSH) triggering the development of follicles with oocytes. The ovaries produce increasing levels of estrogen (E2) resulting in the thickening and decidualization of the endometrium. The surge of lutenizing hormone (LH) at around day 14 provokes the ovulation by releasing the oocyte and the secretory phase begins. The ruptured follicle develops into the corpus luteum secreting rising amounts of progesterone causing further thickening of the endometrium. In case of succsessful implantation of a fertilized oocyte, the corpus luteum begins to produce chorionic gonadotropin (HCG) pregnancy hormone to maintain the progesterone secretion by the corpus luteum. If the oocyte was not fertilized, the corpus luteum degenerates about 14 days after ovulation and the levels of progesterone and E2 drop. That provokes the endometrium to break down and the menstrual cycle starts all over again. Figure kindly provided, adapted, and modified from [2].

1.2 Endometriosis

1.2.1 Epidemiology

Endometriosis is a common, benign, estrogen-dependent, chronic gynecological disorder defined by the presence of endometrial tissue outside the uterus (also designated as ectopic tissue, lesions or implants) – mainly on the pelvic peritoneum, but also in decreasing order, on the ovaries, on the rectovaginal septum, on the bladder, and upper abdomen (figure 2) [3, 4]. The symptoms range widely from asymptomatic to extensive pelvic adhesions and distortion of pelvic anatomy potentially leading to chronic pelvic pain, dyspareunia, dysmenorrhea, bladder/bowel symptoms, and infertility depending on the stage of the disease [3, 4]. Generally, three different clinical forms of endometriosis exist: (I) peritoneal superficial endometriosis (SUP), which is defined by lesions that are on the surface of the peritoneum or the ovaries, (II) endometrioma (OMA), which consists of ovarian endometriotic "choclate" cysts, and (III) deeply infiltrating endometriosis (DIE) which exhibits lesions that are infilitrating *muscularis propria* of structures surrounding the uterus (vagina, bladder, bowel, or uterus) [5]. Deeply infiltrating endometriosis is frequently reinforcing discomforts such as pelvic pain through invasion into vital pelvic organs [6]. Histologically the disease is

also characterized by dense fibrous tissue mainly composed of collagen type I contributing to the severe clinical symptoms, as e.g. chronic pelvic pain or infertility [3, 7].

The association between endometriosis and infertility is well documentated in literature, but the definite cause-effect relationship remains to be elucidated [4]. The estimated prevalence is up to 10 – 15 % in the general female population of reproductive age [8]. The prevalence of endometriosis increases dramatically to 25 – 50 % in infertile women and 30 – 50 % of women with endometriosis suffer from infertility [9]. In normal reproductive women the fecundity rate is estimated to be around 15 – 20 %, while the fecundity rate in women with untreated endometriosis is only about 2 – 10 % [10, 11].

The American Society for Reproductive Medicine (ASRM) has established a staging system for endometriosis. The disease is classified into one of four stages (I-minimal, II-mild, III-moderate, and IV-severe) based on location, amount, extent, and depth of endometrioc lesions as well on presence and severity of adhesions and presence and size of ovarian implants. Most women exhibit minimal or mild endometriosis, which is characterized by superficial implants and mild adhesions. Moderate and severe endometriosis is characterized by chocolate cysts and more severe adhesions. Nevertheless, the stage of endometriosis does not necessarily correlate with the presence or severity of the symptoms, but with stage IV endometriosis, infertility has a high likelihood [12].

The time elapsed from onset of symptoms to diagnosis of the disease can be very long (mean 11.7 years in the USA and 8.0 years in the UK) due to a broad variability in symptoms and their severity that might cause confusion with other disorders [3]. Surgical assessment and removal of ectopic lesions by laparoscopy or laparotomy is still the gold standard for diagnosis and treatment. The lack of potent biomarkers is the reason why no non-invasive diagnostic tests are available so far. Regarding treatment, several other therapeutic options were established (see chapter 1.2.3).
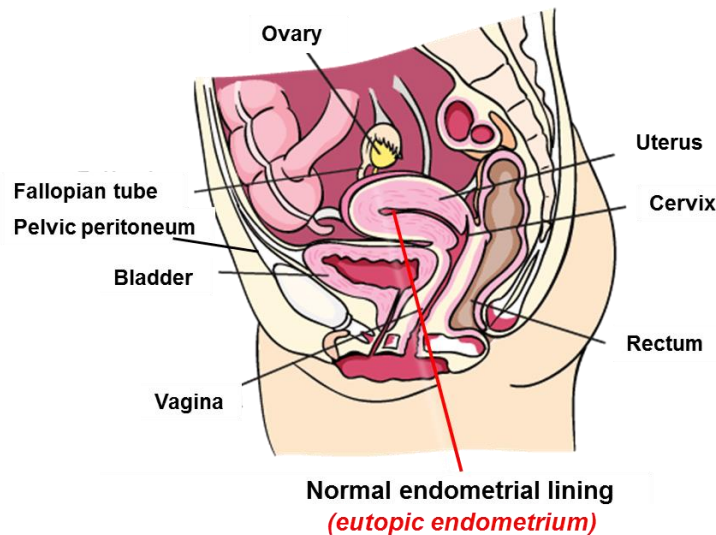
Figure 2: Common sites of endometriosis. Endomteriosis is a disease defined by the presence of endometrial implants outside the uterus causing among others chronic pelvic pain and infertility. Ectopic endometrial lesions are mainly found on the pelvic peritoneum, on the ovaries, on the rectovaginal septum, the bladder, or the fallopian tubes. Figure kindly provided, adapted, and modified from [13].

1.2.2   Pathogenesis

The definite pathogenesis of endometriosis is still unknown. Several theories exist including the retrograde menstruation, altered immunity, coelomic metaplasia, and metastatic spread theory which try to explain the occurrence of endometrial tissue outside the uterus [4]. Newer research is also proposing stem cell and genetic influence on the disease. But also environmental factors seem to play a role in the pathogenesis of endometriosis [3].

Retrograde menstruation

The most widely accepted theory was proposed by Sampson in 1927 stating that the endometrial tissue is transported in a retrograde fashion through the fallopian tubes into the peritoneal cavity during menstruation [3, 14]. The loose endometrial cells then attach to the peritoneal mesothelial cells, invade into the tissue, establish blood supply, proliferate and develop into endometrial implants [4]. Subsequent research provided good support for this theory. Patients with endometriosis have higher volumes of refluxed menstrual blood and endometrial tissue fragements than healthy women [4, 15]. Moreover, endometriosis can be induced in baboons by ligation of the cervix that enables the endometrial fragments to have access to the pelvis [16]. The incidence of endometriosis is increased in young girls with outflow obstruction leading to elevated tubal reflux and retrograde menstruation [4, 17]. But nevertheless, the occurrence of retrograde menstruation is also common in women with and without endometriosis so that this theory alone can not explain the pathogenesis of endometriosis. In fact the underlying mechanisms are most likely multi-factorial.

Besides this more general accepted theory of retrograde menstruation as a pre-requisite of endometriosis further theories exist.

Coelomic metaplasia and metastatic spread (implantation)

Ferguson's theory of coelomic metaplasia was proposed in the 1960's and claims that endometriosis originates from the metaplasia of specialised cells that are present in the mesothelial lining of the visceral and abdominal peritoneum [18, 19]. Another theory states that menstrual cells travel in a metastatic manner from the uterine cavity through the lymphatic channels and veins to distant sites where they establish implants [20]. This implantation approach would explain the exceptionel presence of endometrial tissue far away from the pelvic cavity for example in the brain or the lung [21, 22].

Altered immunity

Several studies show that women with endometriosis have an altered immunity, preventing the by retrograde menstruation refluxed endometrial cells to be eliminiated by the immune system [4, 23]. That would provide an explanation why some women with retrograde menstruation develop endometriosis and others do not. Eventually, the cell-mediated immunity is deficient in patients with the disorder. Women with endometriosis have increased levels of leukocytes and macrophages in and around the ectopic lesions and in the peritoneal fluid but most likely they are unable to detect and to remove endometrial tissue outside its normal location in the uterus [4, 23]. Some studies also propose less cytotoxicity of defective natural killer cells (NK-cells) to endometrial cells [24]. These cells secrete large amounts of cytokines and growth factors such as IL-1, 6 and 8 (interleukin 1, 6 and 8) and TNF (tumor necrosis factor), RANTES (regulated on activation, normal T cell expressed and secreted), and VEGF (vascular endothelial growth factor) into the peritoneal milieu inducing the recruitment of surrounding blood vessels and leukocytes [25-27]. All these conditions lead to higher proliferation and survival of the implants and improved vascular supply. So endometriosis is not only characterized by reduced immunocompetence that prevents ectopic tissue from removal via the immune system, it also exhibits constant low level inflammation that potentiates the establishment of implants [4]. Furthermore, as has been shown by e.g. Mc Allister et al., Gruen et al., or Laux-Biehlmann et al., painful endometriosis certainly originates also from a mixture of inflammatory and neuropathic pathological conditions [28-31]. Therefore, also the therapeutic targeting of inflammatory pain might be appropriate for endometriosis [28, 32].

Stem cells

For tissue homeostasis, adult stem cells exist in the basalis layer of the endometrium [33, 34]. Endometrium-derived stem/progenitor cells residing in the basalis layer can be shed through the fallopian tube to the peritoneal cavity through retrograde menstruation, where they establish endometriotic implants [35, 36].

Newer research also suggests de-novo development of endometrial tissue from endogenous stem cells [37, 38]. These findings help to explain the occurrence of ectopic lesions far away from the uterine cavity. This theory is supported for instance by a study where female allogenic bone marrow transplant recipients received marrow from a single antigen mismatched related female donor that allows the determination of the origin of any cell by the HLA (human leukocyte antigen) type [39]. In endometrial biopsy samples from all bone marrow recipients, donor-derived cells could be detected proposing that endometrial cells can originate from bone marrow derived stem cells [39]. However, the theory of de-novo development of endometrial tissue from endogenous stem cells is not widely accepted owend to the fact that the retrograde menstruation theory is regarded as more plausible.

Genetics

The heritable feature of endometriosis is known for over 20 years, when the risk factor for first-degree relatives of patients with severe endometriosis was reported to be six times higher than that for relatives of healthy women [3, 40]. Familial aggregation has been demonstrated in studies with monozygotic twins, in clinical, and population-based and non-human primate based studies [40-44]. Although the contribution of genetic polymorphisms to endometriosis is not yet clear, they may cause dysregulated expression of genes in the endometrium of both human and non-human primates [45-47].

Genes that are aberrantly expressed in endometriosis include aromatase and 17-beta hydroxysteroid dehydrogenase 2 (HSD17B2) [48, 49]. Aromatase catalyzes the conversion of androstenedione to E2 but due to overexpression of the aromatase in eutopic and ectopic endometrium, high local levels of E2 exist (figure 3) [50, 51]. Usually, the progesterone-dependent HSD17B2 enables the conversion of E2 to the less estronic estrone in the secretory phase [50, 51]. However, the enzyme is downregulated in lesions of affected women causing the E2 dependent growth of implants [50, 51]. Moreover, overexpression of estrogen receptor 2 (ESR2) in ectopic tissue triggers the expression of target genes promoting cellular growth and survival [52]. High levels of E2 also induce increased conversion of arachidonic acid (released by phospholipase A2) to prostaglandin E2 (PGE2) through cyclooxygenase 2 (COX-2) causing inflammation and elevated expression of the

aromatase [50, 51]. Consequently, COX-2 expression levels are also increased in diseased eutopic endometrium and ectopic lesions of diseased women [50, 51]. Endometriosis is also characterized by progesterone resistance coming from downregulation of progesterone receptors (PGR) isofroms PGR-A and PGR-B [53, 54]. Lack of progesterone leads to decreased expression of its target gene HSD17B2 causing the high levels of E2 and the progesterone resistance in lesions [55, 56]. Epigenetics may also play a role in the aberrant expression of ESR1, ESR2, and aromatase. A study by Xue et al. revealed that elevated gene expression of ESR2 results from hypomethylation of the promotor region [52]. Moreover, Wu et al. showed that hypermethylation of the PR-B promotor region causes decreased gene expression which contributes to progesterone resistance [57]. The nuclear receptor steroidogenic factor 1 (SF1) is also overexpressed in endometriotic tissue due to its strong hypermethylation of the promoter region [58]. This protein is activated through PGE2 and triggers the expression of aromatase [50].
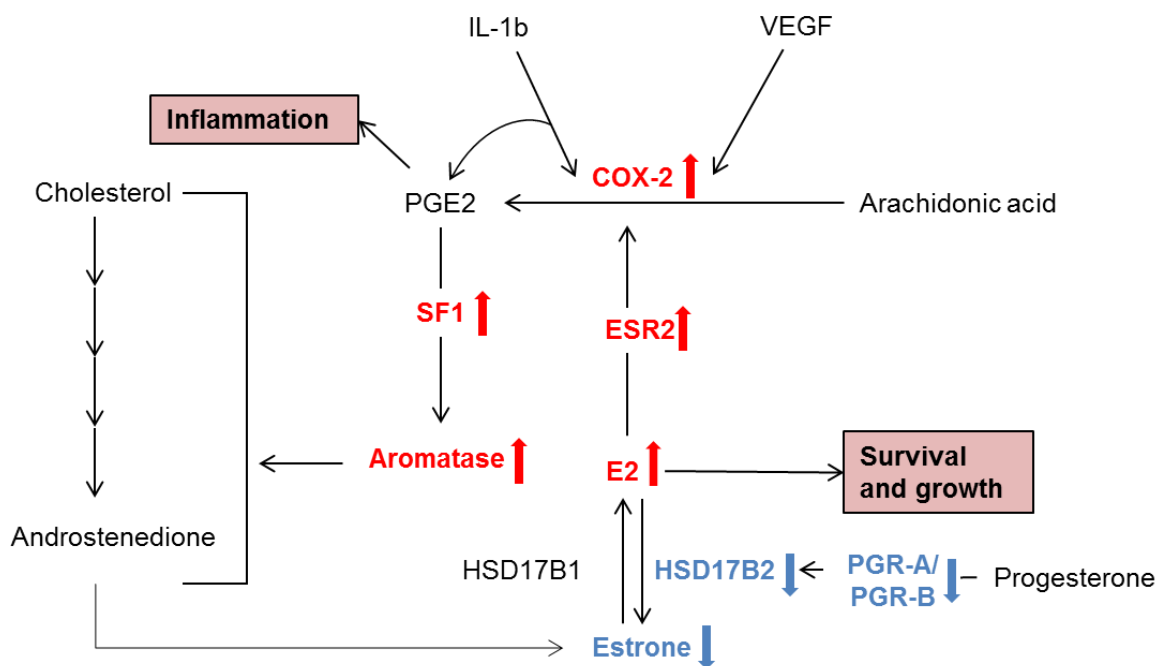
Figure 3: Aberrant gene expression and protein levels in endometriosis. Proteins marked in red are higher and in blue are lower expressed in endometriosis. In normal endometrium cholesterol is converted to androstenedione and estrone, which is further processed to estrogen (E2) through 17-beta hydroxysteroid dehydrogenase 1 (HSD17B1). To elimitate the high potential of E2, progesterone triggers via its receptors A and B (PGR-A and PGR-B) the expression of hydroxysteroid dehydrogenase 2 (HSD17B2), which in turn reconverts E2 to estron. E2 binds to its nuclear receptors 1 and 2 (ESR1 and ESR2) activating the gene expression of cyclooxygenase 2 (COX-2). This enzyme processes arachidonic acid to prostaglandin E2 (PGE2). It mediates inflammation and the gene expression of aromatase via the nuclear receptor steroidogenic factor 1 (SF1). Aromatase further triggers the production of androstenedione and therefore also estrone. Aberrant gene expression in endometriosis leads to disrupted regulation of the entire process resulting in progesterone resistence and high levels of E2 that mediate growth, survival, and inflammation and aromatase expression. Figure reproduced with permission from [50]. Copyright Massachusetts Medical Society.

Environmental factors

Severeal non-primate models have provided important information about environmental factors and their potential impact on endometriosis [3]. A study by Fanton et al. revealed that rhesus monkeys exposed to whole-body proton irradiation have a higher frequency of endometriosis than controls (53 % vs. 26 %) [3, 59]. Rhesus monkeys exposed to 5 – 25 ppm dioxin per day for 4 years also established endometriosis in a dose-dependent manner in staging [3, 60]. These data may explain why Belgium with the highest dioxin pollution in the world has not only the highest incidence of endometriosis but also the highest prevalence of severe endometriosis [61]. However, two subsequent prospective studies from Italy and Belgium did not deliver proof that the significantly increased risk to develop endometriosis in Belgium can be attributed to dioxin exposure [62, 63]. In summary, up to date there is no epidemiological study definitely linking one class of chemicals to the risk of endometriosis, although estrogen-like compounds in the environment have been proposed [3, 64]. People are exposed to a multiplicity of chemicals, with mechanisms of action that may vary in dose, timing of exposue (in utero, childhood, peripubertally, or adult), route of exposure, and synergy with other chemicals, all acting in accordance with an unique genetic background [3, 64].

1.2.3 Treatment

Medical needs are relief of pain, improvement of fertility, or both [3]. By reducing ectopic endometrial implants and restoring normal pelvic anatomy, these medical needs are addressed [4, 65]. Since the growth of the lesions is dependent on ovarian steroid production, endometriosis is an estrogen-dependent benign inflammatory disease of young reproductive women between menarche and menopause [66]. Concerning the dysregulated hormonal conditions of endometriosis, common medical therapies are primarily used to treat on a hormonal basis. For example, gonatropin-releasing hormone (GnRH) reduces the release of FSH and LH and consequently also reduces the ovarian secretion of E2 [50, 51]. Thus, the use of GnRH agonists is one therapeutic option. Other therapies include combined oral contraceptive steroids, prostagens, and androgens, such as danazol, and non-steroidal anti-inflammatory agents [3, 4]. Newer therapies involve selective progesterone-receptor modulators, selective estrogen-receptor modulators, aromatase inhibitors, and antiangiogenic agents [3, 67].

Although all hormonal related approaches are more or less effective by attenuating lesion growth, they translate only late into improvement of pain relief. Fast effects on pain relief by e.g. NSAIDs (non-steroidal anti-inflammatory drugs) such as COX-2 inhibitors are limited due to side effect risks in longterm treatments. Moreover, hormonal related approaches are either

contraceptive itself, or due to potential teratogenic effects they'll need contraceptives in addition.

Another common treatment option is to remove lesions via surgery through laparoscopy or laparotomy which commonly only provides temporary relief for women with pelvic pain. However, symptoms recur in up to 75 % of women within 2 years [3, 68-70].

In general, therapies for pain are not effective for subfertility treatment [3, 71]. Assisted reproduction including controlled ovarian hyperstimulation and intrauterine insemination, or in-vitro fertilisation and embryo transfer are beneficial especially after surgical removal of existing lesions [3, 72-76].

1.3 The WNT pathway

1.3.1 Overview and historical background

WNT (wingless-type MMTV integration site family) proteins are essentially implicated in organismal patterning throughout the animal kingdom during embryogenesis [77]. Apart from that, WNT signaling has been also implicated in adult tissue homeostasis [78]. WNT signals are pleiotropic affecting mitogenic stimulation, cell fate specification, and differentiation [78]. Many studies showed that the WNT pathway is clearly involved in stem cell self-renewal of various different adult stem cells types (for overview [77]).

The Wnt1 gene, originally named Int-1, was discovered in 1982 as a gene activated by the integration of mouse mammary tumor virus proviral DNA in virally induced breast tumors [79]. The *Drosophila Wingless (wg)* gene, which controls segment polarity during larval development, was identified as a homolog of Wnt1 later on from which the term WNT as a combination of Int-1 and *wg* originates [80, 81]. The investigations of relationships among segment polarity mutations were performed by epistasis experiments in 1994 outlining the core of this developmental signal transduction cascade in *Drosophila* [e.g. *Porcupine, Dishevelled*, and *Armadillo* (β-catenin)] [77, 82, 83]. The first assay to study the WNT pathway in vertebrates was established through the injection of mouse Wnt1 RNA into early frog embryos which caused a duplication of the body axis in *Xenopus* [77, 84]. The combined observations from *Drosophila* and *Xenopus* uncovered a highly conserved singaling pathway, commonly designated as the canonical WNT pathway [77]. In the following years more detailed information about the signaling cascade was gained like the identification of T-cell factor/lymphoid enhancer factor (TCF/LEF) transcription factors as WNT nuclear effectors or the identification of frizzleds (FZDs) as WNT receptors working together wih lipoprotein receptor-related proteins (LRPs) as coreceptors [85-88].

In the early 1990s, the WNT pathway was directly connected with human diseases for the first time. Kinzler et al. and Nishido et al. discovered the adenomatous polyposis coli (APC) gene independently in a hereditary cancer syndrome named familial adenomatous polyposis (FAP) in 1991 [89, 90]. Shortly afterwards, it was identified that the large cytoplasmic APC protein is interacting with β-catenin [91, 92]. Within the last two decades, additional pathway components and disease connections were identified indicating the WNT pathway as one of the most important signal transduction pathways in the pathogenesis of many diseases [77].

1.3.2 The canonical WNT pathway

The WNT secretion machinery

WNT proteins have a size of ~ 40 kDa and contain many conserved cysteines [93]. Although WNTs have been discovered almost 30 years ago, their efficient production and biochemical characterization remain challenging [77]. Willert et al. were the first ones who successfully purified mouse Wnt3a in 2003 and they discovered that WNT proteins are lipid modified [94]. These lipids are essential for efficient signaling and may also play a role in WNT secretion (figure 4) [94-96]. Especially Procupine (PORCN) is required for WNT secretion and represents a highly conserved component of the WNT pathway wich is only active in WNT-producing cells. PORCN is a multipass transmembrane O-acetyltransferase in the endoplasmic reticulum (ER) which is essentially involved in the WNT lipid modification and maturation [77, 97, 98]. Loss of PORCN function leads to the retention of Wnt3a in the ER thereby blocking Wnt3a secretion in the *Drosophila* embryo [98, 99].

The seven-transmebrane (7TM) protein Wntless (WLS) plays an essential but less understood role in WNT secretion by possibly serving as a sorting receptor, taking WNTs from the Golgi to the plasma membrane [77, 100-102]. Other proteins and complexes involved in maturation and trafficking such as the retromer are also important for WNT signaling [77, 103, 104].
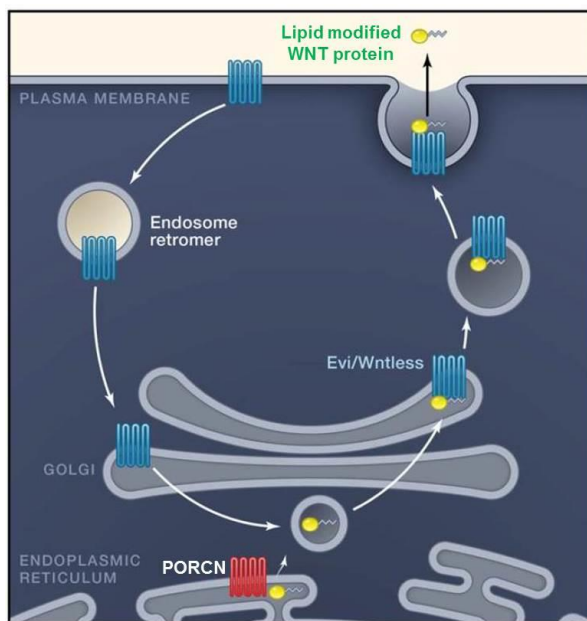
Figure 4: The WNT secretion machinery. WNT proteins are lipid modified by porcupine (PORCN) in the endoplasmic reticulum (ER). The Evi/Wntless (WLS) seven-transmembrane proteine ensures further transportation of WNTs to the plasma membrane. The retromer complex plays an essental role in the recycling of WLS endosomal vesicles. Figure kindly provided, adapted, and modified from [77].

The WNT – receptor interaction

After secretion, WNTs bind a heterodimeric receptor complex consisting of a FZD and a LRP5/6 protein (figure 5) [77]. In summary, there are 10 FZD proteins representing 7TM receptors with large extracellular N-terminal cysteine-rich domains (CRD) providing the core of WNT binding [87, 105, 106]. The WNT-FZD interaction is promiscuous because a single WNT can bind several FZDs and vice versa [77, 87, 106]. In vertebrates, activated FZDs interact with the single-pass transmembrane molecule LRP5 or LRP6 [107, 108]. The ligand-induced dimerization of FZD and LRP leads to a conformational change followed by a phosphorylation step of the key target proteins. Axin binds to the cytoplasmic tail of LRP6 regulated by the phosphorylation of the LRP6 tail by at least two separate kinases, glycogen synthase kinase 3 (GSK3) and casein kinase 1-gamma (CK1γ) [109-111]. GSK3 further phosphorylates serines in several WNT components such as β-catenin, Axin, or APC [112]. The cytoplasmic part of FZD cooperates with Dishevelled (Dvl) triggering the interaction between the LRP tail and Axin [113]. Dvl and Axin also bind to each other through the DIX domain and multimers of receptor-bound Dvl-Axin molecules might further facilitate the FZD-LRP dimerization [114, 115]. The WNT-induced LRP6 phosphorylation titrates Axin away, which is a negative regulator, so that the signal transduction is rather a stoichiometric than a catalytic mechanism [77].

Another small family of 7TM receptors is involved in canonical WNT signaling, the leucine-rich repeat-containing G-protein coupled receptor (LGR) family of receptors. LGRs group B members (LGR4-6) bind with high affinity R-spondins (RSPOs) that essentially leads to the enhancement of WNT signaling especially in low-dose WNT conditions [116-119]. As co-receptors they mediate into WNT signaling through association with the FZD-LRP complex

[117]. LGRs are related to the G-protein coupled receptors (GPCRs) for thyroid-stimulating hormone (TSH), FSH, and LH and they have a large N-terminal extracellular leucine-rich repeat domain providing the platform for glycoprotein binding [77, 120]. Although they bind RSPOs through their large ectodomain, they do not recruit G-proteins [116, 117]. RSPOs are small secreted proteins with two N-terminal furin domains and a thrombospondin domain [77]. The vertebrate genome encodes 4 different RSPOs (RSPO1-4) [77]. Figure 5 gives an overview about WNT-receptor interaction.

Natural WNT inhibitors exist to restrict WNT signaling to prevent overproportional effects. Among these are secreted frizzled-related proteins (SFRPs) and the WNT inhibitory protein (WIF) which can bind WNTs and therefore block the interaction between WNTs and FZDs [77, 121]. Other WNT inhibitors include proteins of the dickkopf (DKK) family, which can disrupt WNT-induced FZD-LRP6 complex formation [77, 122-124].

The cytoplasmatic signaling

The destruction complex plays the key role in canonical WNT signaling. It is responsible for the cytoplasmic stability of β-catenin [77]. The tumor suppressor protein Axin builds the scaffold of the destruction complex by interacting with β-catenin, the tumor suppressor protein APC, and two constitutively active serine-threonine kinases (CK1α/δ and GSK3α/β) (figure 5) [77]. APC presents a large protein that interacts with both β-catenin and Axin [77].

When FZD-LRP receptors are not occupied, CK1 and GSK3 sequentially phosphorylate Axin-bound β-catenin [77]. The phosphorylated motif is then recognized by the F box/WD repeat protein (β-TrCP) as a part of the E3 ubiquitin ligase complex [77]. Consequently, β-catenin is ubiquitinated and targeted for rapid destruction by the proteasome [77, 125]. After activation of WNT signaling through binding of WNTs to the receptors, Axin is recruited to the phosphorylated tail of LRP [77]. This relocalization causes the inhibition of β-catenin ubiquitination within the destruction complex [77]. Consequently, the complex becomes saturated by phosphorylated forms of β-catenin because ubiquitination by β-TrCP is blocked, so newly synthesized β-catenin can accumulate, translocate to the nucleus, and activate gene expression of β-catenin target genes [77, 126].

Additional positive regulation of WNT signaling is mediated by the protein phosphatase PP2A through direct dephosphorylation of β-catenin through its regulatory subunit PR55α [127]. Moreover, tankyrases (TNKS) also trigger WNT signaling through destabilization of Axin by ADP ribosylation thereby creating a dysfunctional distruction complex which causes β-catenin to stabilize and to activate gene expression [128]. Inhibition of TNKS achieves reverse results by stabilizing Axin and therefore also the destruction complex ensuring the ubiquitination and proper destruction of β-catenin [128].
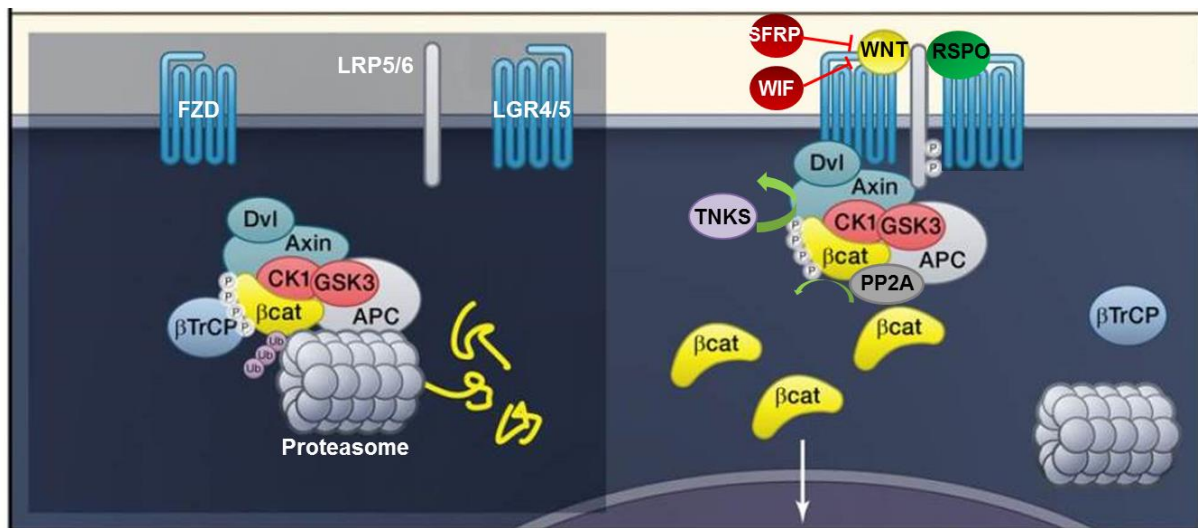
Figure 5: WNT signaling at the receptors and in the cytoplasm. In the abscence of WNTs the destruction complex resides in the cytoplasm, where it binds, phosphorylates, and ubiquitinates β-catenin by β-TrCP. The proteasome finally degrades β-catenin. WNT binding causes the receptors FZD and LRP5/6 to dimerize. The coreceptors LGR4/5 additionally associate with the FZD-LRP complex upon RSPO binding facilitating WNT signaling. The phosphorylation of LRP5/6 leads to the recruitment of Axin therefore stopping β-catenin ubiquitination within the destruction complex. The complex still captures β-catenin but ubiquitination by β-TrCP is blocked. Newly synthesized β-catenin can accumulate and translocate to the nucleus where it activates gene expression of β-catenin target genes. Figure kindly provided, adapted, and modified from [77].

WNT signaling in the nucleus

WNT signaling ultimately acts through gene activation controlled by β-catenin and TCF/LEF (figure 6) [77]. After WNT activation, β-catenin accumulates in the cytoplasm and travels into the nucleus, where it binds DNA-associated TCF/LEF transcription factors [77, 85, 86]. The consensus TCF/LEF motif is conserved among vertebrates and *Drosophila* consisting of the AGATCAAAGG base sequence [77, 129]. If WNT is not activated, TCF/LEF interacts with the corepressor Groucho to prevent gene transcription [77, 130, 131]. Upon WNT activation, the interaction of β-catenin and TCF/LEF leads to the phosphorylation and activation of the transcription factor, thereby inducing gene expression of target genes [77, 132, 133]. AXIN2 is a global target gene and therefore a general indictaor of WNT activity, while most target genes are development stage and tissue specific [134].

The C-terminus of β-catenin acts as a transcriptional activation domain as it binds histone modifiers such as CBP (CREB-binding protein) and Brg-1 (ATP-dependent helicase SMARCA4) or its homolog Cdc73 (cell division cycle 73) [77, 129, 135, 136].
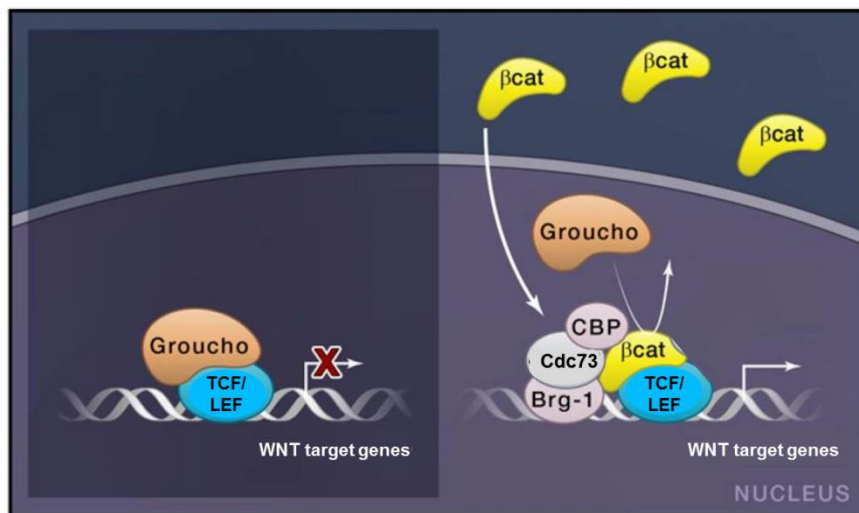
Figure 6: The WNT signaling in the nucleus. In abscence of WNT signals, TCF/LEF is associated with the transcriptional corepressor Groucho preventing gene expression. In presence of WNT signals, β-catenin replaces Groucho from TCF/LEF and recruites transcriptional coactivators such as Brg1, CBP, Cdc73, Bcl9, and Pygopus to activate target gene expression. Figure kindly provided, adapted, and modified from [77].

Direct targets of WNT signaling are defined by the TCF/LEF binding motif and include many genes as cyclin D1 (CDK1), E-cadherin (CDH1), matrix metallopeptidase 2 and 9 (MMP2, MMP9), survivin, VEGF, and octamer-binding transcription factor 4 (OCT4) that are involved in processes such as proliferation, migration, invasion, cell survival, vascularization, and embryonic stem cellness [137-145]. Additionally, several distinct WNT pathway members like WNT3A, RSPO2, LRP6, LGR5, and FZD7 are also direct targets of WNT signaling constituting positive feed-forward circuits that amplifies WNT signaling [146-150]. Other direct or indirect target genes such as SFRP2, DKK1, and AXIN2 provide an autoregulatory negative feedback loop to prevent outranged WNT signaling [134, 151-156]. These various WNT pathway self-regulatory loops mostly occur in a cell-specific manner, generating additional complexity in controlling the amplitude and duration of WNT responses [157].

1.3.3 The non-canonical WNT pathway

The β-catenin-independent WNT signaling is called non-canonical WNT pathway and is transduced through FZD reseptors without involvement of LRPs [158]. Several WNT ligands including WNT4A, WNT5A, WNT7A, WNT11, and WNT16 have been shown to activate the non-canonical WNT pathway [159-161]. WNT5A is the most intensively studied ligand and although it usually activates non-canonical WNT signaling, it can also trigger the canonical WNT pathway under certain conditions [162-166]. Non-canonical WNT signaling includes the WNT/PCP (planar cell polarity) and WNT/Ca2+ pathways (figure 7) [167].

The WNT/PCP pathway requires the WNT/FZD interaction, which in turn promotes the activation of PI3K (phosphatidylinositol 3-kinase) which then activates the AKT/mTOR pathway resulting in increased protein synthesis (shown in green) [158]. The other PCP pathway (colored in blue) leads to the activation of the small GTPase protein Rac (Ras-related C3 botulinum toxin substrate), which in turn induces the ROCK (Rho-associated

protein kinase) pathway and the JNK (c-Jun N-terminal kinase) kinase cascade that finally activates AP1-mediated target gene expression (demonstrated in blue) [168-170].

The WNT/calcium pathway (illustrated in yellow) includes the complex formation between FZD/DVL and G-proteins resulting in PLC (phosphor lipase C) activation which in turn cleaves PIP2 (phosphatidyl inositol 4,5 biphosphate) into DAG (diacylglycerol) and IP3 (inositol 1,4,5-triphosphate) [168]. Consequently, PKC (protein kinase C) gets activated through DAG while IP3 initiates calcium release from the ER enhancing the phosphorylation and activation of PKCs [168]. Moreover, the activation of Ca^{2+}-calmodulin-dependent calcineurin (CN) and CAMKII (Ca^{2+}-calmodulin dependent kinase II) is promoted causing NFAT (nuclear factor of activated T-cells) and NLK (nemo like kinase) translocation [168]. NFAT acts as a transcription activator for appropriate target genes while NLK serves as a canonical WNT pathway inhibitor since it degradates TCF/LEF transcription coactivators [168, 171]. If not stated differently, in this study WNT signaling generally means the canonical WNT pathway.
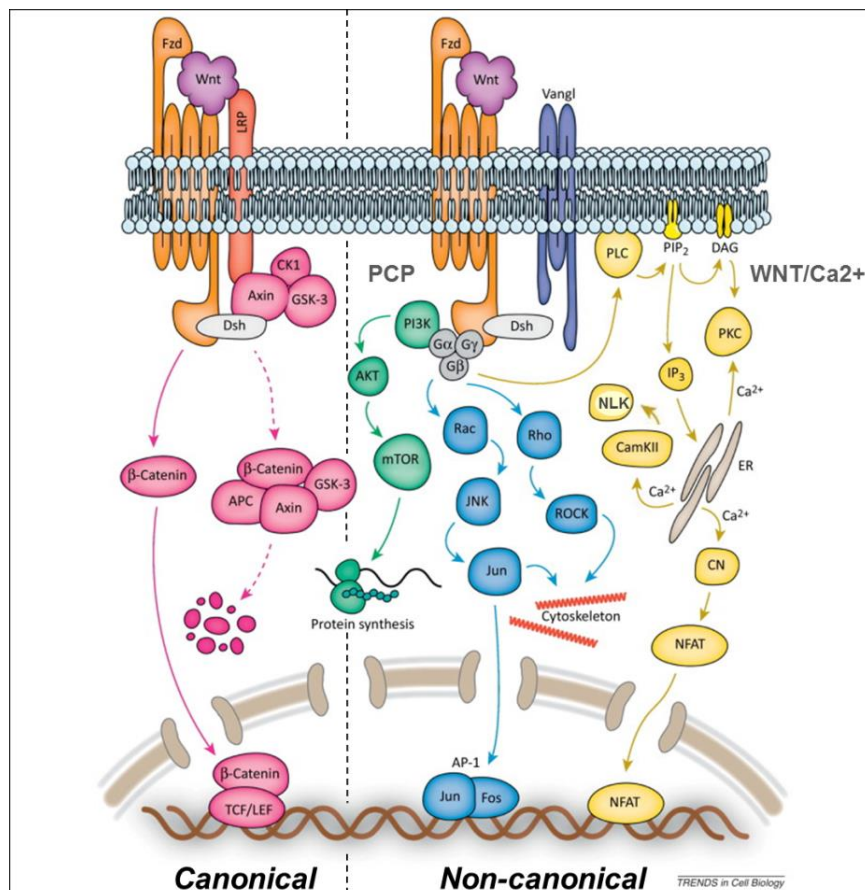
Figure 7: The canonical and the non-canonical WNT pathway. Interaction of WNT/FZD leads to either JNK, ROCK or AKT/mTOR activation (PCP pathway), or PKCs activation through the cleavage of PIP2 to DAG by PLCs with subsequent NFAT transactivation caused by the calcium release by IP3, or inhibition of β-catenin activity through Ca^{2+} dependent binding of NLK to TCF/LEF (WNT/Ca^{2+} pathway). Figure kindly provided and adapted from [158].

1.3.4 Canonical WNT signaling in disease

Several studies connect WNT signaling with e. g. bone biology and disease [77, 172]. For example LRP5, LRP6, and FZD9 mutations are associated with hereditary disorders that are characterized among others by osteoporosis, coronary artery disease, and metabolic syndrome [77, 173-175]. In addition, dysfunctional WNT proteins contribute to an impaired bone development like mutated WNT3 or WNT7A proteins that cause among others limb-malformations with various degrees of limb aplasia/hypoplasia [176, 177]. Since WNT activates osteoblasts and influences bone mass, secreted WNT agonists have become attractive targets for antibody therapy in osteoporosis [77].

Mutations in RSPOs have been found in two human hereditary disorders so far [77]. RSPO1 dysfunctions cause XX sex reversal and skin abnormalities with predisposition to squamous cell carcinomas and disrupted RSPO4 is associated with anonychia and severe hypoplasia of finger- and toenails [77, 178, 179]. Mutations of RSPO2 have not yet been associated with human diseases, but Rspo2 knock out mice show diverse developmental defects involving limbs, lung, and craniofacial anatomy [77, 180-182]. Furthermore, inactivating mutations in the PORCN gene have been shown to cause a X-linked disorder with skin and digital malformations and additional ocular and dental dysfunctions [183, 184]. Since the gene is X-linked, mutations in PORCN are lethal in male causing early embryonic lethality coming from gastrulation defects observed in mouse knockout embryos [77, 185, 186]. Females can survive with focal defects because of random X inactivation [77].

Also defects of LGR5 have been investigated. Lgr4 and Lgr5 were neonatal lethal in mutant knockout mice. Pleiotropic phenotypes were identified in male reproductive organs, eye, gall bladder, kidney, hair follicles, and a varity of other organs for Lgr4 [77, 187]. In contrast, Lgr5 mutant mice showed only a single abnormality of the lower jaw and tongue [187]. A strong genetic interaction between Lgr4 and Lgr5 was identified in the gut of double-mutant mice [117, 188]. Lgr5 marks adult stem cells in a varity of actively self-renewing organs, including the intestinal tract and hair follicles [189, 190]. This together with the fact that it also acts as a coreceptor in WNT signaling through the binding of RSPOs, suggests a strong connection between WNT signaling and the activation of adult stem cells [77]. Therefore, LGR5 has been implicated in colon cancer and also serves as a target gene in this disease [191].

Not only LGR5 is involved in cancer. Since WNT signaling generally plays an important role in adult stem cell biology, it is not surprising that various WNT pathway mutations are frequently associated to cancer, especially in tissue that depends on WNT for self-renewal and repair [77]. Loss-of-function mutations of APC result in hereditary cancer syndrome FAP or sporadic colorectal cancer [77, 89, 90]. A global exome-sequencing study confirmed that

the overwhelming majority of colorectal cancer patients carry inactivating mutations in the APC gene [192]. This study also revealed a rare but recurrent fusion of VTI1A (vesicle transport through interaction with t-SNAREs 1A) and TCF7L2 (the gene coding TCF4) in colon cancer [193]. In other rare cases of colon cancer and hepatocellular carcinomas, AXIN2 or β-catenin are mutated [77, 194, 195]. Defective β-catenin has also been implicated in various other solid tumors such as melanomas or pilomatricomas [77, 196].

Also metabolic diseases were linked to WNT signaling. For example specific single-nucleotide polymorphisms (SNPs) in WNT5B, WNT10B, and TCF7L2 were associated with an increased risk for type II diabetis [197-199].

1.3.5 WNT signaling in endometriosis

Since many WNT-associated genes are essentially involved in mechanisms such as cell proliferation, migration, and invasion, the connection with endometriosis is likely [3, 200]. Indeed, several studies have demonstrated that dysregulated WNT signaling may contribute to the pathophysiology of endometriosis (for overview [201]). The abnormal activation of the WNT pathway in the menstrual endometrium of diseased women might promote the development of endometriosis through increased cell migration and invasion. Moreover, the aberrant activation of WNT signaling may also enable the growth of lesions through increased invasiveness and resistance to apoptosis of endometriotic cells. Furthermore, the dysregulated WNT pathway might also cause the persistence of the proliferative phenotype resulting in impaired decidualization in the mid-secretory endometrium of infertile endometriosis patients. Abnormal activation of WNT signaling may be also the molecular and cellular mechanism leading to fibrosis in endometriosis. Upon treatment with a small molecule WNT inhibitor, the progession of fibrosis could be reversed in a xenograft model of endometriosis in immunodeficient nude mice [202]. Finally, there are several *in vivo* experiments proposing a potential contribution of WNT signaling in the molecular mechanisms that underly chronic pelvic pain in endometriosis (for overview [201]). Altogether these findings suggest an important role of the WNT pathway in the pathogenesis of endometriosis [201].

1.3.6 Small molecule canonical WNT modulators

The extensive involvement of the WNT pathway in the pathogenesis of many diseases and especially in cancer has promoted the research to target WNT signaling with small molecules. Table 1 lists a selection of published molecules. The most effective and selective target would be the complex between TCF/LEF and β-catenin. But research proved that this target is rather elusive since its structure consists of a large binding surface which cannot be

easily disrupted by chemical compounds [203]. Compounds such as PKF115-584 have been suggested to inhibit WNT signaling at this level. However, although they potently antagonize cellular effects of β-catenin activities *in vitro* and *in vivo*, their specifity and efficacy have to be further established so that no clinical trails were initiated so far [77, 204]. Consequently, compounds are needed that target the WNT pathway upstream.

The most specific and most upstream located target to block WNT signaling is the inhibition of PORCN which is the enzyme that catalyses acetylation of WNT proteins and therefore enables their secretion in adjacent cells. IWP is able to inactivate PORCN with a high degree of selectivity [205]. However, its use is limitied to *in vitro* experiments, because its hydrophobicity excludes the usage *in vivo*. Nevertheless, the variant C56 and its advanced derivate LGK974 from Novartis are useful for this application and they did also show effective inhibition of WNT signaling resulting in decreased tumor growth *in vivo* [206, 207]. LGK974 is currently tested in a phase I clinical trial to treat pancreatic adenocarcinoma, rapidly accelerated fibrosarcoma (BRAF) mutant colorectal cancer and other tumor types with documented genetic alterations (clinical trial registry number: NCT01351103).

Some chemical compounds activate WNT signaling trough blockade of natural WNT inhibitors. WAY-316606 is a small molecule which prevents SFRP1 to bind to FZD receptors [208]. Therfore, WNTs can easily interact with the FZD receptors leading to increased WNT signaling and bone formation in murine calvarial organ culture assay [208].
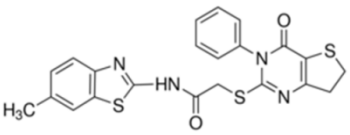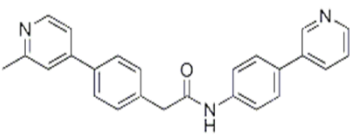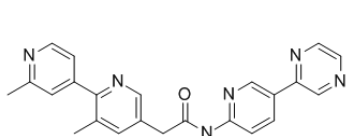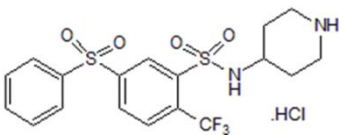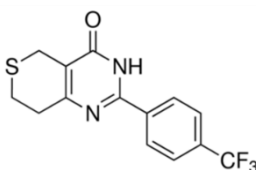
Other small molecules such as XAV939 or NVP-TNKS656 function by stabilizing AXIN and therefore destabilizing β-catenin through inhibition of TKNS [128, 209]. IWR is a small molecule directly interacting with AXIN promoting its stabilization [205]. Whereas IWR and XAV939 have been only tested successfully *in vitro*, NVP-TNKS656 has been reported to also cause more robust apoptosis and antitumor activity both *in vitro* and *in vivo* [210].
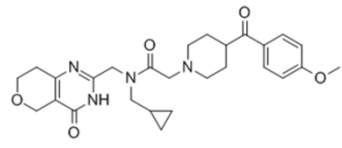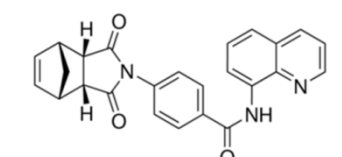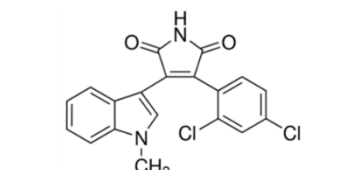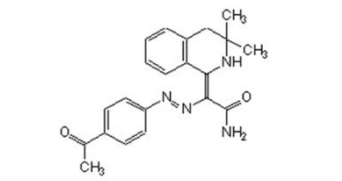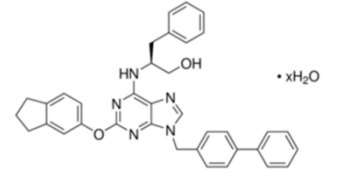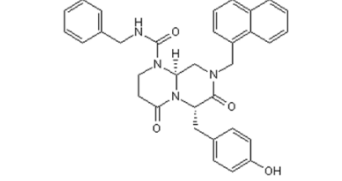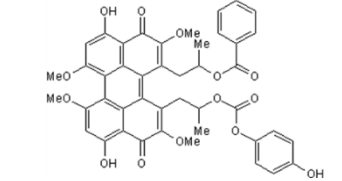
The most widely used strategy to affect WNT signaling is to target GSK3β. Chemicals such as lithiumchlorid (LiCl) can activate the enzyme leading to phosphorylation of AXIN-bound β-catenin which in turn initiates its degradation [77]. In contrast, SB-216763 inhibits GSK3β causing the activation of the WNT pathway and therefore inducing the expression of a β-catenin-TCF/LEF reporter gene in HEK293 cells [77, 204]. However, GSK3β is involved in various signaling events in cells and its targeting has pleiotropic effects [77]. Another activator is IQ1, a small molecule that targets PP2A which facilitates the direct dephosphorylation of β-catenin [211]. QS11 certainly increases the WNT pathway through affecting protein trafficking by inhibiting the GTPase activating protein of ADP-ribosylation factor 1 (ARFGAP1) [212].

ICG-001 operates more downstream in the WNT pathway by inhibiting the transcriptional coactivator CBP [213]. The small molecule selectively induces apoptosis in transformed colon cells, reduces growth of colon carcinoma cells *in vitro*, and shows efficacy in the Min mouse and nude mouse colon cancer xenograft models *in vivo* [213].

In summary, a small set of chemical compounds to target WNT signaling is available allowing further investigation of the pathway. However, their use is limited and screens for further molecules are ongoing. Since our understanding of the WNT pathway is still incomplete, much space for improving new small molecules is left. Furthermore, most compounds are only suitable for *in vitro* studies showing the urge to develop molecules that can be also applied *in vivo*.

Table 1: Small molecule modulators of the WNT pathway.

Molecule	Structure	Target	Effect on target	Effect on signaling	Reference
IWP		PORCN	inhibits	**inhibits**	Chen et al., 2009 [205]
C59		PORCN	inhibits	**inhibits**	Proffitt et al., 2013 [206]
LGK974		PORCN	inhibits	**inhibits**	Liu et al., 2013 [207]
WAY-316606		SFRP1	inhibits	**activates**	Bodine et al., 2009 [208]
XAV939		TNKS1/2	inhibits	**inhibits**	Huang et al., 2009 [128]

NVP-TNKS656		TNKS2	inhibits	**inhibits**	Shultz et al., 2013 [209]
IWR		AXIN2	activates	**inhibits**	Chen et al., 2009 [205]
SB-216763		GSK3β	inhibits	**activates**	Coghlan et al., 2000 [214]
IQ1		PP2A	activates	**activates**	Miyabayashi et al., 2007 [211]
QS11		ARFGAP1	activates	**activates**	Zhang et al., 2007 [212]
ICG-001		CBP	inhibits	**inhibits**	Emami et al., 2004 [213]
PKF115-584		TCF/LEF/ β-catenin	inhibits	**inhibits**	Lepourcelet et al., 2004 [204]

1.4   Aim of the work

Goal of the thesis was to investigate the involvement of the WNT pathway in endometriosis. Broadening our knowledge in this field can contribute to disease understanding and may help to discover new therapeutic options. Finally, the need for biomarkers for a non-invasive diagnosis of endometriosis shall be addressed.

A previous clinical study (EMMA – Endometriosis Marker Austria) using laser capture microdissection (LCM) and gene arrays indicated that WNT signaling was dysregulated in endometriosis. Several WNT pathway members, that were particularly noticeable, were selected and further examined. Firstly, the gene array data of the WNT candidate genes WNT2B, WNT7A, FZD7, LGR5, and RSPO1 needed to be validated within the same patient cohort via TaqMan and within a different cohort via immunohistochemistry. Moreover, mRNA expression of the clinical samples concerning additional genes associated with e.g. migration or proliferation were measured with TaqMan, since these mechanisms are also implicated in endometriosis and might be regulated by WNT signaling. Furthermore, the selected WNT candidate genes were examined in endometrial stromal cells (ESCs) *in vitro*. Manipulation of mRNA and protein levels ought to give information about their impact on WNT activity, viability, cell death rate, and caspase and migration activity to determine whether they affect WNT signaling and corresponding cellular responses. Additionally, an *in vivo* experiment with a small molecule that targets WNT signaling in a retrograde menstruation model for endometriosis in mice has been carried out to elucidate the effect of WNT inhibition on the establishment of the disease. Therefore, disease burden in terms of lesion size and number was measured. Finally, the mRNA expression of WNT pathway genes, that are involved in e.g. migration, proliferation, or vascularization was measured in the *ex vivo* samples, to draw a direct connection between the WNT pathway and mechanisms that could contribute to endometriosis.

2 MATERIALS

The following section lists all chemicals, buffers, kits, TaqMan probes, siRNAs, expression plasmids, antibodies, cell culture media and supplements, consumables, technical devices, and softwares that were used in this study.

2.1 Chemicals and buffers

1 x PBS	Gibco, Carlsbad, CA, USA
10 x PBS	Gibco, Carlsbad, CA, USA
2-Mercaptoethanol	Gibco, Carlsbad, CA, USA
Acetic acid	Sigma Aldrich Corp., St. Louis, MO, USA
Albumin Standard	Thermo Fisher Scientific, Braunschweig, Germany
BD FACS Flow™	BD Bioscience, San Jose, USA
BD FACS™ Accudrop Beads	BD Bioscience, San Jose, USA
BD™ CompBeads Anti-Mouse Ig K	BD Bioscience, San Jose, USA
BD™ CompBeads Negative Control	BD Bioscience, San Jose, USA
Bovine serum albumin, 30% in PBS	Sigma Aldrich Corp., St. Louis, MO, USA
Calcein-AM	Invitrogen GmbH, Darmstadt; Germany
Celsior® organ storage solution	Genzyme, Cambridge, USA
Complete Tablets Mini EDTA-free, EASY Pack	Roche, Basel, Switzerland
Cytomation Target Retrieval Solution, pH 9	Dako, Jena, Germany
DAB Peroxidase (HRP) Substrate Kit (with Nickel), 3,3'-diaminobenzidine	Vector Laboratories, Burlingame, CA, USA
DAKO Real™Antibody Diluent	Dako, Jena, Germany
DAPI (1 mg/ml)	Thermo Fisher Scientific, Braunschweig, Germany
Destilled Water	Gibco, Carlsbad, CA, USA
Dual Endogenous Enzyme Block	Dako, Jena, Germany
Ehanol 70 Vol-%, reinst	Bernd Kraft GmbH, Duisburg, Germany
EnVision + System-HRP labelled Polymer Anti-Mouse	Dako, Jena, Germany
EnVision + System-HRP labelled Polymer Anti-Rabbit	Dako, Jena, Germany
Ethanol	Sigma Aldrich Corp., St. Louis, MO, USA
Eukitt®	O. Kindler GmbH, Freiburg im Breisgau, Germany
FACS Flow ™	BD Bioscience, San Jose, USA
Fluoromount™ Aqueous Mounting Medium	Sigma Aldrich Corp., St. Louis, MO, USA
Formalin solution, neutral buffered, 10%	Sigma Aldrich Corp., St. Louis, MO, USA
Mayer´s Hematoxylin (Lillie´s Modification)	Dako, Jena, Germany

Histoacryl ® tissue adhesive	B. Braun, Melsungen, Germany
HyClone HyPure™ Molecular Biology Grade Water	GE Healthcare, Little Chalfont, UK
Ketavet®, 100 mg/ml	Zoetis, Berlin, Germany
Lipofectamine® 2000	Life Technologies, Carlsbad, CA, USA
Methanol	Sigma Aldrich Corp., St. Louis, MO, USA
Passive Lysis Buffer, 5 x	Promega, Madison, WI, USA
Permanent AP Red Kit	Zytomed Systems GmbH, Berlin, Germany
Pierce® RIPA Buffer	Thermo Fisher Scientific, Braunschweig, Germany
Pierce™ BCA Protein Assay Reagent A and B	Thermo Fisher Scientific, Braunschweig, Germany
Poly(ethylene glycol) 400	Fluka, St. Louis, MO, USA
Protease inhibitor cOmplete ULTRA Tablets, Mini, EASYpack	Roche, Basel, Switzerland
Protein Block, Serum-Free, Ready-To-Use	Dako, Jena, Germany
Recovery™ Cell culture Freezing Medium	Gibco, Carlsbad, CA, USA
Rompun, 2%	Bayer Health Care, Berlin, Germany
Sodium azid	Sigma Aldrich Corp., St. Louis, MO, USA
TBS	Fisher Scientific GmbH, Schwerte, Germany
Trypan Blue	Biochrom GmbH, Berlin, Germany
Tween®	AppliChem, Darmstadt, Germany
Water, sterile	Merck Millipore, Darmstadt, Germany
Xylol	Sigma Aldrich Corp., St. Louis, MO, USA
ZytoChem Plus AP Polymer anti-Mouse	Zytomed Systems GmbH, Berlin, Germany

2.2 Kits

Agilent 6000 Nano Reagents Part I	Agilent Technologies Inc., Santa Clara, USA
Agilent 6000 Pico Reagents Part I	Agilent Technologies Inc., Santa Clara, USA
ApoTox-Glo™ Triplex Assay	Promega, Madison, WI, USA
CellTiter-Glo® Luminescent Cell Viability Assay	Promega, Madison, WI, USA
Cignal TCF/LEF Reporter Assay Kit (LUC)	Qiagen, Hilden, Germany
Dual-Luciferase® Reporter Assay System	Promega, Madison, WI, USA
MinElute Reaction Cleanup Kit	Qiagen, Hilden, Germany
Ovation PicoSL WTA System V2 Kit	NuGEN Technologies, Inc., San Carlos, CA, USA
Peggy Sue or Sally Sue-Mouse (12-230 kDa)	
Size Separation Master Kit (anti-mouse-HRP)	ProteinSimple, San Jose, USA
RNeasy Micro Kit	Qiagen, Hilden, Germany
RNeasy Mini Kit	Qiagen, Hilden, Germany

Super Script® VILO™	Invitrogen GmbH, Darmstadt; Germany
TaqMan® 2X Universal PCR Master Mix	Thermo Fisher Scientific
TaqMan® Fast Universal PCR Master Mix	Thermo Fisher Scientific, Braunschweig, Germany
Tumor Dissociation Kit (Human)	Miltenyi Biotec, GmbH, Bergisch Gladbach, Germany

2.3   TaqMan probes

All TaqMan probes were obtained from Thermo Fisher Scientific, Braunschweig, Germany.

18s rRNA	Hs99999901_s1
Axin 2	Mm00443610_m1
BAX	Hs00180269_m1
Bax	Mm00432051_m1
BCL2	Hs00608023_m1
Bcl2	Mm00477631_m1
CAV1	Hs00971716_m1
Cav1	Mm00483057_m1
CD10	Hs00153510_m1
Cdh1	Mm01247357_m1
Cdk1	Mm00772472_m1
DKK3	Hs00951307_m1
Dkk3	Mm00443800_m1
EPCAM	Hs00901885_m1
ESR1	Hs00174860_m1
Esr1	Mm00433149_m1
ESR2	Hs00230957_m1
Esr2	Mm00599821_m1
FGF9	Hs00181829_m1
Fgf9	Mm00442795_m1
FZD7	Hs00275833_s1
Fzd7	Mm00433409_s1
GAPDH	Hs99999905_m1
Hif1a	Mm00468869_m1
KRT18	Hs02827483_g1
LGR5	Hs00969422_m1
Lgr5	Mm00438890_m1
LRP1	Hs00233856_m1
Lrp1	Mm00464608_m1
MAPK10	Hs00373461_m1
Mapk10	Mm00436518_m1
MKI67	Hs01032443_m1
Mki67	Mm01278617_m1
MME (CD10)	Hs00153510_m1
MMP2	Hs01548727_m1
Mmp2	Mm00439498_m1

MMP9	Hs00234579_m1
Mmp9	Mm00442991_m1
PGR	Hs01556702_m1
Pgr	Mm00435628_m1
Pou5f1/Oct4	Mm03053917_g1
RSPO1	Hs00543475_m1
Rspo1	Mm00507077_m1
SFRP1	Hs00610060_m1
Sfrp1	Mm00489161_m1
SFRP2	Hs00293258_m1
Sfrp2	Mm01213947_m1
Snai2	Mm00441531_m1
SOSTDC1	Hs00383602_m1
TBX18	Hs01385457_m1
Tbx18	Mm00470177_m1
THY-1	Hs00174816_m1
THY-1 (CD90)	Hs00174816_m1
Vcam1	Mm01320970_m1
Vegfa	Mm00437306_m1
VIM	Hs00174816_m1
Vim	Mm01333430_m1
WIF1	Hs00183662_m1
Wif1	Mm00442355_m1
WNT2B	Hs00921614_m1
Wnt2b	Mm00437330_m1
WNT7A	Hs01114990_m1
Wnt7a	Mm00437356_m1

2.4   siRNAs

All siRNAs were obtained from Dharmacon, Lafayette, CO, USA.

FZD7	SMARTpool: siGENOME FZD7 siRNA
LGR5	SMARTpool: siGENOME LGR5 siRNA
Non-Targeting	siGENOME Non-Targeting siRNA #1
RSPO1	SMARTpool: siGENOME RSPO1 siRNA
WNT7A	SMARTpool: siGENOME WNT7A siRNA

2.5   Overexpression plasmids

All overexpression plasmids were obtained from OriGene Technologies, Inc., Rockville, MD, USA.

Control	pCMV6-Entry, mammalian vector with C-terminal Myc- DDK Tag
FZD7	(Myc-DDK-tagged)-Human frizzled family receptor 7
LGR5	(Myc-DDK-tagged)-Human leucine-rich repeat containing G protein-coupled receptor 5

2.6   Antibodies

ACE	LSC105463, Genxbio, Shakarpur, India
Anti-Mouse (GaM)-FITC	1010-02, SouthernBiotech, Birmingham, AL, USA
anti-Mouse Secondary Antibody	Peggy Sue/Sally SueMaster Kit, ProteinSimple; San Jose, USA
Anti-Rabbit (GaR)-PE	Cat.: 4050-09S, SouthernBiotech, Birmingham, AL, USA
Biotin-FITC	130-090-857, Milteny Biotec, Bergisch Gladbach, Germany
CACN1A-Biotin	ABIN751305, Antibodies-online, Aachen, Germany
CACN1A-PE	ABIN751313, Antibodies-online, Aachen, Germany
CD10-PE	130-099-669, Miltenyi Biotec, Bergisch Gladbach, Germany
CD13-Biotin	ab25723, Abcam, Cambridge, UK
CD140B-Biotin (Mouse)	130-096-272, Miltenyi Biotec, Bergisch Gladbach, Germany
CD140B-PE	323605, BioLegend, San Diego, CA, USA
CD166-PE	12-1668-41, Affymetrix eBioscience, Santa Clara, CA, USA
CD248-Biotin	ABIN677575, antibodies-online; Aachen, Germany
CD34-PE	130-098-140, Miltenyi Biotec, Bergisch Gladbach, Germany
CD36-PE	130-100-149, Miltenyi Biotec, Bergisch Gladbach, Germany
CD45	Clones 2B11 + PD7/26, DAKO, Jena, Germany
CD74-FITC	11-0748, Affymetrix eBioscience, Santa Clara, CA, USA
CD90-PE	130-097-932, Miltenyi Biotec, Bergisch Gladbach, Germany
CD9-Biotin	13-0098-80, Affymetrix eBioscience, Santa Clara, CA, USA
CD9-FITC	ab18241, Abcam, Cambridge, UK
CLDN3-FITC	FAB4620F, R&D Systems GmbH, Wiesbaden, Germany
Cytokeratin	orb43708, Biorbyt, Cambridge, UK
E-Cadherin-Biotin	13-3249, Affymetrix eBioscience, Santa Clara, CA, USA
EpCAM-FITC	130-098-113, Miltenyi Biotec, Bergisch Gladbach, Germany
FAP	ab28244, Abcam, Cambridge, UK
Flex Negative Control Mouse Cocktail of mouse IgG1, IgG2A, IgG2B, IgG3 and IgM	DAKO, Jena, Germany
FZD7	ARP41251_P050, Aviva Systems Biology, San Diego, CA, USA
Gapdh	NB300-221, Novus Biologicals, Littleton, CO, USA

IC IgG1-FITC	400137, BioLegend, San Diego, CA, USA
IC IgG1-PE	12-4714-81, Affymetrix eBioscience, Santa Clara, CA, USA
IC IgG2A-Biotin	ab97679, Abcam, Cambridge, UK
KI67	M7240, DAKO, Jena, Germany
LGR5	Tier 2, monospezifischer IgG, Eva Simon [215]
MUC-1-FITC	559774, BD Biosciences, San Jose, USA
RSPO1	HPA046154, Sigma, Sigma Aldrich Corp., St. Louis, MO, USA
Streptavidin-PE	7100-09M, SouthernBiotech, Birmingham, AL, USA
TICAM2	ab77169, Abcam, Cambridge, UK
TMEM87A	MAB7966, R&D Systems GmbH, Wiesbaden, Germany
TMEM97	ab126490, Abcam, Cambridge, UK
TMEM9B	ab122414, Abcam, Cambridge, UK
Vimentin	orb98455, IgG1, Biorbyt, Cambridge, UK
WNT2B	ab178418, Abcam, Cambridge, UK
WNT7A	PA5-28289, Thermo Scientific Pierce Antibodies, Braunschweig, Germany
β-catenin	610153, BD Bioscience, San Jose, USA

2.7 Recombinant proteins

Recombinant human RSPO1 (4645-RS-025)	R&D Systems GmbH, Wiesbaden, Germany
Recombinant human WNT3A (5036-WN/CF)	R&D Systems GmbH, Wiesbaden, Germany
Recombinant human WNT7A (3008-WN-025)	R&D Systems GmbH, Wiesbaden, Germany
Recombinant mouse WNT2B (3900-WN-025)	Hölzel Diagnostika, Cologne, Germany

2.8 Cell culture media and supplements

DMEM + 4,5 g/l Glucose	Gibco, Carlsbad, CA, USA
DMEM/F-12 + GlutaMAX™	Gibco, Carlsbad, CA, USA
GlutaMAX™, 100 x	Gibco, Carlsbad, CA, USA
Heat Inactivated Fetal Bovine Serum	Gibco, Carlsbad, CA, USA
Human Insulin	Biochrom, Berlin, Germany
L-Glutamine, 100 x	Gibco, Carlsbad, CA, USA
McCoy's 5A	Gibco, Carlsbad, CA, USA
MEM	PAA Laboratories GmbH, Coelbe, Germany
Non-Essential Amino Acids	PAA Laboratories GmbH, Coelbe, Germany
Opti-MEM™	Gibco, Carlsbad, CA, USA
Penicillin/Streptomycin, 100 x	Gibco, Carlsbad, CA, USA
TrypLE™ Express	Gibco, Carlsbad, CA, USA

2.9   Consumables

5 ml Polypropylene Round-Bottom Tubes (FACS)	BD Biosciences, San Jose, USA
Bio-Bottle™	bio-bottle New Zealand Ltd, Auckland, New Zealand
Biosphere® Filter Tips, 10 µl, 20 µl, 200 µl, 1000 µl	Sarstedt, Numbrecht, Germany
Caps for glas vials, 13 mm	WICOM Germany GmbH, Heppenheim, Germany
CoolPack mini	Coolike-Regnery GmbH, Bensheim, Germany
Costar® Stripette	Corning®, New, York, USA
Countess® Cell Counting Chamber Slides	Thermo Fisher Scientific, Braunschweig, Germany
Coverslips	Menzel-Glaeser, Braunschweig, Germany
Coverslips	Menzel-Glaeser, Braunschweig, Germany
Cryo Tubes®	Thermo Fisher Scientific, Braunschweig, Germany
Cytofunnel™	Shandon, Braunschweig, Germany
Cytospin Filter Crad	Shandon, Braunschweig, Germany
Falcon® Centrifuge Tubes 15 and 50 ml	Corning®, New, York, USA
gentleMACS C Tubes	Miltenyi Biotec, Bergisch Gladbach, Germany
Glas vials, 4 ml	WICOM Germany GmbH, Heppenheim, Germany
HTS FluoroBlok™ Multiwell Insert System, 24 and 96 well, 3 µm	Corning®, New, York, USA
Invitrolon™ PVDF	Life Technologies, Carlsbad, CA, USA
Matrix Tips 30 µl and 125 µl	Thermo Fisher Scientific, Braunschweig, Germany
Micro Amp® Optical 384-Well Reaction Plate with Barcode	Applied Biosystems, Foster City, CA, USA
Micro Amp™ Optical Adhesive Film	Thermo Fisher Scientific; Braunschweig, Germany
Microplates for Life Science Research, 96 well	PerkinElmer™, Waltham, MA, USA
Needle 100 Sterican® GR	B. Braun, Melsungen, Germany
Nunc MaxiSorp® 96 well plate	Affymetrix eBioscience, Santa Clara, CA, USA
PCR Tube Strips 0.2 ml	Eppendorf AG, Hamburg, Germany
Precellys Lysing Kit CK14_0.5 ml	Bertin Corp., Rockville, MD, USA
Pre-sparation Filters 70 µm	Miltenyi Biotec, Bergisch Gladbach, Germany
Reaction tubes 0.5, 1.5 and 2 ml	Eppendorf AG, Hamburg, Germany
RNA Nano Chips	Agilent Technologies Inc., Santa Clara, USA
RNA Pico Chips	Agilent Technologies Inc., Santa Clara, USA
Rotor Adapters	Qiagen, Hilden, Germany
Single Use Syringes, 1 ml	Codan, Lensahn, Germany
Slides Super Frost Color	Menzel-Glaeser, Braunschweig, Germany
S-Monovette®	Sarstedt, Numbrecht, Germany

Sterican® Needle, 18G x 1 1/2	B. Braun, Melsungen, Germany
Syringe Omnifix® ml	B. Braun, Melsungen, Germany
T25-, T75- and T162 Flasks	Corning®, New, York, USA
VWR® Disposable Pipetting Reservoirs	VWR International, Darmstadt, Germany

2.10   Devices

Matrix Pipette,30 µl and 125 µl	Thermo Fisher Scientific, Braunschweig, Germany
2100 Bioanalyzer	Agilent Technologies Inc., Santa Clara, USA
7900 HT Fast Real-Time PCR System	Life Technologies, Carlsbad, CA, USA
-80°C Freezer	Heraeus, Cologne, Germany
8-Channel Multi-Pipette, 100 µl	Eppendorf, Hamburg, Germany
Automated cell counter Countess™	Invitrogen GmbH, Darmstadt; Germany
Automated nucleic acid purificator QIAcube	Qiagen, Hilden, Germany
Binocular Stemi 2000-C	Zeiss, Oberkochen, Germany
Camera Power Shot A640	Canon, Tokio, Japan
Cell sorter BD FACS Aria™ IIu	BD Biosciences, San Jose, USA
Centrifuge Biofuge Fresco	Heraeus, Cologne, Germany
Centrifuge Galaxy Mini	VWR International, Darmstadt, Germany
Centrifuge Megafuge 1.0	Thermo Fisher Scientific, Braunschweig, Germany
Centrifuge Multifuge 3SR+	Thermo Fisher Scientific, Braunschweig, Germany
Clean Bench Hera Safe	Life Technologies, Carlsbad, CA, USA
Coverslipper workstation Leica CV5030	Leica, Wetzlar, Germany
Cycler T-Gradient	Biometra, Goettingen, Germany
Cytospin III Cytocentrifuge	Shandon, Braunschweig, Germany
FACS Aria II	BD Biosciences, San Jose, USA
Fluorescence microscope Olympus BH-2	Olympus, Tokio, Japan
Fluorescence/lumiescence reader POLARstar Omega BMG	Labtech International Ltd., East Sussex, UK
Freezer	Liebherr, Bulle, Germany
Fridge	Liebherr, Bulle, Germany
Gentle MACS Dissociator	Miltenyi Biotec, Bergisch Gladbach, Germany
Glass chamber	Assistenti
Hermetically sealed chamber	Santo Plastic, Hongkong, China
Incubator HERAcell 240i	Thermo Fisher Scientific, Braunschweig, Germany
Micro Centrifuge	Thermo Fisher Scientific, Braunschweig, Germany
Microplate reader POLARstar Omega	BMG Labtech, Ortenberg, Germany
Microscope Primo Vert	Zeiss, Oberkochen, Germany
Microwave	Bosch, Stuttgart, Germany
Mini Rocker-Shaker PR-30	Grant bio, Essex, UK
NanoDrop® 8 Sample Spectrophotometer ND-8000	Thermo Fisher Scientific, Braunschweig, Germany

Peggy Sue™	ProteinSimple, San Jose, USA
Pipettes, 10 µl, 20 µl, 200 µl and 1000 µl	Eppendorf, Hamburg, Germany
Pipettus	Integra Bioscience, Biebertal, Germany
Precellys 24	Peqlab Biotechnology GmbH, Erlangen, Germany
Roller Mixer SRT1	Stuart Scientific, Staffordshire, UK
Shaker THERMOstar	BMG Labtech, Ortenberg, Germany
Slide clamps	Shandon, Braunschweig, Germany
Slide scanner Mirax Midi	Zeiss, Oberkochen, Germany
ULTRA-TURRAX®	Sigma Aldrich Corp., St. Louis, MO, USA
Vortex Genie2	Scientific Industries, Inc., New York, USA

2.11 Software

2100 Expert Software, Bioanalyzer	Agilent Technologies Inc., Santa Clara, USA
BD FACSDiva Software v.8	BD Biosciences, San Jose, USA
Compass V. 2.7.1	ProteinSimple, San Jose, USA
Control Program for BMG LABTECH Omega Readers, Fluorescence Reader	BMG Labtech, Ortenberg, Germany
EndNote X7	Microsoft, Redmond, WA, USA
Excel 2010	Microsoft, Redmond, WA, USA
Ingenuity Pathway Analysis	Qiagen, Hilden, Germany
ND-8000 V2.1.0, Nanodrop	Thermo Fisher Scientific, Braunschweig, Germany
POLARstar Omega, Fluorescence Reader	BMG Labtech, Ortenberg, Germany
PowerPoint	Microsoft, Redmond, WA, USA
Prism 6	GraphPad Software, Inc., La Jolla, CA, USA
RQ Manager 1.2.1, TaqMan	Applied Biosystems, Foster City, CA, USA
SDS 2.4, TaqMan	Applied Biosystems, Foster City, CA, USA
Word 2010	Microsoft, Redmond, WA, USA
Zeiss AxioVision 40 V4.6.3.0, Microscope	Zeiss, Oberkochen, Germany

3 METHODS

3.1 Patient characteristics and sample acquisition

All patients offering samples for the different studies were pseudonymized and analyzed anonymously, so no individual-related data are contained in the database.

In general, premenopausal women undergoing diagnostic or therapeutic laparoscopy because of suspected endometriosis, pelvic pain of unknown origin, benign adnexal masses or leiomyoma uteri were included in these studies. Only subjects between 18 and 50 years of age, who gave written, informed consent, were included. Known infectious or chronic autoimmune diseases, perioperative hormonal or anti-hormonal treatment, and preexisting malignant diseases were defined as exclusion criteria.

3.1.1 TaqMan Arrays

For the TaqMan analyses, patients were recruited by the Department of Gynecology and Obstetrics at the University Hospital in Vienna from 2010 – 2012. Approval for this study was obtained from the institutional ethics committee of the Medical University of Vienna (EK 545/2010) and it was supported by Bayer Pharma AG. All samples were received as fresh frozen sample blocks.

Eutopic endometrial tissue was obtained by curettages from 21 reproductive-aged women. They were subdivided into two groups by the presence (patients; n = 12) or absence (healthy controls; n = 9) of ectopic endometrial tissue in the peritoneal cavity (table 2). Ectopic peritoneal lesions were resected during surgery and diagnosed by a trained pathologist. Eutopic endometrial samples were assigned to the proliferative or the secretory cycle by histological examination (table 2).

Table 2: Patient characteristics for TaqMan analyses.

	No endometriosis			Endometriosis		
	Total	Prolifera-tive	Secretory	Total	Prolifera-tive	Secretory
Number (n) of patients	9	5	4	12	5	7
Mean age (range)	36.1 (27 – 49)	35.6 (27 – 49)	36.8 (32 – 44)	34.0 (25 – 46)	33.0 (25 – 38)	34.7 (28 – 46)
Mean height (range), cm	165.1 (155 – 180)	165.2 (158 – 180)	165.0 (155 – 177)	170.7 (164 – 178)	171.6 (166 – 175)	170.0 (164 – 178)
Mean weight (range), kg	79.8 (58 – 111)	88.0 (70 – 111)	69.5 (58 – 86)	61.4 (50 – 77)	64.8 (57 – 77)	59.0 (50 – 68)
Mean BMI (range), kg/m2	29.3 (20 – 35)	32.1 (28 – 34)	25.8 (20 – 35)	21.1 (18 – 26)	22.1 (19 – 26)	20.4 (18 – 24)
Mean gravity (range)	1.5 (0 – 4)	2.4 (0 – 4)	0.0 (0 – 0)	0.5 (0 – 2)	0.0	0.7 (0 – 2)
Mean ASRM stage (range)	0.0	0.0	0.0	2.5 (1 – 4)	2.8 (1 – 4)	2.3 (1 – 3)
Mean parity (range)	2.0 (0 – 3)	2.0 (0 – 3)	0.0	0.0	0.0	0.0

3.1.2   Fluorescence-activated cell sorting (FACS)

For FACS, patients were recruited by the Department of Gynecology and Obstetrics at the Vivantes Humboldt Hospital in Berlin from 2014 – 2015. The local ethics committee Ärztekammer Berlin (Eth-02/14) gave approval for this study. All samples were received as fresh tissue samples.

Eutopic endometrium was derived from curettages from 10 reproductive-aged women. They were subdivided into two groups by the presence (patients; n = 8) or absence (healthy controls; n = 2) of ectopic endometrial tissue in the peritoneal cavity (table 3). Eutopic endometrial samples were dedicated to the proliferative or the secretory cycle based on a histological assessment by an expert (table 3).

Table 3: Patient characteristics for FACS.

	No endometriosis			Endometriosis		
	Total	**Prolifera-tive**	**Secretory**	**Total**	**Prolifera-tive**	**Secretory**
Number (n) of patients	2.0	1.0	1.0	8.0	6.0	2.0
Mean age (range)	44.0 (44 – 44)	44.0	44.0	31.8 (28 – 40)	31.8 (28 – 40)	33.0 (31 – 35)
Mean height (range), cm	157.0 (154 – 160)	154.0	160.0	165.3 (154 – 170)	166.8 (162 – 170)	159.5 (159 – 160)
Mean weight (range), kg	53.5 (47 – 60)	47.0	60.0	62.8 (52 – 98)	59.5 (52 – 73)	77.0 (56 – 98)
Mean gravity (range)	1.5 (1 – 2)	2.0	1.0	2.2 (0 – 5)	2.3 (0 – 6)	2.5 (0 – 5)

3.1.3   Immunohistochemistry

All tissue samples were obtained as tissue slides from Provitro GmbH (Berlin) originating from patients between 26 and 49 years of age.

Eutopic endometrium obtained from resectates from 35 reproductive-aged women (table 4). They were subdivided into two groups by the presence (patients eutopic; n = 13) or absence (healthy controls; n = 22) of ectopic endometrial tissue in the peritoneal cavity. Ectopic peritoneal lesions (patients ectopic; n = 12) were resected during laparoscopy and examined by a trained pathologist. Eutopic endometrial samples were assigned to the proliferative or the secretory cycle phase resulting from a histological examination by a pathologist.

Table 4: Patient characteristics for immunohistochemistry.

	No endometriosis			Endometriosis		
	Total	**Proliferative**	**Secretory**	**Total**	**Proliferative**	**Secretory**
Number (n) of patients	22.0	12.0	10.0	25.0	11.0	14.0
Mean age (range)	38.0 (29 – 49)	39.5 (33 – 49)	36.9 (29 – 44)	36.2 (26 – 47)	36.0 (26 – 47)	36.4 (30 – 47)

3.2 Molecular biological methods

3.2.1 Immunohistochemistry

Immunohistochemical staining

Double immunostaining was carried out with antibodies against CD45, FZD7, KI67, RSPO1, WNT2B and WNT7A, whereas anti-CD45 always served as the second primary antibody (table 5).

For deparaffinization, sections were incubated in xylene two times for 5 minutes each. Rehydration of sections was done by incubation in a descending ethanol gradient: absolute ethanol (two times for 2 minutes each) and 96 % and 70 % ethanol (one time for 2 minutes each). If necessary, sections were cooked in the microwave at 900 W for 2.5 minutes and 180 W for 10 minutes in 1 X Target Retrieval Solution (DAKO). Before proceeding to the next step, sections were cooled down to room temperature (RT) and washed 3 times in Tris-buffered saline with Tween20 (TBST, Fisher Scientific) for 5 minutes each. Subsequently, blocking with Dual Endogenous Enzyme Block (DAKO) for 10 minutes, threefold wash in TBST for 5 minutes each and 5 minutes treatment with Protein Block (DAKO) followed. All antibodies were diluted in DAKO Real™Antibody Diluent (table 5). The incubation with the primary antibody was performed in a moist chamber at 4 °C overnight. The next day, slides were washed 3 times with TBST for 5 minutes each followed by the incubation of the ready-to-use polymer labelled secondary antibodies EnVision + System-HRP labelled Polymer Anti-Rabbit or Anti-Mouse (DAKO) for 30 minutes at RT in a moist chamber. Immunoreactions were visualized with DAB Peroxidase Substrate Kit (Vector) according to the manufacturer's instructions for 5 – 10 minutes at RT followed by 3 washing steps with TBST for 5 minutes each. For double staining of antibodies both originating from mice, the free binding sites of the polymers had to be blocked previous to staining of the second primary antibody (anti-CD45) by incubating the slides with Flex Negative Control Mouse Cocktail (DAKO) for 20 minutes at RT in the moisture chamber. Afterwards, anti-CD45 antibody was added to the samples for 1 hour at RT in the moisture chamber with subsequent 3 washing steps with TBST for 5 minutes each. The secondary ready-to-use polymer-linked antibody ZytoChem Plus AP Polymer anti-Mouse (Zytochem Systems) was incubated for 30 minutes at RT in the moisture chamber and the visualization of the immunoreactions was performed with the Permanent AP Red Kit (Zytomed Systems) following the manufacturer's protocol. Omission of the primary antibody served as negative controls.

The specimens were counterstained with hematoxylin (diluted 1:2 in destilled water, DAKO) for 30 seconds following blueing under running tab water for 3 minutes. Afterwards, slides

were dehydrated via an ascending alcohol series through 30 seconds 70 %, 96 %, and 2 x 100 % ethanol each terminated with 2 x xylene for 2 minutes each. Finally, the tissue sections were covered with Eukitt® quick-hardening mounting medium (O. Kindler) and cover slips.

Table 5: Antibodies used for immunohistochemical staining.

Antigens (primary antibodies)	Dilution	Treatment	Secondary antibodies	Chomogen
CD45 (DAKO)	1:400		ZytoChem AP Polymer anti-Mouse	Permanent AP Red
FZD7 (Aviva Systems Biology)	1:100	Microwave	EnVision HRP labelled Polymer Anti-Rabbit	DAB
				DAB
RSPO1 (Sigma)	1:20			DAB
WNT2B (Abcam)	1:100			DAB
WNT7A (Thermo Scientific)	1:500			DAB
KI67 (DAKO)	1:75	Microwave	EnVision HRP labelled Polymer Anti-Mouse	DAB

Evaluation of immunohistochemical stainings

Immunostaining of eutopic and ectopic endometrial tissue were evaluated by a trained pathologist. Scoring was applied using a semiquantitative scoring system. Briefly, immunoreactivity of the glandular and stromal endometrial compartments was displayed as percentage of immunoreactive cells. Staining pattern and intensity were very inhomogeneous. Therefore, immunohistology was disregarded.

3.2.2   FACS of fresh tissue samples

Tissue dissociation

Curettages from patients were obtained as fresh tissue and transported in Celsior® organ storage solution (Genzyme) in 50 mL falcon tubes. The tissue was removed from the solution and cut into 1 mm pieces and dissociated with the Human Tumor Dissociation kit (Miltenyi Biotec) on the GentleMACS® Dissociator (Miltenyi Biotec) with several incubation steps at 37°C according to the manufacturer's protocol. The final single cell suspension was filtered through a 70 µm pre-separation filter. After centrifugation at 300 rpm for 5 minutes, the pellet was resuspended in 5-7 ml RPMI medium (Gibco), counted, and prepared for FACS.

Antibody staining

Previously, all falcon tubes and FACS sorting tubes were blocked with fetal calf serum (FCS; Gibco) at RT for several minutes.

Depending on the cell number $1 \times 10^6 - 1 \times 10^7$ viable cells from the cell suspension were stained with fluorescently labelled antibodies for FACS. During the establishment of the procedure various antibodies for staining of stromal and epithelial cells were used according to table 6 following the manufacturer's declarations. About 1×10^6 viable cells were either stained with an epithelial specific antibody or with a stromal specific antibody according to the protocol below. For selected antibodies of the most promising potential epithelial and stromal markers, isotype controls (IC) were performed to examine unspecific binding. They represented antibodies of the same isotype originating from the same species in combination with the same secondary antibody (table 7). ICs were commercially available and CD140B-Biotin (Mouse) is an antibody which only binds murine antigens and therefore also serves as an appropriate IC for antigens of human origin.

Later on anti-CD90 (Miltenyi Biotec) was used for sorting of stromal cells and anti-EpCAM (Miltenyi Biotec) for epithelial cells.

The fluorescence intensity originating from every antibody bound to its antigen was normalized against its background fluorescence using a sample lacking antibodies. The resulting normalized fluorescence intensity gave information about the binding efficiency of the different antibodies.

Table 6: Application of the different antibodies for the FACS sorting following the manufacturer's instructions.

Antigens 1 (primary antibodies)	Application	Antigens 2 (secondary antibodies)	Application
ACE (Genxbio)	3 µl	**Anti-mouse (GaM)-FITC** (SouthernBiotech)	1 µg
CACNA1A-Biotin (Antibodies-online)	1 µg	**Anti-rabbit (GaR)-PE** (SouthernBiotech)	0.5 µg
CACNA1A-PE (Antibodies-online)	1 µg	**Biotin-FITC** (Miltenyi Biotec)	10 µl
CD10-PE (Miltenyi Biotec)	10 µl	**Streptavidin-PE** (SouthernBiotech)	0.5 µg
CD13-Biotin (Abcam)	1 µg	*Isotype controls*	*Application*
CD140B-PE (BioLegend)	5 µl	**IC IgG1-FITC** (BioLegend)	1 µg
CD166-PE (eBioscience)	0.1 µg	**CD140B-Biotin** (Mouse; Miltenyi Biotec)	10 µl
CD248-Biotin (Antibodies-online)	1 µg	**IC IgG1-PE IC** (eBioscience)	1 µg

CD34-PE (Miltenyi Biotec)	10 µl	**IC IgG2A-Biotin IC** (Abcam)	1 µg
CD36-PE (Miltenyi Biotec)	10 µl		
CD74-FITC (eBioscience)	0.125 µg		
CD90-PE (Miltenyi Biotec)	10 µl		
CD9-Biotin (eBioscience)	0.5 µg		
CD9-FITC (Abcam)	20 µl		
CLDN3-FITC (R&D Systems)	10 µl		
E-Cadherin-Biotin (eBioscience)	0.25 µg		
EpCAM-FITC (Miltenyi Biotec)	10 µl		
FAP (Abcam)	2 µg		
MUC-1-FITC (BD Bioscience)	20 µl		
TICAM2 (Abcam)	1 µg		
TMEM87A (R&D Systems)	2.25 µg		
TMEM97 (Abcam)	0.05 µg		
TMEM9B (Abcam)	0.25 µg		

Table 7: Antibodies with their appropriate isotype control (IC) combinations.

Antigens (antibody)	*Isotype Control (IC)*
EpCAM-FITC	IC IgG1-FITC
MUC-1-FITC	IC IgG1-FITC
CD9-FITC	IC IgG1-FITC
CD9 + Biotin-FITC	CD140B (Mouse)+ Biotin-FITC
CD90-PE	IC IgG1-PE IC
CD10-PE	IC IgG1-PE IC
CD13 + Strep-PE	IC IgG2A + Strep-PE

Firstly, the cells were centrifuged at 300 rpm for 5 minutes to remove RMPI medium. Subsequently, the pellet was resuspended in 100 µl FACS buffer and stained with 10 µl anti-CD90-PE (or other potential stromal or epithelial markers) for stromal cells with an incubation time of 15 minutes on ice. Then 500 µl FACS buffer was added and a washing step with centrifugation for 5 minutes at 300 rpm followed. After the supernatant was discarded, the pellet was resuspended in 100 µl fresh FACS buffer and staining of epithelial cells via the addition of 10 µl anti-EpCAM-FITC antibody and the incubation on ice for 15 minutes was performed. Afterwards, 1 µg/ml DAPI (Thermo Fisher Scientific) was added to the cell suspension and a final washing step with 500 µl FACS buffer with a subsequent centrifugation step followed. According to the cell number, the pellets were resuspended in 1

– 2 ml fresh FACS buffer and transferred to FACS tubes after the supernatant was removed and the samples were ready for FACS.

FACS

For setup of the FACS Aria II (BD Bioscience) instrument, Accudrop Beads (BD Bioscience) were used to adjust the drop drive and drop delay. BD™ CompBeads Anti-Mouse Ig K and BD™ CompBeads Negative Control (BD Bioscience) helped to calibrate the sorter and to set the gates. Filter 1 was used to capture very small cells and 1 X PBS in FACS Flow™ (BD Bioscience) served as sheath buffer. Gate P1 of forward scatter (FSC) and sideward scatter (SSC) separated intact cells of desired size from cell debris. P2 from FSC-Width (FSC-W) versus FSC-Height (FSC-H) and P3 from SSC-Width (SSC-W) versus SSC-Hight (SSC-H) filtered single cells from duplets and triplets. P4 eliminated dead DAPI-positive cells. Epithelial and stromal cells were sorted through gate P5 [Fluorescein isothiocyanate (FITC)-positive epithelial cells] and P6 [Phycoerythrin (PE)-positive stromal cells] into 500 µl RLT buffer (Qiagen).

The laser settings were adjusted according to table 8 and the gating strategy is depicted in figure 8.

Table 8: Laser settings used for FACS sorting.

Laser	Voltage Sort [V]
FSC	0-30
SSC	408
FITC	520
PE	400
DAPI	330
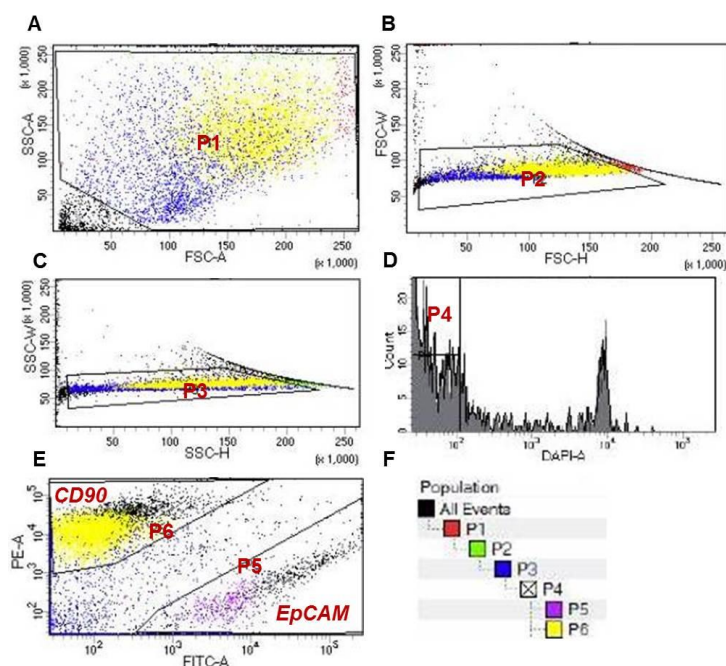
Figure 8: Sorting strategy used for sorting of epithelial and stromal cells. (A): Gate P1 for separating intact cells from cell debris through FSC versus SSC. **(B)** and **(C)**: Gate P2 and P3 for filtering single cells through gates FSC-W against FSC-H and SSC-W against SSC-H. **(D)**: Gate P4 for removing dead DAPI-positive cells. **(E)**: Gate P5 and P6 for sorting FITC-positive epithelial and PE-positive stromal cells. **(F)**: Population hierarchy scheme.

3.2.3   RNA isolation

For every 100 µl sorted cell suspension, 250 µl of RLT buffer (Qiagen) and 250 µl of 100 % EtOH were added to the sample and the RNA was isolated using the RNeasy® Micro Kit (Qiagen) according to the manufacturer's manual. RNA quality and quantity were examined with RNA Pico Chips and appropriate kits (Agilent Technologies) on the 2100 Bioanalyzer instrument (Agilent Technologies) following the manufacturer's protocol.

For the RNA isolation of samples obtained from cell culture and depending on the cell amount, the RNeasy® Mini or RNeasy® Micro kit (Qiagen) were used respective the manufacturer's instructions. RNA quality and quantity were examined by the NanoDrop® Spectrophotometer (Thermo Fisher Scientific).

For isolation of RNA from *ex vivo* samples, tissue was homogenated in precellys vials (Bertin Corp.). Uteri were chopped and homogenated in 600 µl RLT buffer with the Precellys 24 instrument (Peqlab Biotechnology GmbH) prior to the storage at -80°C. Up to two lesions were directly frozen in 400 µl RLT buffer at -80°C and homogenated after storage. Afterwards, RNA was isolated with the help of the RNeasy® Mini kit according to the manufacturer's protocol. RNA quality and quantity was evaluated using the NanoDrop® Spectrophotometer.

3.2.4   Preamplification and cDNA synthesis

Prior to TaqMan analyses and depending on the RNA concentration, 300 – 0.1 ng of RNA from sorted cells were preamplified and converted to cDNA with the Ovation® PicoSL WTA Systems V2 kit (NuGen) according to the manufacturer's instructions. The sample quality and quantity was assesed using the NanoDrop® Spectrophotometer.

Preamplified cDNA was subsequently cleaned up with the MinElute Reaction Cleanup Kit (Qiagen) according to the manufacturer's protocol. Quality and quantity of cDNA was assessed with the NanoDrop® Spectrophotometer.

If RNA was not obtained from sorted samples, preamplification was not necessary. In this case and depending on the RNA concentration, 1 – 0.2 µg cDNA was synthezised with the help of the SuperScript® Vilo™ kit (Invitrogen) respective the manufacturer's protocol.

3.2.5   Quantitative real time polymerase chain reaction (qRT-PCR)

Quantitative real time (qRT) PCR reactions were performed using the TaqMan technology as described elsewhere [216]. The entire TaqMan equipment including the probes was obtained from Thermo Fisher Scientific. For single TaqMan assays or standard TaqMan arrays the 2X

Universal PCR Master Mix was used according to tables 9 and 10. All TaqMan primer probes are listed in chapter 2.3. For single assays and depending on the amount of cDNA, 10 – 50 ng per reaction and for the TaqMan arrays, 10-20 ng of cDNA per reaction was used. All arrays and assays ran on the ABI Prism 7900 HT (Life Technologies) instrument. The master mix conditions for single TaqMan assays and TaqMan arrays and the cycler settings are listed in tables 11 and 12. All samples ran as triplicates.

Table 9: Master mix conditions for single TaqMan reactions.

Reagent	Volume
2X Universal PCR Master Mix	5.5 µl
Primer probes	0.5 µl
cDNA (10 - 50 ng)	x µl
DEPC-Water	to 12 µl

Table 10: Master mix conditions per port for the TaqMan arrays.

Reagent	Volume
2X Universal PCR Master Mix	55 µl
cDNA (20 - 30 ng)	x µl
DEPC-Water	to 110 µl

Table 11: Thermal cycler settings for single TaqMan reactions.

Step	Temperature [°C]	Time [min:sec]	Repetitions
1	50	2:00	0
2	95	10:00	0
3	95	0:15	39
4	60	1:00	0

Table 12: Thermal cycler settings for TaqMan arrays.

Step	Temperature [°C]	Time [min:sec]	Repetitions
1	50	2	0
2	94.5	10:00	0
2	97	0:30	39
3	59.7	1:00	0

The relative mRNA content was normalized to glyderaldehyde-3-phosphate dehydrogenase (GAPDH) mRNA expression in human samples and to eukaryotic 18s rRNA mRNA expression in murine samples. Probes labelled with Mm detected murine genes and probes with Hs detected human genes (chaper 2.3). Using the $2^{-\Delta\Delta CT}$ method described by Livak et al. in 2001, the normalization of the mRNA expression of the gene of interest (GOI) with the house keeping genes (HKG) generated the ΔCT [217]. After $2^{-\Delta CT}$ transformation the relative gene expression of the GOI in comparison to the HKG could be obtained. For evaluating mRNA expression differences between treatment and control samples, the ΔΔCT had to be

calculated by subtracting the ΔCT of the control sample from the ΔCT of the treated samples followed by the $2^{-\Delta\Delta CT}$ transformation. By the calculation of $[(2^{-\Delta CT}$ or $2^{-\Delta\Delta CT}) – 1]$ x 100, the fold change or percentage change of mRNA expression could be evaluated.

The calculations for analyzing qRT-PCR results are listed in table 13.

Table 13: Calculation steps for analyzing qRT-PCR results.

Formulas
ΔCT = CT of gene of interest (GOI) – CT of house keeping gene (HKG)
$2^{-\Delta CT}$ = mRNA expression of GOI in comparison with HKG
ΔΔCT = ΔCT Treatment – ΔCT Control
$2^{-\Delta\Delta CT}$ = difference of mRNA expression treatment vs. control
$[(2^{-\Delta CT}$ or $2^{-\Delta\Delta CT}) - 1]$ x 100= Fold change/percentage change mRNA expression

3.2.6 Western blot analysis by Peggy Sue

Protein isolation and quantification

Ex vivo samples from the mouse experiment were stored in precellys vials at -80°C. After thawing of the samples, uterus fragments were homogenated in 250 µl and lesions in 100 µl RIPA buffer (Thermo Fisher Scientific) supplemented with protease inhibitor (Roche) (1 tablet in 7 ml buffer) using the Precellys 24 instrument for 30 seconds at 5200 rpm. Afterwards, the samples were centrifuged at 15,000 x g for 20 minutes at 4°C. The clear supernatant containing the solubilized proteins was obtained and the concentration was measured with the help of an albumin (BSA - Thermo Fisher Scientific) standard curve including 100 µl of 0.8 mg/ml, 0.4 mg/ml, 0.2 mg/ml, 0.1 mg/ml, 0.05 mg/ml, and 0 mg/ml. The samples were diluted 1:10 – 1:50 in destilled water. Following the manufacturer's instructions, bicinchoinic acid (BCA) Protein Assay Reagents A and B (Thermo Fisher Scientific) were mixed 50:1 and 200 µl of the mixture were added to each well. After shaking the samples for several minutes at RT, the protein amount was measured at 532 nm and the concentration of the triplicates was quantified through the BSA standard curve.

Peggy Sue Western blotting

For Western blotting, the Peggy Sue system from PtoteinSimple was used allowing a size-based separation of proteins in capillaries in a 96-well format with subsequent immunoblotting on the same plate in an automated fashion (figure 9) as established by Nguyen et al. in 2011 [218]. All steps were performed according to the manufacturer's protocol. Therefore, the capillaries had to be prepared by loading the stacking and separation matrix followed by adding the samples into the cappillaries automatically with a concentration through the matrix. Then the separated proteins were immobilized to the capillary wall via a

proprietary, photoactivated capture chemistry. Target proteins were detected using primary antibodies against β-catenin (BD Bioscience, dilution 1:50) and Gapdh (Novus Biologicals) as a HKG control (dilution 1:50). The immunodetection was performed using undiluted HRP-conjugated anti-mouse secondary antibodies from the Peggy Sue or Sally SueMaster Kit and the appropriate chemiluminescent substrate.

The consequent chemiluminescent signal in the form of peaks was identified in the capillaries and evaluated with the Compass software from ProteinSimple (figure 9). These peaks could be also depicted as lanes virtually. The peak height of a sample represents the abundant amount of the specific protein and is quantifiable. But first of all, the peak height of the target protein had to be normalized through devision with the related peak heigh of Gapdh (HKG) from the same sample. Afterwards, the resulting quotient is comparable between the different samples and allows statements of potential protein expression differences.

$$\textit{Normalized protein expression} = \frac{\textit{Peak height of sample}}{\textit{Peak height of Gapdh (HKG)}}$$
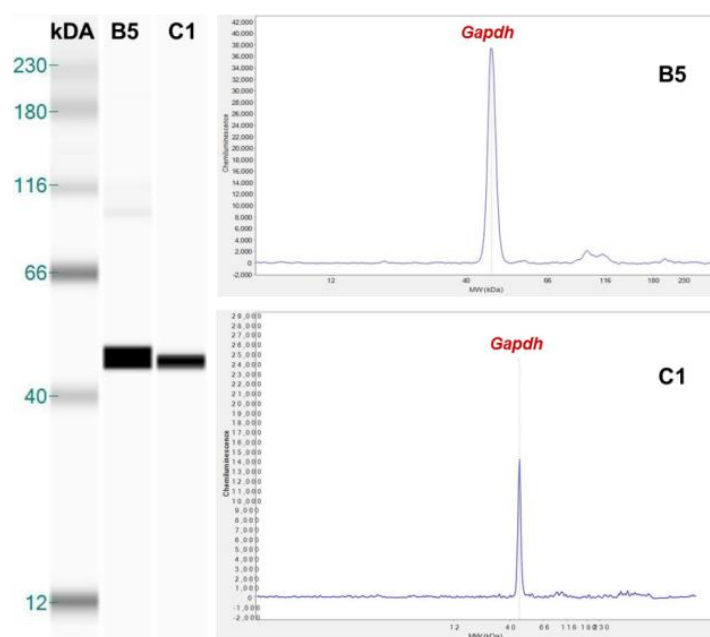

Figure 9: Chemiluminescent signals of the detected protein in the form of lanes and peaks using the Peggy Sue instrument. The height of the peaks represents the abundant amount of the specific protein and is quantifiable. After normalization of target genes with the HKG Gapdh, protein expression differences between different samples could be evaluated.

3.3   Cell culture methods

3.3.1   Cultivation of cell lines

All cell lines were of human origin and cultured at 37°C and 5 % CO_2 according to table 14. Appropriate media with respective supplements are listed in table 15. For splitting of the cells, medium was removed, cells were washed with sterile PBS (Gibco), detached with TrypLE (Gibco), and incubated at 37°C and 5 % CO_2 for several minutes. Subsequently, cells were resuspended 1:1 in appropriate pre-warmed medium with respective supplements (Gibco, Biochrome or PAA Laboratories – see chapter 2.8). After they were centrifuged at 500 x g for 5 minutes and the supernatant was removed, they were resuspended in 1 – 4 ml appropriate medium and splitted accordingly. For cell lines which were not splitted after 3 – 4 days, the culture medium was changed with a washing step using sterile PBS in between.

Table 14: Cell lines and cultivation conditions used.

Cell type	Cell line	Origin/description	Cultivation [splitting ratio]	References
Epithelial	AN3-CA	Endometrial adenocarcinoma	1:3 - 1:4 every 3 - 4 days	Dawe et al., 1964 [219]
	ECC1	Endometrial adenocarcinoma	1:3 - 1:5 every 3 - 4 days	Satyaswaroop and Tabibzadeh, 1991 [220]
	EM42	Endometrial cell line originating from benign proliferative endometrium spontaeously immortalised	1:3 - 1:4 every 3 - 4 days	Desai et al., 1994 [221]
	HEC-1-A	Endometrial adenocarcinoma	1:2 - 1:4 every 3 - 4 days	Kuramoto et al., 1972 [222]
	Ishikawa	Endometrial adenocarcinoma	1:20 - 1:30 every 5 - 7 days	Nishida et al., 1985 [223]
	KLE	Endometrial adenocarcinoma	1:2 every 3 - 4 days	Richardson et al., 1984 [224]
	RL95-2	Endometrial adenocarcinoma	1:2 - 1:4 every 3 - 4 days	Way et al., 1983 [225]
	Z11	SV40 immortalised endometrial cells originating from peritoneal lesions	1:2 every 5 - 7 days	Zeitvogel et al., 2001 [226]

	Z12	SV40 immortalised endometrial cells originating from peritoneal lesions	1:2 - 1:5 every 3 - 4 days	Zeitvogel et al., 2001 [226]
Stromal	*22B*	SV40 immortalised endometrial cells originating from peritoneal lesions	1:2 every 5 - 7 days	Zeitvogel et al., 2001 [226]
	ESC	SV40 immortalised endometrial cells	1:3 - 1:4 every 3 - 4 days	*in-house*
	MES-SA	Uterus sarcoma cells	1:2 - 1:4 every 3 - 4 days	Harker et al., 1983 [227]

Table 15: Media composition of the cell lines used.

Cell line	Media composition
22B, Z11, Z12	DMEM 1g/L Glukose w/o Phenolrot 10% FCS 1 % L-Glutamine 1 % Pen/Strep
AN3-CA	MEM 10 % FCS 1 % Pen/Strep
ECC1	DMEM + 4,5 g/L Glukose w/o Phenolrot 5 % FCS 1 % L-Glutamine 1 % Human Insulin 1 % Pen/Strep
EM42, ESC, KLE	DMEM/F-12 + GlutaMAX™ 10 % FCS 1% Pen/Strep
HEC-1-A, MES-SA	McCoy's 5A 10% FCS 1 % L-Glutamine 1 % Pen/Strep
Ishikawa	MEM 5 % FCS 1 % L-Glutamine 1 % Non-Essential Amino Acids 1 % Pen/Strep
RL95-2	DMEM/F-12 + GlutaMAX™ 1 % Human Insulin 1 % Pen/Strep

3.3.2 Freezing and thawing of cells

If necessary, cells were freezed. Therefore, with TypLE detached cells were resuspended 1:1 in appropriate medium and counted. Afterwards, they were centrifuged for 5 minutes at 500 x g, the supernatant was removed, and 1×10^6 viable cells were resuspended in 1 ml freezing medium (Gibco) and stored at -80°C. Longterm storage of cells was ensured by liquid nitrogen.

For taking cryo conserved cells back in culture, they were thawed fastest possible at 37°C and resuspended in 6 ml culture medium with a subsequent centrifugation step at 500 x g for 5 minutes to remove the freezing medium with DMSO in the supernatant. Afterwards, cells were resuspended in a T25-flask filled with about 6 ml fresh culture medium and cultivated accordingly.

3.3.3 Counting of cells

Cells were counted by using the Countess® automated cell counter (Invitrogen) which calculates the amount of viable cells per ml through trypane blue (Gibco) staining. Therefore, 10 µl of a 1: 1 mixture of cells and trypane blue was loaded to Cell Counting Chamber Slides. With the help of digital image technology, the instrument took pictures and the software was able to analyse cell number, concentration per ml, size, and viability of the cells.

3.3.4 Transfection

All cell lines were transfected via liposomes delivering nucleic acids into a cell through merging with the cell membrane [228].

Around 3×10^5 viable cells were seeded into 12-well plates filled with 1 ml appropriate medium each 24 hours prior to transfection. The cells were cultivated as described before (see chapter 3.3.1). After 24 hours the culture medium was removed, wells were washed with 1 ml sterile PBS, and 1 ml pure Opti-MEM™ (Gibco) was added. The transfection approach was prepared by using 95 µl Lipofectamine® 2000 (Life Technologies) and 5 µl pure OptiMEM™ mixture according to table 16 followed by an incubation for 10 minutes at RT. Afterwards, the transfection mixture was added to the wells and the cells were cultivated at 37°C and 5 % CO_2 for 24 hours before further use.

Table 16: Transfection mixture used for 3×10^5 viable cells per well in a 12-well plate.

Reagent	Volume
Lipofectamine® 2000	5 µl
OptiMEM™	95 µl

3.3.5   siRNA knockdown

Knockdown of target genes was achieved by siRNA (small interfering RNA) knockdown as described elsewhere [229]. Complementary single stranded siRNA attaches to mRNA preventing it from transcription by initiating its degeneration through RISC (RNA-induced silencing complex). Therefore, cells had to be transfected with 60 pmol siRNA (Dharmacon) respective table 17.

Table 17: Transfection mixture for siRNA knockdown experiments of 3 x 10^5 viable cells per well in a 12-well plate.

Reagent	Volume
Lipofectamine® 2000	5 µl
SiRNA(s) (2 µM → final 60 pmol)	30 µl
OptiMEM™	to 100 µl

After 24 hours of incubation at 37°C and 5 % CO_2, the medium was removed, cells were washed with 1 ml sterile PBS, detached with 250 µl TrypLE™ for 3 – 5 minutes at 37°C, and subsequently resuspended in 250 µl appropriate medium. They were counted and seeded in 96-well plates with 1.5 x 10^4 viable cells per well for further experiments.

Remaining cells were centrifuged at 500 x g for 5 minutes, resuspended in 350 µl RLT buffer, and stored at -80°C until RNA isolation, cDNA conversion, and qRT-PCR (see chapters 3.2.3 – 3.2.5).

SiRNA knockdown efficiency was calculated after qRT-PCR through dividing the $2^{-\Delta\Delta}$ CT of the siRNA knockdown sample through the $2^{-\Delta\Delta}$ CT of the "Non-Targeting siRNA" sample resulting in the fold change of RNA activity. The conversion [(normalized RNA activity- 1) x 100] indicates the percentage change of RNA activity.

$$\textit{Normalized RNA activity} = \frac{2^{-\Delta\Delta\,CT}\;\textit{siRNA sample}}{2^{-\Delta\Delta\,CT}\;\textit{„Non-Targeting" siRNA sample}}$$

$$\textit{Percentage change of RNA activity} = \textit{(Normalized RNA activity – 1) x 100}$$

3.3.6   mRNA overexpression (transfection of expression plasmids)

Through the transfection of expression plasmids of several WNT candidate genes their mRNA overexpression was achieved.

Therefore, cells had to be transfected with 1 µg expression plasmid (OriGene) according to table 18 and chapter 3.3.4.

Table 18: Transfection mixture for overexpression experiments of 3 x 10^5 viable cells per well in a 12-well plate.

Reagent	Volume
Lipofectamine® 2000	5 µl
Expression plasmid (1 µg)	10 µl
OptiMEM	to 100 µl

After 24 hours of incubation at 37°C and 5% CO2, the medium was removed, wells were washed with 1 ml sterile PBS, and trypzinated with TypLE at 37°C and 5 % CO_2 for several minutes. Afterwards, they were resuspended 1:1 in appropriate medium, counted, and respectively seeded in 96-well plates with 1.5 x 10^4 viable cells per well for further experiments.

Remaining cells were centrifuged at 500 x g for 5 minutes, resuspended in 350 µl RLT buffer, and stored at -80°C until RNA isolation, cDNA conversion, and qRT-PCR (see chapters 3.2.3 – 3.2.5).

Overexpression efficiency was calculated after qRT-PCR through dividing the $2^{-\Delta\Delta}$ CT of the overexpression sample through the $2^{-\Delta\Delta}$ CT of the "Empty plasmid" sample resulting in the fold change of expression activity. The conversion [(normalized expression activity - 1) x 100] indicates the percentage change of expression activity.

$$\text{Normalized expression activity} = \frac{2^{-\Delta\Delta\ CT}\ \text{overexpression sample}}{2^{-\Delta\Delta\ CT}\ \text{„Empty plasmid" sample}}$$

$$\begin{array}{l}\textbf{Percentage change} \\ \textbf{of expression activity} =\end{array} \quad \begin{array}{l}\textbf{(Normalized expression activity – 1)} \\ \textbf{x 100}\end{array}$$

3.3.7 Cytospin

T-flasks with adherent cells were washed with sterile PBS and detached with TrypLE as indicated previously. Subsequently, cells were resuspended 1:1 in appropriate pre-warmed medium and counted (see chapter 3.3.3). Cytospin elements (Shandon) were assembled (slide with Cytospin filter cards and Cytofunnel fixed with a respective clamp) and one Cytofunnel was loaded with 1 x 10^4 viable cells following centrifugation in an appropriate Cytospin cytocentrifuge (Shandon) for 5 minutes at 500 x g. Afterwards, cell spots were air-dried for 10 – 20 minutes. Subsequently, cells were fixed and permeabilized with 95 %/5 %

ethanol/acidic acid for 20 minutes at -20°C following a threefold washing step with PBS for 5 minutes each in glass chambers. The liquid was removed entirely from the slides and they were put into a hermetically sealed chamber. About 50 µl of 1:10 diluted antibodies [anti-Cytokeratin or anti-Vimentin (both from Biorbyt)] were added to the cell spots and incubated for 25 minutes with a subsequent threefold washing step with PBS for 5 minutes each in glass chambers. Finally, slides were covered with 40 µl Fluoromount (Sigma Aldrich) and a coverslip and analyzed under a fluorescent microscope.

3.4 Functional cell culture based *in vitro* assays

All functional cell culture based *in vitro* assays were performed in endometrial stromal cells (ESCs). These cells were tested for the WNT pathway and migration activity previously to ensure that they represent a suitable cell culture for these assays. Since they do not secrete WNTs naturally, the pathway had to be activated through WNT3A addition beforehand.

3.4.1 WNT activity assay

The TCF/LEF reporter assay kit (Qiagen) consists of the reporter representing a WNT responsive luciferase construct. It encodes the firefly luciferase reporter gene under the control of a minimal (m)CMV promoter and tandem repeats of the WNT specific TCF/LEF transcriptional response element (TRE) similar to the TOPflash plasmid [130]. The negative control is a construct of a non-inducible firefly luciferase gene lacking the CMV promotor and the positive control is constitutively expressing firefly luciferase [230]. If the WNT pathway is active, the WNT specific transcription factors TCF and LEF bind to TRE and activate the transcription of the luciferase reporter gene and WNT activity can be quantified through luminescence signals (figure 10).
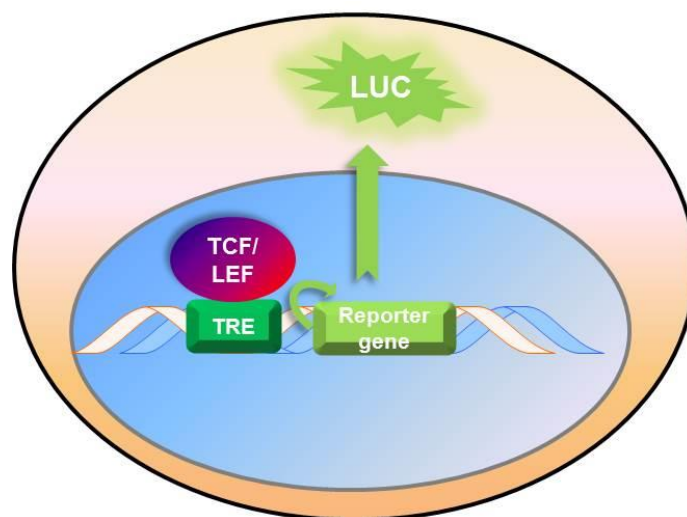
Figure 10: Principle of the TCF/LEF reporter assay measuring the WNT activity. In case of active WNT signaling, β-catenin nudges the transcription factors TCF and LEF to bind to TCF/LEF transcriptional response elements (TRE) initiating the transcription of the luciferase reporter gene. Luciferase intensity indicates WNT activity. Figure adapted and modified from [230].

For the WNT activity assay, 1 µg of the constructs were transfected according to table 19 following the procedure in chapter 3.3.4. In case of simultaneous transfection, 1 µg TCF/LEF reporter construct with either 60 pmol siRNA or 1 µg overexpression plasmids (see chapters 3.3.5 and 3.3.6) for the transfection mixtures were used in accordance with tables 20 and 21.

Table 19: Transfection mixture for the TCF/LEF reporter constructs.

Reagent	*Volume*
Lipofectamine® 2000	5 µl
TCF/LEF reporter or negative control or positive control	10 µl (1 µg)
OptiMEM	to 100 µl

Table 20: Transfection mixture for the simultaneous transfection of TCF/LEF reporter constructs and siRNA.

Reagent	*Volume*
Lipofectamine® 2000	5 µl
TCF/LEF reporter or negative control or positive control	10 µl (1 µg)
SiRNA (2µM → final 60 pmol)	30 µl
OptiMEM	to 100 µl

Table 21: Transfection mixture for the simultaneous transfection of TCF/LEF reporter constructs and overexpression plasmids.

Reagent	*Volume*
Lipofectamine® 2000	5 µl
TCF/LEF reporter or negative control or positive control	10 µl (1 µg)
Expression plasmids (final 1 µg)	30 µl
OptiMEM	to 100 µl

After 24 hours of incubation at 37°C and 5 % CO_2, the medium was removed, wells were washed with 1 ml sterile PBS, and detached with 250 µl TrypLE™ for 3 – 5 minutes at 37°C. Afterwards, cells were resuspended in 250 µl appropriate medium and counted. Around 1.5 x 10^4 viable cells per well were seeded in 96-well plates for further experiments. If necessary, the WNT pathway was activated through 400 ng/ml WNT3A (R&D Systems) per well. Without treatment (e. g in case of siRNA knockdown) the WNT activity was measured 22 hours after WNT3A addition. In case of treatment with recombinant proteins or small molecules, treatment was performed after 5 hours of incubation with or without WNT3A followed by a 17 hour long incubation at 37°C and 5 % CO_2. The next day, cells were lysed in 25 µl 1 x Passive Lysis Buffer (Promega) per well and the luciferase activity was measured with the Dual Luciferase Reporter Assay System kit (Promega) according to the manufacturer's instructions. The main procedure for measuring the WNT activity right away or after siRNA knockdown, overexpression, or treatment with compounds or recombinant proteins is summarized in figure 11.
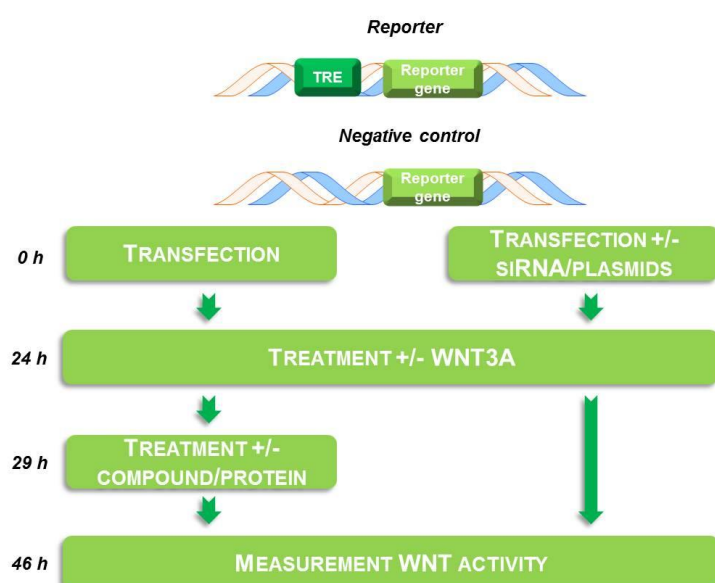

Figure 11: Protocol of the WNT activity measurement. Around 3 x 10^5 viable cells were transfected in 12-well plates with the TCF/LEF constructs and 60 pmol siRNA or 1 µg expression plasmids if necessary. After 24 hours of incubation at 37°C and 5 % CO_2, culture medium was removed, cells were washed with PBS, and detached with TrypLE. Afterwards, they were resuspended 1:1 in appropriate medium and counted. Around 1.5 x 10^4 viable cells per well were seeded in 96-well plates treated with WNT3A (400 ng/ml) for WNT pathway activation, if necessary. Either WNT activity was measured after 22 hours of incubation or cells were treated with recombinant proteins or small molecules after they were incubated for 5 hours with or without WNT3A. The measurement of the WNT activity followed after additional 17 hours of incubation with the Dual Luciferase Reporter Assay System kit according to the manufacturer's instructions.

WNT activity was evaluated through calculation of its fold increase or decrease (fold change = FC). All samples ran in triplicates. First of all, in one experiment a mean of the luciferase signals from the technical replicates of the sample "Reporter + WNT3A" was calculated. Afterwards, the fold change in WNT activity for every single replicate of all samples resulted from the quotient of the mean of sample "Reporter + WNT3A", which marked 100% WNT activity. Generally, these single fold changes from several experiments were condensed in one graph, of which one mean and standard deviation was calculated.

$$\textit{Normalized WNT activity [FC]} = \frac{\textit{WNT activity of the replicate}}{\textit{Mean WNT activity triplicates "Reporter + WNT3A"}}$$

$$\textit{Percentage change of WNT activity} = \textit{(Normalized WNT activity – 1) * 100}$$

3.4.2 ApoTox-Glo™ Triplex assay

ApoTox-Glo™ Triplex Assay (Promega) was used to measure the cell death rate and apoptosis activity (caspase 3/7 activity) in the same well according to the manufacturer's protocol (figure 12 and 13) [231]. In case of the measurement of the cell death rate, the cell impermeant dye bis-AAF-R110 can not enter the intact cell membrane of living cells. Consequently, it is not processed to the fluorescent dye R110 by the dead-cell proteases which are released from dead cells with perforated cell membranes. The fluorescence can be measured at $485_{EX}/520_{EM}$. Afterwards, the cells are lysed and the caspase3/7 activity can be quantified by dissociated aminoluciferin causing the luciferase reaction and production of light.
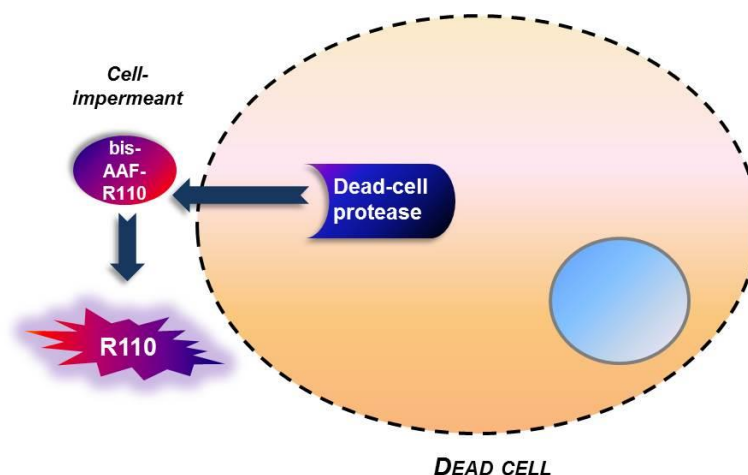

Figure 12: Principle of the ApoTox-Glo™ assay measuring the cell death rate. In case of dead cells, the cell impermeant dye bis-AAF-R110 gets activated trough cleavage by the dead-cell proteases which are released from dead cells with perforated cell membranes. The resulting fluorescent dye can be quantified at a wavelength of $485_{EX}/520_{EM}$. Figure adapted and modified from [231].
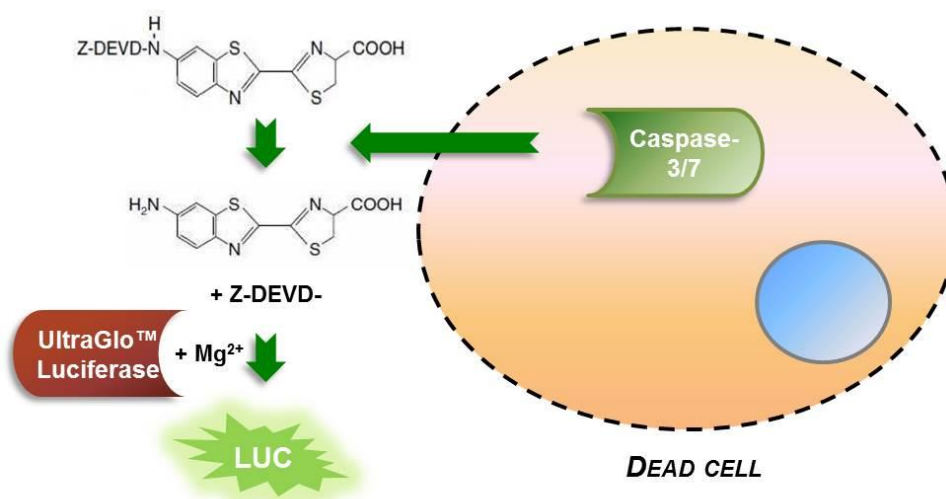
Figure 13: Principle of the ApoTox-Glo™ assay measuring the caspase 3/7 activity. After quantifying the cell death rate, the cells are lysed enabling the measurement of the caspase 3/7 activity. Perforated cells release, if present, caspase 3/7 which dissociates aminoluciferin causing the luciferase reaction and production of light. Figure adapted and modified from [231].

Cells were prepared and transfected (with or without siRNA or expression plasmids but always with TCF/LEF reporter constructs) respective chapters 3.3.4 – 3.3.6 obtaining 96-well plates with 1.5×10^4 viable cells per well. Either cell death rate and caspase activity were measured after 22 hours of treatment with/without WNT3A or recombinant proteins or small molecules were added after 5 hours of WNT3A (400 ng/ml) addition and cells were incubated for further 17 hours. For the evaluation of the cell death rate and apoptosis activity, the ApoTox-Glo™ assay was performed according to the manufacturer's protocol. The entire procedure of performing the assay is depicted in figure 14.
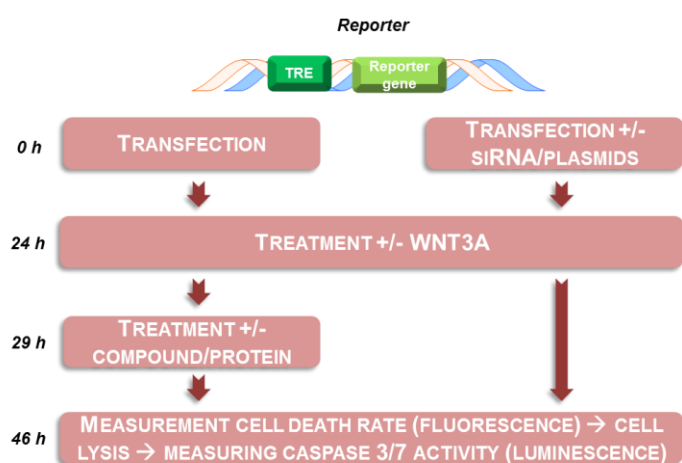

Figure 14: Protocol of measuring the cell death rate and caspase 3/7 activity. Around 3×10^5 viable cells were transfected in 12-well plates with the TCF/LEF constructs and 60 pmol siRNAs or 1 µg expression plasmids if necessary. After 24 hours of incubation at 37°C and 5 % CO_2, culture medium was removed, cells were washed with PBS, and detached with TrypLE. Afterwards, they were resuspended 1:1 in appropriate medium and counted. Around 1.5×10^4 viable cells per well were seeded in 96-well plates and treated with or without WNT3A (400 ng/ml) for WNT pathway activation. Cell death rate and caspase activity were measured after 22 hours of incubation or cells were treated with recombinant proteins or small molecules after they were incubated for 5 hours with or without WNT3A. The measurement of cell death rate and caspase activity followed after additional 17 hours of incubation. The next day the ApoTox-Glo Triplex assay kit was performed according to the manufacturer's instructions with quantifying the fluorescence resulting from dead cells at a wavelength of $485_{EX}/520_{EM}$ following cell lysis and measurement of the luminescence coming from the caspase 3/7 activity.

Cell death rate and caspase activity were evaluated through calculation of its fold increase or decrease. All samples ran in triplicates. First of all, in one experiment a mean of the

fluorescent or luciferase signals from the technical replicates of the sample "Reporter + WNT3A" was determined. Afterwards, the fold change in WNT activity for every single replicate of all samples was calculated through the quotient of the mean of sample "Reporter + WNT3A", which marked 100% cell death rate or caspase activity respectively. Therefore, one graph consists of single fold changes of single assays with one common mean and standard deviation.

$$\text{Normalized cell death rate or caspase activity [FC]} = \frac{\text{Cell death rate or caspase activity of the replicate}}{\text{Mean cell death rate or caspase activity of triplicates "Reporter + WNT3A"}}$$

$$\text{Percentage change of cell death rate or caspase activity} = (\text{Normalized cell death rate or caspase activity} - 1) * 100$$

3.4.3   CellTiter-Glo® viability assay

The CellTiter-Glo® assay (Promega) was used to measure the viability of cells [232]. Induced cell lysis releases ATP (adenosine triphosphate) from living cells enabling the conversion of beetle luciferin to oxyluciferin through UltraGlo™ luciferase which in turn causes the production of light which can be directly linked to the viability of the cells (figure 15).
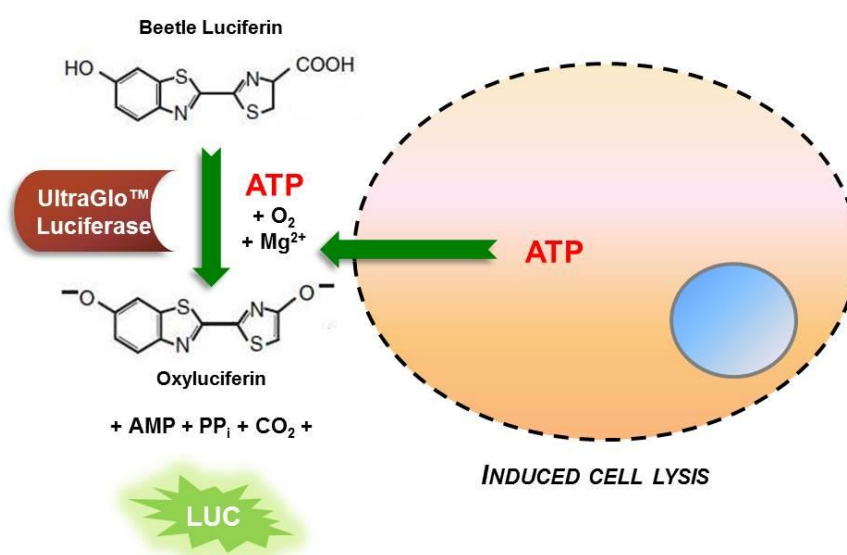

Figure 15: Principle of the CellTiter-Glo® assay measuring the viability. Induced cell lysis releases ATP from living cells enabling the cleavage of beetle luciferin to oxyluciferin through UltraGlo™ luciferase causing the production of light which can be directly linked to the viability of the cells. Figure adapted and modified from [232].

Cells were prepared and transfected (with or without siRNA or expression plasmids but always with TCF/LEF reporter constructs) respective chapters 3.3.4 – 3.3.6 generating 96-well plates with 1.5×10^4 viable cells per well. Either viability was measured after 22 hours of treatment with/without WNT3A or recombinant proteins or small molecules were added after 5 hours of WNT3A (400 ng/ml) addition and cells were incubated for further 17 hours. For the evaluation of the viability, the CellTiter-Glo assay was performed according to the manufacturer's protocol. The entire procedure is represented in figure 16.
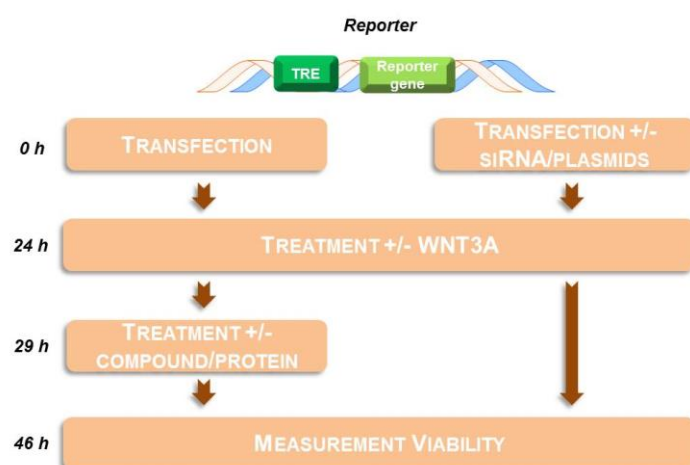

Figure 16: Protocol of measuring the viability. Around 3×10^5 viable cells were transfected in 12-well plates with the TCF/LEF constructs and 60 pmol siRNAs or 1 µg expression plasmids if necessary. After 24 hours of incubation at 37°C and 5 % CO_2, culture medium was removed, cells were washed with PBS, and detached with TrypLE. Afterwards, they were resuspended 1:1 in appropriate medium and counted. Around 1.5×10^4 viable cells per well were seeded in 96-well plates and treated with or without WNT3A (400 ng/ml) for WNT pathway activation. Either viability was measured after 22 hours of incubation or cells were treated with recombinant proteins or small molecules after they were incubated for 5 hours with or without WNT3A. The measurement of the viability followed after additional 17 hours of incubation. The CellTiter-Glo® assay kit was performed according to the manufacturer's instructions with quantifying the luminescence coming from the luciferase reaction activated through ATP from living cells.

The viability was evaluated through calculation of its fold increase or decrease. All samples ran in triplicates. First of all, in one experiment a mean of the luciferase signals from the technical replicates of the sample "Reporter + WNT3A" was established. Afterwards, the fold change in WNT activity for every single replicate of all samples was determined through the quotient of the mean of sample "Reporter + WNT3A", which marked 100% viability. Generally, these single fold changes from several experiments were resumed in one graph, of which one mean and standard deviation was calculated.

$$\textit{Normalized viability [FC]} = \frac{\textit{Viability of the replicate}}{\textit{Mean viability of triplicates "Reporter + WNT3A"}}$$

$$\textit{Percentage change of viability} = \textit{(Normalized viability – 1) * 100}$$

3.4.4   Migration assay

Migration was investigated with a fluorescence based Boyden chamber assay [233]. The FluoroBlok transwell system (Corning®) allows the fluorescence measurement of calcein stained cells which migrate through the 3 µm pores of the membrane. The cells were seeded in the upper well with appropriate medium lacking FCS. The bottom well contained appropriate medium with FCS stimulating the migration of the cells. Once the cells traveled through the FluoroBlok membrane, they were stained by calcein (Invitrogen) which was added to the medium previously. The resulting fluorescence indicated the migration activity (figure 17).
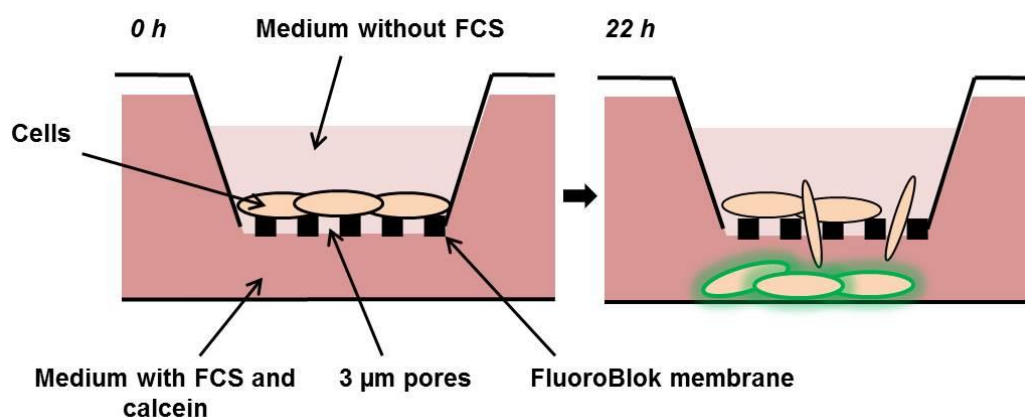

Figure 17: Principle of the migration assay. Cells were seeded in the upper wells with medium lacking FCS. The lower well contained medium with FCS stimulating the migration. Once cells traveled through 3 µm pores of the FluoroBlok membrane, they were stained with calcein (0.1 mg/ml) in the lower well. The resulting fluorescence indicated the migration activity after 22 hours.

Cells were prepared and transfected (with or without siRNA or expression plasmids but always with TCF/LEF reporter constructs) respective chapters 3.3.4 – 3.3.6. After 24 hours of incubation with the transfection approaches, medium was removed, cells were washed with sterile PBS, and detached with TypLE at 37°C and 5 % CO_2 for several minutes. Afterwards, cells were resuspended 1:1 in appropriate medium without FCS and counted. Around 2 – 3.5 x 10^4 viable cells were seeded in the upper well of a 24-well plate and 1.5 x 10^4 viable cells were seeded in the upper well of a 96-well plate. Exactly 650 µl (24-well plate) or 225 µl (96-well plate) appropriate medium with FCS and 0.1 mg/ml calcein was added to the lower wells. If necessary, the WNT pathway was activated with 400 ng/ml WNT3A per well. Either the migration activity was evaluated after 22 hours of incubation at 37°C and 5 % CO_2 after WNT3A addition or small molecules or recombinant proteins were added after 5 hours of incubation with WNT3A following an incubation of further 17 hours at 37°C and 5 % CO_2. The next day the fluorescence indicating the migration activity was measured at a wavelength of 520 nm with the POLARstar Omega BMG device (Labtech). The entire procedure of the migration assay is represented in figure 18.
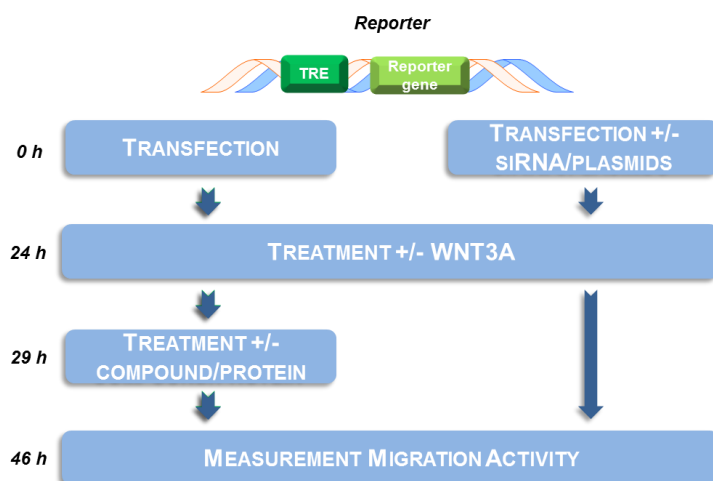
Figure 18: Protocol for the migration assay. Around 3×10^5 viable cells were transfected in 12-well plates with the TCF/LEF constructs and 60 pmol siRNAs or 1 µg expression plasmids if necessary. After 24 hours of incubation at 37°C and 5 % CO_2, culture medium was removed, cells were washed with PBS, and detached with TrypLE. Afterwards, they were resuspended 1:1 in appropriate medium and counted. Around $2 – 3.5 \times 10^4$ viable cells were seeded in the upper well of a 24-well plate and 1.5×10^4 viable cells were seeded in the upper well of a 96-well plate with appropriate medium without FCS. The lower wells contained appropriate medium with FCS and 0.1 mg/ml calcein. Cells were treated with or without WNT3A (400 ng/ml) for WNT pathway activation. Either migration activity was measured after 22 hours of incubation or cells were treated with recombinant proteins or small molecules after they were incubated for 5 hours with or without WNT3A. Then the measurement of the migration followed after additional 17 hours of incubation.

The migration activity was evaluated through calculation of its fold increase or decrease. All samples ran in triplicates. First of all, in one experiment a mean of the luciferase signals from the technical replicates of the sample "Reporter + WNT3A" was determined. Afterwards, the fold change in WNT activity for every single replicate of all samples was calculated through the quotient of the mean of sample "Reporter + WNT3A", which marked 100% migration activity. In general, one graph depicts these single fold changes from several experiments of which one mean and standard deviation was calculated.

$$\text{Normalized migration activity [FC]} = \frac{\text{Migration of the replicate}}{\text{Mean migration of triplicates "Reporter + WNT3A"}}$$

$$\text{Percentage change of migration activity} = (\text{Normalized migration activity} – 1) * 100$$

3.5 *In vivo* methods

3.5.1 Animals

Female adult BALB/c mice (≈20 g, 8-12 weeks old) were purchased from Charles River Laboratories. They were allowed to acclimate for 1 week beforehand and maintained in a 12 hours light/dark cycle with access to Altromin standard diet and water *ad libitum*. The animals were randomized and housed in groups of six per cage containing wood shavings, bedding, and a shelter. All experiments were performed in strict compliance with company, regional, and federal guidelines for the use of laboratory animals. The experiments were approved and

executed in accordance with policies and directives of LAGESO (Landesamt für Gesundheit und Soziales Berlin; Germany) and all efforts were made to minimize suffering.

3.5.2   Mice inoculation model for endometriosis

The mice inoculation model was performed as established once by Somigliana in 1999 and was further defined in-house [29, 234]. Retrograde menstruation was mimicked by injecting uterus fragments in the peritoneum (endometrium challenge/inolculation) mimicking detached endometrial cells in the menstrual blood flowing back through the fallopian tubes into the pelvic cavity instead of out of the body [234].

For tissue removal, mice were anaesthetized using a ketamine (Ketavet, 100mg/ml from Zoetis) and xylazine (Rompun, 20mg/ml from Bayer) solution (ketamine:xylazine:water; 1:1:8, 250µl/mouse). The uterine horns were removed and opened longitudinally on a suitable dish. The tissue was kept wet all the time with sterile PBS. Tissue punches were received using a sample corer (2 mm diameter) and suspended in 400µl sterile PBS (12 punches/400µl PBS) afterwards.

Recipient mice were anesthetized subcutaneously as described above and the abdomen shaved and desinfected. Into the peritoneal skin a cut of approximately 5 mm was made followed by the carefully lifting of the skin to expose inner skin lining of the peritoneal cavity. The exactly 12 tissue fragments containing solution was injected with a 18-gauge needle (B. Braun) directly into the peritoneum. Finally, the cut was closed with the help of Histoacryl® tissue adhesive (B. Braun).

In the experiments using the WNT inhibitor, animals were randomized into treatment groups. Every group included 5 animals [LGK974 (Novartis) and vehicle control]. The compounds were formulated in PEG400/water 80:20 (Fluka/Millipore) and administered by oral gavage. LGK974 was dosed with 5 mg/kg twice a day. The peri oral route and drug dose used in this study have been previously reported for LGK974 by Jiang et al. in 2013 to be efficacious regarding tumor reduction [235].

Body weight was monitored once a week. On day 7 or 14 after inoculation mice were sacrificed. The abdomens were inspected, potential lesions were carefully removed, and their surface areas were measured using the Stemi 2000-C binocular (Zeiss) at magnification 1.0, the Power Shot A640 camera (Canon) and the AxioVision software (Zeiss). The Uteri were also removed.

For RNA expression analyses up to two lesions were freezed at -80°C in 400 µl RLT buffer. Uteri were chopped and homogenated in precellys vials by adding 600 µl RLT buffer and using the ULTRA-TURRAX® instrument (IKA®) prior to freezing at -80°C. For protein

expression experiments, uteri fragments and lesions were quick-freezed with nitrogen in precellys vials and stored at -80°C. Blood samples at the day of sacrifice should give information about plasma concentration of the compound and was measured according to established Bayer guidelines in the Pharmocokinetics lab of Reinhard Nubbemeyer. Blood was taken from the vena cava.

If limited amount of lesions were available, storage for RNA isolation was the highest priority and only remaining lesions could be freezed for protein expression analyses.

The experimental design of the *in vivo* experiment is illustrated in figure 19. For the investigation of *ex vivo* samples, see chapter 3.2.
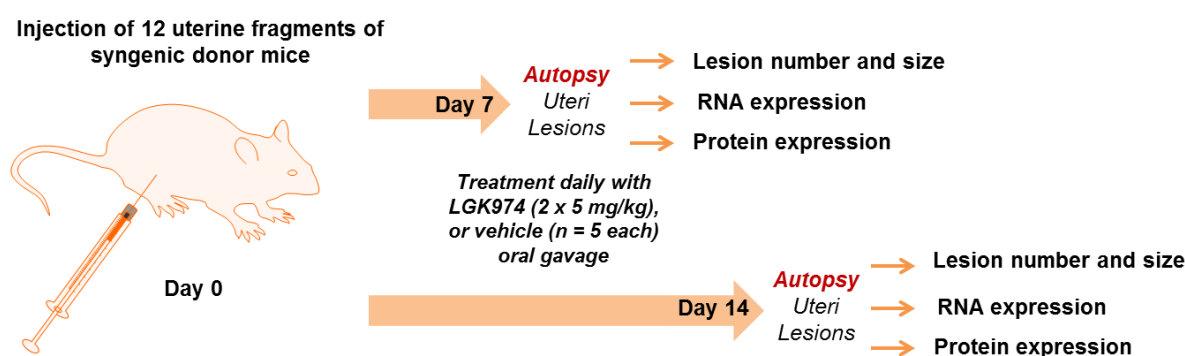

Figure 19: Experimental design of the *in vivo* study using the mice inoculation model. Exactly 12 uterus tissue fragments of 2 mm diameter each of donor mice were injected at day 0 in syngenic recipient mice. Body weight was measured once a week. Mice were treated with LGK974 or vehicle at doses of 5 mg/kg twice a day. Every group contained 5 mice. After 7 or 14 days mice were sacrificed and the lesion were counted and surface areas were measured. Additionally, lesions and uteri were freezed for RNA and protein expression experiments in decreasing priority.

3.6   Statistical analysis

For statistical analysis GraphPad Prism (Version 6) was used. Data are either expressed as bars or scatter dot plot with mean and standart deviation in both directions, as bars with mean and standart deviation in one direction, or as box and whiskers ranging from Min (minimum) to Max (maximum) including the median and box bounderies at the 25th and 75th percentiles. Generally, to determine differences between samples, the unpaired t-test assuming Gaussian distribution was performed. For the analysis of the TaqMan arrays from the clinical study or the mouse experiment the unpaired Mann-Whitney test was used without multiple corrections.

P-values below 0.05 (*) are indicated as significant, below 0.01 (**) as very significant, below 0.001 (***) as extremely significant, and below 0.0001 (****) also as extremely significant.

4 RESULTS

4.1 Confirmation of the gene array data in the same patient cohort

4.1.1 TaqMan analyses confirmed most selected candidate genes from the gene array analysis in the same patient cohort.

The previous clinical study (EMMA) had been performed to investigate the gene expression of eutopic and ectopic endometrium of diseased women in comparison to controls in order to find potential biomarkers or therapeutic targets. It included the separation of epithelial and stromal cells via LCM followed by mRNA expression analyses with Illumina gene arrays. Bioinformatic analysis revealed that the WNT pathway members WNT2B, WNT7A, LGR5, RSPO1, and FZD7 were upregulated in lesions from endometriosis patients. The same RNA should now be used to confirm the selected WNT candidate genes via the TaqMan method, which is considered to be more sensitive and precise.

In TaqMan analysis all selected candidate genes were found to be elevated in endometriosis (figure 20). While the general trend of elevated mRNA expression was consistently observed, the significance as judged by p-value varied. In some cases TaqMan arrays revealed significant deregulated mRNA expression that showed only a strong trend previously (RSPO1) or the significant deregulated gene expression was not observed anymore in the TaqMan data. However, as emphasized above, the trend and direction of deregulation in mRNA expression is similar to the findings of the gene array analysis. Generally, the gene expression of the WNT candidate genes were increased in implants compared to diseased or healthy eutopic endometrium. Almost always the mRNA expression of eutopic endometrium of patients and controls did not differ, indicating that aberrant mRNA expression of WNT pathway genes might not play a relevant role in the eutopic endometrium.

Frequently, the abnormal gene expression significantly correlated to cycle phase and cell type.

WNT2B was higher expressed in endometrial lesions.

As can be seen in figure 20, analysis of the gene arrays showed that WNT2B was highly expressed in all lesions of all cell types and cycle phases. It was always elevated compared to eutopic endometrium of endometriosis patients, except for epithelial cells of the secretory

phase, where WNT2B upregulation was observed in comparison to healthy tissue. Additionally, significantly increased mRNA expression of the WNT ligand was found in ectopic tissue compared to healthy eutopic endometrium in stromal cells of the proliferative phase. TaqMan analyses of corresponding samples confirmed significant upregulation of WNT2B in lesions compared to eutopic endometrium of patients in stromal cells of both cycle phases. However, most of the other significant aberrant gene expression findings of the gene array study showed a similar tendency and direction after TaMan analysis.

WNT7A was upregulated in ectopic tissue.

Results from the gene arrays suggested that WNT7A was significantly upregulated in all implants, except for stromal cells of the proliferative phase. Epithelial cells of both cycle phases showed significantly increased mRNA expression in comparison with eutopic diseased endometrium. Epithelial and stromal cells from the secretory cycle phase additionally revealed upregulation of the WNT ligand compared to healthy tissue. Upon TaqMan analyses, the significant elevated mRNA expression of WNT7A in epithelial cells of the secretory phase could be confirmed. The other significant deregulated gene expression findings of the gene array study exhibited also a similar trend after TaqMan measurement. The results of the experiments are summarized in figure 20.

LGR5 was elevated in implants.

In the gene arrays, LGR5 mRNA was significantly increased in all ectopic samples except for stromal cells of the proliferative cycle phase. Epithelial cells from both cycle phases exhibited elevated mRNA levels in comparison with eutopic endometrium of endometriosis patients, whereas epithelial and stromal cells from the secretory phase showed upregulation of the co-receptor compared to controls. Via TaqMan, increased mRNA expression of LGR5 was confirmed in implants of epithelial cells of both cycle phases compared to eutopic diseased tissue. In addition, TaqMan analyses revealed raised LGR5 mRNA levels in secretory phase ectopic stromal cells in comparison to eutopic endometrium from patients (figure 20).

FZD7 was increased in endometrial lesions.

Results from gene arrays are presented in figure 20. They show that besides from the proliferative phase epithelial cells, FZD7 was significantly upregulalted in all ectopic samples. Upregulation of the WNT receptor was observed in stromal cells of all cycle phases compared to both healthy and diseased eutopic endometrium. Epithelial cells from the secretory phase exhibited significantly elevated mRNA levels when compared to controls. Unless the last observation, which shows also a trend of deregulated mRNA expression respectively, all significant findings of the gene array study could be confirmed via TaqMan.

Moreover, TaqMan analyses showed decreased FZD7 mRNA expression in proliferative phase eutopic endometrium of diseased women compared to controls.

RSPO1 was also upregulated in ectopic tissue.

In gene arrays, RSPO1 was significantly upregulated in implants of epithelial or stromal cells from the proliferative phase or secretory phase respectively compared to healthy endometrium. These findings could not be confirmed via TaqMan. However, the TaqMan method revealed significantly increased mRNA levels of RSPO1 in ectopic samples of both epithelial and stromal cells of the proliferative phase compared to eutopic endometrium of patients. However, the trend of elevated mRNA expression of RSPO1 in proliferative ectopic epithelial and stromal cells in comparison to diseased eutopic tissue was already observed in the gene array study (figure 20).
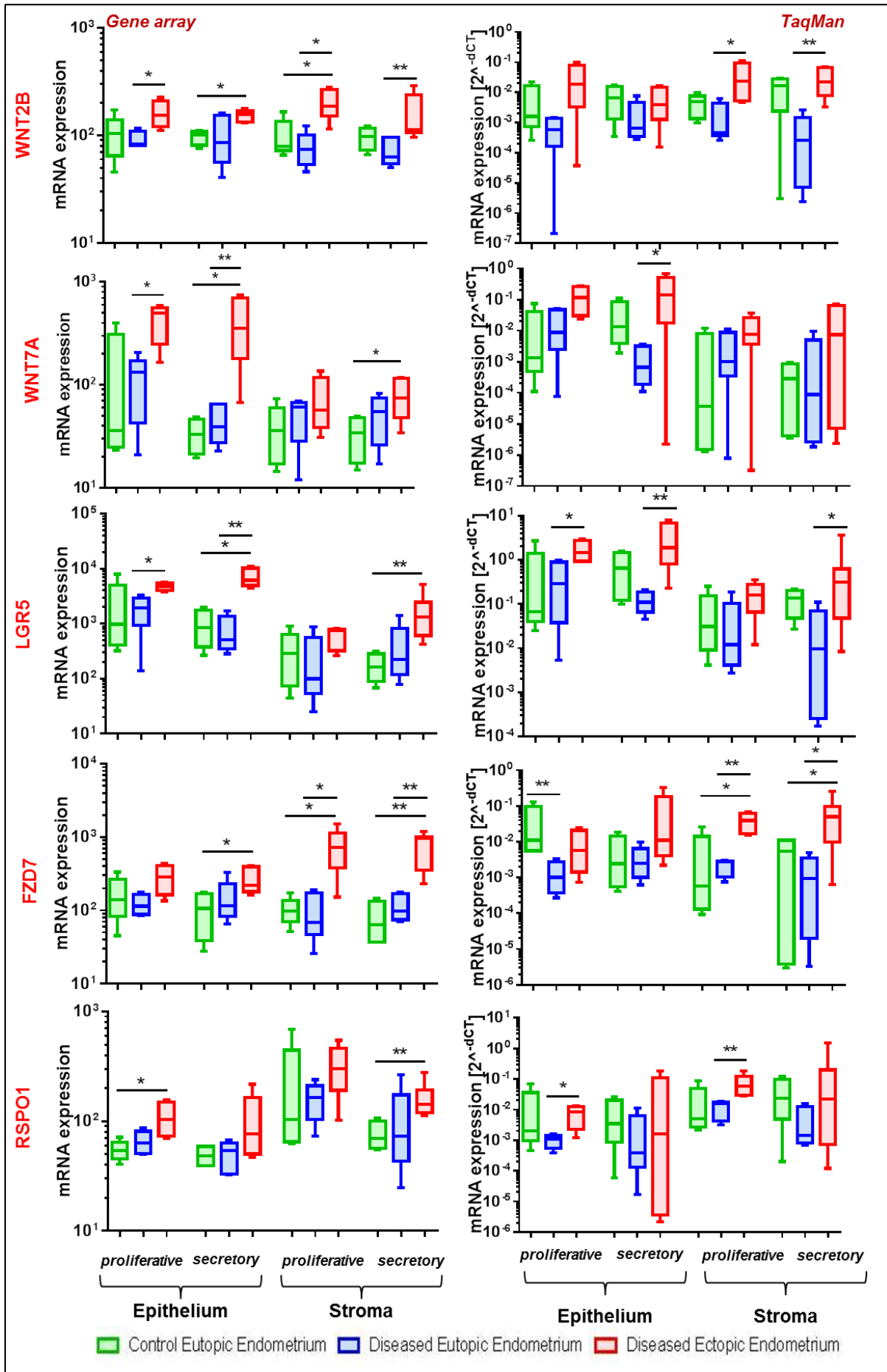
Figure 20: Gene array versus TaqMan analyses of the selected WNT candidate genes WNT2B, WNT7A, LGR5, FZD7, and RSPO1 of the different cycle phases and cell types. Green bars indicate control eutopic endometrium, blue bars represent eutopic endometrium of endometriosis patients, and red bars demonstrate lesions. Box boundaries: 25th and 75th percentiles; solid line: median; whiskers: Min to Max. * indicates p < 0.05 and ** p < 0.01.

4.1.2 Further WNT pathway genes were dysregulated in endometriosis.

With the RNA from the clinical study, TaqMan analyses were also performed for further WNT pathway genes that are either directly or indirectly regulated through WNT signaling. Direct WNT target genes contain TCF-binding sites and are immediately activated through WNT signaling [for overview see "the WNT homepage" from the Stanford University (http://web.stanford.edu/group/nusselab/cgi-bin/wnt/, last call 13.06.2016)]. Genes that are indirectly affected through WNT signaling were identified using the Ingenuity Pathway Analysis (IPA) by Qiagen. Other genes, without connection to the WNT pathway were chosen due to their potential role in endometriosis (e.g. hormone receptors). Generally, all these genes are associated with mechanisms such as migration, proliferation, or apoptosis that might play a role in lesion formation in endometriosis. Table 22 contains all genes and their appropriate annotations, of which the mRNA expression was measured.

Table 22: Annotations of 23 genes measured by TaqMan in the clinical samples. All genes highlighted in orange are WNT pathway genes, which are either directly or indirectly regulated through WNT signaling according to IPA. If stated, they contain the TCF/LEF binding motif and are direct traget genes of WNT signaling. IPA = Ingenuity Pathway Analysis, BMP = bone morphogenetic proteins, ECM = Extracellular matrix, TF = Transcription factor.

Gene	Full name	Annotation
BAX	Bcl-2-like protein 4	Apoptosis [236]
BCL2	B-cell lymphoma 2	Anti-apoptosis [237]
CAV1	Caveolin-1	Tissue growth (inhibition anoikis) [238]
DKK3	Dickkopf WNT signaling pathway inhibitor 3	WNT inhibitor by disruption FZD/WNT interaction [239]
ESR1	E2 receptor 1	Hormone receptor
ESR2	E2 receptor 2	Hormone receptor
FGF9	Fibroblast growth factor 9	Proliferation, cell survival [240]
FZD7	Frizzled-7	WNT receptor [241], direct WNT target gene [149]
LGR5	Leucine-rich repeat-containing G-protein coupled receptor 5	WNT coreceptor, direct WNT target gene [150, 242]
LRP1	Low density lipoprotein receptor-related protein 1	WNT inhibitor by interacting with FZD1 [243], migration [244, 245]
MAPK10	Mitogen-activated protein kinase 10	Proliferation [246]
MKI67	Marker of proliferation Ki-67	Proliferation [247]
MMP2	matrix metalloproteinase 2	ECM degradation → migration [248], direct WNT target gene [142]
MMP9	matrix metalloproteinase 3	ECM degradation → migration [249], direct WNT target gene [142]
PGR	Progesterone receptor	Hormone receptor
RSPO1	R-spondin 1	WNT ligand [250]
SFRP1	Secreted frizzled-related protein 1	WNT inhibitor by binding WNTs [251]

SFRP2	Secreted frizzled-related protein 2	WNT inhibitor by binding WNTs [251], eventually direct WNT target gene [151]
SOSTDC1	Sclerostin domain containing 1	BMP antagonist, inhibition proliferation/differentiation [252]
TBX18	T-Box 18	TF → cell differentiation [253]
WIF1	WNT inhibitory factor 1	WNT inhibitor by binding WNTs [251]
WNT2B	Wingless-type MMTV integration site family, member 2B	WNT ligand [254]
WNT7A	Wingless-type MMTV integration site family, member 7A	WNT ligand [254]

Proliferative phase – epithelial cells

The greatest difference in gene expression was observed between ectopic and matching eutopic endometrium of patients, whereas the mRNA expression of eutopic tissue from diseased women versus healthy controls was almost similar (figure 21 and table 23).

The comparison of diseased eutopic tissue with controls revealed only DKK3 as significantly downregulated in the endometrium of patients. DKK3 is a WNT inhibitor and WNT signaling associated.

Ectopic tissue compared to healthy or diseased eutopic endometrium exhibited significantly increased mRNA levels of SFRP2, CAV1, and SOSTDC1. In addition, lesions exhibited elevated mRNA expression of TBX18 compared to eutopic tissue of healthy women and LRP1, WIF1, SFRP1, and MMP2 compared to eutopic endometrium of endometriosis patients. All these genes are connected to the WNT pathway. SFRP1, SFRP2, and WIF1 are WNT inhibitors suggesting elevated WNT inhibition in lesions. TBX18 is a transcription factor that is essentially implicated in cell differentiation and CAV1 has been associated with tissue growth by inhibiting anoikis. Interestingly, SOSTDC1 plays a role in the inhibition of proliferation referring to reduced proliferation of ectopic epithelial cells. MMP2 and LRP1 are both involved in cell motility. MMPs are responsible for extracellular matrix (ECM) degradation and therefore cause cell migration. Consequently, increased mRNA levels of MMP2 and LRP1 propose elevated migration activity of ectopic cells. The results from this experiment are shown in figure 21 and summarized in table 23.
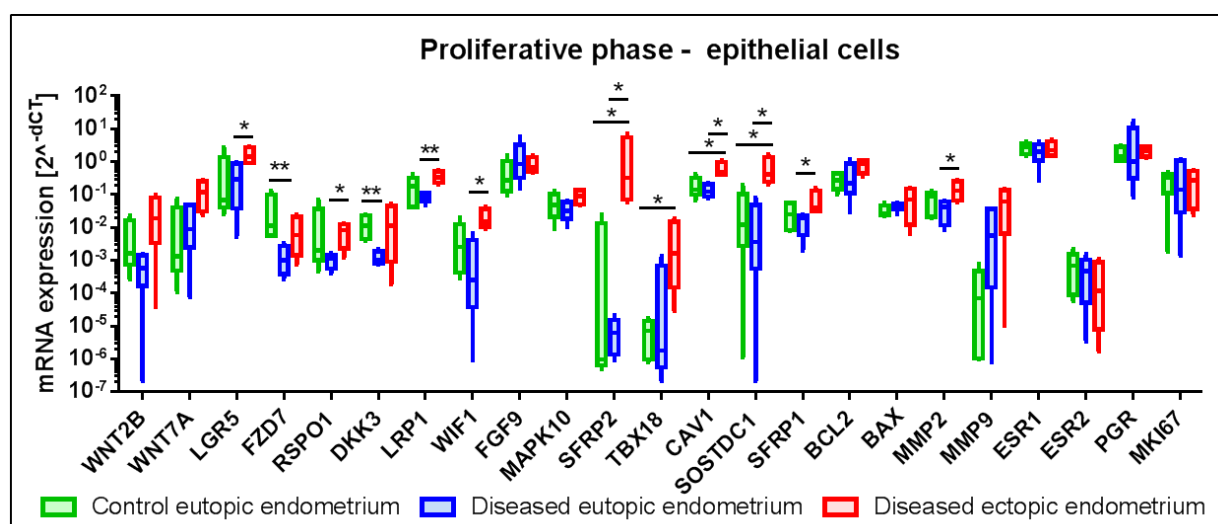
Figure 21: TaqMan mRNA expression analysis in proliferative phase epithelial cells. Green bars indicate control eutopic endometrium, blue bars represent eutopic endometrium of patients, and red bars demonstrate lesions. Box boundaries: 25th and 75th percentiles; solid line: median; whiskers: Min to Max. * indicates p < 0.05 and ** p < 0.01.

Diseased eutopic vs. control			Diseased ectopic vs. control			Diseased ectopic vs. diseased eutopic		
Gene	FC	p-Value	Gene	FC	p-Value	Gene	FC	p-Value
WNT2B	0.10	0.220	WNT2B	4.72	0.413	WNT2B	45.84	0.191
WNT7A	1.29	0.691	WNT7A	8.02	0.064	WNT7A	6.21	0.064
LGR5	0.73	0.670	LGR5	2.91	0.111	*LGR5*	*3.98*	*0.032*
FZD7	*0.03*	*0.008*	FZD7	0.21	0.286	FZD7	6.49	0.111
RSPO1	0.07	0.151	RSPO1	0.51	0.556	*RSPO1*	*7.68*	*0.040*
DKK3	*0.10*	*0.008*	DKK3	1.43	0.730	DKK3	14.98	0.286
LRP1	0.47	0.651	LRP1	1.99	0.191	*LRP1*	*4.25*	*0.008*
WIF1	0.30	0.222	WIF1	3.60	0.111	*WIF1*	*12.02*	*0.016*
FGF9	3.06	0.421	FGF9	1.64	0.206	FGF9	0.54	0.905
MAPK10	0.62	0.548	MAPK10	1.54	0.413	MAPK10	2.48	0.111
SFRP2	0.00	0.841	*SFRP2*	*371.95*	*0.016*	*SFRP2*	*246802*	*0.016*
TBX18	37.26	0.999	*TBX18*	*749.12*	*0.016*	TBX18	20.11	0.111
CAV1	0.72	0.691	*CAV1*	*3.21*	*0.040*	*CAV1*	*4.44*	*0.016*
SOSTDC1	0.45	0.580	*SOSTDC1*	*15.14*	*0.016*	*SOSTDC1*	*33.76*	*0.016*
SFRP1	0.50	0.452	SFRP1	2.26	0.413	*SFRP1*	*4.49*	*0.016*
BCL2	1.54	0.889	BCL2	2.75	0.064	BCL2	1.78	0.286
BAX	1.32	0.341	BAX	2.31	0.556	BAX	1.75	0.905
MMP2	0.53	0.222	MMP2	2.12	0.413	*MMP2*	*3.99*	*0.032*
MMP9	76.72	0.222	MMP9	338.40	0.111	MMP9	4.41	0.413
ESR1	0.83	0.738	ESR1	1.00	0.977	ESR1	1.21	0.905
ESR2	0.67	0.548	ESR2	0.43	0.413	ESR2	0.64	0.556
PGR	2.42	0.651	PGR	1.14	0.500	PGR	0.47	0.730
MKI67	1.70	0.999	MKI67	0.98	0.905	MKI67	0.58	0.905

Table 23: Fold changes (FC) and p-values from the TaqMan mRNA expression analysis of proliferative phase epithelial cells. Rows highlighted in red indicate significant results.

Proliferative phase – stromal cells

Again, the greatest difference in mRNA expression is observed when comparing ectopic and matching eutopic endometrium of patients, whereas the mRNA expression of eutopic tissue from diseased women versus healthy controls did not differ (figure 22 and table 24).

Ectopic tissue compared to healthy or diseased eutopic endometrium demonstrated significantly elevated mRNA levels of LRP1, WIF1, SFRP2, and TBX18. Moreover, lesions

compared to eutopic tissue of patients exhibited increased DKK3 and MAPK10 mRNA expression. Except for MAPK10, which plays generally a role in increased cell proliferation, all other genes are WNT pathway genes. LRP1 is involved in cell motility and TBX18 plays a role in cell differentiation. SFRP2, WIF1, and DKK3 are WNT inhibitiors (figure 22 and table 24).

When gene expression in epithelial and stromal cells from ectopic tissue is compared against those in corresponding cells derived from eutopic diseased tissue, genes involved in cell migration were upregulated in ectopic epithelial cells. On the other hand, in ectopic stromal cells MAPK10, which is important for cell proliferation, was significantly upregulated.
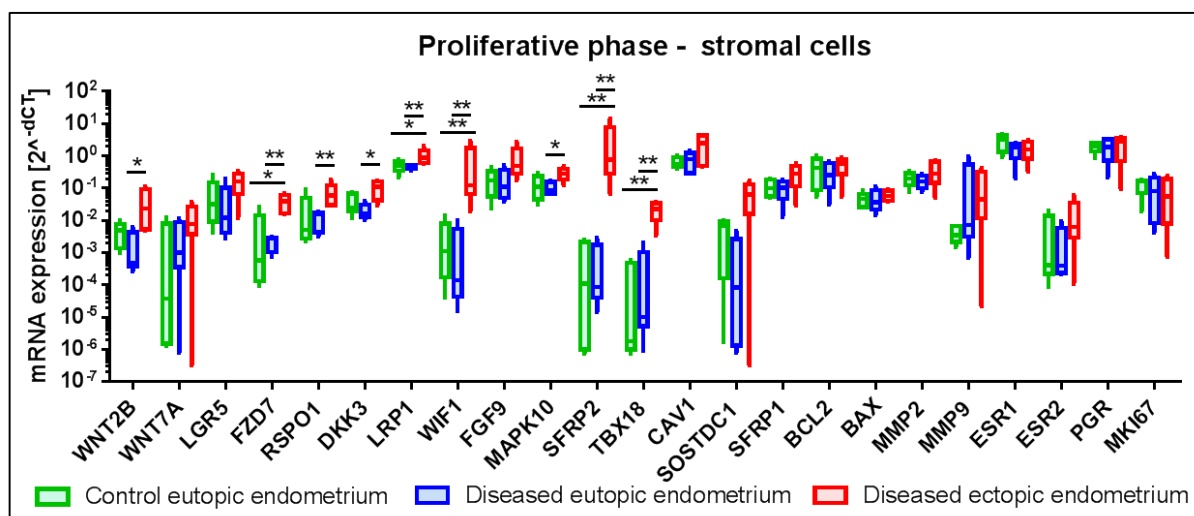

Figure 22: TaqMan mRNA expression analysis in proliferative phase stromal cells. Green bars indicate control eutopic endometrium, blue bars represent eutopic endometrium of patients, and red bars demonstrate lesions. Box boundaries: 25th and 75th percentiles; solid line: median; whiskers: Min to Max. * indicates $p < 0.05$ and ** $p < 0.01$.

Table 24: Fold changes (FC) and p-values from the TaqMan mRNA expression analysis of proliferative phase stromal cells. Rows highlighted in red indicate significant results.

Diseased eutopic vs. control			Diseased ectopic vs. control			Diseased ectopic vs. diseased eutopic		
Gene	FC	p-Value	Gene	FC	p-Value	Gene	FC	p-Value
WNT2B	0.43	0.198	WNT2B	9.59	0.095	*WNT2B*	*22.23*	*0.032*
WNT7A	1.21	0.841	WNT7A	4.30	0.310	WNT7A	3.57	0.310
LGR5	0.64	0.421	LGR5	2.42	0.310	LGR5	3.78	0.111
FZD7	0.37	0.310	*FZD7*	*6.71*	*0.032*	*FZD7*	*18.31*	*0.008*
RSPO1	0.54	0.452	RSPO1	3.24	0.095	*RSPO1*	*6.01*	*0.008*
DKK3	0.52	0.210	DKK3	2.67	0.087	*DKK3*	*5.18*	*0.016*
LRP1	0.91	0.524	*LRP1*	*1.98*	*0.032*	*LRP1*	*2.18*	*0.008*
WIF1	0.64	0.421	*WIF1*	*222.20*	*0.008*	*WIF1*	*344.55*	*0.008*
FGF9	1.02	0.999	FGF9	4.70	0.064	FGF9	4.60	0.095
MAPK10	0.79	0.999	MAPK10	2.14	0.095	*MAPK10*	*2.70*	*0.032*
SFRP2	0.81	0.841	*SFRP2*	*3861.04*	*0.008*	*SFRP2*	*4775.72*	*0.008*
TBX18	2.11	0.691	*TBX18*	*112.34*	*0.008*	*TBX18*	*53.25*	*0.008*
CAV1	1.16	0.999	CAV1	3.60	0.310	CAV1	3.11	0.222
SOSTDC1	0.21	0.222	SOSTDC1	13.39	0.151	SOSTDC1	65.19	0.151
SFRP1	0.90	0.999	SFRP1	2.61	0.151	SFRP1	2.91	0.095
BCL2	0.75	0.841	BCL2	1.22	0.691	BCL2	1.63	0.421
BAX	1.12	0.968	BAX	1.35	0.397	BAX	1.20	0.421
MMP2	0.82	0.691	MMP2	1.86	0.421	MMP2	2.27	0.246
MMP9	53.04	0.310	MMP9	33.99	0.151	MMP9	0.64	0.841
ESR1	0.58	0.310	ESR1	0.60	0.246	ESR1	1.05	0.999
ESR2	0.43	0.841	ESR2	2.86	0.548	ESR2	6.62	0.310
PGR	1.03	0.999	PGR	1.16	0.548	PGR	1.13	0.999
MKI67	0.81	0.421	MKI67	0.71	0.421	MKI67	0.87	0.889

Secretory phase – epithelial cells

Results from the TaqMan analysis with the secretory phase epithelial cell samples are demonstrated in figure 23 and table 25. Again, the greatest difference in gene expression exhibited ectopic versus matching eutopic endometrium of patients, whereas the mRNA expression of the eutopic tissue from diseased women versus healthy controls was almost similar.

Comparison of control versus diseased eutopic endometrium revealed, that only CAV1 and BAX were significantly lower expressed in diseased patients.

The comparison of implants with healthy or diseased eutopic endometrium exhibited significantly increased LRP1 and SFRP1 mRNA levels. Additionally, mRNA expression of LRP1, WIF1, FGFP9, MAPK10, SFRP2, TBX18, CAV1, SOSTDC, SFRP1, MMP2, and PGR was significantly increased in lesions compared to eutopic tissue of endometriosis patients. Except for MAPK10 and PGR, all these genes are associated to WNT signaling. SFRP1, SFRP2, and WIF1 are involved in WNT inhibition. LRP1 and MMP2 play a role in cell migration, FGF9 and MAPK10 in proliferation, and CAV1 in tissue growth through inhibition of anoikis. SOSTDC1 is implicated in the inhibition of proliferation. Interestingly, PGR was also significantly higher expressed in implants compared to diseased eutopic endometrium. That

would contradict the progesterone resistance theory in endometriosis, which includes downregulation of PGR in lesions, causing progesterone insensitivity (see chapter 1.2.2).
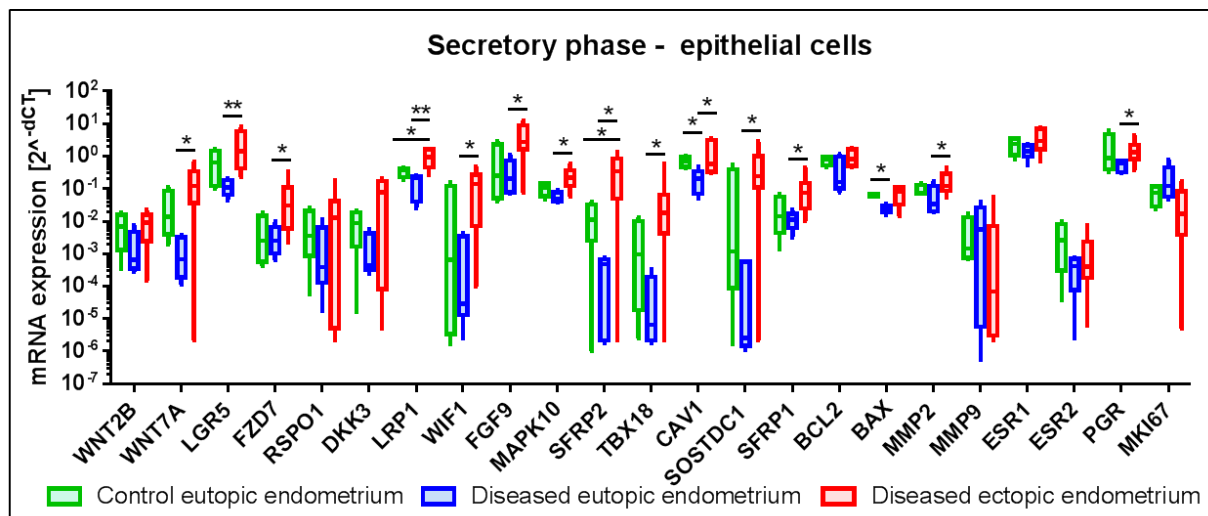

Figure 23: TaqMan mRNA expression analysis in secretory phase epithelial cells. Green bars indicate control eutopic endometrium, blue bars represent eutopic endometrium of patients, and red bars demonstrate lesions. Box boundaries: 25th and 75th percentiles; solid line: median; whiskers: Min to Max. * indicates $p < 0.05$ and ** $p < 0.01$.

Table 25: Fold changes (FC) and p-values from the TaqMan mRNA expression analysis of secretory phase epithelial cells. Rows highlighted in red indicate significant results.

Diseased eutopic vs. control			Diseased ectopic vs. control			Diseased ectopic vs. diseased eutopic		
Gene	FC	p-Value	Gene	FC	p-Value	Gene	FC	p-Value
WNT2B	0.26	0.286	WNT2B	1.19	0.999	WNT2B	4.54	0.106
WNT7A	0.04	0.064	WNT7A	5.60	0.164	*WNT7A*	*132.63*	*0.048*
LGR5	0.16	0.191	LGR5	3.62	0.152	*LGR5*	*22.12*	*0.003*
FZD7	0.60	0.999	FZD7	14.69	0.067	*FZD7*	*24.57*	*0.029*
RSPO1	0.32	0.413	RSPO1	4.67	0.788	RSPO1	14.66	0.343
DKK3	0.19	0.286	DKK3	8.68	0.230	DKK3	44.55	0.268
LRP1	0.47	0.111	*LRP1*	*2.74*	*0.039*	*LRP1*	*5.87*	*0.003*
WIF1	0.03	0.910	WIF1	4.12	0.110	*WIF1*	*121.17*	*0.010*
FGF9	0.42	0.999	FGF9	5.51	0.152	*FGF9*	*13.22*	*0.028*
MAPK10	0.54	0.191	MAPK10	2.47	0.110	*MAPK10*	*4.57*	*0.010*
SFRP2	0.02	0.286	*SFRP2*	*30.37*	*0.042*	SFRP2	1262.45	0.030
TBX18	0.02	0.318	TBX18	27.56	0.110	*TBX18*	*1271.32*	*0.030*
CAV1	*0.30*	*0.032*	CAV1	2.16	0.927	*CAV1*	*7.27*	*0.018*
SOSTDC1	0.00	0.413	SOSTDC1	5.58	0.152	*SOSTDC1*	*3330.00*	*0.015*
SFRP1	0.46	0.556	SFRP1	4.78	0.110	*SFRP1*	*10.41*	*0.018*
BCL2	0.61	0.413	BCL2	1.32	0.688	BCL2	2.15	0.149
BAX	*0.39*	*0.016*	BAX	1.14	0.746	BAX	2.92	0.064
MMP2	0.69	0.318	MMP2	1.96	0.230	*MMP2*	*2.84*	*0.048*
MMP9	2.28	0.999	MMP9	1.81	0.527	MMP9	0.79	0.755
ESR1	0.67	0.381	ESR1	1.62	0.527	ESR1	2.40	0.097
ESR2	0.11	0.191	ESR2	0.46	0.530	ESR2	4.40	0.530
PGR	0.27	0.381	PGR	0.86	0.649	*PGR*	*3.16*	*0.015*
MKI67	3.05	0.286	MKI67	0.71	0.315	MKI67	0.23	0.135

Secretory phase – stromal cells

Again, the greatest difference in mRNA levels was observed when ectopic tissue is compared to matching eutopic endometrium of diseased women, whereas the gene expression of eutopic cells from patients versus healthy controls was the same (figure 24 and table 26).

As can be seen in figure 24 and table 26 the comparison of diseased ectopic tissue with either control or diseased endometrium revealed SFRP1 and SFRP2 as significantly upregulated. Furthermore, lesions compared to eutopic endometrium of endometriosis patients exhibited significantly increased mRNA levels of WIF1, FGF9, and TBX18. All these genes are associated with WNT signaling. WIF1, SFRP1, and SFRP2 function as WNT inhibitors. FGF9 is involved in proliferation and TBX18 plays a role in cell differentiation.

When the gene expression results from ectopic versus eutopic diseased tissue from epithelial and stromal cells are compared, generally more WNT associated genes are deregulated in epithelial cells. Moreover, epithelial cells exhibited a greater number of aberrantly activated genes that are involved in proliferation or migration.
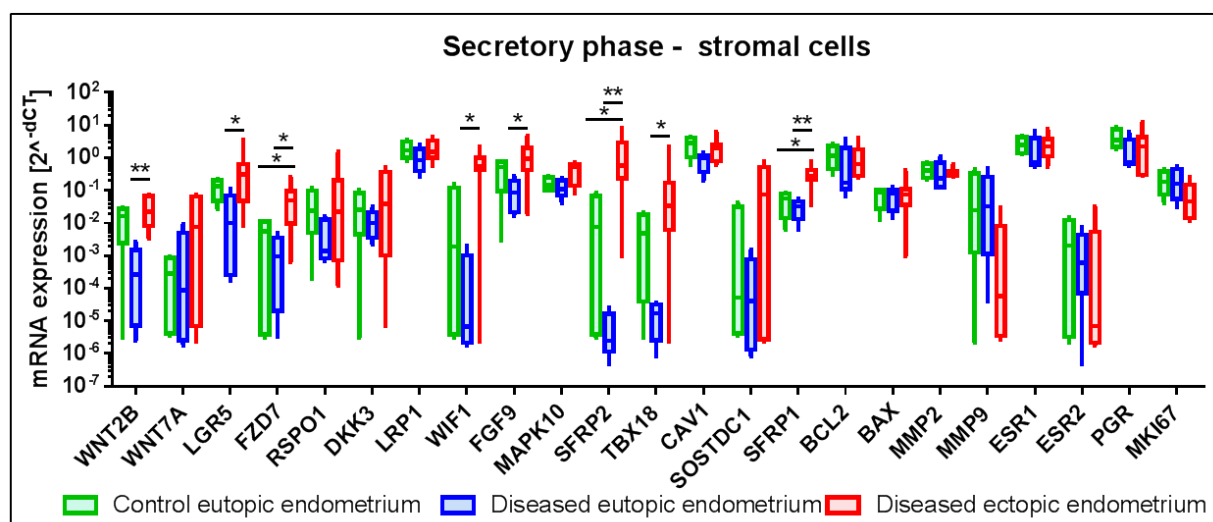

Figure 24: TaqMan mRNA expression analysis in secretory phase stromal cells. Green bars indicate control eutopic endometrium, blue bars represent eutopic endometrium of patients, and red bars demonstrate lesions. Box boundaries: 25th and 75th percentiles; solid line: median; whiskers: Min to Max. * indicates $p < 0.05$ and ** $p < 0.01$.

Table 26: Fold changes (FC) and p-values from the TaqMan mRNA expression analysis of secretory phase stromal cells. Rows highlighted in red indicate significant results.

Diseased eutopic vs. control			Diseased ectopic vs. control			Diseased ectopic vs. diseased eutopic		
Gene	FC	p-Value	Gene	FC	p-Value	Gene	FC	p-Value
WNT2B	0.04	0.191	WNT2B	1.99	0.649	*WNT2B*	*1.48*	*0.003*
WNT7A	5.25	0.730	WNT7A	72.64	0.315	WNT7A	1.14	0.343
LGR5	0.23	0.079	LGR5	5.77	0.527	*LGR5*	*1.25*	*0.048*
FZD7	0.29	0.833	*FZD7*	*13.46*	*0.018*	*FZD7*	*1.46*	*0.018*
RSPO1	0.14	0.286	RSPO1	6.03	0.927	RSPO1	1.45	0.343
DKK3	0.32	0.413	DKK3	3.76	0.413	DKK3	1.12	0.267
LRP1	0.56	0.286	LRP1	1.02	0.961	LRP1	1.02	0.164
WIF1	0.01	0.413	WIF1	17.76	0.073	*WIF1*	*18.85*	*0.030*
FGF9	0.23	0.286	FGF9	3.35	0.109	*FGF9*	*1.15*	*0.030*
MAPK10	0.80	0.510	MAPK10	2.38	0.315	MAPK10	1.03	0.149
SFRP2	0.00	0.191	*SFRP2*	*81.61*	*0.024*	*SFRP2*	*2703.17*	*0.003*
TBX18	0.00	0.191	TBX18	45.94	0.230	*TBX18*	*205.35*	*0.030*
CAV1	0.31	0.111	CAV1	0.82	0.558	CAV1	1.03	0.115
SOSTDC1	0.03	0.556	SOSTDC1	21.90	0.527	SOSTDC1	8.22	0.202
SFRP1	0.60	0.413	*SFRP1*	*6.73*	*0.043*	*SFRP1*	*1.11*	*0.006*
BCL2	0.68	0.191	BCL2	0.88	0.527	BCL2	1.01	0.149
BAX	0.96	0.999	BAX	1.52	0.999	BAX	1.02	0.876
MMP2	0.88	0.413	MMP2	0.81	0.564	MMP2	1.01	0.321
MMP9	0.92	0.905	MMP9	0.05	0.412	MMP9	1.00	0.149
ESR1	0.75	0.318	ESR1	1.07	0.894	ESR1	1.01	0.249
ESR2	0.39	0.905	ESR2	1.27	0.927	ESR2	1.03	0.999
PGR	0.42	0.111	PGR	0.77	0.649	PGR	1.02	0.785
MKI67	1.09	0.905	MKI67	0.37	0.164	MKI67	1.00	0.149

Summary of the gene expression analysis of clinical samples

Generally, a high number of directly or indirectly regulated WNT pathway genes were deregulated in endometriosis, indicating that the WNT pathway indeed was affected. Already eutopic endometrium from diseased women exhibited upregulation of WNT associated genes in comparison to controls. However, the highest upregulations were observed in ectopic tissue compared to diseased eutopic endometrium. Furthermore, many of these genes are implicated in mechanisms such as migration or proliferation that are involved in the pathogenesis of endometriosis.

In the eutopic endometrium of patients compared to healthy controls, more WNT associated genes were deregulated in the proliferative phase than in the secretory phase, raising the possibility that in this menstrual phase the WNT pathway might be stronger involved. In addition to the WNT pathway, further genes that are implicated in cell motility showed also an increased expression. However, diseased proliferative phase eutopic endometrium exhibited more deregulated mRNA expression than diseased secretory phase eutopic endometrium.

Implants compared to matching eutopic endometrium of endometriosis patients showed even more WNT pathway genes that were significantly upregulated than diseased eutopic samples compared to healthy controls. That suggests that the WNT pathway is even more activated and therefore possibly more relevant in lesions. Also cell migration and proliferation were

affected, although there was a difference between the cycle phases and cell types. In ectopic epithelial cells from the secretory cycle, cell motility and proliferation seems to play a more important role than in their stromal counterparts, since more migration-associated genes were deregulated. In the proliferative phase this difference was not observed, since both cell types expressed different genes that are implicated in cell migration or proliferation.

4.2 Confirmation of the gene array data from the clinical study in a different patient cohort

To confirm the findings of the clinical study, the involvement of the WNT pathway was investigated in additional patient samples. For that purpose, two approaches were chosen. On the one hand, protein expression analysis via IHC was performed and on the other hand, a protocol for separating stromal and epithelial cells via FACS with subsequent mRNA expression analysis was established.

4.2.1 Confirmation of the results from the clinical study via IHC

CD45 expressing immune cells showed a patient specific distribution independent from cycle phase, disease state and tissue type.

CD45 is the common leukocyte antigen and is expressed by immune cells. In the clinical study, LCM only allowed the separation of the entire stromal compartment from epithelial cells. Consequently, the stromal cell population also included e. g. endothelial or immune cells. Therefore, the immunohistochemical staining should give information about the specific spatial distribution of CD45-positive immune cells in the eutopic and ectopic endometrium of endometriosis patients and controls.

Generally, no difference in CD45-positivity between the proliferative or secretory phase or between lesions and eutopic endometrium of patients or healthy women was observed (figure 26). The amount and distribution of immune cells differed individually, ranging from very few to many CD45-positive cells that were either evenly dispersed or formed focal accumulations. All these findings were independent from cycle phase, disease state, and tissue type. Figure 25 summarizes these findings with 4 representative co-stainings together with KI67.
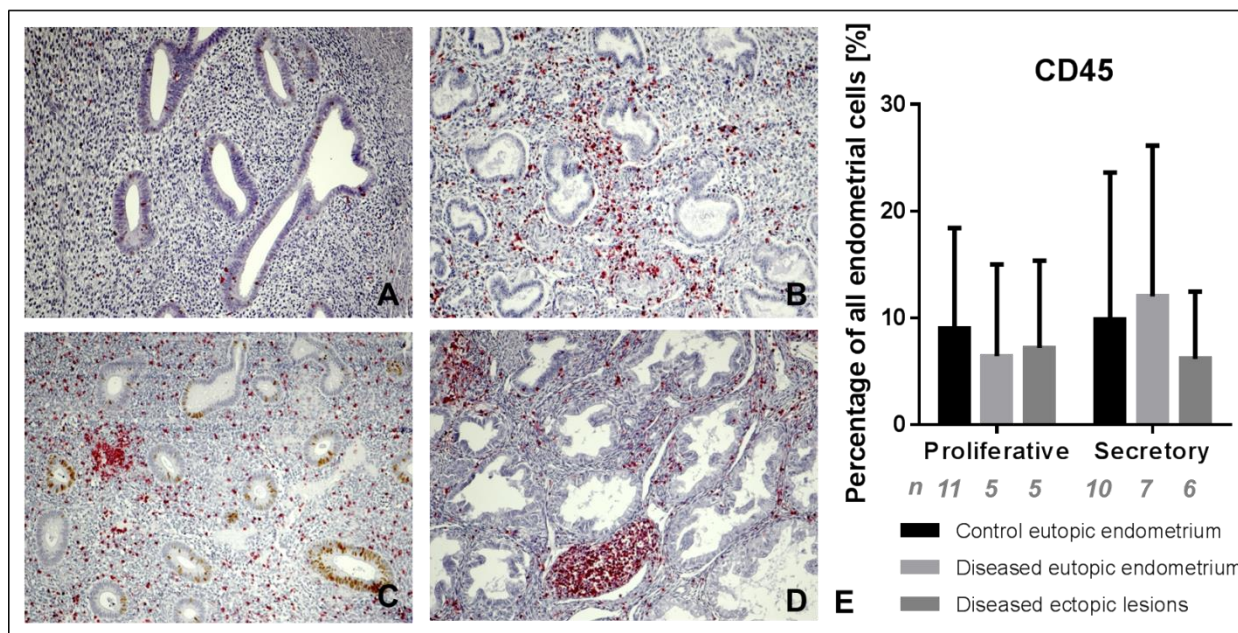
Figure 25: Immunohistochemical staining of CD45 (red) and KI67 (brown) in eutopic endometrium of patients and controls and in lesions. Representative examples of CD45 and KI67 protein expression in eutopic endometrium from **(A)** the proliferative cycle phase of a healthy women, **(B)** from the secretory cycle phase of a healthy woman, **(C)** from the proliferative cycle phase of an endometriosis patient, and **(D)** from the secretory cycle phase of a healthy woman. **(E)** Evaluation of the percentage of CD45-positive cells of all endometrial cells from all samples by a trained pathologist. Bars include mean and standard deviation. Original magnification x 100.

Protein expression of **KI67** tended to be higher in eutopic endometrium of endometriosis patients and was reduced in lesions.

Results from the clinical samples indicated that the mRNA levels of the proliferation marker KI67 tended to be higher in secretory phase eutopic epithelial cells from endometriosis patients in comparison to respective controls from the same cycle phase. Lesions exhibited a trend to reduced mRNA expression of KI67 compared to diseased eutopic endometrium.

The data from the immunohistochemistry experiments with KI67 are summarized in figure 26 with 4 representative co-stainings together with CD45. The previous observations were largely also found in immunohistochemical stainings for all cell types and cycle phases. Diseased eutopic endometrium showed a trend of elevated proliferation as indicated by increased KI67 protein levels, whereas lesions tended to proliferate less. As expected, the proliferative phase exhibited more KI67-positive cells than tissue from the secretory cycle phase in general. Thereby, most of the KI67-positive cells occurred in epithelial glandular cells than in the surrounding stroma.
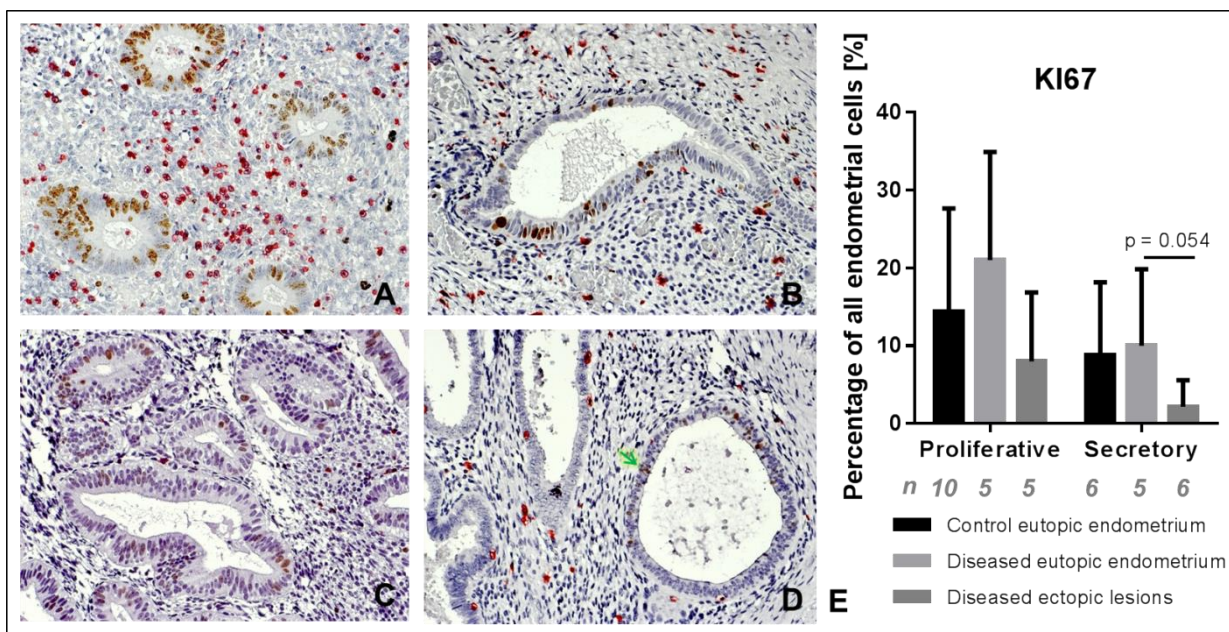
Figure 26: Immunohistochemical staining of KI67 (brown) and CD45 (red) in eutopic endometrium of patients and controls and in lesions. Representative examples of KI67 and CD45 protein expression **(A)** in eutopic endometrium of an endometriosis patient from the proliferative phase, **(B)** in a lesion from the proliferative phase, **(C)** in eutopic endometrium from the secretory phase of an endometriosis patient, and **(D)** in a lesion from the secretory phase. **(E)** Evaluation of the percentage of KI67-positive cells of all endometrial cells from all samples by a trained pathologist. Bars include mean and standard deviation. Green arrow marks one KI67-positive glandular cell. Original magnification x 200.

FZD7 was highly upregulated in lesions compared to eutopic tissue of diseased or healthy women from both cycle phases.

Altogether, immunohistochemical stainings showed that in both cycle phases the protein expression of the WNT receptor FZD7 was highly increased in lesions. Eutopic endometrium exhibited very low FZD7 protein levels in general. These findings match the results from the previous clinical study. Interestingly, FZD7 staining was stronger in glandular cells than in the surrounding stroma, while FZD7 mRNA expression was higher in the stromal compartment in the clinical study. However, FZD7-staining was observed to vary widely between the different individuals. The results are summarized in figure 27 with 4 representative co-staings together with CD45.
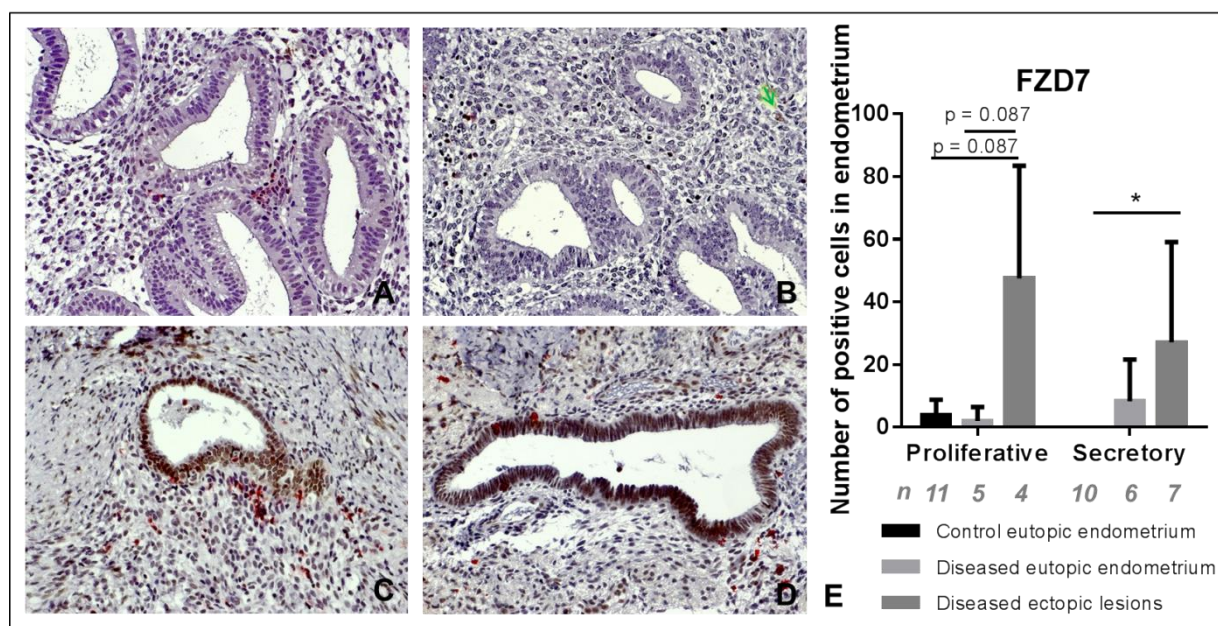
Figure 27: Immunohistochemical staining of FZD7 (brown) and CD45 (red) in eutopic endometrium of patients and controls and in lesions. Representative examples of FZD7 protein expression in eutopic endometrium **(A)** from the secretory cycle phase of a healthy woman, and **(B)** from the secretory cycle phase of an endometriosis patient, and in lesions **(C)** from the secretory cycle phase, and **(D)** from the proliferative cycle phase. **(E)** Evaluation of the number of FZD7-positive cells of all endometrial cells from all samples by a trained pathologist. * indicates $p < 0.05$. Bars include mean and standard deviation. Original magnification x 200.

WNT2B protein levels tended to be elevated in diseased eutopic endometrium and were further increased in lesions independent from cycle phase or cell type.

The results from the clinical study of generally upregulated WNT2B mRNA levels in endometriotic implants tended to be confirmed on protein level in a different patient cohort (figure 28). Immunohistochemical stainigs revealed a gradually increase of the WNT ligand protein levels from controls to lesions independent from cell type or cycle phase. However, TaqMan analyses with the clinical samples exhibited elevated mRNA levels of WNT2B in stromal cells of lesions compared to eutopic endometrium of endometriosis patients of both cycle phases. Moreover, in contrast to these findings, WNT2B protein levels did not differ between stromal or epithelial cells upon immunohistochemical satining. However, also WNT2B-staining varied widely between the different individuals.
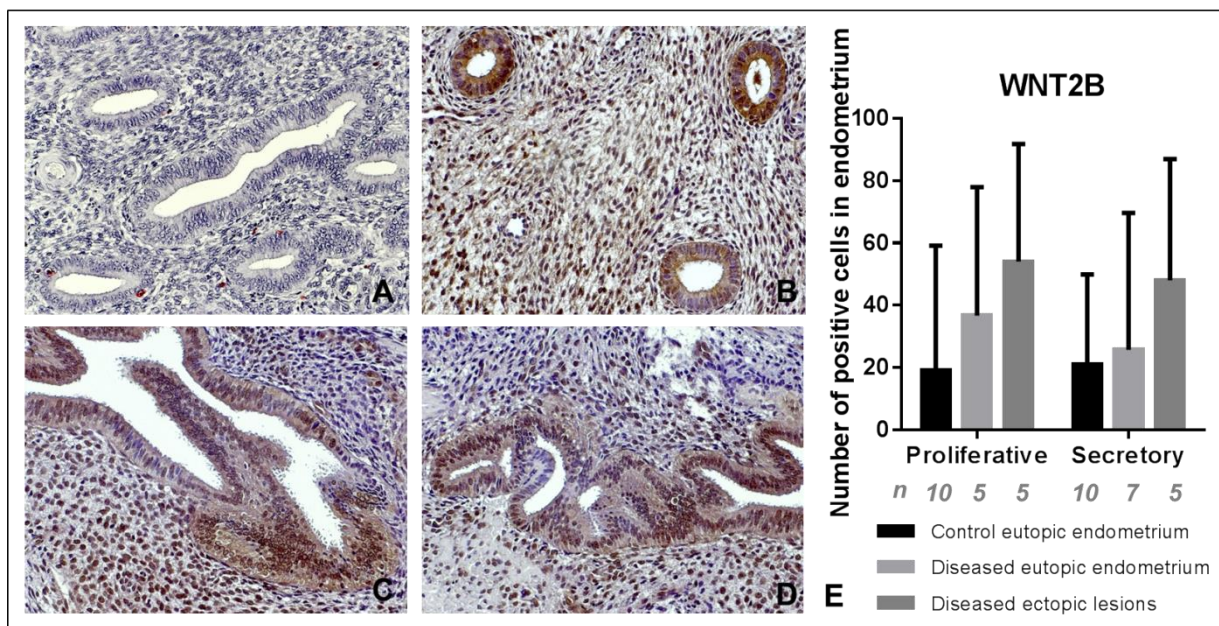
Figure 28: Immunohistochemical staining of WNT2B (brown) and CD45 (red) in eutopic endometrium of patients and controls and in lesions. Representative examples of WNT2B protein expression in eutopic endometrium **(A)** from the proliferative cycle phase of a healthy women, and **(B)** from the proliferative cycle phase of an endometriosis patient, and in lesions **(C)** from the secretory cycle phase, and **(D)** from the proliferative cycle. **(E)** Evaluation of the number of WNT2B-positive cells of all endometrial cells from all samples by a trained pathologist. Bars include mean and standard deviation. Original magnification x 200.

WNT7A tended to be upregulated in diseased eutopic endometrium from the proliferative phase.

TaqMan analyses of the clinical samples revealed significantly higher WNT7A mRNA expression in epithelial cells of lesions compared to diseased eutopic endometrium from the secretory phase. These results could not be confirmed with immunohistochemical stainings. However, a tendency of increased protein expression of the WNT ligand in the eutopic endometrium of endometriosis patients compared to controls or lesions from the proliferative cycle phase was observed. Moreover, the clinical study uncovered increased WNT7A mRNA expression in epithelial cells, but on protein level WNT7A -positive cells were observed to be ubiquitary present in both epithelial and stromal compartments. However, also WNT7A-staining exhibited a wide variation between the different individuals. The results from the immunohistochemical stainings of WNT7A are summarized in figure 29 with 4 representative co-stainings.
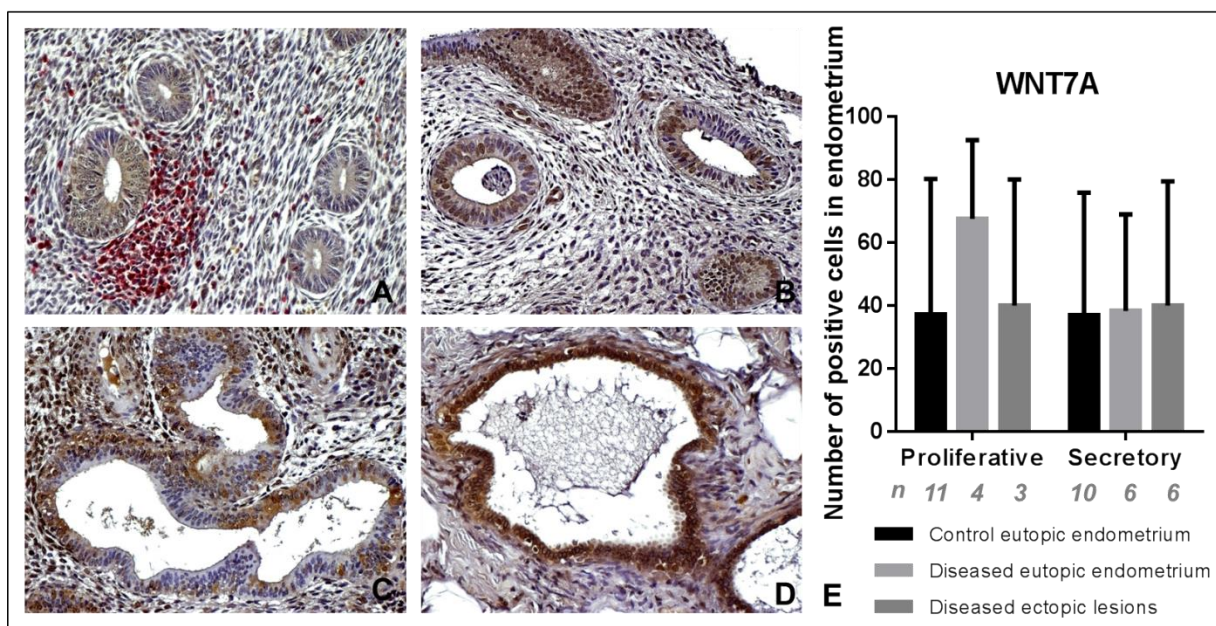
Figure 29: Immunohistochemical staining of WNT7A (brown) and CD45 (red) in eutopic endometrium of patients and controls and in lesions. Representative examples of WNT7A protein expression in eutopic endometrium **(A)** from the proliferative cycle phase of a healthy women, **(B)** from the proliferative cycle phase of an endometriosis patient, and **(C)** from the secretory cycle phase of an endometriosis patient, and in an ectopic lesion **(D)** from the secretory cycle phase. **(E)** Evaluation of the number of WNT7A-positive cells of all endometrial cells from all samples by a trained pathologist. Bars include mean and standard deviation. Original magnification x 200.

RSPO1 tended to be generally upregulated in diseased eutopic endometrium and lesions.

Both TaqMan data and immunohistochemical staining exhibited generally upregulated RSPO1 levels in lesions (figure 30). Furthermore, in both studies ubiquitous mRNA and protein levels of RSPO1 in both epithelial and stromal cells was detected. However, TaqMan analyses demonstrated a significant upregulation of RSPO1 in lesions compared to diseased eutopic endometrium of the proliferative phase, whereas IHC showed a trend of gradually increased RSPO1 protein levels from control to endometriotic tissue from both cycle phases. Also RSPO1-staining varied widely between the different individuals.
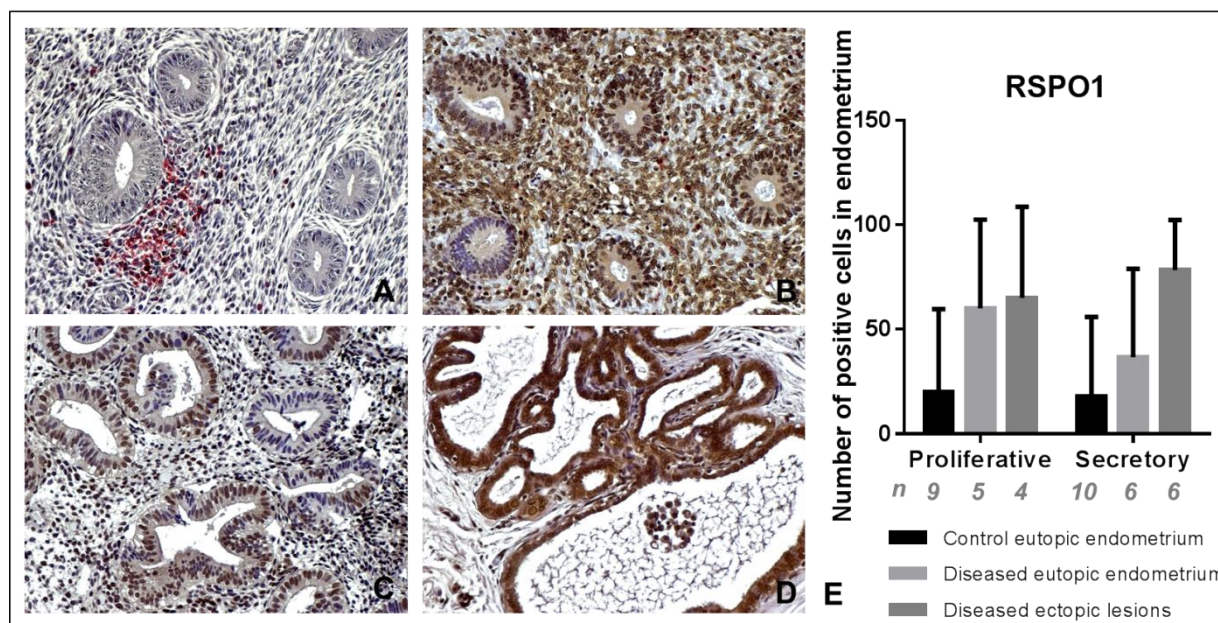
Figure 30: Immunohistochemical staining of RSPO1 (brown) and CD45 (red) in eutopic endometrium of patients and controls and in lesions. Representative examples of RSPO1 protein expression in eutopic endometrium **(A)** from the proliferative cycle phase of a healthy women, **(B)** from the proliferative cycle phase of an endometriosis patient, and **(C)** from the secretory cycle phase of an endometriosis patient and in a lesion **(D)** from the secretory cycle. **(E)** Evaluation of the number of RSPO1-positive cells of all endometrial cells from all samples by a trained pathologist. Bars inlcude mean and standard deviation. Original magnification x 200.

Technical issues prevented the **LGR5** staining to deliver reliable results for protein expression.

For LGR5 two commercial available antibodies [bs-1117R (Bioss Inc.) and ab75732 (Abcam)] and one by Eva Simon developed antibody (LGR5-11b, Tier 2) against LGR5 were tested on endometrial tissue slides obtained from the clinical study. Endometrium ought to be positive for LGR5 according to the Human Protein Atlas (http://www.proteinatlas.org/ENSG00000139292-LGR5/tissue; last call 26.07.2016) and the previous clinical study. However, no antibody could be identified to establish an appropriate staining and all examined slides were negative.

RESULTS

4.2.2 Separation of epithelial and stromal cells of eutopic endometrium by FACS

A FACS protocol was established in parallel to LCM as an alternative methodology to separate epithelial and stromal cells to enable subsequent mRNA expression analyses. LCM is hampered by the problem that only the entire stromal compartment can be obtained, which also includes e.g. endothelial or immune cells. FACS was expected to yield stromal cell populations of higher purity by using stromal cell-specific antibodies.

For that purpose, epithelial and stromal cell lines had to be identified that allowed a cell separation via cell-type specific antibodies. Literature or the provider's claim clearly defined the origin of the cell lines used in this study (table 27). Fluorescence staining of intracellular epithelial (cytokeratin) or stromal (vimentin) markers was performed to check the cell type of the different cell lines. Surprisingly, the cell type of various cell lines was obviously not always decisive. AN3-CA for example was obtained from the global biological materials resource ATCC who declared this cell line to be of epithelial origin which could not be confirmed in this study. On the contrary, the cells were clearly positive for vimentin, the stromal intracellular marker. Furthermore, some cell lines were positive for both intracellular markers (e.g. Z11). The results from this experiment are summarized in table 27.

Table 27: Intracellular staining of epithelial (cytokeratin) and stromal (vimentin) markers of the available cell lines. The left column indicates the cell type definition based on literature or provider's claim. Grey = negative staining, light orange = slightly positive staining, orange = strong positive staining, IC = isotype control.

	Cell line	Pan-Cytokeratin	Vimentin	IC IgG1
Epithelial	AN3-CA			
	Z11			
	Z12			
	EM42			
	KLE			
	Ishikawa			
	ECC1			
	HEC-1A			
	RL95-2			
Stromal	22 B			
	ESC			
	MES-SA			

However, these results show that the identification of epithelial and stromal markers for the separation of these specific cell types is not trivial, since the cell lines did not always exhibit distinct phenotypes. Nevertheless, these cell lines were used to establish the FACS protocol.

79

For cell separation of stromal and epithelial cells from unfixed fresh tissue by FACS, cell specific epithelial and stromal surface antigens had to be identified first. Based on literature research various markers were identified (table 28).

Table 28: Epithelial and stromal surface markers that were further analyzed by FACS for their ability to separate epithelial and stromal cells.

Stromal markers		Epithelial markers	
Name		**Name**	
CACNA1A	Calcium channel, voltage-dependent	ACE	Angiotensin I converting enzyme
CD10	Neprilysin	CD9	Cell growth-inhibiting gene 2 protein or Tetraspanin-29
CD13	Alanyl aminopeptidase	CD74	HLA class II histocompatibility antigen gamma chain
CD34	Hematopoietic progenitor cell antigen CD34	CD133	Prominin 1
CD36	Thrombospondin receptor	CD166	Activated leukocyte cell adhesion molecule
CD90	Thymus cell antigen 1	CLDN3	Claudin-3
CD140B	Platelet-derived growth factor receptor	E-Cad	E-Cadherin
CD248	Endosialin	EpCAM	Epithelial cell adhesion molecule
FAP	Fibroblast activation protein	MUC1	Mucin 1
		TICAM2	Toll-like receptor adaptor molecule 2
		TMEM87A	Transmembrane protein 87A
		TMEM97	Transmembrane protein 97
		TMEM9B	Transmembrane protein 9B

With the help of the cell lines and appropriate fluorescently labelled antibodies these markers were further investigated via FACS for their ability to separate epithelial and stromal cells. The fluorescence intensity emerging from every antibody bound to its antigen on the cell surface was measured and normalized against the background fluorescence obtained from a sample lacking antibodies. This resulting normalized fluorescence intensity gave information about the binding efficacy of the antibodies. This procedure was performed for every cell line (see table 27) and every marker (see table 28). The results are depicted in figure 31. For the most promising epithelial markers MUC1, EpCAM, and CD9 and stromal markers CD90, CD10, and CD13 appropriate isotype controls were performed to investigate unspecific binding. As can be seen in figure 32, almost no unspecific binding occurred, indicating that the antibodies bound their epithelial or stromal antigens specifically.
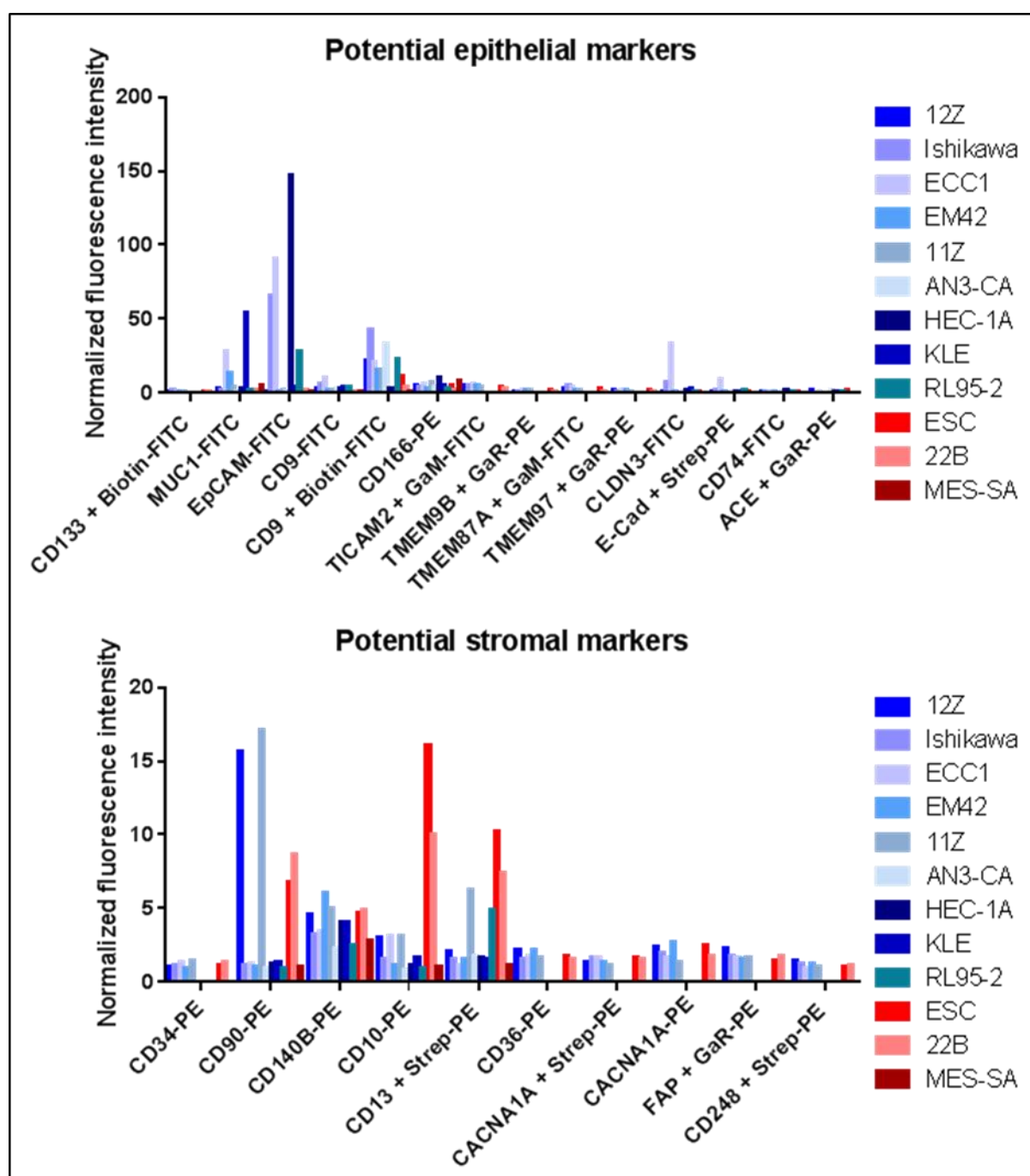
Figure 31: Normalized fluorescence intensity of specific antibodies bound to potential epithelial and stromal cell surface markers. Blue bars indicate cell lines defined as epithelial and red bars indicate cell lines defined as stromal.
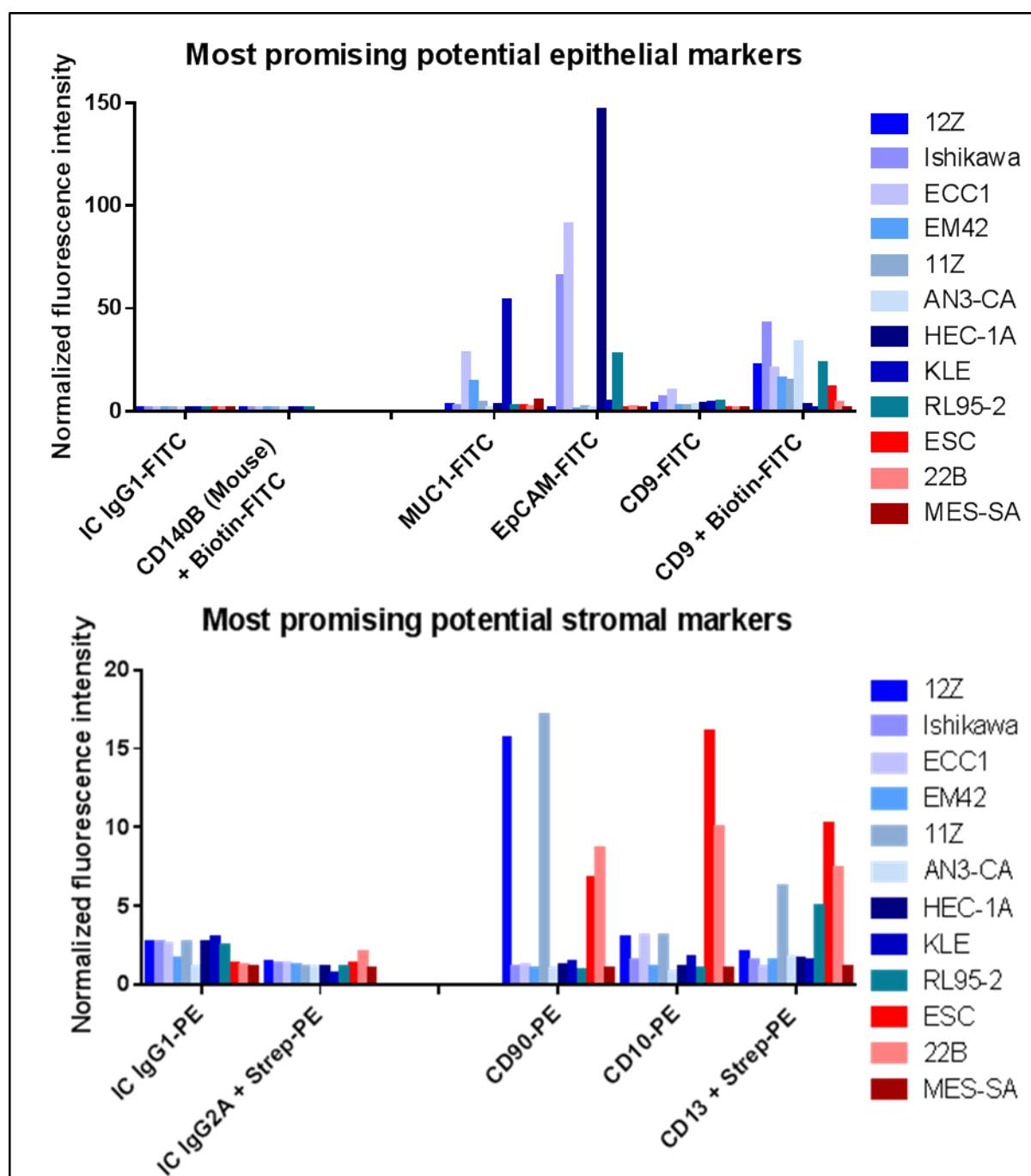
Figure 32: Normalized fluorescence intensity of specific antibodies against the the most promising potential epithelial and stromal cell surface markers. Blue bars indicate cell lines defined as epithelial and red bars indicate cell lines defined as stromal. IC = Isotype control.

The next step to validate these markers was to isolate cells from murine uteri, to sort them via FACS with the help of the selected epithelial and stromal markers, and to stain them with anti-cytokeratin or anti-vimentin to examine the success of cell sorting. Due to severe technical problems with the isolation and sorting of murine cells in addition to altered antibody affinities, these experiments could only give hints about the sorting efficiency of the different antibodies (data not shown). However, in this context CD90 and EpCAM were the most suitable antigens for this approach. Therefore, they were chosen to test the isolation and separation of epithelial and stromal cells from human endometrium.

The entire procedure from tissue dissociation, single cell isolation, cell separation, and RNA isolation with subsequent quality and quantity examination from unfixed fresh tissue was tested exemplarily with a curettage of patient NID55. Subsequently, TaqMan analysis was done with epithelial and stromal specific probes against KRT18 and EpCAM and CD90 and CD10 respectively to evaluate the purity of the obtained sorted populations.

As can be seen in figure 33, high quality RNA (RIN ~ 9) could be obtained from the curettage of patient NID55 upon cell separation via FACS. Moreover, subsequent TaqMan analysis confirmed that the sorted cell populations were of high purity. Anti-EpCAM antibodies were able to enrich epithelial cells to a high degree, whereas anti-CD90 antibodies were so stringently binding stromal cells that the epithelial cells were entirely eliminated from this population. So both antigens were suitable for separating these cell types and the resulting high quality RNA would enable proper RNA expression analyses (figure 34).
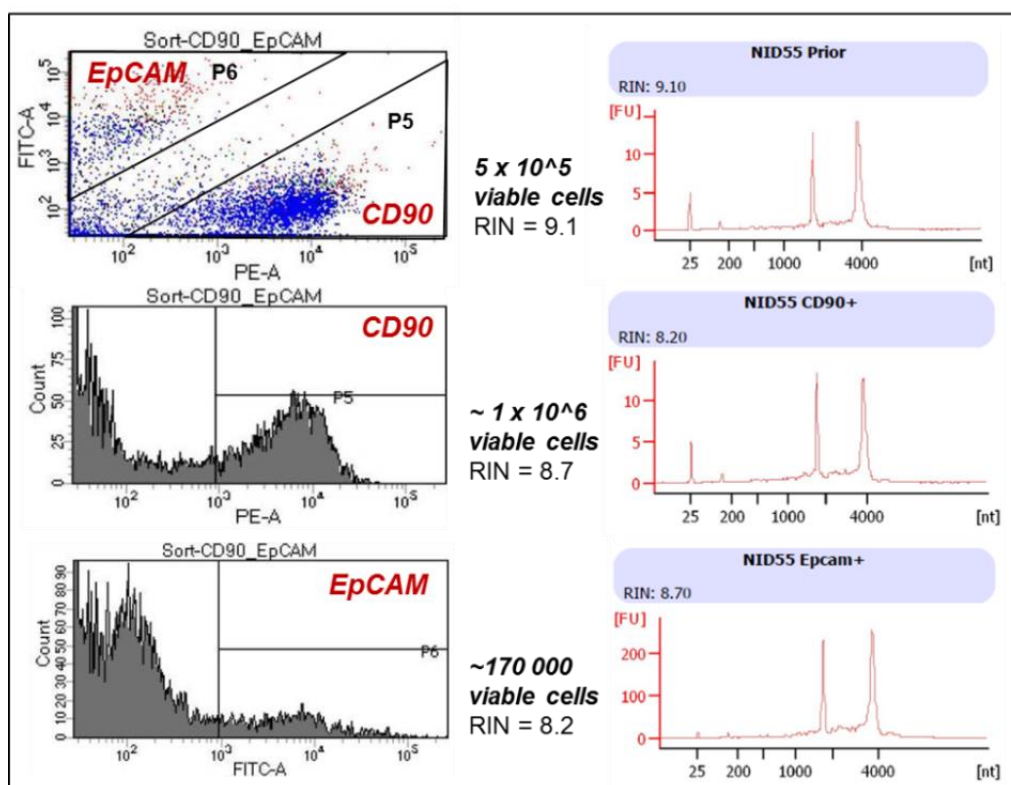

Figure 33: Cell separation of epithelial and stromal cells via FACS using the epithelial marker EpCAM and the stromal marker CD90 with subsequent mRNA isolation. A curettage from patient NID55 has been used to test this approach. Sample „Prior" indicates unsorted cells; P = Sorting gate.
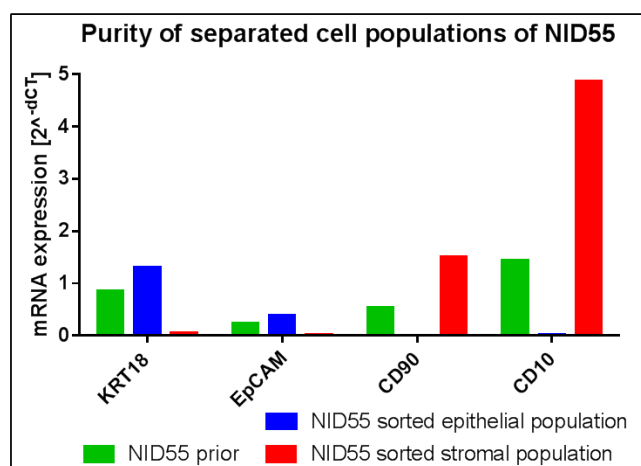
Figure 34: TaqMan analyses with stromal and epithelial specific probes to evaluate the purity of the cell popualtions obtained by FACS. Green bars indicate unsorted cell population (prior), blue bars indicate sorted epithelial cells using EpCAM, and red bars indicate sorted stromal cells using CD90. KRT18 and EpCAM were used as epithelial and CD90 and CD10 as stromal specific TaqMan probes.

The purity of FACS separated cell populations was significantly higher than those separated by LCM. Generally, the comparison of epithelial or stromal cell populations with the unseparated control group or with each other revealed more significant differences between the FACS-related samples than between the LCM-related samples. These results indicate that FACS is more suitable for the separation of epithelial and stromal cells. Figure 35 demonstrates these results and significant differences are indicated accordingly. However, during the establishment of the method it turned out, that this procedure was only suitable for eutopic endometrium, since ectopic samples often contained insufficient cell numbers.
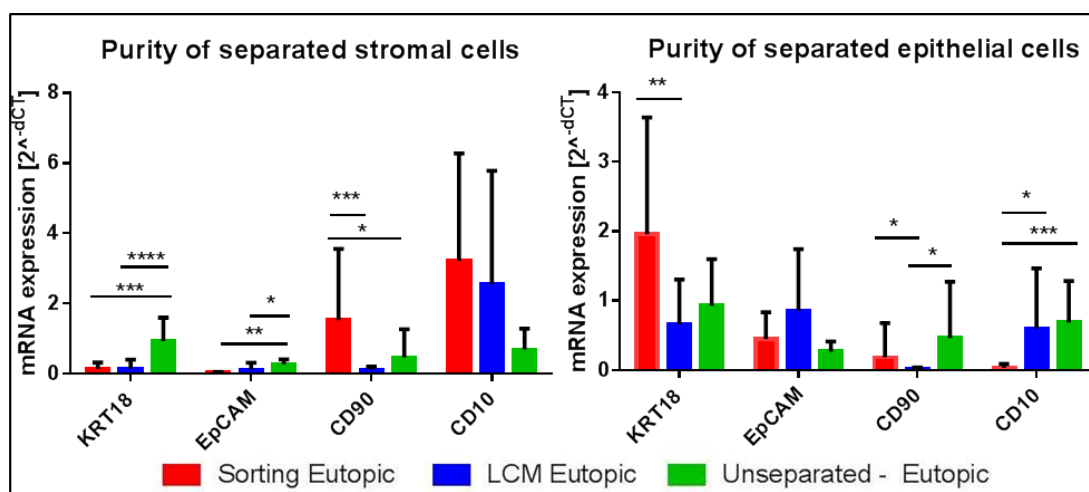

Figure 35: TaqMan analyses with epithelial and stromal specific probes to evaluate the purity of the cell populations obtained by FACS or by LCM. Bars include mean and standard deviation. * indicates $p < 0.05$, ** represents $p < 0.01$, *** indicates $p < 0.001$ and **** $p < 0.0001$.

Finally, the protocol has been successfully established and for the in-depth investigation of eutopic samples, FACS is the more favourable approach than LCM. However, since in this study also ectopic samples should be investigated, this procedure was not suitable and immunohistochemistry was used instead. Nevertheless, this approach has been applied to

clinical samples, but the number of recruited samples was not sufficient to enable proper statistical analysis (data not shown).

4.3   Investigation of the WNT pathway *in vitro*

Based on the clinical study, WNT candidate genes WNT2B, WNT7A, FZD7, LGR5, and RSPO1 were selected for further investigation of their potential involvement in endometriosis. TaqMan analyses and immonhistochemistry already confirmed that their mRNA and protein levels were increased in lesions. Now, the WNT candidate genes were particularly examined in endometrial stromal cells (ESCs) *in vitro*. This cell line has been once established from a human sample internally by Florian Prinz. Their mRNA levels were manipulated through siRNA knockdown or overexpression by transfection of expression plasmids. Furthermore, cellular perturbation studies were performed by the addition of recombinant WNT ligands to WNT receptors expressing ESCs. The impact on WNT activity and its subsequent influence on viability, cell death rate, caspase activity, and migration activity were then analyzed.

4.3.1   Targeting of the selected WNT pathway genes via siRNA knockdown, overexpression, or recombinant proteins

For the WNT receptors LGR5 and FZD7 siRNA knockdown and transfection with an overexpression plasmid were performed. Since the WNT ligands WNT2B, WNT7A, and RSPO1 are not expressed in ESCs, whereby transfection approaches would not be feasible, they were tested through the addition of the respective recombinant proteins to the cells. Both receptors and ligands were tested in WNT3A activated cells. However, WNT ligands were also examined in non-activated cells, since their own activation potential, synergies with the prototypic activator WNT3A, or inhibition should be evaluated.

First, WNT activity was measured to show that the WNT pathway was affected. In conjunction with siRNA knockdown or overexpression experiments, the mRNA expression of the respective genes was also examined to calculate the knockdown or overexpression efficiency. Afterwards functional assays to quantify viability, proliferation, apoptosis, and migration were performed.

Generally, controls were performed to prove the integrity of the WNT activity assay. Negative controls with inoperative mCMV promoters were used to investigate, whether the emerging signals were WNT specific. Moreover, either non-targeting (NT) siRNAs, empty backbone plasmids, or BSA (for recombinant proteins) were used to evaluate, if the appearing WNT signals or functional readouts were specific for the individual candidate genes.

LGR5 significantly influenced WNT activity, viability, cell death, caspase activity, and migration activity of endometrial stromal cells.

Upon siRNA knockdown, the WNT activity could be significantly reduced by ~ 59 % or increased by ~ 72 % after LGR5 overexpression. RNA expression levels confirmed that knockdown and overexpression efficiency were significant. Generally, the negative controls had no influence on the WNT activity suggesting that the emerging signals were WNT specific. Results of the WNT activity assay with LGR5 are summarized in figure 36.

After siRNA knockdown of the WNT co-receptor LGR5, a significant reduction of the viability and an increase in cell death rate appeared. Overexpression exhibited reverse results. Reduced levels of LGR5 also led to significantly increased caspase activity indicating activated apoptosis. However, overexpression of LGR5 did not reduce caspase activity accordingly (figure 37). The migration activity was not changed significantly but siRNA knockdown led to a reduced migration by trend, whereas elevated LGR5 mRNA levels tended to result in increased migration of ESCs (figure 38). Non-targeting siRNAs did generally not affect functional readouts proposing that observed effects were specifically influenced by changing levels of the WNT receptor.

Altogether these results demonstrate that altered mRNA levels of LGR5 change the WNT activity accordingly, resulting in modified viability, cell death rate, and/or apoptosis and migration activity in ESCs.
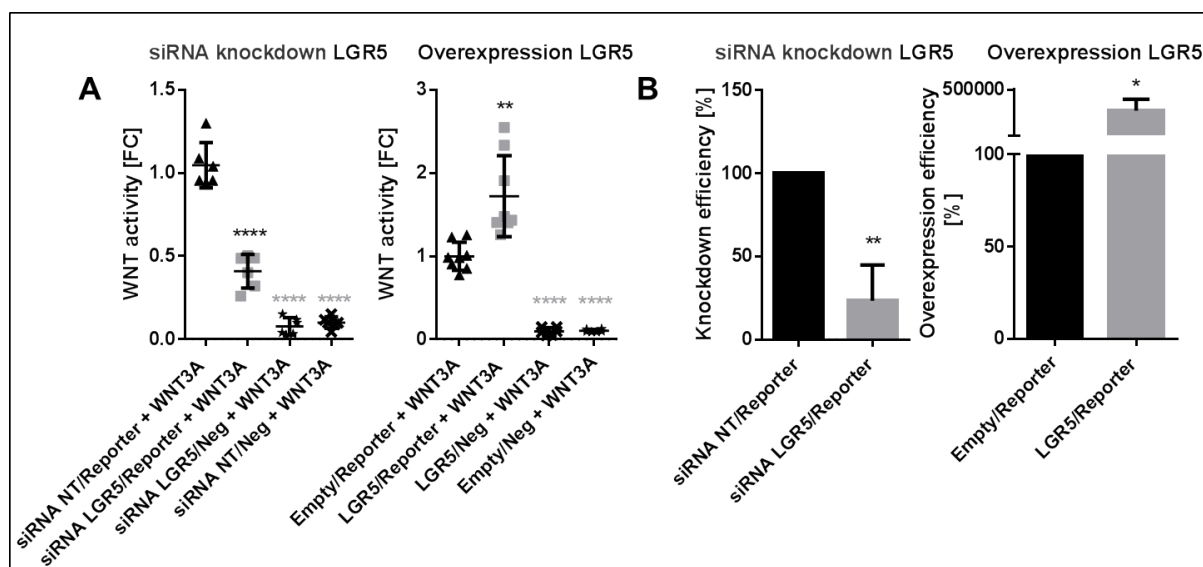
Figure 36: WNT activity and knockdown/overexpression efficiency after LGR5 siRNA knockdown or overexpression. (A) WNT activity assay. **(B)** Knockdown and overexpression efficiency. NT = non-targeting, Neg = Negative control of WNT activity assay, Empty = empty backbone plasmids. Fold changes (FC) were calculated versus (siRNA NT or Empty)/Reporter + WNT3A. Scatter dot plots and bars include mean and standard deviation. * indicates p < 0.05, ** represents p < 0.01, *** indicates p < 0.001 and **** p < 0.0001.
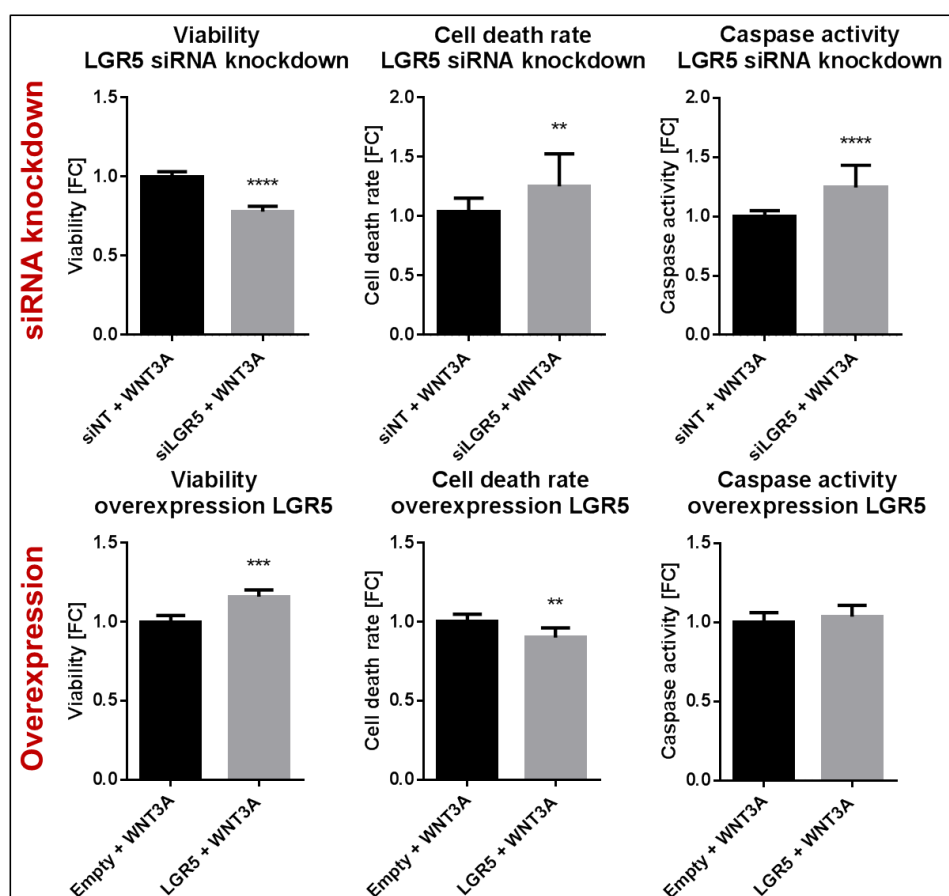

Figure 37: Results of the cell based assays after siRNA knockdown or overexpression of LGR5. NT = non-targeting, Empty = empty backbone plasmids. Fold changes (FC) were calculated versus (siNT or Empty)/Reporter +WNT3A. Bars include mean and standard deviation. ** represents p < 0.01, *** indicates p < 0.001 and **** p < 0.0001.
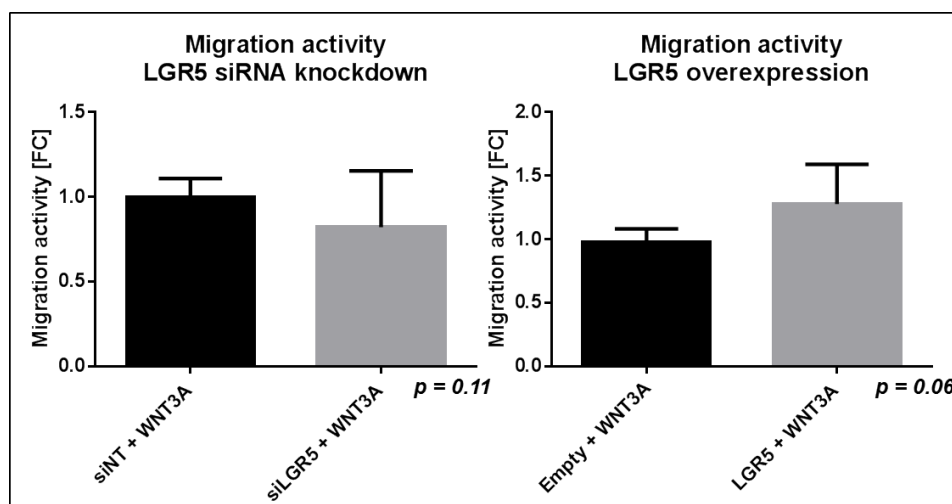
Figure 38: Migration activity after siRNA knockdown or overexpression of LGR5. NT = non-targeting, Empty = empty backbone plasmids. Fold changes (FC) were calculated in comparision to „siNT/Empty + WNT3A" control. Fold changes (FC) were calculated versus (siNT or Empty)/Reporter +WNT3A. Bars include mean and standard deviation.

Both, siRNA knockdown or overexpression of **FZD7** significantly decreased WNT activity and influenced viability, cell death, caspase activity, and migration activity.

After siRNA knockdown the WNT activity could be significantly reduced by ~ 63 %. The RNA expression did also significantly decrease by ~ 57 % respectively indicating a high knockdown efficiency. However, although RNA levels of FZD7 significantly increased by ~ 3 % upon transfection with the FZD7 expression plasmid, the appropriate WNT activity did not raise. On the contrary, the WNT activity significantly dropped by ~ 52 %. Changes of the WNT activity were WNT pathway specific as indicated by the negative control (figure 39).

The viability significantly declined after siRNA knockdown of the WNT receptor FZD7, whereas the cell death rate did not exhibit changes, although a significant elevation of the caspase activity suggests activated apoptosis. Overexpression of the receptor by transfection with the FZD7 expression plasmid resulted in significantly increased viability and decreased cell death rate accordingly. But unaltered caspase activity proposes that no apoptosis was involved in the reduced cell death rate (figure 40). The migration activity was not changed dramatically but siRNA knockdown showed a tendency of reduced migration, whereas increased FZD7 mRNA levels resulting from plasmid transfection led to significantly increased migration activity (figure 41). Effects on the functional readouts were FZD7 specific as indicated by the non-targeting siRNA control.
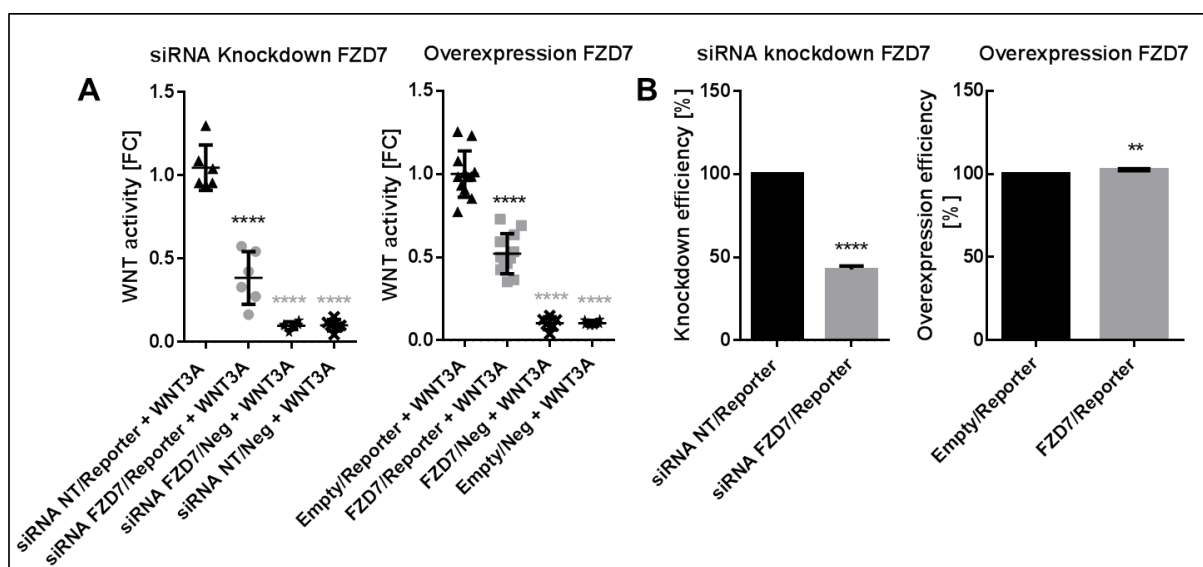
Figure 39: WNT activity and knockdown/overexpression efficiency after FZD7 siRNA knockdown or overexpression. (A) WNT activity assay. **(B)** Knockdown and overexpression efficiency. NT = non-targeting, Neg = Negative control of WNT activity assay. Fold changes (FC) were calculated versus (siRNA NT or Empty)/Reporter +WNT3A. Scatter dot plots and bars include mean and standard deviation ** represents p < 0.01 and **** p < 0.0001.
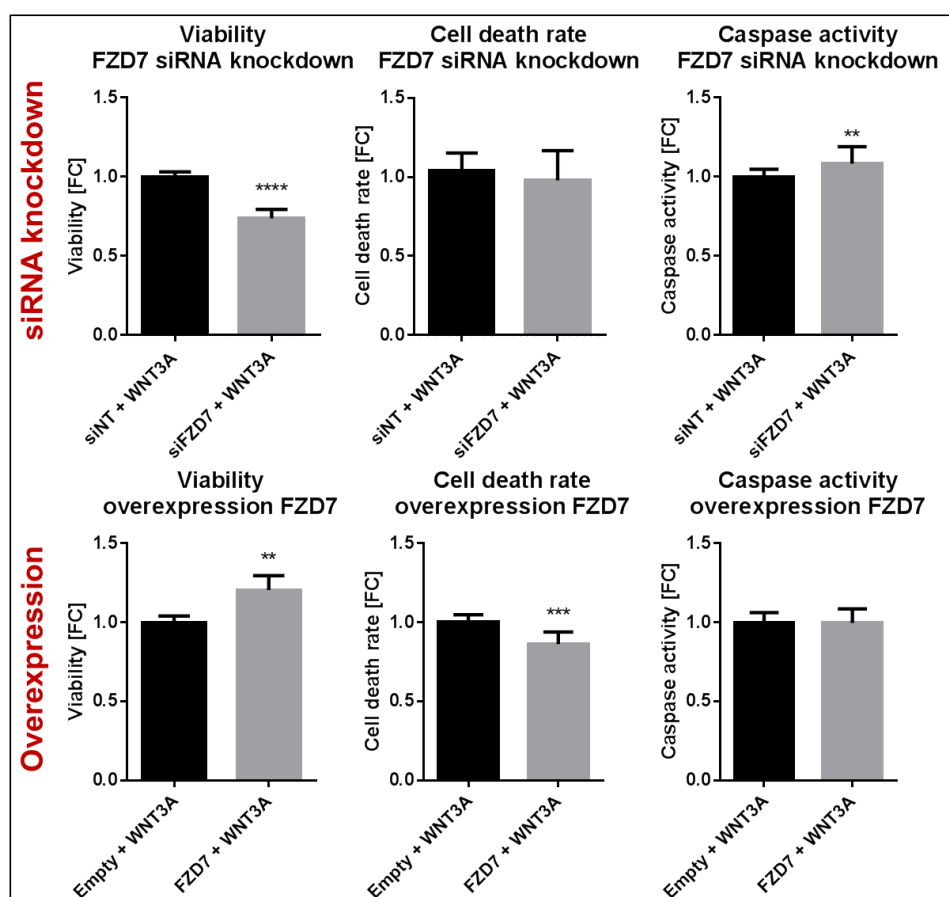

Figure 40: Results of cell based assays after siRNA knockdown or overexpression of FZD7. NT = non-targeting, Empty = empty backbone plasmids. Fold changes (FC) were calculated versus (siNT or Empty)/Reporter +WNT3A. Bars include mean and standard deviation. ** represents p < 0.01, *** indicates p < 0.001 and **** p < 0.0001.
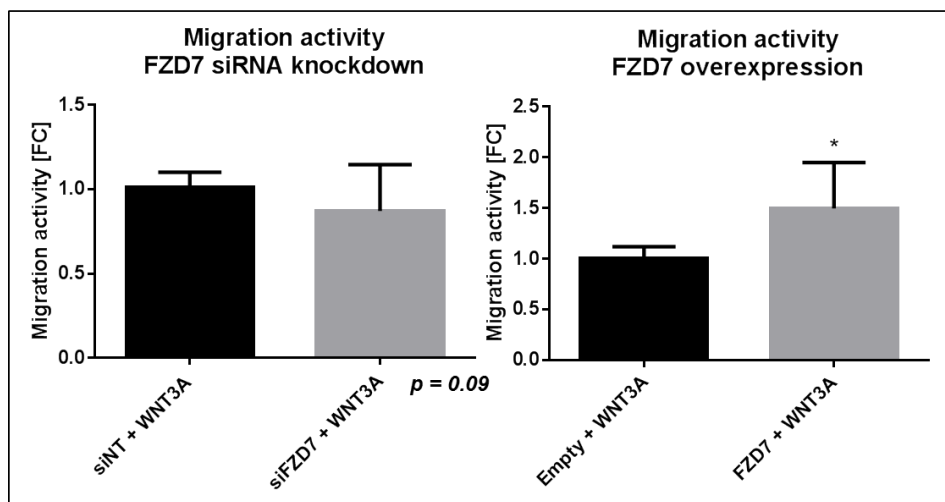
Figure 41: Migration activity after siRNA knockdown or overexpression of FZD7. NT = non-targeting, Empty = empty backbone plasmids. Fold changes (FC) were calculated in comparision to „siNT/Empty + WNT3A" control. Fold changes (FC) were calculated versus (siNT or Empty)/Reporter +WNT3A. Bars include mean and standard deviation. * indicates p < 0.05.

RSPO1 had no significant effects on WNT activity, viability, cell death rate, and caspase or migration activity.

Interestingly, the WNT ligand alone was not able to elevate WNT activity, but in combination with WNT3A, the WNT pathway was significantly increased by ~ 60 % compared to the "Reporter + WNT3A" control, which marked 100 % WNT activity. But if samples "BSA + WNT3A" and "RSPO1 + WNT3A" are compared, no significant difference in WNT activity can be noticed, although the WNT activity of the BSA sample does not significantly differ from that of the sample "Reporter + WNT3A". In general, the negative control indicates that emerging effects on the WNT activity assay were WNT pathway specific. The results from the WNT activity assay are demonstrated in figure 42.

Generally, in the experiments with recombinant proteins it was observed, that there was only a tendency of increased viability of ESCs after WNT3A addition. That would suggest just a minor role of the activated WNT pathway in the viability of endometrial cells. All other functional readouts regarding cell death rate or caspase and migration activity were not altered through WNT3A activation. However, BSA affected viability and migration activity positively. The viability was elevated by BSA in both WNT-activated and non-activated ESCs. Regarding the migration, BSA alone was not able to have an effect, whereas in combination with WNT3A, BSA significantly increased the migration activity of ESCs. These observations suggest that viability might be influenced by BSA in a WNT-independent manner, whereas the migration activity induced by BSA depended on WNT signaling. However, effects on viability by BSA were little and not significant, while the shift in migration activity after BSA treatment was distinct and significant.

RSPO1 treatment did not change cell viability. Eventually, in combination with WNT3A, cells tended to show an enhanced viability level comparable to that of BSA controls. But since the viability of WNT-activated cells did not vary between BSA or RSPO1 treatment, this effect is not of relevance. Only in non-activated ESCs, a significant increase of the viability upon RSPO1 treatment compared to BSA controls was demonstrated (figure 42).

Concerning the cell death rate, caspase or migration activity, no relevant effects could be observed. Although the cell death rate and caspase activity were slightly but significantly decreased upon RSPO1 addition in WNT-activated cells in comparison to the sample "Reporter + WNT3A", no distinction to the respective BSA control was demonstrated. The migration activity could be significantly enhanced by ~ 60 % after RSPO1 and 30 % after BSA treatment in WNT3A-activated cells. Nonetheless, the variation in migration activity between these two proteins was not significant. In non-activated cells no alterations at all were exhibited in any of these functions. All these findings are illustrated in figures 42 and 43.
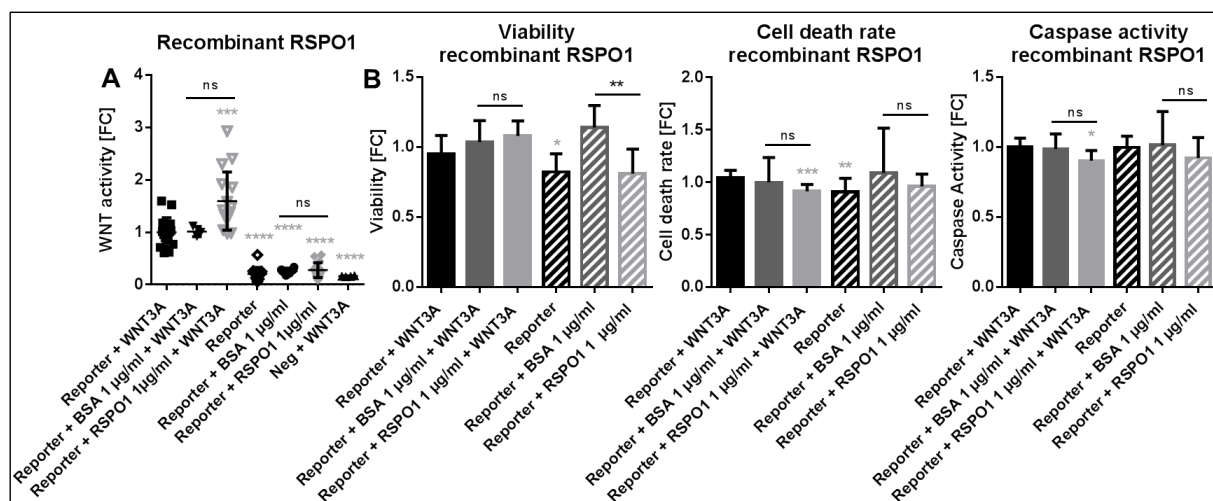

Figure 42: WNT activity and results of the cell based assays after treatment with recombinant RSPO1. (A) WNT activity assay. **(B)** Cell based assays measuring viability, cell death rate, and caspase activity. Neg = Negative control of WNT activity assay. Fold changes (FC) were calculated versus „Reporter +WNT3A" and significant results are indicated through grey stars. Black horizontal bars indicate differences between respective samples. Black stars present significant differences. Scatter dot plots and bars include mean and standard deviation. * indicates $p < 0.05$, ** represents $p < 0.01$, *** indicates $p < 0.001$ and **** $p < 0.0001$, ns = not significant.
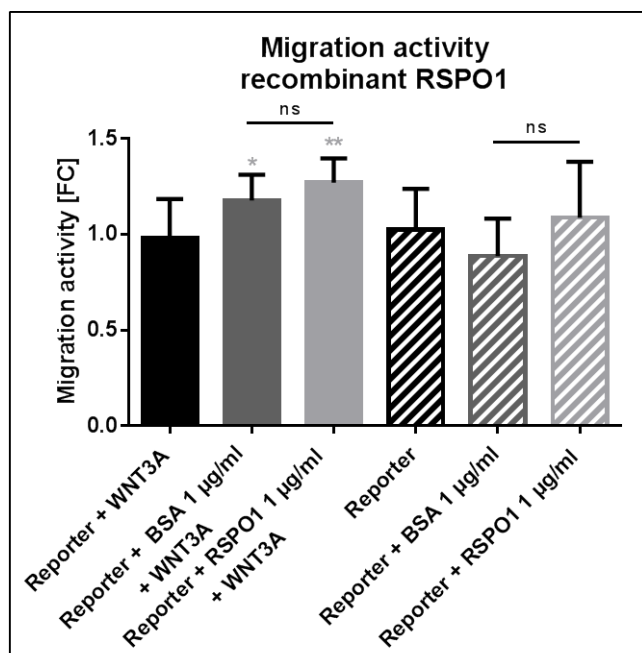
Figure 43: The migration activity of ESCs after treatment with recombinant RSPO1. Fold changes (FC) were calculated versus „Reporter +WNT3A" and significant results are indicated through grey stars. Black horizontal bars indicate differences between respective samples. Bars include mean and standard deviation. * indicates p < 0.05 and ** p < 0.01, ns = not significant.

To sum up, although WNT activity, cell death rate, and caspase and migration activity could be significantly altered through the ligand in WNT3A-activated cells in comparison to "Reporter + WNT3A" samples, the direct relation to BSA controls revealed that these effects were not relevant.

WNT2B significantly reduced WNT signaling, viability, and migration activity but did not show pronounced effects on cell death or caspase activity.

Surprisingly, addition of recombinant WNT2B did significantly decrease WNT signaling by ~ 25 % in WNT-activated cells compared to "Reporter + WNT3A", which marked 100 % activity. Even in relation to "BSA + WNT3A", the reduction is still significant and as indicated by the negative control, WNT pathway specific. The addition of the WNT ligand alone was not able to affect the WNT activity. In figure 44 the resulting WNT activity upon WNT2B treatment is illustrated.

Treatment with WNT2B did not only show a significant decrease of viability and migration activity when compared to "Reporter + WNT3A" but also in relation to BSA controls in cells activated with WNT3A, indicating relevant findings. These alterations might be a consequence of the reduced WNT activity. In non-activated ESCs no significant observations were made. That would mean that the drop in viability and migration activity upon WNT2B addition was WNT pathway-dependent. Interestingly, enhanced cell death rate and caspase activity should follow reduced viability, but that could not be demonstrated in this experiment in either WNT-activated or non-activated cells (figures 44 and 45).
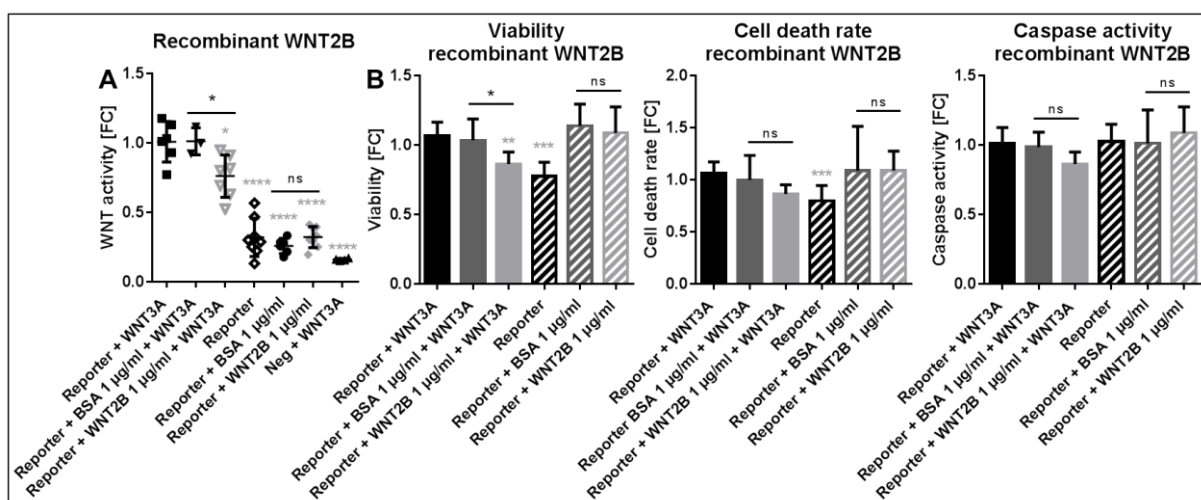
Figure 44: WNT activity and results of the cell based assays after treatment with recombinant WNT2B. (A) WNT activity assay. **(B)** Cell based assays measuring viability, cell death rate, and caspase activity. Neg = Negative control of WNT activity assay. Fold changes (FC) were calculated versus "Reporter +WNT3A" and significant results are indicated through grey stars. Black horizontal bars indicate differences between respective samples. Black stars present significant differences. Scatter dot plots and bars include mean and standard deviation. * indicates $p < 0.05$, ** represents $p < 0.01$, *** indicates $p < 0.001$ and **** $p < 0.0001$, ns = not significant.
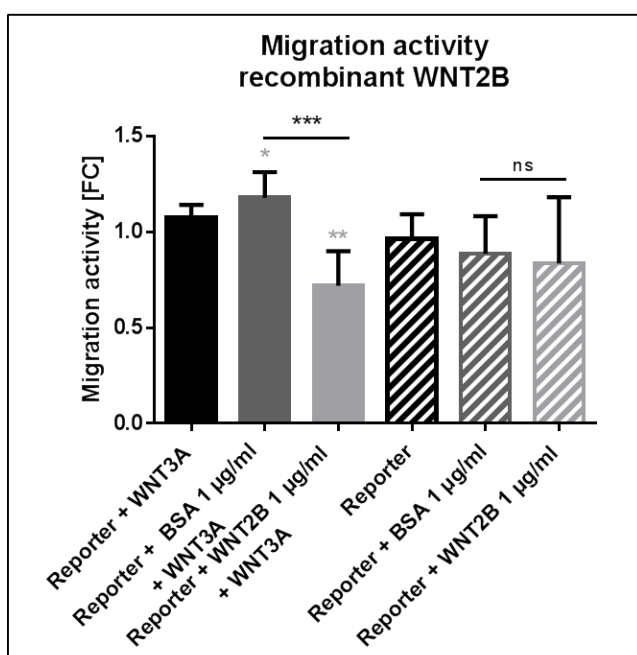

Figure 45: The migration activity of ESCs after treatment with recombinant WNT2B. Fold changes (FC) were calculated versus „Reporter +WNT3A" and significant results are indicated through grey stars. Black horizontal bars indicate differences between respective samples. Black stars present significant differences. Bars include mean and standard deviation. * indicates $p < 0.05$, ** represents $p < 0.01$ and *** $p < 0.001$, ns = not significant.

WNT7A dramatically decreased viability, whereas no significant effects on WNT activity, cell death rate, and caspase and migration activity were observed.

The addition of the recombinant protein alone was not able to affect WNT activity. In combination with WNT3A, the WNT pathway was significantly enhanced by ~ 34 % compared to the sample "Reporter + WNT3A", marking 100 % WNT activity. But in relation to the BSA control of WNT-activated cells, the difference was not significant and therefore not

relevant anymore. Figure 46 illustrates the resulting WNT activity after addition of the WNT ligand.

However, after WNT7A treatment a dramatically decrease by ~ 36 % in the viability of WNT-activated and non-activated cells was observed, which was still significant in comparison to respective BSA controls. Interestingly, significantly reduced cell death rate and/or caspase activity and increased migration activity were not observed in relation to BSA controls but in comparison to "Reporter + WNT3A" samples (figures 46 and 47).

In summary, only the viability of ESCs was affected through treatment with the WNT ligand, but in a WNT independent manner. Moreover, subsequent elevated cell death rate and caspase activity were absent, indicating that no apoptosis or cell death in general occurred.
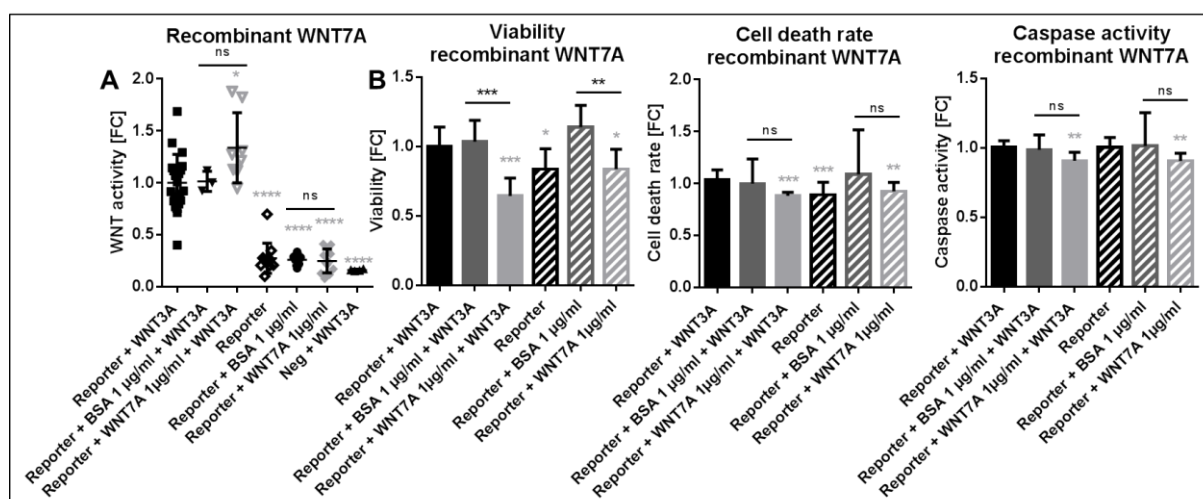

Figure 46: WNT activity and results of the cell based assays after treatment with recombinant WNT7A. (A) WNT activity assay. **(B)** Cell based assays measuring viability, cell death rate, and caspase activity. Neg = Negative control of WNT activity assay. Fold changes (FC) were calculated versus "Reporter +WNT3A" and significant results are indicated through grey stars. Black horizontal bars indicate differences between respective samples. Black stars present significant differences. Scatter dot plots and bars include mean and standard deviation. * indicates $p < 0.05$, ** represents $p < 0.01$, *** indicates $p < 0.001$ and **** $p < 0.0001$, ns = not significant.
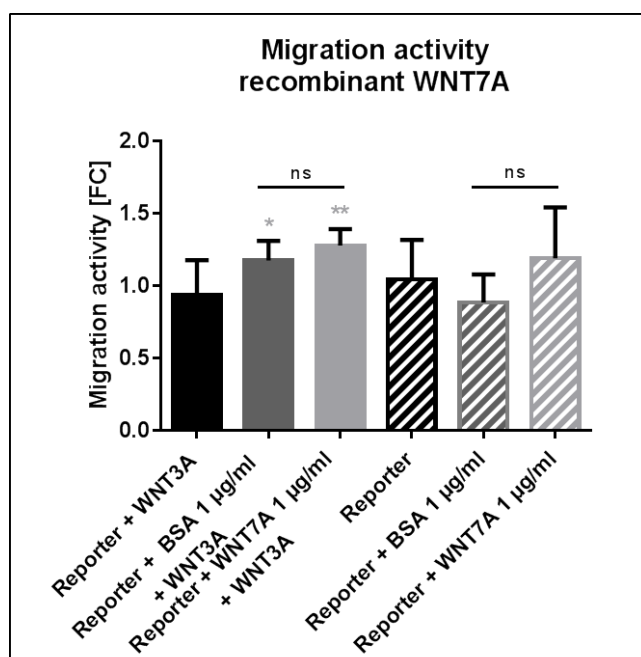
Figure 47: The migration activity of ESCs after treatment with recombinant WNT7A. Fold changes (FC) were calculated versus „Reporter +WNT3A" and significant results are indicated through grey stars. Black horizontal bars indicate differences between respective samples. Bars include mean and standard deviation. * indicates $p < 0.05$ and ** $p < 0.01$, ns = not significant.

With the WNT activity assay and the functional assays also natural WNT inhibitors SFRP1, SFRP2, SFRP4 and WIF1 were investigated but these experiments did not reveal striking findings (data not shown).

4.3.2 Screening of small molecules revealed activity of C59, NVP-TNKS656, ICG-001 and PKF115-584 in endometrial cells *in vitro.*

So far, this study revealed that LGR5 is the most promising candidate, since altered mRNA expression showed large effects on WNT activity, viability, cell death, caspase activity, and migration activity of ESCs. These are all mechanisms that might also play a role in lesion formation in endometriosis. Moreover, as a co-receptor, LGR5 marks an important interface within the WNT pathway by dramatically influencing WNT activity. Due to the lack of LGR5 specific antibodies or small molecules, the protein could not be specifically targeted *in vivo.* LGR5 null mice exhibit 100% neonatal lethality characterized by gastrointestinal tract dilation [255]. Conditional Lgr5 knockout mice in the female reproductive organs by progesterone receptor-Cre have been described before, but were not available [256]. Consequently, various compounds, that influence WNT signaling on different levels, were screened *in vitro* in ESCs to identify chemicals that would allow further investigation of the WNT pathway *in vitro* and *in vivo* later on. Table 29 lists all small molecules that were tested.

Table 29: List of all small molecules that were tested *in vitro* in ESCs.

Molecule	Target	Effect on target	Effect on signaling	Reference
IWP	PORCN	inhibits	**inhibits**	Chen et al., 2009 [205]
C59	PORCN	inhibits	**inhibits**	Proffitt et al., 2013 [206]
WAY-316606	SFRP1	inhibits	**activates**	Bodine et al., 2009 [208]
XAV939	TNKS1/2	inhibits	**inhibits**	Huang et al., 2009 [128]
NVP-TNKS656	TNKS2	inhibits	**inhibits**	Shultz et al., 2013 [209]
IWR	AXIN2	activates	**inhibits**	Chen et al., 2009 [205]
SB-216763	GSK3β	inhibits	**activates**	Coghlan et al., 2000 [214]
IQ1	PP2A	activates	**activates**	Miyabayashi et al., 2007 [211]
QS11	ARFGAP1	activates	**activates**	Zhang et al., 2007 [212]
ICG-001	CBP	inhibits	**inhibits**	Emami et al., 2004 [213]
PKF115-584	TCF/LEF/ β-catenin	inhibits	**inhibits**	Lepourcelet et al., 2004 [204]

All compounds were found by literature review and tested in the WNT activity assay first to evaluate their effects on the WNT pathway.

The controls proved the integrity of the WNT activity assay. LiCl is known to further facilitate WNT signaling, but was not able to initiate the WNT pathway on its own. The highest concentration of DMSO used in the compound screen (10 µM) did not affect WNT activity suggesting that the effects observed in the single assays were specific to the small molecules. Moreover, negative controls, which contained an inoperative mCMV promoter, demonstrated that the emerging signals were indeed WNT specific (figure 48).

For the screening of the WNT inhibitors, WNT signaling had to be activated through WNT3A to investigate their inhibitory potential. WNT inhibitors tested included IWP, C59, XAV939, NVP-TNKS656, IWR, ICG-001, and PKF115-584. Most of the compounds were able to effectively inhibit WNT signaling. The concentration of 1 µM of IWP was able to significantly decrease WNT activity by ~ 64 %, whereas the treatment with a higher concentration of the compound did only show a tendency of reduced WNT signaling by ~ 36 %. The concentration of 1 µM of XAV939 only slightly decreased WNT signaling by ~ 2.5 %. Surprisingly, 10 µM of XAV939 significantly increased the WNT pathway by ~ 39 %. The concentration of 10 µM of ICG-001 or PKF115-584 significantly decreased the WNT pathway by ~ 86 % or ~ 96 % accordingly. The tankyrase inhibitor NVP-TNKS-656, IWR, and C59 exhibited WNT inhibition in a dose-dependent manner. The concentration of 1 µM or 5 µM of NVP-TNKS-656 resulted in a decrease of ~ 32 % and ~ 41 % respectively. For IWR, 1 µM of the small molecule significantly inhibited WNT signaling by ~ 71 % and 10 µM increased the effect to 85 % WNT inhibition. 10 nM of C59 by trend reduced WNT signaling by ~ 4 %, 100 nM showed already significantly decerased WNT activity by ~ 48 % and 1 µM even increased the effect to 97 % WNT inhibition. The results of the screening of WNT inhibitors in the WNT activity assay are summarized in figure 48.

WNT activators were tested in both WNT-activated and non-activated cells to examine their own activating potential and eventual synergistic or inhibitory effects. Tested WNT activators included WAY-3166061, SB-216763, IQ1, and QS11. Generally, only few WNT activators were able to effectively initiate or increase WNT signaling. Some of them even reduced the WNT activity. Except for WAY-3166061 and SB-216763 at concentrations of 100 nM or 10 µM respectively, no other compound could initiate the WNT pathway. In combination with WNT3A and depending on the concentration, the assay measured either a trend of or significantly elevated or reduced WNT activity. WAY-3166061 decreased WNT signaling by ~ 15 % (10 nM) or significantly lowered WNT activity by ~ 85 % (100 nM) or 50 % (1 µM). SB-216763 only tended to enhance WNT signaling by ~ 288 % at 10 µM but at 1 µM the compound even inhibited the WNT pathway by ~ 31 %. Also IQ1 exhibited a WNT reduction

of ~ 17 % and ~ 76 % at 1 µM and 10 µM respectively. QS11 demonstrated a significantly decrease of WNT activity by ~ 65 % at lower concentration (2 µM) and a tendency of elevated WNT signaling by ~ 34 % at higher concentration (10 µM). The screening of WNT activators in the WNT activity assay is demonstrated in figure 49.
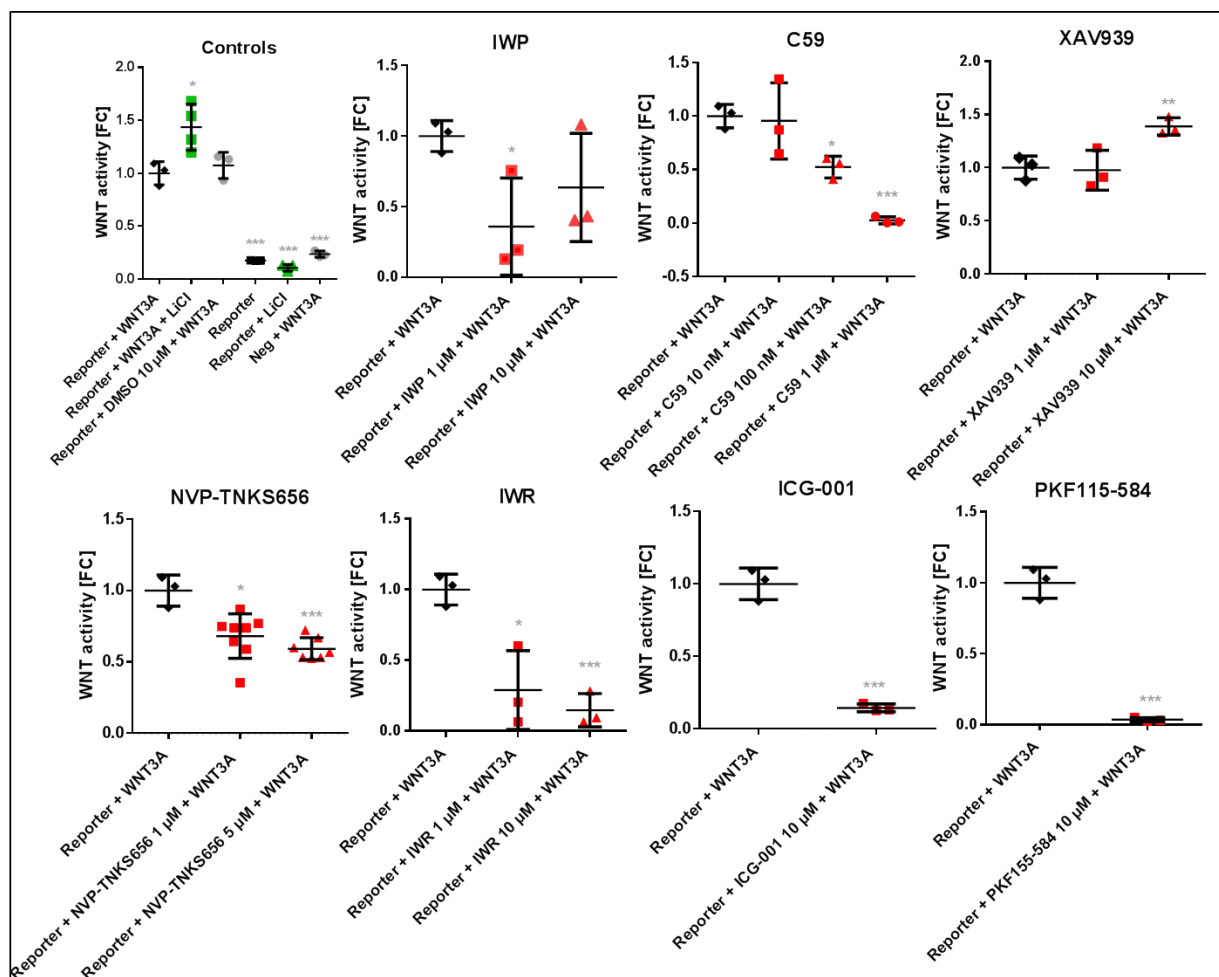

Figure 48: WNT activity after the treatment with controls and selected WNT inhibitors. Fold changes (FC) were calculated versus "Reporter +WNT3A" and significant results are indicated through grey stars. Scatter dot plots include mean and standard deviation. * indicates p < 0.05, ** represents p < 0.01 and *** p < 0.001.

Figure 49: WNT activity after the treatment with selected WNT activators. Fold changes (FC) were calculated versus "Reporter +WNT3A" and significant results are indicated through grey stars. Scatter dot plos include mean and standard deviation. * indicates $p < 0.05$, ** represents $p < 0.01$ and *** $p < 0.001$.
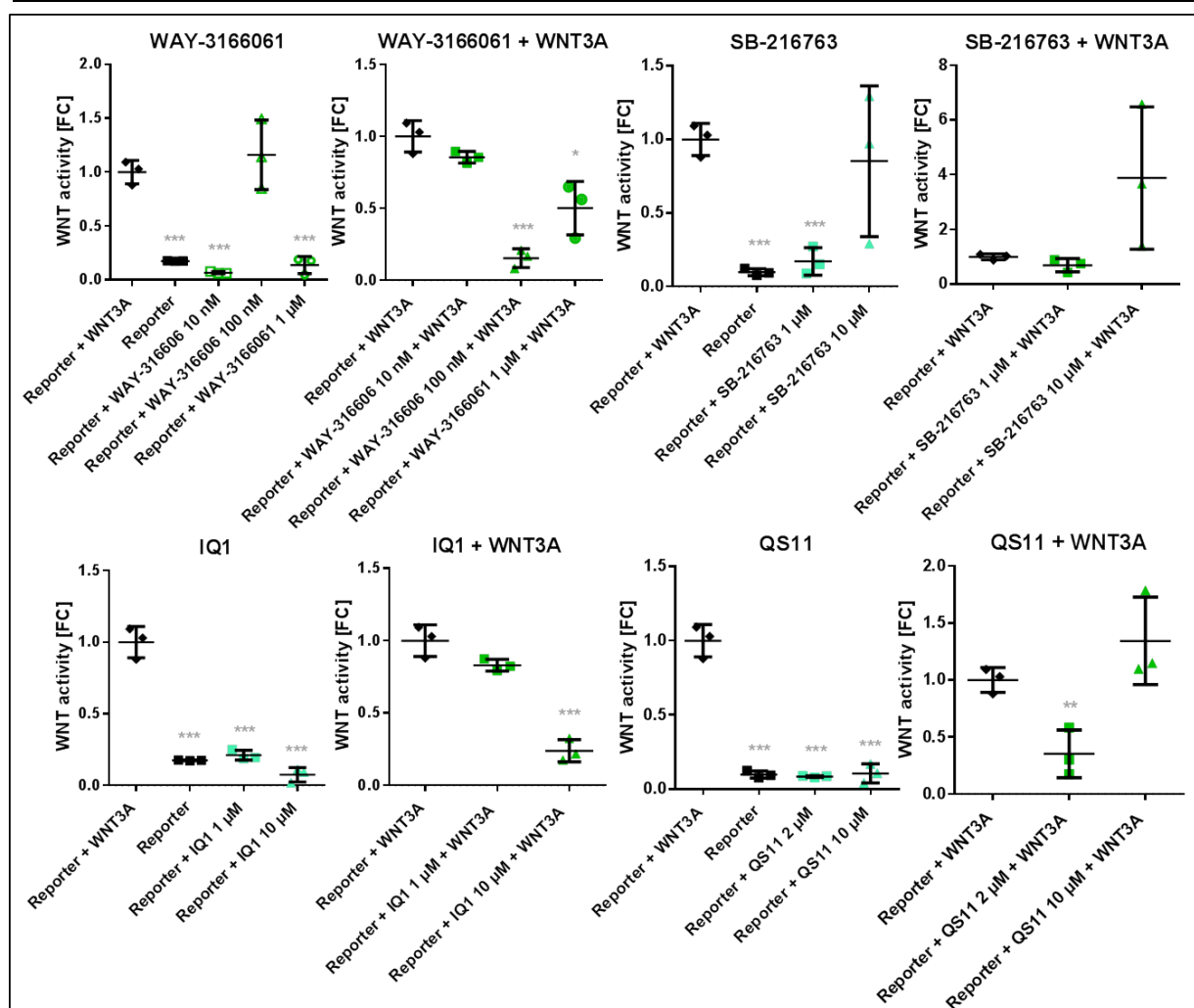
In summary only few compounds exhibited appropriate effects on WNT activity, restricting the number of suitable small molecules for potential *in vivo* usage.

4.3.3 Dose response experiments revealed NVP-TNKS656 for the potential use *in vivo*.

Due to their promising inhibitory effects on the WNT pathway, C59, NVP-TNKS656, ICG-001, and PKF115-584 were further investigated *in vitro*. Dose response experiments were performed using WNT-activated ESCs to determine the half maximal inhibitory concentration (IC_{50}), which represents the concentration of the compound, which is required to inhibit 50 % of a maximum effect (figure 50). From the activators no small molecule was selected for further examination due no favourable activating effects.
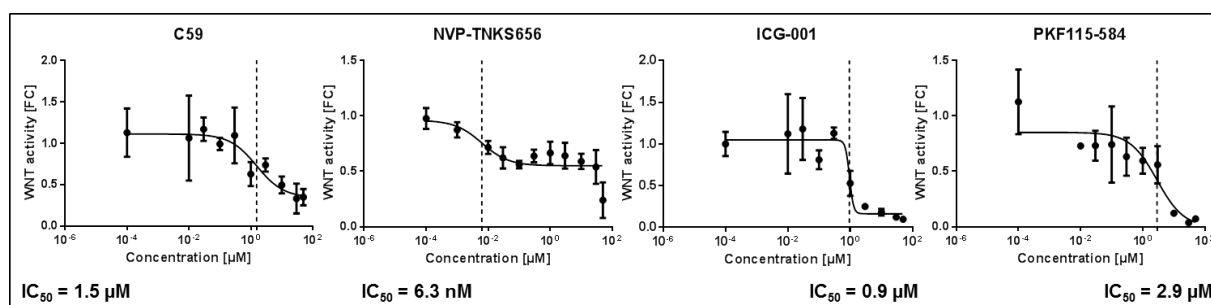
Figure 50: Dose response experiments with WNT-activated ESCs and small molecule inhibitors C59, NVP-TNKS656, ICG-001 and PKF115-584. IC_{50} = maximal inhibitory concentration.

From the dose response experiments an IC_{50} of 1.5 µM for C59, 6.3 nM for NVP-TNKS656, 0.9 µM for ICG-001, and 2.9 µM for PKF115-586 was calculated.

Based on the literature, all compounds have already been applied *in vivo* without showing high toxicity. C59 blocked the progression of mammary tumors in MMTV-WNT1 transgenic mice while downregulating Wnt/β-catenin target genes without exhibiting apparent toxicity [206]. NVP-TNKS656 demonstrated more robust apoptosis and antitumor activity in a xenograft model with SW480 colon cancer cells in female athymic nude mice [210]. ICG-001 was efficacious in Min mouse and nude mouse xenograft models of colon cancer by initiating programmed cell death through downregulation of survivin, which inhibits apoptosis [213]. PKF115-584 for instance was tested in a chronic lymphatic leukaemia (CLL)-like xenograft model in nude mice and tumor inhibition of 57% was observed when compared with vehicle-treated controls and the intervention was well tolerated [257].

However, except for NVP-TNKS656, the IC_{50} values detected were relatively high, rising the concerns, that for visible effects in an *in vivo* endometriosis model, required doses of the compounds would be high and might therefore cause severe side effects. Furthermore, C59 as a PORCN inhibitor blocks WNT secretion. ESCs are not able to secrete WNTs in an autocrine fashion, so there is no basis for WNT inhibition at this level in these cells. Consequently, the small molecule should not show any effects in these cells. Indeed, dose response-dependent inhibition of WNT activity by C59 was observed, suggesting, that these effects might be unspecific. But its derivative LGK974, which has the same mechanism of action, was more specific since it did not show any effects in ESCs (data not shown). Moreover, it has been already successfully used in several *in vivo* studies at well-tolerated doses [207, 235]. It demonstrated induced tumor regression in a MMTV-WNT1 murine breast cancer model and inhibition of proliferation and induction of differentiation of RNF43-mutant pancreatic adenocarcinoma xenograft models [207, 235].

4.3.4 NVP-TNKS656 significantly reduced viability, cell death rate and migration activity in endometrial cells *in vitro*.

Based on the results from the dose response experiments and the consequent considerations, NVP-TNKS656 was selected for further examination *in vitro* in terms of viability, cell death, caspase, and migration activity before its usage *in vivo*. LGK974 has been also shortlisted but could be not pre-tested in ESCs. It acts on PORCN consequently blocking WNT secretion but ESCs are not able to secrete WNTs naturally.

The WNT pathway activity in WNT-activated cells was significantly decreased by ~ 36 % upon NVP-TNKS656 treatment in comparison to the respective DMSO control. As indicated by the negative control, this effect was WNT pathway specific. As expected, the compound alone was not able to affect WNT signaling in non-activated ESCs. DMSO alone could also not influence the WNT pathway (figure 51).

After the treatment of WNT-activated ESCs with the small molecule, the viability significantly decreased by ~ 22 % in relation to the appropriate DMSO sample as illustrated in figure 51. Consequently, the cell death rate significantly increased by ~ 19 % respectively in WNT-activated cells. Interestingly, also in non-activated cells the viability dropped by ~ 20 % compared to DMSO upon NVP-TNKS656 treatment. Moreover, the caspase activity did not reveal any alterations through any of the conditions suggesting that programmed cell death is not responsible for the raised cell death rate.

The migration activity of WNT activated and non-activated cells was significantly decreased by ~ 28 % and 33 % respectively through the tankyrase inhibitor NVP-TNKS656 in relation to DMSO controls (figure 52).

To sum up, NVP-TNKS656 had an impact on WNT activity and viability, cell death rate, and migration activity respectively. Interestingly, the caspase activity did not change suggesting that apoptosis was not involved in increased cell death.
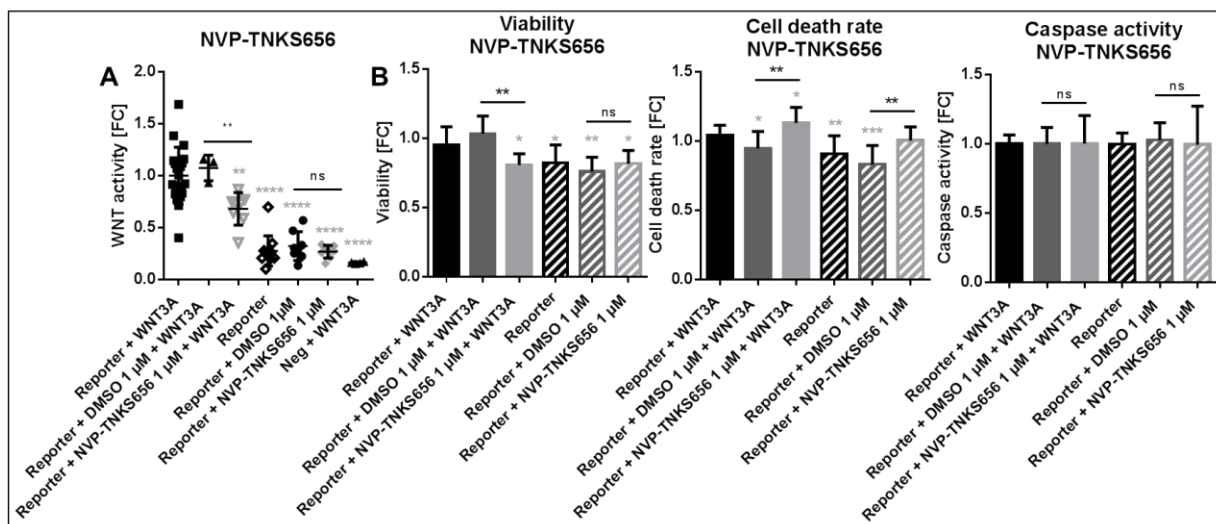
Figure 51: WNT activity and results of the cell based assays after treatment with NVP-TNKS656. (A) WNT activity assay. **(B)** Cell based assays measuring viability, cell death rate, and caspase activity. Neg = Negative control of WNT activity assay. Fold changes (FC) were calculated versus „Reporter +WNT3A" and significant results are indicated through grey stars. Black stars indicate significant differences between respective samples. Scatter dot plots and bars include mean and standard deviation.* indicates $p < 0.05$, ** represents $p < 0.01$, *** indicates $p < 0.001$ and **** $p < 0.0001$, ns = not significant.
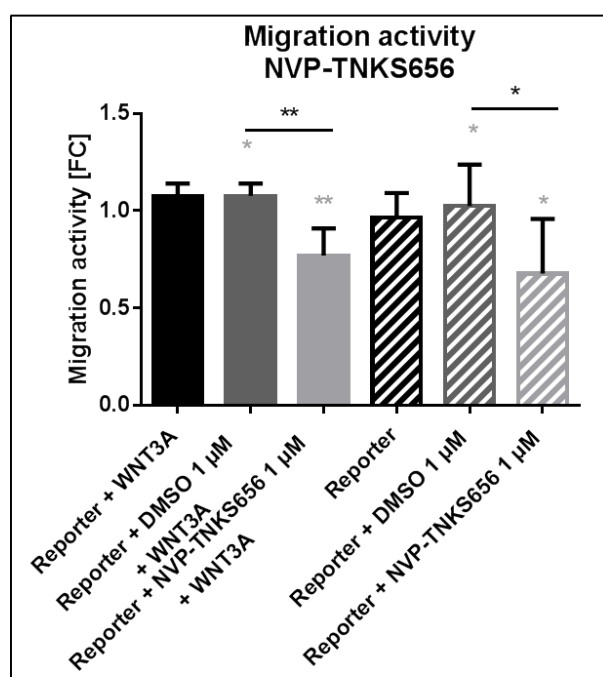

Figure 52: The migration activity of ESCs after the treatment with NVP-TNKS656. Fold changes (FC) were calculated versus „Reporter +WNT3A" and significant results are indicated through grey stars. Black stars indicate significant differences between respective samples. Bars include mean and standard deviation. * indicates $p < 0.05$ and ** represents $p < 0.01$.

4.4 Investigation of the WNT pathway *in vivo*

Based on the *in vitro* results, NVP-TNKS656 and LGK974 were chosen for the *in vivo* experiment. However, a pilot study with both small molecules in mice revealed that NVP-TNKS5656 treatment caused a high mortality. Therefore further *in vivo* experiments with this compound were not reasonable (data not shown). Nevertheless, the pilot study with LGK974 was promising allowing a final *in vivo* experiment with the mice inoculation model for endometriosis. An advantage of the PORCN inhibitor LGK974 is that it acts further upstream within the WNT pathway than the tankyrase inhibitor NVP-TNKS656 enabling a broader inhibition of WNT signaling. Moreover, since it blocks WNT secretion, it also affects the WNT pathway further upstream than the WNT receptors and ligands LGR5, FZD7, WNT2B, WNT7A, and RSPO1. Consequently, potential observed effects might be also attained in a similar way through inhibition of these WNT candidate genes.

Mice were inoculated with 12 uterine fragments on day 0 and treated with 5 mg/kg LGK974 or vehicle twice a day by oral gavage, as described in chapter 3.5.2. Body weight was measured once a week and mice were sacrificed 7 or 14 days after inoculation. Number and size of lesions were measured to evaluate disease burden. Blood samples taken on the day of sacrifice should give information about plasma concentrations of the compound. Furthermore, mRNA expression of the selected WNT candidate genes, additional WNT associated genes and genes without connection to WNT siganling was investigated due to their described or potential role in endometriosis (e.g. hormone receptors). Moreover, protein levels of β-catenin were also measured to evaluate β-catenin degradation indicating WNT activity.

4.4.1 LGK974 significantly reduced disease burden in the mice inoculation model *in vivo*.

Upon 7 days of treatment with LGK974, the lesion number tended to be reduced, although the morphology of the lesions did not vary between the control and the compound group. On day 14, lesion number as well as total lesion size significantly decreased by ~ 47 % and 71 % respectively upon LGK974 treatment. Also the morphology of the lesions did change. While lesions from the control group were big and cystic, samples from the compound group were small and degraded. Consequently, the disease burden could be reduced through WNT pathway inhibition.

Figure 53 depicts lesions taken form day 7 and 14 of treatment with LGK974. Three representative samples were chosen for each condition. Lesion number and total lesion sizes on day 7 and 14 are demonstrated in figure 54.
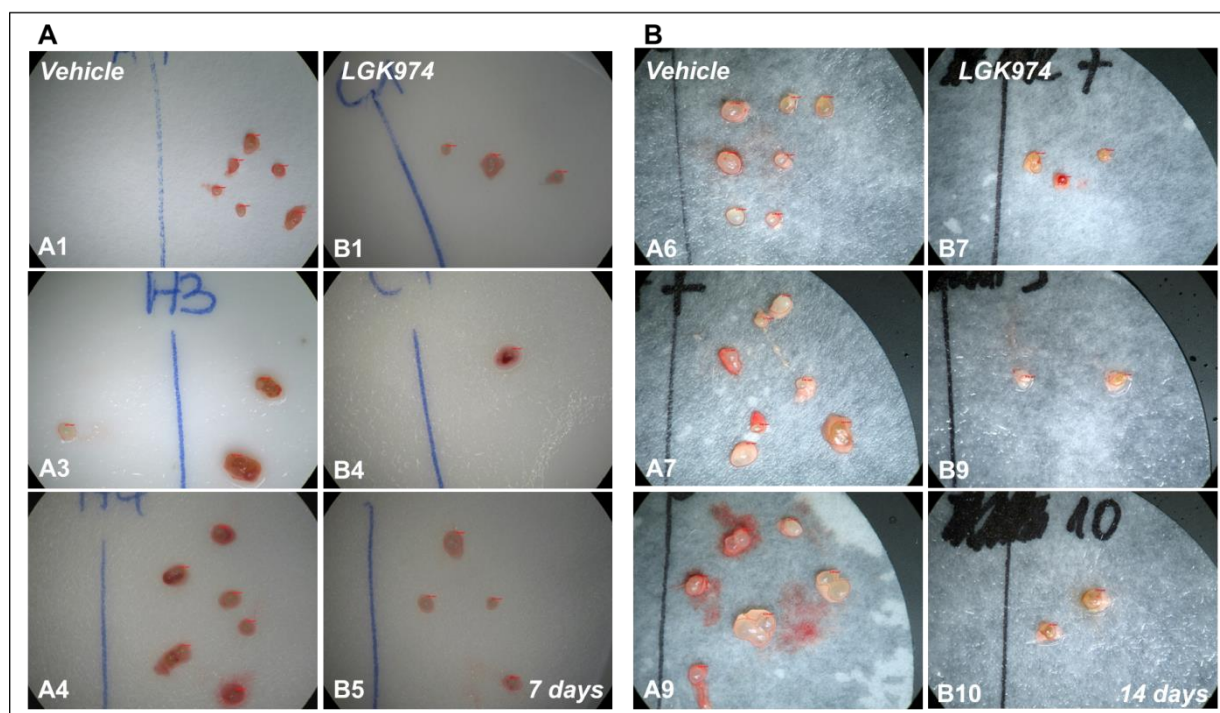
Figure 53: Lesions taken 7 or 14 days after endometrium challenge of the compound and the vehicle group. (A) Lesions taken on day 7 after treatment. **(B)** Lesions taken on day 14 after treatment. Samples "A" were collected from the vehicle group and "B" from the compound group. Samples to the left of the line indicate loose lesions, and samples to the right of the line present adherent lesions.
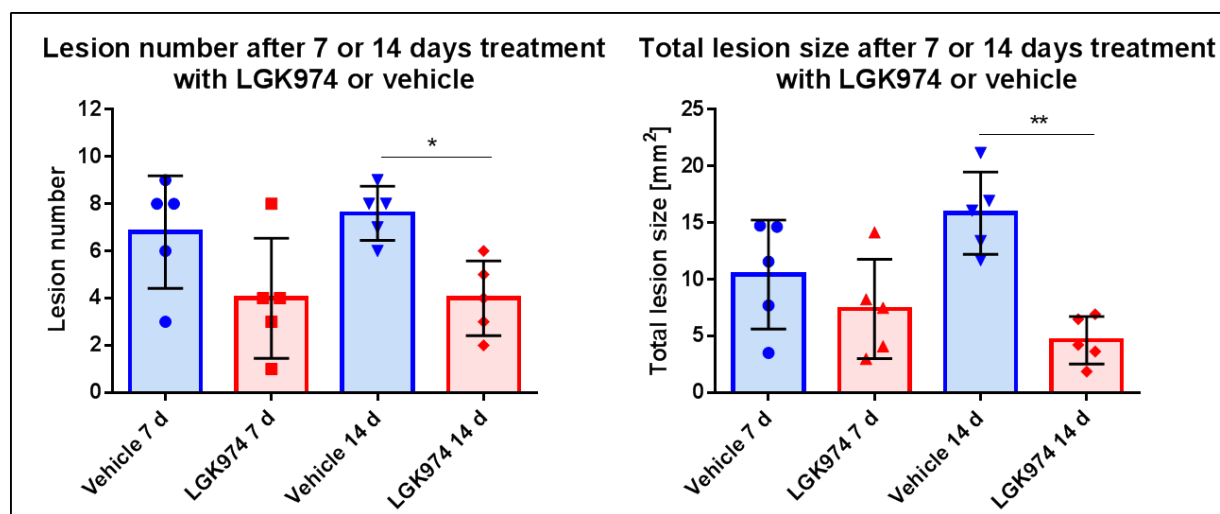

Figure 54: Lesion number and total lesion size after 7 or 14 days of treatment with LGK974 or the vehicle. D = days. Black stars indicate significant differences between respective samples. Bars include mean and standard deviation. * indicates $p < 0.05$ and ** represents $p < 0.01$.

The molecular mode of action from the *in vivo* study was also examined. Generally, expression levels of the direct WNT target gene Axin2 demonstrated that it was downregulated upon LGK974 treatment. In the uterus, already after 7 days the Axin2 mRNA expression was significantly reduced compared to controls. But after 14 days an increase in variability of Axin2 expression did not allow to measure significant effects anymore, though the degree of downregulation was comparable to day 7. In lesions, Axin2 mRNA expression showed a trend of reduction after 7 days and a significant reduction after 14 days in relation

to the vehicle group suggesting that the WNT pathway might be generally inhibited in implants through LGK974 (figure 55B).

The overall β-catenin protein levels were expected to drop upon WNT inhibition. Protein isolation was only possible from the uteri and some samples had to be excluded due to degradtion. However, protein levels of overall β-catenin did not change in the uteri at either day 7 or day 14 after treatment with LGK974 (figure 55A).

Plasma concentrations of LGK974 proved that the levels were sufficient to assume that the observed effects could indeed result from drug action. An IC_{50} value of 0.4 nM had been previously determined by Liu at al. in a relative luciferase WNT co-culture assay [207]. Since ESCs do not secrete WNT3A in an autocrine fashion, the IC_{50} could not be investigated in a comparable way in this study (figure 55C).

The compound was well tolerated as illustrate in figure 56. Although the mice lost body weight of about 5 % compared to the vehicle group at day 5 of the treatment, they entirely recovered and expressed high vitality afterwards.
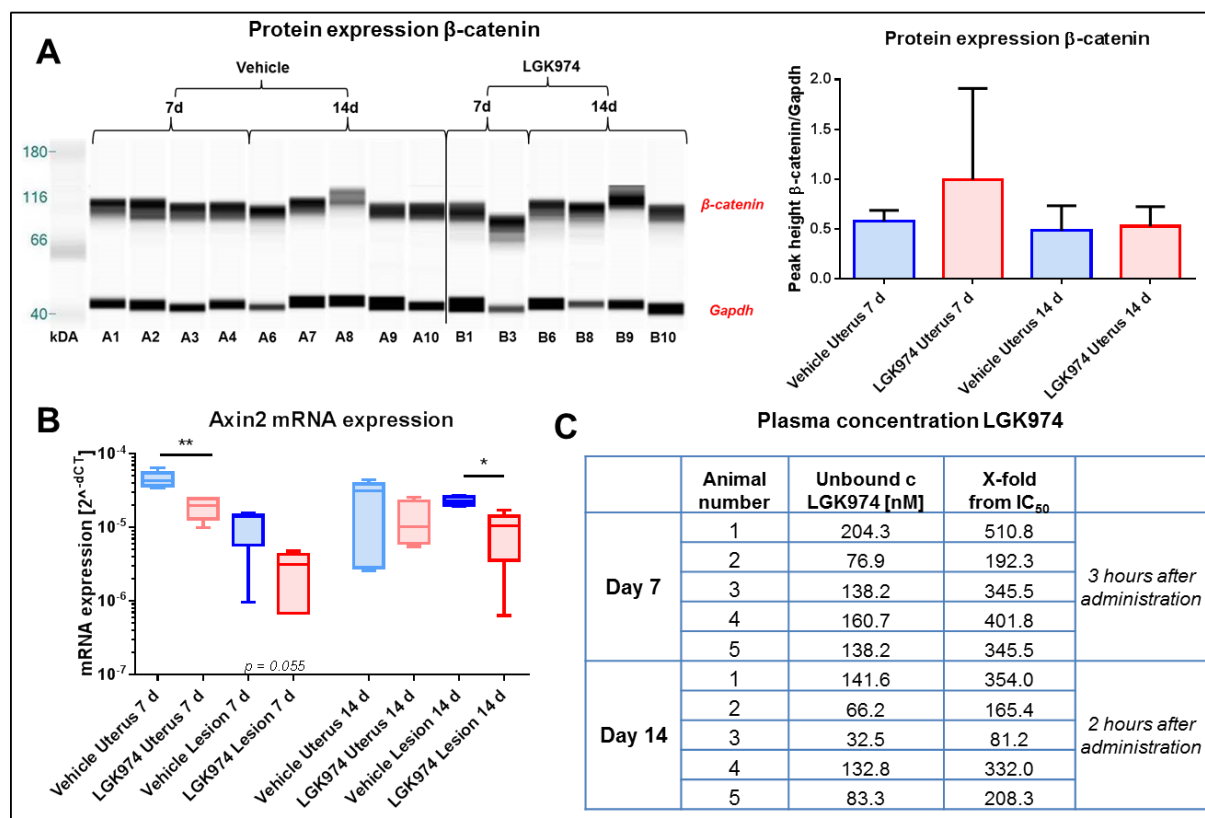

Figure 55: Molecular mode of action of LGK974 in the mice inoculation model for endometriosis. (A) Protein levels of overall β-catenin. **(B)** Axin2 mRNA expression. **(C)** Plasma concentrations of LGK974. The cellular IC_{50} value of 0.4 nM was taken from the literature [207]. d = days, samples "A", were collected from the vehicle group and "B" from the compound group. Black stars indicate significant differences between respective samples. Bars include mean and standard deviation. * indicates $p < 0.05$ and ** represents $p < 0.01$.
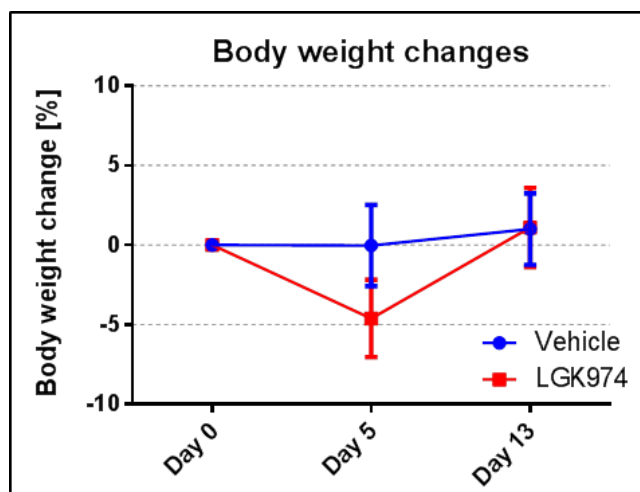
Figure 56: The body weight of mice on day 5 and 13 after treatment with LGK974 or the vehicle.

4.4.2 After 14 days of treatment with LGK974, the mRNA expression of many WNT pathway genes and genes that are involved in migration or vascularization were reduced.

With the *ex vivo* samples TaqMan analyses were performed for WNT pathway genes and also for genes that are connected to mechanisms such as migration, proliferation, or apoptosis which might also play a role in lesion formation in endometriosis. Table 30 lists all genes, of which the mRNA expression was anaylzed.

Table 30: Annotations of 29 genes measured by TaqMan in the *ex vivo* samples. All genes highlighted in orange are WNT pathway genes, which are either directly or indirectly regulated through WNT signaling according to IPA. If stated, they contain the TCF/LEF binding motif and are direct target genes of WNT signaling. IPA = Ingenuity Pathway Analysis, ECM = Extracellular matrix, EMT = Epithelial mesenchymal transition, TF = Transcription factor.

Gene	Full name	Annotation
Bax	Bcl-2-like protein 4	Apoptosis [236]
Bcl2	B-cell lymphoma 2	Anti-apoptosis [237]
Cav1	Caveolin-1	Metastatic growth (inhibition anoikis) [238]
Cdh1	E-Cadherin	Adhesion [258], direct WNT target gene (inverse regulated) [138, 139]
Cdk1	Cyclin D1	Proliferation [259], direct WNT target gene [137]
Dkk3	Dickkopf WNT signaling pathway inhibitor 3	WNT inhibitor by disruption FZD/WNT interaction [239]
Esr1	E2 receptor 1	Hormone receptor
Esr2	E2 receptor 2	Hormone receptor
Fgf9	Fibroblast growth factor 9	Proliferation, cell survival [240]
Fzd7	Frizzled-7	WNT receptor [241], direct WNT target gene [149]
Hif1a	Hypoxia-inducible factor 1-alpha	Angiogenesis [260]
Lgr5	Leucine-rich repeat-containing G-protein coupled receptor 5	WNT coreceptor, direct WNT target gene [150, 242]
Lrp1	Low density lipoprotein receptor-related protein 1	WNT inhibitor by interacting with FZD1 [243], migration [244, 245]

Mapk10	Mitogen-activated protein kinase 10	Proliferation [246]
Mki67	Marker of proliferation Ki-67	Proliferation [247]
Mmp2	matrix metalloproteinase 2	ECM degradation → migration [248], direct WNT target gene [142]
Mmp9	matrix metalloproteinase 3	ECM degradation → migration [249], direct WNT target gene [142]
Pgr	Progesterone receptor	Hormone receptor
Pou5f1/Oct4	Octamer-binding transcription factor 4	Stem cell self-renewal [261], direct WNT target gene [262]
Rspo1	R-spondin 1	WNT ligand [250]
Sfrp1	Secreted frizzled-related protein 1	WNT inhibitor by binding WNTs [251]
Sfrp2	Secreted frizzled-related protein 2	WNT inhibitor by binding WNTs [251], eventually direct WNT target gene [151]
Snai2	Snail family zinc finger 1	Represses Cdh1 → Migration [263]
Tbx18	T-Box 18	TF → cell differentiation [253]
Vcam1	Vascular cell adhesion protein 1	Adhesion immune cells[264]
Vegfa	Vascular endothelial growth factor A	Angiogenesis [265], direct WNT target gene [144]
Wif1	Wnt inhibitory factor 1	WNT inhibitor by binding WNTs [251]
Wnt2b	Wingless-type MMTV integration site family, member 2B	WNT ligand [254]
Wnt7a	Wingless-type MMTV integration site family, member 7A	WNT ligand [254]

LGK974 versus vehicle after 7 and 14 days of treatment

The gene expression of uteri and lesions from the *in vivo* experiment were measured via TaqMan and compared between treatment and control group after 7 and 14 days.

After 7 days the uteri of mice treated with the small molecule exhibited many WNT pathway genes that were downregulated. One of them is the direct WNT target gene and pathway member Lgr5. Further genes were Sfrp2 and Wif1, which are involved in WNT pathway inhibition, Cdk1 that triggers proliferation, Vegfa, which is responsible for angiogenesis and the transcription factor Tbx18 that plays a role in cell differentiation. Mki67 and Pgr are not WNT pathway genes, but they were also downregulated in the uteri of the compound group. Interestingly, after 14 days the gene expression of the uteri recovered and normalized. Except for Cdh1, compound and vehicle group did not differ in mRNA expression anymore. Cdh1 was significantly upregulated in the uteri form mice treated with LGK974. It is a direct target gene and inversely regulated by the WNT pathway. Cdh1 encodes E-cadherin, which plays a role in adhesion. Figure 57 and table 31 summarize these results.

In lesions, the direct target gene Lgr5 was 100 fold downregulated after 7 and 14 days of treatment with LGK974. In addition, after 7 days the WNT inhibitor Wif1 exhibited a 100 fold reduction in mRNA expression. Moreover, the non-WNT associated genes Bcl2, which has antiapoptotic functions, and Esr2 showed a tendency of decreased mRNA levels upon WNT

inhibition. After 14 days the gene expression pattern of lesions changed. Except for Lgr5, different genes were deregulated when compared to the samples after 7 days of treatment. The WNT pathway genes Rspo1, Sfrp2, Sfrp1, and Cdk1 were downregulated in the compound group. Sfrp1 and Sfrp2 are WNT inhibitors and decreased mRNA levels of Cdk1 suggest reduced proliferation in implants upon WNT inhibition. Moreover, Pgr mRNA, which is not a WNT pathway gene, was also almost significantly decreased in ectopic tissue upon LGK974 treatment for 14 days (figure 58 and table 32).

Altogether, many WNT pathway or non-WNT associated genes were downregulated upon WNT inhibition. After 7 days of treatment the effect seemed to be higher on uteri than on lesions, since more genes were deregulated. Interestingly, after 14 days the gene expression pattern changed. In the uteri, the mRNA expression normalized, so that mRNA levels did not strongly differ between treatment and control group. By contrast, the number of downregulated genes in lesions of the compound group increased. However, except for Lgr5 different genes were deregulated in lesions after 14 days of treatment.
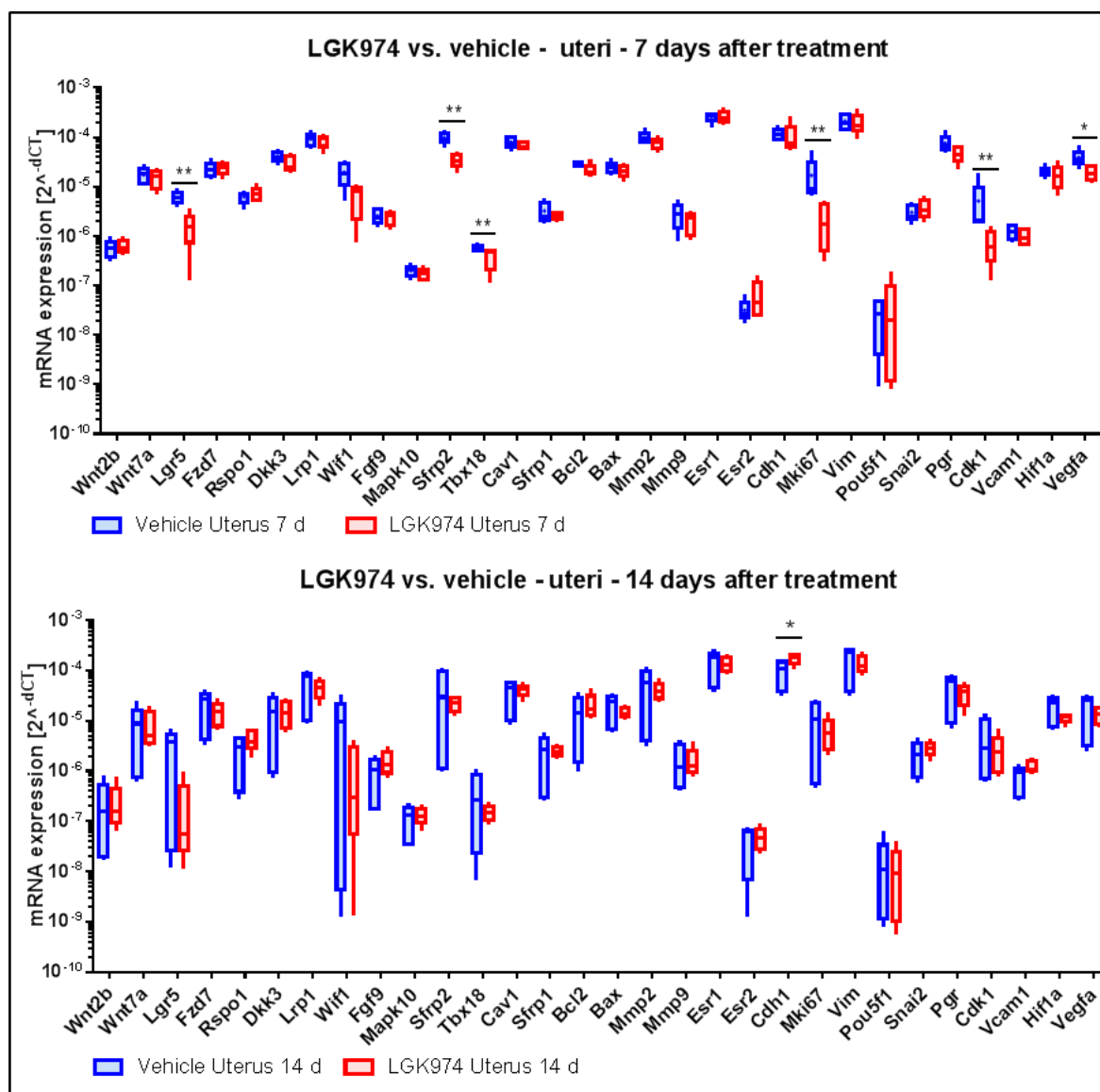
Figure 57: TaqMan mRNA expression analysis of *ex vivo* uteri after 7 and 14 days of treatment with LGK974 compared to the vehicle group. Blue bars indicate vehicle group and red bars indicate compound group. Box boundaries: 25th and 75th percentiles; solid line: median; whiskers: Min to Max. d = days. * indicates p < 0.05 and ** represents p < 0.01.

Table 31: Fold changes (FC) and p-values from the TaqMan mRNA expression analysis of *ex vivo* uteri after 7 and 14 days of treatment with LGK974 compared to the vehicle group. Red highlighted rows indicate significant results and orange highlighted rows indicate mRNA expression differences with trend to significance.

| LGK974 uterus vs. vehicle uterus					
7 days			**14 days**		
Gene	**FC**	**p-Value**	**Gene**	**FC**	**p-Value**
Wnt2b	1.10	0.841	Wnt2b	0.99	0.841
Wnt7a	0.87	0.548	Wnt7a	0.98	0.841
Lgr5	*0.26*	*0.008*	Lgr5	0.08	0.421
Fzd7	1.07	0.841	Fzd7	0.71	0.691
Rspo1	1.15	0.999	Rspo1	1.76	0.310
Dkk3	0.74	0.222	Dkk3	1.03	0.999
Lrp1	0.94	0.999	Lrp1	0.84	0.691
Wif1	*0.32*	*0.056*	Wif1	0.12	0.548
Fgf9	0.91	0.691	Fgf9	1.65	0.548
Mapk10	0.88	0.548	Mapk10	1.13	0.999
Sfrp2	*0.36*	*0.008*	Sfrp2	0.48	0.691
Tbx18	*0.66*	*0.008*	Tbx18	0.37	0.691
Cav1	0.85	0.548	Cav1	1.16	0.881
Sfrp1	0.81	0.999	Sfrp1	1.05	0.999
Bcl2	0.75	0.135	Bcl2	1.39	0.691
Bax	0.85	0.421	Bax	0.74	0.691
Mmp2	0.77	0.421	Mmp2	0.79	0.841
Mmp9	0.71	0.548	Mmp9	0.91	0.841
Esr1	1.02	0.889	Esr1	0.93	0.841
Esr2	2.05	0.310	Esr2	1.16	0.999
Cdh1	0.90	0.151	*Cdh1*	*1.79*	*0.032*
Mki67	*0.14*	*0.008*	Mki67	0.55	0.841
Pou5f1	1.62	0.651	Pou5f1	0.76	0.999
Snai2	1.24	0.548	Snai2	1.32	0.548
Pgr	*0.61*	*0.095*	Pgr	0.80	0.691
Cdk1	*0.14*	*0.008*	Cdk1	0.52	0.841
Vcam1	0.82	0.286	Vcam1	1.63	0.151
Hif1a	0.82	0.310	Hif1a	0.61	0.548
Vegfa	*0.49*	*0.016*	Vegfa	0.72	0.691
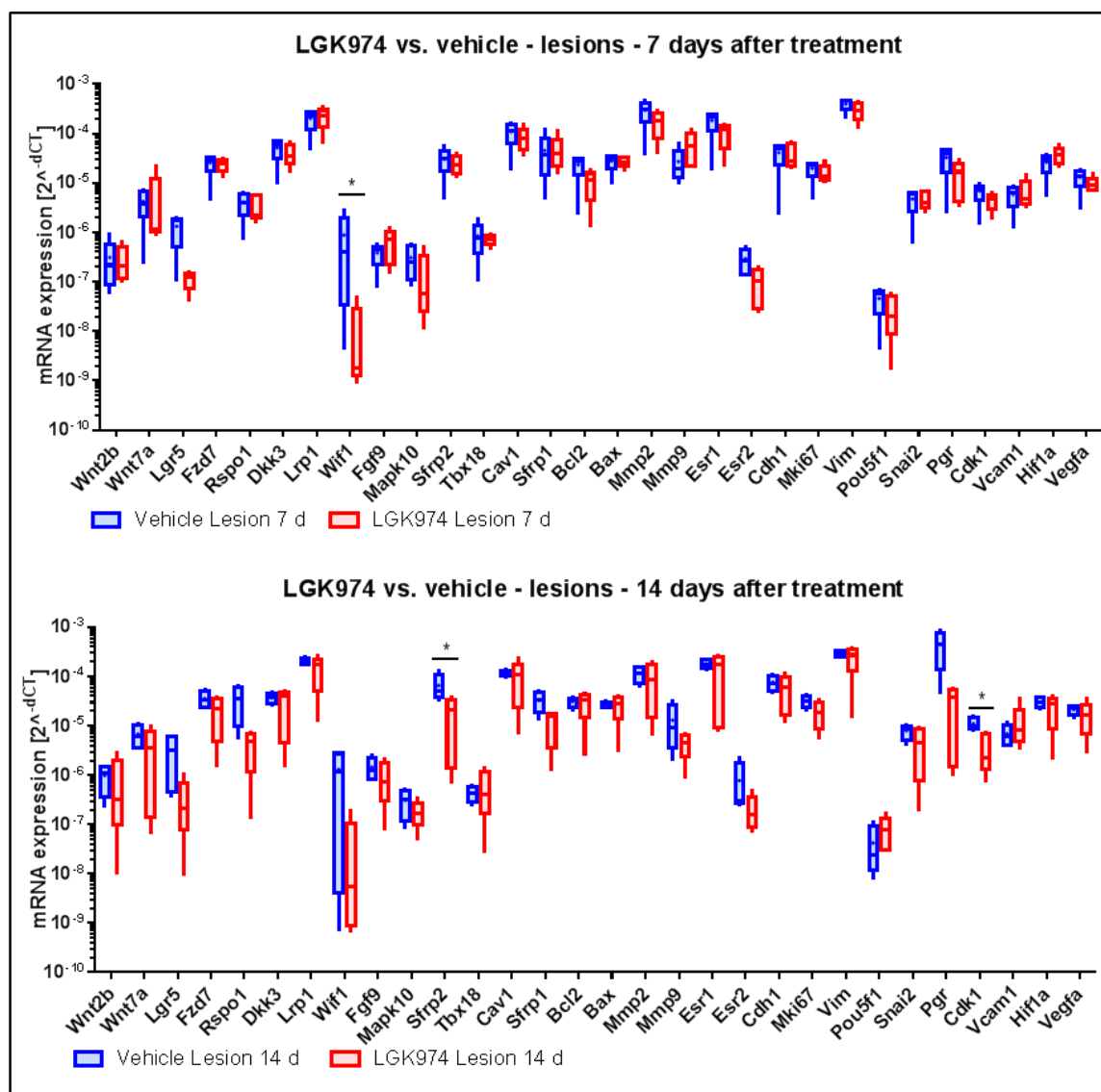
Figure 58: TaqMan mRNA expression analysis of *ex vivo* lesions after 7 and 14 days of treatment with LGK974 compared to the vehicle group. Blue bars indicate vehicle group and red bars indicate compound group. Box boundaries: 25th and 75th percentiles; solid line: median; whiskers: Min to Max. d = days. * indicates p < 0.05 and ** represents p < 0.01.

Table 32: Fold changes (FC) and p-values from the TaqMan mRNA expression analysis of *ex vivo* lesions after 7 and 14 days of treatment with LGK974 compared to the vehicle group. Red highlighted rows indicate significant results and orange highlighted rows indicate mRNA expression differences with trend to significance.

LGK974 lesion vs. vehicle lesion					
7 days			**14 days**		
Gene	**FC**	**p-Value**	**Gene**	**FC**	**p-Value**
Wnt2b	0.95	0.999	Wnt2b	0.91	0.556
Wnt7a	1.30	0.548	Wnt7a	0.57	0.413
Lgr5	0.09	0.056	Lgr5	0.11	0.064
Fzd7	0.91	0.310	Fzd7	0.59	0.191
Rspo1	0.83	0.548	Rspo1	0.12	0.064
Dkk3	0.77	0.548	Dkk3	0.78	0.905
Lrp1	1.09	0.841	Lrp1	0.69	0.318
Wif1	*0.01*	*0.032*	Wif1	0.03	0.413
Fgf9	1.64	0.421	Fgf9	0.67	0.286
Mapk10	0.51	0.167	Mapk10	0.59	0.286
Sfrp2	0.80	0.421	*Sfrp2*	*0.28*	*0.032*
Tbx18	0.84	0.841	Tbx18	1.40	0.905
Cav1	0.75	0.421	Cav1	0.89	0.595
Sfrp1	1.04	0.841	Sfrp1	0.35	0.111
Bcl2	0.45	0.095	Bcl2	0.94	0.905
Bax	0.97	0.548	Bax	0.97	0.730
Mmp2	0.59	0.151	Mmp2	0.83	0.905
Mmp9	2.21	0.151	Mmp9	0.34	0.191
Esr1	0.54	0.151	Esr1	0.76	0.960
Esr2	0.34	0.095	Esr2	0.27	0.111
Cdh1	0.94	0.999	Cdh1	0.75	0.556
Mki67	0.81	0.548	Mki67	0.60	0.191
Pou5f1	0.60	0.310	Pou5f1	1.93	0.191
Snai2	1.00	0.999	Snai2	0.60	0.286
Pgr	0.45	0.151	Pgr	0.07	0.064
Cdk1	0.64	0.151	*Cdk1*	*0.34*	*0.016*
Vcam1	1.14	0.841	Vcam1	1.75	0.730
Hif1a	1.38	0.548	Hif1a	0.77	0.730
Vegfa	0.73	0.310	Vegfa	0.79	0.365

Lesion versus uteri – vehicle and LGK974 after 7 and 17 days of treatment

After 7 days, the comparison between lesions and uteri from the control group revealed both, the significant reduction and elevation of the gene expression of many WNT pathway genes. Wnt7a, Lgr5, Wif1, Fgf9, Sfrp2, and Vegfa were significantly expressed at lower levels. Wnt7a and Lgr5 are WNT pathway members, Wif1 and Sfrp2 are WNT inhibitors and Fgf9 is involved in proliferation and cell survival. Nevertheless, other WNT pathway genes showed increased mRNA levels. Sfrp1 and Mmp9 were significantly increased. Sfrp1 is a WNT pathway inhibitor and Mmp9 is implicated in ECM degradation and therefore could contribute to cell invasion. Cdh1 mRNA expression, which is inversely regulated through WNT signaling and plays a role in migration, was significantly reduced in implants. Consequently, its downregulation could also support cell migration in implants. Vegfa downregulation in lesions proposes reduced vascularization. Other genes without connection to WNT signaling were also deregulated in endometriotic implants. Vcam plays a role in the adhesion of immune cells and was significantly upregulated. Consequently, elevated mRNA expression of Vcam would suggest that immune cells increasingly adhere to ectopic tissue. Elevated mRNA levels of Esr2 and decreased mRNA expression of Pgr and Esr1 were also observed. After 14 days, all emerging deregulated WNT pathway genes in lesions exhibited invariably elevated mRNA expression (Wnt2b, Rspo1, Dkk3, Lrp1, Cav1, Sfrp1, Mmp9, and Snai2). That suggests that the WNT pathway is indeed hyperactive in lesions. Rspo1 and Wnt2b are WNT pathway members and Dkk3 and Sfrp1 function as WNT inhibitors. Cav1, Mmp9, Lrp1, and Snai2 are all implicated in cell migration suggesting elevated migration activity of endometriotic cells (figure 59 and table 33).

Lesions compared to uteri taken from mice treated with LGK974 exhibited similar results after 7 days of treatment. Again, many WNT pathway genes were expressed at lower and higer levels in implants. Wnt2b, Wnt7a, Lgr5, Rspo1, Lrp1, Wif1, Fgf9, and Vegfa exhibited reduced mRNA levels, while the mRNA expression of Tbx18, Sfrp1, Mmp9, and Cdk1 was increased. Tbx18 is involved in cell differentiation. Although dropped levels of Fgf9 indicate reduced proliferation in lesions, raised mRNA expression of Cdk1 and the non-WNT pathway gene Mki67 suggest increased proliferation in ectopic cells. Cdh1, which is inversely regulated through the WNT pathway, was significantly decreased. Other genes without association to WNT signaling were also deregulated in implants. Vcam1 and Hif1a mRNA levels were increased, while Pgr, Esr1, and Hif1 gene expression was significantly decreased. Although dropped levels of Vegfa in the implants of LGK974 treated animals suggest decreased angiogenesis, elevated Hif1a mRNA expression may have supported this process. Moreover, reduced Bcl2 mRNA expression proposes increased apoptosis of

endometriotic cells. After 14 days the number of deregulated genes dropped upon WNT inhibition making uterus and lesion more similar in terms of mRNA expression. Except for Cdh1, the gene expression of most of the WNT pathway genes recovered and normalized. Wif1 and Mmp9 for example just exhibited a tendency of deregulated gene expression. The direct WNT target gene Pou5f1/Oct4 was significantly expressed at higher levels in lesions of the compound group proposing increased self-renewal of stem cells. Redarding non-WNT pathway genes the mRNA expression of Esr2, Mki67, and Vcam1 was increased. In comparison to 7 days of treatment with LGK974 the proliferation of ectopic cells as indicated by Mki67 was reduced. The adhesion of immune cells and consequent altered immunity mediated through elevated mRNA levels of Vcam1 might have been raised. Gene expression of Esr2 was also raised after 14 days in relation to 7 days of treatment (figure 60 and table 34).

In summary, ectopic samples from both the vehicle and the compound group showed, that the WNT pathway was rather downregulated in the beginning but aberrantly activated at a later time point. Additionally, many genes, which are implicated in migration, angiogenesis, proliferation, immunity, or apoptosis exhibited deregulated mRNA expression levels in both groups after 7 days. However, after 14 days, treatment with LGK974 normalized the gene expression of many WNT pathway genes in lesions and therefore also positively influenced mechanisms such as migration or proliferation.
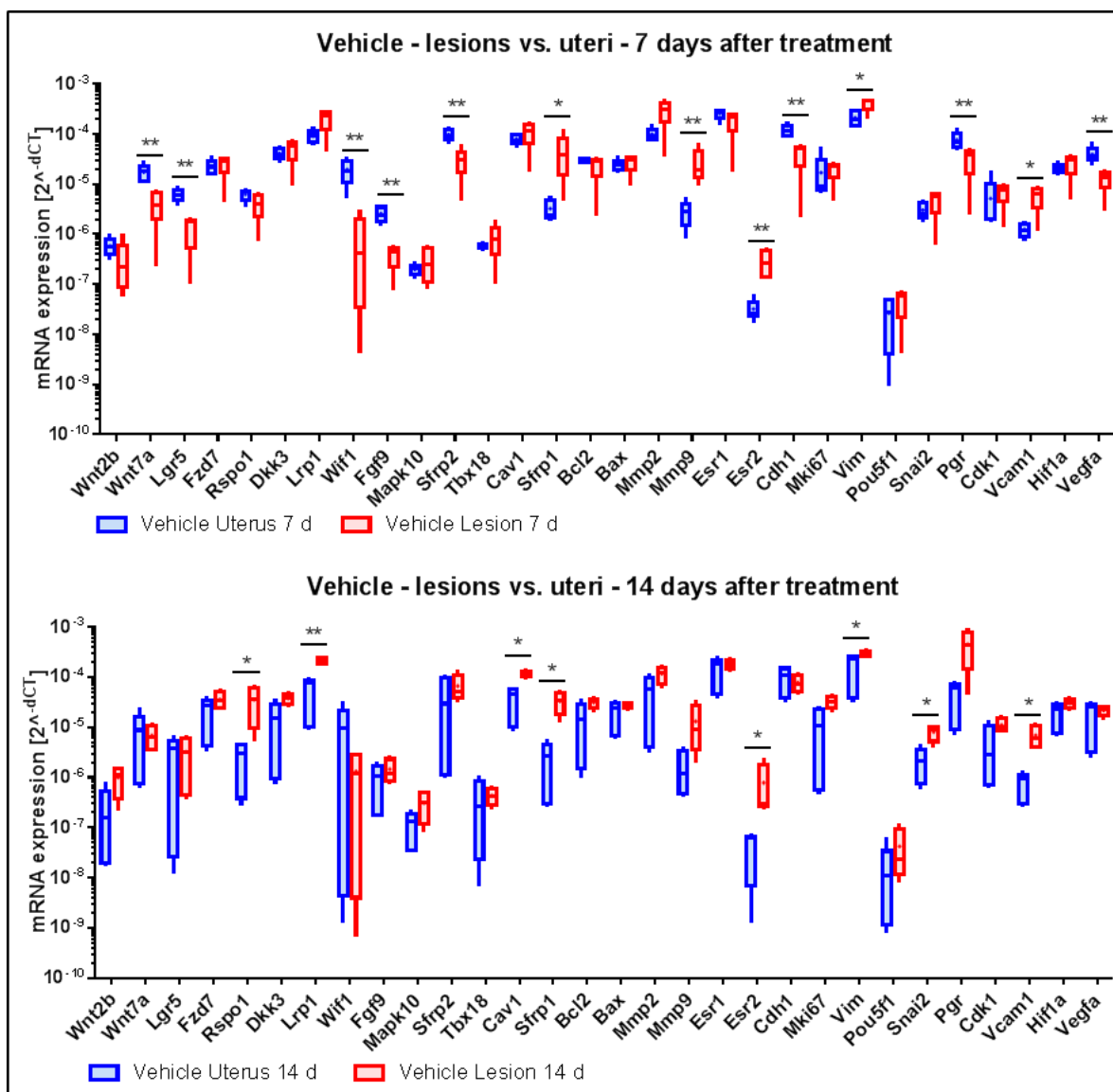
Figure 59: TaqMan mRNA expression analysis of *ex vivo* lesions versus uteri of the vehicle group after 7 and 14 days. Blue bars indicate vehicle group and red bars indicate compound group. Box boundaries: 25th and 75th percentiles; solid line: median; whiskers: Min to Max. d = days. * indicates p < 0.05 and ** represents p < 0.01.

Table 33: Fold changes (FC) and p-values from the TaqMan mRNA expression analysis of *ex vivo* lesions versus uteri of the vehicle group after 7 and 14 days. Red highlighted rows indicate significant results and orange highlighted rows indicate mRNA expression differences with trend to significance.

| Vehicle lesion vs. vehicle uterus					
7 days			**14 days**		
Gene	**FC**	**p-Value**	**Gene**	**FC**	**p-Value**
Wnt2b	0.54	0.151	Wnt2b	4.01	0.064
Wnt7a	*0.24*	*0.008*	Wnt7a	0.80	0.905
Lgr5	*0.22*	*0.008*	Lgr5	1.13	0.730
Fzd7	1.15	0.548	Fzd7	1.71	0.413
Rspo1	0.66	0.156	*Rspo1*	*13.88*	*0.016*
Dkk3	1.25	0.222	Dkk3	2.54	0.064
Lrp1	2.23	0.156	*Lrp1*	*3.95*	*0.016*
Wif1	*0.04*	*0.008*	Wif1	0.13	0.413
Fgf9	*0.15*	*0.008*	Fgf9	1.52	0.556
Mapk10	1.56	0.841	Mapk10	2.67	0.191
Sfrp2	*0.31*	*0.008*	Sfrp2	1.48	0.413
Tbx18	1.47	0.222	Tbx18	1.08	0.905
Cav1	1.37	0.156	*Cav1*	*3.27*	*0.016*
Sfrp1	*14.14*	*0.016*	*Sfrp1*	*13.71*	*0.016*
Bcl2	0.81	0.691	Bcl2	2.07	0.191
Bax	1.13	0.421	Bax	1.34	0.730
Mmp2	3.01	0.151	Mmp2	2.27	0.111
Mmp9	*9.69*	*0.008*	Mmp9	7.25	0.064
Esr1	0.73	0.095	Esr1	1.26	0.905
Esr2	*9.19*	*0.008*	*Esr2*	*18.81*	*0.016*
Cdh1	*0.35*	*0.008*	Cdh1	0.80	0.905
Mki67	1.16	0.548	Mki67	2.75	0.064
Pou5f1	1.75	0.206	Pou5f1	2.60	0.286
Snai2	1.56	0.151	*Snai2*	*3.71*	*0.016*
Pgr	*0.43*	*0.008*	Pgr	10.34	0.111
Cdk1	1.34	0.548	Cdk1	2.16	0.111
Vcam1	*4.75*	*0.032*	*Vcam1*	*9.05*	*0.016*
Hif1a	1.28	0.151	Hif1a	1.62	0.191
Vegfa	*0.34*	*0.008*	Vegfa	1.19	0.683
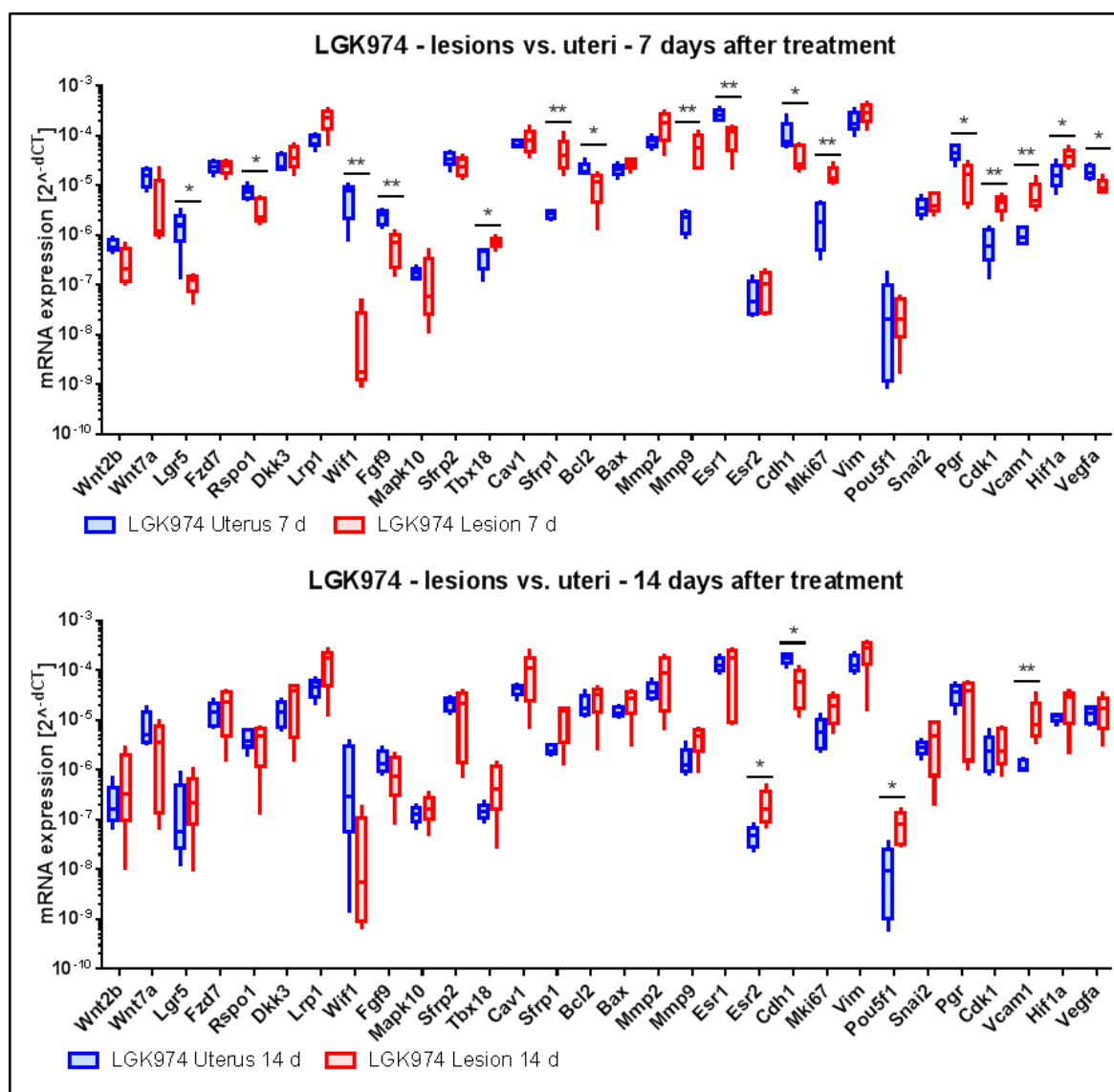
Figure 60: TaqMan mRNA expression analysis of *ex vivo* lesions versus uteri of the compound group after 7 and 14 days. Blue bars indicate vehicle group and red bars indicate compound group. Box boundaries: 25th and 75th percentiles; solid line: median; whiskers: Min to Max. d = days. * indicates p < 0.05 and ** represents p < 0.01.

Table 34: Fold changes (FC) and p-values from the TaqMan mRNA expression analysis of *ex vivo* lesions versus uteri of the compound group after 7 and 14 days. Red highlighted rows indicate significant results and orange highlighted rows indicate mRNA expression differences with trend to significance.

LGK974 lesion vs. vehicle uterus					
7 days			**14 days**		
Gene	**FC**	**p-Value**	**Gene**	**FC**	**p-Value**
Wnt2b	0.47	0.056	Wnt2b	3.68	0.310
Wnt7a	0.37	0.095	Wnt7a	0.47	0.421
Lgr5	0.07	0.032	Lgr5	1.58	0.421
Fzd7	0.99	0.999	Fzd7	1.42	0.691
Rspo1	0.47	0.032	Rspo1	0.93	0.999
Dkk3	1.31	0.548	Dkk3	1.91	0.548
Lrp1	2.58	0.095	Lrp1	3.28	0.151
Wif1	0.00	0.008	Wif1	0.03	0.095
Fgf9	0.27	0.008	Fgf9	0.61	0.222
Mapk10	0.90	0.310	Mapk10	1.38	0.548
Sfrp2	0.69	0.151	Sfrp2	0.85	0.999
Tbx18	1.86	0.016	Tbx18	4.04	0.151
Cav1	1.21	0.841	Cav1	2.51	0.421
Sfrp1	18.16	0.008	Sfrp1	4.53	0.151
Bcl2	0.49	0.016	Bcl2	1.40	0.421
Bax	1.29	0.222	Bax	1.76	0.151
Mmp2	2.30	0.151	Mmp2	2.38	0.691
Mmp9	29.95	0.008	Mmp9	2.70	0.095
Esr1	0.39	0.008	Esr1	1.03	0.841
Esr2	1.54	0.452	Esr2	4.42	0.016
Cdh1	0.36	0.016	Cdh1	0.34	0.016
Mki67	6.91	0.008	Mki67	3.02	0.095
Pou5f1	0.65	0.691	Pou5f1	6.63	0.032
Snai2	1.26	0.421	Snai2	1.69	0.691
Pgr	0.31	0.016	Pgr	0.85	0.999
Cdk1	5.92	0.008	Cdk1	1.40	0.841
Vcam1	6.62	0.008	Vcam1	9.73	0.008
Hif1a	2.16	0.032	Hif1a	2.04	0.151
Vegfa	0.50	0.032	Vegfa	1.30	0.600

5   DISCUSSION

5.1   The WNT pathway is globally involved in endometriosis.

A clinical study to investigate the mRNA expression of healthy and diseased human eutopic and ectopic samples via gene arrays exhibited upregulation of the WNT pathway in endometriosis. Stromal and epithelial tissue was separated via LCM previously to gain a higher resolution of the gene expression. TaqMan analysis with the same samples confirmed these findinigs.

This study enabled the detection of new genes dysregulated in endometriosis such as SFRP2 or WIF1. It was discovered that selected WNT pathway members LGR5, FZD7, RSPO1, WNT2B, and WNT7A were significantly upregulated in ectopic samples compared to matching diseased or healthy eutopic endometrium. Some of the WNT members were found to be dysregulated in endometriosis for the first time (figure 20). These findings are supported by a recent study by de Mattos et al. which also reports significantly increased WNT activity in endometriotic lesions compared to matching eutopic endometrium in a rat model of endometriosis [266]. The gene expression of Wnt4 and Wnt7b were significantly increased and the gene expression of Gsk3β and Cdh1 were decreased [266]. Furthermore, upregulated WNT signaling was indicated by significantly elevated levels of stromal and nuclear β-catenin in these implants compared to matching eutopic tissue [266]. Altogether, these findings support the theory of the involvement of the WNT pathway in endometriosis.

In our study, apart from the selected WNT pathway members, many inhibitory WNT downstream genes such as DKK3, SFRP2, SFRP1, or WIF1 were elevated indicating upregulation of the WNT pathway in diseased eutopic endometrium compared to healthy controls or in lesions compared to eutopic endometrium of patients (figures 21 – 24 and tables 23 – 26). All these genes are regulated through WNT signaling. WNT pathway inhibitory genes AXIN2 and DKK1 have been previously described as direct WNT target genes by containing the TCF/LEF motif and they are activated through WNT signaling [153, 156]. It was suggested that they participate in an autoregulatory negative feedback loop to limit outraged WNT activity [153, 156]. DKK3 also contains the TCF/LEF motif. Therefore, it is conceivable that DKK3 and all the other inhibitory genes are upregulated to counter-regulate aberrantly upregulated WNT activity in endometriosis. Moreover, SFRP1 has been also previously described to be significantly increased in endometriotic tissue compared to controls [267]. Potentially, hyperactivation of the WNT pathway causes numerous WNT

facilitating genes to be excessively active but possibly less mediators of the negative feedback loops exist and therefore activation of WNT signaling exceeds its inactivation. However, this had to be measured on the endpoints of WNT pathway activation by the investigation of proliferation, cell death, or migration.

Generally, mRNA expression levels of the eutopic endometrium of endometriosis patients were already slightly different from that of healthy controls, a finding that corroborates previous reports [268, 269]. However, the greatest distinction in gene expression was found between diseased eutopic endometrium and lesions, which has been also already described by other studies (e.g. [270, 271]). Since healthy and diseased eutopic endometrium exhibit an almost comparable gene expression, the search for potential biomarkers enabling non-invasive diagnosis is challenging.

5.1.1 WNT pathway members indicative for migration and proliferation are higher expressed in endometriosis patients.

In this study, further WNT pathway genes, that might contribute to the establishment and maintenance of endometriotic implants by affecting migration (CAV1, MMP2 or LRP1) or proliferation (MAPK10 or FGF9) were deregulated in endometriosis (see for annotation table 22 and [238, 240, 244-246, 248]) upon gene array or TaqMan analysis of the mRNA expression in clinical samples (figures 21 – 24 and tables 23 – 26). Most of them were found to be dysregulated for the first time.

LRP1 and CAV1 for example were not yet directly linked to endometriosis. Their expression levels have been described to be highly elevated in endometrial carcinomas previously [272, 273]. Moreover, LRP1 induced the expression of MMP2 in human glioblastoma U87 cells and MMP2 increased the migration activity of endometrial cells [245, 274, 275]. It was shown that the total and active forms of this protein were significantly higher in menstrual epithelial and stromal cells of endometriosis patients compared to those of healthy individuals [275]. Generally, endometriotic epithelial and stromal cells were more invasive than those of matching eutopic endometrium of the same diseased women and their invasiveness could be significantly decreased by the treatment with a WNT inhibitor [275]. These results are in agreement with previous findings, where ectopic cells showed invasive and metastatic phenotypes similar to carcinoma cells [226, 276]. After treatment with a WNT inhibitor, levels of active MMP2 in endometrial epithelial cells and levels of total and active MMP9 in endometrial stromal cells were significantly reduced compared to those of matching eutopic endometrium [275]. That proposes a decrease of the invasive phenotype and that aberrant WNT signaling might be involved in this process [275]. Therefore, it is likely that also LRP1, which is described to operate upstream from MMP2, and CAV1 contribute to the invasive

phenotype in this disease. Generally, these findings are in accordance with the implantation theory postulating that migration and invasion appear to be critical in the pathogenesis of endometriosis and aberrant activation of WNT signaling may be involved in these mechanisms [3, 201].

In our study, for the first time elevated mRNA levels of MAPK10 and FGF9 were observed in endometriosis that might contribute to increased proliferation of lesions. MAPK10 is a member of Ras/Raf/MEK/ERK signaling (MAPK10 has been originially named ERK - MAPK (mitogen-activated protein kinases, originally called ERK - extracellular signal-regulated kinases), which is apart from cell cycle transition, implicated in many other cellular processes such as apoptosis and differentiation [277]. So upregulated MAPK10 might cause increased Ras/Raf/MEK/ERK signaling (or MAPK signaling respectively) which in turn leads to dysregulated proliferation, apoptosis, and differentiation that potentially further contributes to the formation and establishment of implants. MAPK10 itself has not yet been directly linked to endometriosis or endometrial cancer so far but Yotova et al. observed increased Ras/Raf/MEK/ERK (MAPK) signaling in endometrial stromal cells of patients with endometriosis [278]. FGF9 has been described as an endometrial growth factor [279]. Ovarian endometrioid adenocarcinomas have a connection to endometriosis and Hendrix et al. have already discovered FGF9 as a key factor and downstream target of WNT signaling in this disease [280]. Moreover, FGF9 has been found to be elevated in endometriotic implants and its expression and mitogenic effect was regulated by aberrant production of E2 [279, 281]. So possibly, both upregulated WNT signaling and aberrant E2 production in endometrial cells contribute to elevated FGF9 protein levels and Ras/Raf/MEK/ERK signaling respectively. Both increase proliferation and could result in ectopic lesion formation and maintenance. Elevated proliferation of implants has been already demonstrated in previous studies (e.g. [282]). All these finding support the theory that in endometriotic cells the menstrual cycle phases are abrogated and that they are stuck in the proliferative phase.

However, immunohistochemical stainings of KI67 revealed decreased proliferation in lesions compared to eutopic endometrium of diseased or healthy women contrary to the notion of raised proliferation in endometriotic implants (figure 26). TaqMan analyses of the clinical samples exhibited hints of reduced proliferation in implants as well. These results are in agreement with other studies and might explain the small size of many lesions [283, 284]. Also the study by Matsuzaki et al. proposed that WNT signaling might not be essential for cell proliferation of endometriotic cells since the inhibitory effect of WNT compounds on cell proliferation of ovarian, deep infiltrating, and superficial peritoneal endometriotic tissue was lower than on matching eutopic endometrium of the same patients [275]. SOSTDC1 inhibits proliferation and was upregulated in some samples of endometriotic implants compared to

diseased or healthy eutopic controls in our clinical study [252]. Either it was increased due to reduced proliferation in implants, or its upregulation was also due to outraged WNT pathway activation. SOSTDC1 (also known as WISE) is also able to inhibit the canonical WNT signaling in a context-dependent fashion through interacting with LRP6 [285]. So potentially, it also contributes to auto-regulatory negative feedback loops through WNT signaling indicating that the WNT pathway is aberrantly active in endometriosis.

In our study immunohistochemical stainigs of KI67 did not show differences between eutopic endometrium of diseased or healthy women and quantification of immunohistochemical signals are tricky. However, some studies revealed increased proliferation of diseased eutopic endometrium compared to healthy controls (e.g. [286]). Also TaqMan analyses of the clinical samples gave hints into that direction. This might be the basis of lesion formation, since these hyperproliferative endometrial cells could reach the peritoneum through retrograde menstruation. Previous findings suggest that the WNT pathway might be aberrantly activated in the eutopic endometrium of infertile patients during the mid-secretory phase [201, 287-289]. Matsuzaki et al. also showed that the basal cell proliferation of endometrial stromal and epithelial cells in the mid-secretory phase of patients with endometriosis is significantly higher compared to healthy individuals [275]. Moreover, the mRNA expression of the WNT target gene CDK1 was significantly elevated in endometrial epithelial cells in the mid-secretory phase of diseased women compared to healthy controls [275]. Already a previous study has demonstrated that CDK1 tended to be expressed at higher levels in the secretory phase stromal cells of patients with endometriosis [290]. Upon treatment with a WNT inhibitor, CDK1 gene expression and cell proliferation could be effectively decreased in epithelial and stromal cells of patients with endometriosis [275]. CDK1 is a direct WNT target gene supporting the theory that this increased proliferation of the uterine lining is WNT driven. Potentially, proliferation then drops upon lesion establishment but the WNT pathway may still be dysregulated and promotes further processes such as vascularization or invasion. Consequently, the WNT pathway may not be as involved in cell proliferation of diseased ectopic cells than in diseased eutopic endometrial cells [201].

However, it has to be noticed that besides from the cycle phase, the mRNA expression also depends on the cell type underlining the importance of previous cell separation as done in this study. Particularly, the stromal compartment is characterized by further heterogeneity. Not only stromal cells, but also e.g. endothelial or immune cells reside there, which hardly can be separated via LCM. This hast o be kept in mind during the analysis and interpretation of the results. To circumvent these limitations, another protocol using FACS was established and the separation of epithelial and stromal cells through cell type specific antibodies was

achieved with high purity. But due to technical reasons, this procedure was only applicable for eutopic endometrial cells but this study was supposed to adress the investigation of eutopic and ectopic tissue. But for in-depth examination of eutopic samples, FACS is the more favourable approach than LCM and might also enable the identification of biomarkers.

5.1.2 In vivo study in mice further supports the involvement of the WNT pathway in endometriosis.

LGK974 is suitable for *in vivo* usage.

Several compounds were pretested in ESCs regarding their ability to influence WNT signaling, viability, cell death rate, caspase activity, and migration activity in order to identify one small molecule that might be suitable for the usage in the mice inoculation model to investigate the WNT pathway *in vivo*.

The tankyrase inhibitor NVP-TNKS656 exhibited a desirable IC_{50} of 6.3 nM, showed promising effects on viability, cell death rate, and migration activity *in vitro* and was already successfully used in a mouse model (figures 50-52). However, hints of mortality from a pilot study led to the decision to abandon the small molecule from *in vivo* usage in this study [210]. LGK974 did not exhibit an increased mortality. On the contrary, mice were highly vital (figure 56). To understand why the PORCN inhibitor LGK974 was less toxic than NVP-TNKS656 it is worthwhile to take a look at the mode of action. Possibly, LGK974 acts more WNT-specific compared to NVP-TNKS656. Tankyrases are ADP-ribosyltransferases and they catalyse the transfer of an ADP-ribose from the co-substrate NAD+ on a target proteins leading to the attachment of one or several ADP-ribose (ADPr) molecules to the target proteins [291, 292]. Therefore, tankyrases are involved in numerous posttranslational processes. Consequently, they have been not only linked to WNT signaling but also to additional cellular signaling pathways that mediate processes such as mitotic progression, glucose metabolism, stress granule formation, and possibly proteasome regulation [293-297].

The WNT pathway is downregulated in an early stage and upregulated in later stages of endometriosis *in vivo*. WNT inhibition through LGK974 dramatically reduces disease burden.

LGK974 has been used in the mice inoculation model for endometriosis to investigate its effect on disease burden and gene expression. Lesion number and lesion size were significantly decreased upon WNT inhibition indicating reduced disease burden (figures 53 and 54). Although β-catenin protein levels did not alter upon treatment with LGK974,

decreased mRNA expression of the direct target gene Axin2 indicates successful WNT inhibition (figures 55). The investigation of WNT pathway genes revealed that aberrant activitiy of WNT signaling occurs to a later time point during the development of the disease (figures 59 – 60 and tables 33 - 34).

Reduced disease burden was specific for biochemical PORCN inhibition. Plasma concentration of free LGK974 of ~ 117 nM was sufficient in comparison to the IC_{50} of 0.4 nM (figure 55) [207]. These very high levels might raise the suspicion that also OFF-target effects may have caused the results. The measurement of mRNA of the direct target gene Axin2 and protein levels of β-catenin in comparison between vehicle and compound group should give information about the degree of WNT inhibition [134]. The mRNA expression of Axin2 was significantly reduced in uteri of the compound group after 7 days of treatment and in lesions after 14 days of treatment in relation to controls suggesting ON-target effects (figure 55). Moreover, the applied concentration of the drug was in accordance with a previously published study, in which this concentration was used successfully without exhibiting toxicity [207]. Furthermore, the body weight values of the experiment demonstrate high vitality of the mice (figure 56) [207].

The mRNA expression of Axin2 and protein levels of β-catenin give information about the degree of WNT inhibition. In the uteri of compound treated mice, the Axin2 mRNA expression was significantly reduced after 7 days compared to the controls. After 14 days the Axin2 mRNA expression only exhibited a trend of decreased expression compared to the vehicle group. However, the mean of the Axin2 mRNA expression of the treatment groups after 7 and 14 days was comparable. Either Axin2 mRNA expression was also decreased through LGK974 after 14 days and the significance was eliminated through the huge scatter or it was not decreased anymore due to an eventual counter-regulation in the uterus ensured the recovery and subsequent maintenance of constant WNT activity. When the vehicle group and treatment group are compared, overall mRNA expression of the uteri after 14 days did not show substantial differences anymore, supporting the theory of counter-regulation. Moreover, overall β-catenin protein levels both after 7 or 14 days of treatment did not change between control and compound group (figure 55). Unaltered protein expression after 14 days might be due to counter-regulation in the uterus. WNTs are essential in the uterine development in mice. Defects of Wnt ligand genes (Wnt4, 7a and 5a) or Wnt pathway components (β-catenin or Lef-1) cause developmental defects in uterine glands [298-305]. Conditional Lgr4 knockout mice are subfertile with impaired development of the embryo in the oviduct during early pregnancy [306, 307]. Histologically, the uteri of Lgr4(K5 KO) mice have altered epithelial differentiation, reduced expression of morphogenesis regulatory genes related to WNT signaling, and the uteri failed to undergo decidualization [306, 307].

Many studies show, that the WNT pathway plays an essential role in uterine development and function, so precise regulation is necessary to ensure proper function in terms of gland formation, decidualization, and implantation [308]. The reason why overall β-catenin protein levels did not drop after 7 days of treatment, although Axin2 mRNA expression was already significantly reduced, could not be investigated in this study. Phosphorylation of β-catenin is more dynamic than overall protein levels and would give more exact information about the state of β-catenin [77]. However, β-catenin phosphorylation was not analysed. Nonetheless, β-catenin protein levels can also be influenced through a WNT-independent fashion. Increased E2 levels in endometriosis cause increased conversion of arachidonic acid to PGE2 through COX-2 [50, 51]. PGE2 then activates protein kinase A (PKA) and increases the transcriptional activity of TCF in HEK293 cells [309]. Hin et al. discovered, that activation of PKA increases cytoplasmatic and nuclear β-catenin protein levels through direct phosphorylation of β-catenin, thereby inhibiting its ubiquitination and consequent degradation [310]. Consequently, increased E2 levels in endometriosis do not only possibly increase WNT signaling and induce mechanisms such as migration, proliferation, and angiogenesis, they also influence β-catenin protein levels. Possibly, increased β-catenin protein levels through PKA and decreased β-catenin protein levels through LGK974-mediated WNT inhibition were balanced in the uteri of the mice in this study. Technical difficulties hampered protein isolation from lesions to obtain sufficient protein of good quality to perform Western blots to investigate the amount of β-catenin.

To sum up, regardless unaltered β-catenin protein levels, Axin2 mRNA expression levels indicate successful WNT inhibition. After 7 days a trend and after 14 days significant reduction of Axin2 gene expression upon LGK974 treatment was demonstrated. Furthermore, effective WNT inhibition was identified through significant downregulation of WNT candidate genes (Lgr5) and WNT inhibiting genes (Wif1 and Sfrp2) in uteri and lesions after 14 days also suggesting autoregulatory feedback loops (figures 57-58 and tables 31-32). These findfings are also in accordance with significantly reduced disease burden in terms of lesion size and number (figures 53 and 54).

Outraged WNT pathway activity occurs to a later time point in the development of endometriosis. The comparison of lesions and uteri of the vehicle group or the compound group respectively revealed that both groups were alike after 7 days. Similar genes were dergulated in lesions compared to matching uteri (figures 57-58 and tables 31-32). Moreover, genes of the WNT pathway were expressed at a lower level (significantly: Wnt7a, Lgr5, Rspo1, Wif1, and Sfrp2, by trend: Wnt2b) in lesions compared to uteri after 7 days. However, after 14 days the WNT pathway was significantly upregulated in lesions compared to uteri of the vehicle group (significantly: Rspo1 and Sfrp1, by trend: Wnt2b and Dkk3) (figure 59 and

table 33). Lesions compared to uteri of the compound group showed no elevated expression of WNT pathway members suggesting that WNT inhibition was successful (figure 60 and table 34). Consequently, these data propose that in the early stage of the disease WNT signaling is not elevated. Successively aberrant upregulation of the WNT pathway over time may finally lead to the establishment and maintenance of the disease. Consequently, WNT inhibition through LGK974 successfully returned WNT signaling to a normal eutopic level and significant reduction of disease burden and changes in gene expression after 14 days occurred. Possibly, these effects would have been even more pronounced after a longer treatment time. In summary, the WNT pathway seemed to be slightly downregulated in lesions in the beginning of experimental endometriosis. Over time, WNT signaling significantly increased in lesions and could be therefore effectively targeted by LGK974 leading to decreased disease burden. So far there are no studies published proving this theory and the investigation of lesions taken from women with endometriosis would not give insight in the establishment of the implants. Only one other mouse study for endometriosis with a WNT inhibitor (CGP049090) has been performed so far [202]. They demonstrated, that no significant differences in fibrosis between endometrium and endometriotic implants on day 0 or 7 was visible, but fibrosis significantly increased in endometriotic cells after 14 days and was even further increased after 28 days compared to the eutopic endometrium at the onset of the experiment [202]. They did not evaluate WNT pathway genes, so no statement can be made about WNT signaling activity but possibly also an increase in WNT signaling over time occurred. The situation is different in several cancer entities. Cancer generally exhibits very strong aberrantly active WNT signaling, so effects upon WNT inhibition such as decreased tumor growth can be investigated very early in according mouse models, while for endometriosis *in vivo* studies an extended time frame should be chosen [207].

Altogether, in our study WNT activity increased over time of the disease progession. Consequently, rising WNT signaling possibly aggravates symptoms of endometriosis.

WNT inhibition through LGK974 reduces mechanisms such as migration, proliferation or angiogenesis.

The measurement of mRNA expression of genes associated with mechansisms such as migration, proliferation, or angiogenesis revealed that WNT inhibition through LGK974 generally decreased their expression levels, possibly contributing to reduced disease burden.

Interestingly, after 7 days of treatment, differences in mRNA expression of genes associated with e.g. migration or proliferation between vehicle and treatment group were only visible in uteri and not in lesions (figures 57-58 and tables 31-32). This might be a consequence of

lower mRNA expression of the WNT pathway members in lesions in the early stage of the experiment.

Uteri treated with LGK974 for 7 days exhibited already less mRNA expression of proliferation (Mki67 and Cdk1) and angiogenesis (Vegfa) markers compared to controls (figure 57). Mki67 and Cdk1 are reliable markers for proliferation, which is a mechanism that has been associated with endometriosis previously and was already discussed (see chapter 5.1.1) [3, 247, 259]. After 14 days of WNT inhibition, Cdk1 was still significantly reduced in lesions (figure 59). Vegfa plays an important role in angiogenesis and is even a direct target gene of the WNT pathway [144, 265, 311]. In healthy eutopic endometrium, VEGF expression is enhanced by E2 and cyclic changes throughout the menstrual cycle with maximal expression in the secretory phase and menstruation occur (for overview [311]). However, endometriotic cells can also synthesize and secrete VEGF and some studies demonstrated increased concentration of VEGF in endometriotic tissue, peritoneal fluid, and eutopic glandular epithelium of endometriosis patients [311, 312]. Our study revealed decreased levels of Vegfa mRNA in the uteri of animals treated with LGK974. It has to be considered that not only endometrial cells are able to express and secrete VEGF, but also activated macrophages and neutrophils [313, 314]. In endometriosis a constant low level inflammation is observed, so infiltration of proinflammatory immune cells into the eutopic endometrium is likely (for overview [4]). Since the entire uteri were obtained and no tissue or cell separation was performed, also the mRNA expression of immune cells that resided in the endometrium and myometrium was included. One could therefore speculate that WNT inhibition either also reduced Vegfa mRNA expression of the infiltrated uterine immune cells and endometrial and myometrial cells, or led to a decreased infiltration of immune cells in general, therefore creating an environment with less inflammation.

E-cadherin (Cdh1) increases cell-cell adhesion and consequently reduces cell migration and invasion [258]. Loss of E-cadherin has been associated with the initiation and progression of many human tumors including endometrial carcinomas [315, 316]. Additionally, E-cadherin is a direct WNT target gene and its expression is inversely regulated by the WNT pathway, whereby inhibition of WNT signaling should result in elevated E-cadherin mRNA expression levels [138]. After 14 days of treatment, E-cadherin was significantly elevated in the uteri upon WNT inhibition (figure 57 and table 31). Although some studies did not find altered E-cadherin protein levels in peritoneal endometriotic lesions compared to matching eutopic endometrium, our study reveals that a connection to endometriosis is likely. Some studies reported, that loss of E-cadherin causes local aggressiveness and invasiveness of peritoneal implants [315, 317-319]. Indeed, a study by de Mattos et al. revealed decreased mRNA levels of E-cadherin in implants in an endometriosis rat model [266]. Moreover, β-catenin and

Cdh1 proteins are directly linked to each other in epithelial cell–cell adhesions and are together included in the maintenance of tissue architecture [318].

Altogether these results are in accordance with previous finding from our clinical study. Other studies also showed, that mechanisms such as proliferation, angiogenesis, and migration are strongly correlated with endometriosis (for overview [3]). Moreover, the comparison of uteri and lesions from both groups of the *in vivo* study further confirms that these mechanisms obviously play a role in lesion formation, since mRNA expression levels of certain genes were dysregulated respectively in implants especially after 7 days of endometrium inoculation (figures 58-59 and tables 33-34). Upon WNT inhibition with LGK974 these processes could be positively influenced, which may have also caused the reduction in disease burden after 14 days of treatment.

In summary, the WNT pathway seems to be essentially involved in the pathogenesis of endometriosis and many genes associated with mechanisms such as migration, proliferation, and angiogenesis and the WNT pathway are also significantly dysregulated. Upon WNT inhibition the mechanisms could be altered, consequently leading to a decrease in disease burden. However, from a clinical point of view, endometriosis is a benign disease of young women. The WNT pathway is involved in numerous processes so its pharmacological targeting would have pleiotropic effects. Especially potential side effects on stem cell maintenance and tissue homeostasis have to be considered and the therapeutic use of WNT inhibitors in young patients with a potential desire to have children has to be profoundly analysed in further studies [201, 320, 321]. WNT inhibition is more restricted to usage in malignant diseases such as cancer, where several compounds are already implicated in clinical trials. Nevertheless, several WNT pathway members may serve as potential biomarkers for endometriosis allowing non-invasive diagnose, which would improve patient's quality of life. Moreover, this study helped to broaden our understanding of the underlying pathological mechansims in the disease.

5.2 Involvement of LGR5 and its ligand RSPO1 in the pathogenesis of endometriosis

5.2.1 LGR5 plays an important role in endometriosis through dysregulated WNT signaling and may serve as a biomarker.

In vitro, increased or decreased WNT signaling induced via elevated or reduced levels of LGR5 mRNA accordingly resulted in respective effects on viability, cell death rate, caspase activity, and migration activity in endomtrial cells (figures 36-38). Hence, the WNT co-

receptor directly influences WNT signaling and further regulates functional processes. In clinical samples, the WNT co-receptor mRNA was significantly upregulated in lesions compared to matching diseased eutopic endometrium suggesting a potential involvement in the pathogenesis of the disease (figure 20). However, this could not be analysed by immunohistochemistry, since no appropriate antibody could be established. The mouse study exhibited significantly reduced Lgr5 mRNA expression in lesions compared to uteri in both groups at the beginning. But the mRNA levels normalized later on (figures 59-60 and tables 33-34). So in the retrograde menstruation mouse model, WNT signaling indicated by Lgr5 was initially reduced but recovered over time. Assuming that the time course plays a relevant role in dysregulated WNT signaling, the observed time frame within the experiment was potentially too short to establish aberrantly high mRNA levels of Lgr5. Unfortunately this theory cannot be proven in clinical samples taken from patients with well-established endometriosis. However, upon WNT inhibition Lgr5 was further decreased in uteri and lesions of the compound group compared to controls after 7 days of treatment, so Lgr5 mRNA expression was directly affected through WNT inhibition (figures 57-58 and tables 31-32). This again suggests a potential implication of the co-receptor in lesion establishment. But after 14 days, in the uteri of both groups Lgr5 did not show aberrant mRNA expression anymore compared to lesions suggesting a potential counter-regulation (figures 59-60 and tables 33-34).

For uterine function, LGR5 seems to play an important role. A study by Sun et al. discovered, that Lgr5 is highly expressed in the uterine epithelium of immature mice and it is dramatically downregulated as soon as mice resume estrous cycle [322]. The downregulation is mediated through E2 and progesterone via their cognate nuclear receptors [322]. They speculate that this might also be causative for the observed increase of Lgr5 expression after ovariectomy [322]. In many publications endometriosis is characterized by progesterone resistance (see chapter 1.2.2). Decreased levels of progesterone receptor signaling might cause increased LGR5 expression and WNT activity, which in turn induces mechanisms such as migration, proliferation, and angiogenesis that facilitate lesion formation and maintenance.

Adult stem cells have been found in the human uterus [35, 323-326]. Gil-Sanchis et al. proposed that Lgr5 might serve as an endometrial stem cell marker [327]. Altogether these studies are in line with Sampson's retrograde menstruation theory. Possibly, endometrial stem cells as indicated through LGR5 reach the peritoneum by retrograde menstruation. Upon differentiation of these misplaced cells, they form endometriotic lesions. Another study further substantiated this theory. It revealed that the WNT target gene SOX9 is also expressed in human endometrial basal glandular epithelial cells containing a rare subpopulation of cells with nuclear β-catenin [201, 328]. These findings suggest that the

WNT pathway is already activated in the basal epithelium of patients. Lesions also expressed SOX9 and the expression pattern matched those of the basal epithelium in the eutopic endometrium suggesting that implants might be originating from the basalis before being disseminated by retrograde menstruation [328]. Most likely the WNT pathway is essentially involved in this process providing a novel therapeutic strategy for prevention and treatment of endometriosis [201]. In cancer, LGR5 was also defined as an adult stem cell marker that often plays a role in cancer stem cells [150, 329]. Among others, overexpression correlates with poor survival of colon cancer in mice as well as in patients [150, 329]. Therefore, LGR5 has been described as a promising biomarker for stage I and II gastric cancer and as a predictive marker in colon cancer patients treated with 5-fluorouracil-based adjuvant chemotherapy [330, 331]. Since therapeutic targeting of LGR5 will be challenging due to expected severe side effects, LGR5 might at least serve as a biomarker to reliably diagnose endometriosis non-invasively. However, in the examinated patient cohort, LGR5 was upregulated in peritoneal lesions and not in the eutopic endometrium of endometriosis patients compared to healthy women. Consequently, non-invasive diagnostic tests would not be applicable. Since in our study Lgr5 was also affected by LGK974-mediated WNT inhibition in the uteri of mice, an involvement and potential role of LGR5 also in the eutopic endometrium is likely and has to be further investigated. Although plenty of studies on endometriosis biomarkers have been performed thus far, neither a single biomarker nor a panel of biomarkers has been validated for non-invasive diagnostic tests with sufficient sensitivity and specificity so far [332, 333].

5.2.2 RSPO1 might be involved in the pathogenesis of endometriosis.

RSPO1 is the ligand of the co-receptor LGR5 and was significantly upregulated in endometriotic lesions compared to diseased and healthy eutopic endometrium in our clinicial study (figure 20). In immunohistochemical stainings RSPO1 showed only slightly elevated levels in ectopic tissue compared to eutopic endometrium in general (figure 30). However, evaluation of protein levels by immunohistochemistry was generally not suitable. The establishment and performance of the method was challenging due to difficulties to receive adequate samples of good quality. The histological samples were obtained commercially and no detailed information about fixation or further processing of the tissue was available. Unfortunately, tissue and resulting staining quality was often dissatisfying and even caused the dismissal of various samples leading to the very small sample size. Generally, it has to be noticed that the results of the immunohistochemical stainings varied greatly between the different individuals proving that endometriosis is most likely a multifactorial disease and the WNT pathway dysregulation strongly depends on the individual background referring to such as environmental factors or genetics.

Results from the *in vivo* experiment show that in lesions of the vehicle group, Rspo1 mRNA levels were not altered after 7 days but significantly upregulated after 14 days of inoculation compared to uteri (figure 59 and table 33). In lesions of the compound group, the ligand was significantly downregulated after 7 days but normalized after 14 days of treatment (figure 60 and table 34). Accordingly, Rspo1 gene expression was reduced by trend upon WNT inhibition after 14 days in lesions compared to controls (figure 58 and table 32). So successful WNT inhibition normalized Rspo1 mRNA levels and might have contributed to a reduced lesion maintenance over a longer period of time. That would fit to the clinical findings from our previous study. *In vitro* treatment with recombinant RSPO1 caused no changes in cell death rate, caspase, and migration activity, but statistically significantly decreased viability in non-activated ESCs compared to the respective BSA control (figures 42-43). RSPO1 was not expressed in ESCs and no other cell line expressing the ligand could be found. So possibly, the WNT pathway regarding this protein is insufficiently represented and e.g. potential interaction partners are also not expressed. Consequently, targeting through recombinant proteins would not activate WNT signaling and therefore not influence cellular functions in ESCs.

In line with the findings of our study, there are other reports indicating a potential role in gender-related pathways in the female reproductive tract. In the ovar RSPO1 is expressed in somatic cells and regulates the WNT4 signaling pathway that is essential for ovarian determination [334-336]. Loss of RSPO1 causes 46XX female-to-male sex reversal and 46XY individuals with duplication of the region of chromosome 1 encompassing the RSPO1 and WNT4 genes, suffer from male-to-female sex reversal [178, 336, 337]. This hints to direct or indirect hormonal control of RSPO1 activity and fits to the results of this study as endometriosis as an E2-driven disease.

In cancer, also a relationship to RSPO1 was described. In one study RSPO1 regulated keratinocyte proliferation and differentiation and rendered keratinocytes prone to squamous cell carcinoma [178, 338]. Coi et al. introduced RSPO1 as a prognostic marker in invasive ductal breast cancer for disease-free survival [338].

In summary, our study revealed a potential connection of RSPO1 with endometriosis for the first time helping to broaden our understanding of the pathogenesis of the disease. But again therapeutic targeting of RSPO1 will be challenging due to expected severe side effects. Since in the clinical study RSPO1 was not significantly altered in diseased eutopic endometrium compared to healthy samples, it is probably not a suitable biomarker for a non-invasive diagnosic.

5.3 The role of the receptor FZD7 and its ligands WNT7A and WNT2B

WNT2B and WNT7A have been described to be ligands of FZD7 In the intestine or the skeletal muscle respectively [339-341]. In our study, these WNT candidate genes were found to be significantly upregulated in ectopic samples (figure 20). Immunohistochemical staining confirmed increased protein expression of FZD7 in lesions (figure 27). WNT2B protein levels were slightly increased in ectopic samples and WNT7A did not exhibit changed protein expression in lesions (figures 28 and 29). Again it is notable that the results of the immunohistochemical stainings varied greatly between the different individuals. In the mouse model of endometriosis Wnt7a was significantly and Wnt2b slightly reduced in lesions compared to uteri after 7 days of inoculation. Fzd7 showed no altered gene expression. Wnt7a mRNA expression levels normalized after 14 days and Wnt2b exhibited increased mRNA levels (figures 59-60 and tables 33-34). So in this study downregulation of mRNA expression of several WNT candidate genes in an early stage and normalization in later stages of endometrium challenge could be demonstrated. However, aberrantly upregulated expression of Fzd7, Wnt7a or Wnt2b could not be confirmed in the *in vivo* experiments, possibly because the time course of the experiment was too short. Consequently, their expression levels were not affected by LGK974 treatment (figures 57-58 and table 31-32). Fzd7 is even a direct target gene of the WNT pathway by containing the TCF/LEF binding motif and should show decreased mRNA expression upon WNT inhibition [149]. This could not be observed in this experiment. Auto-regulatory negative feedback loops in terms of Fzd7 mRNA expression for counter-regulation of WNT inhibition in uteri and lesions might be an explanation.

In vitro, both efficient knockdown and overexpression of FZD7 mRNA levels in ESCs successfully decreased WNT activity (figure 39). Knockdown of the receptor led to a significant reduction of cell viability and elevation of caspase activity (figure 40). Overexpression led to significantly increased cell viability and migration activity and decreased cell death rate (figures 40 and 41). It is notable, that upon mRNA overexpression, the mRNA levels only increased by about 3 %. Possibly, cellular functions react very senstive on slightest changes of FZD7 mRNA levels, so that an increase of 3 % is sufficient to affect viability and migration activity. So how can an increase in viability and migration activity and decreased cell death rate be explained in combination with a concurrent drop in WNT activity despite FZD7 overexpression? Possibly, FZD7 expression is highly sensitive, so that slightest increases in mRNA levels cause inhibition of the WNT pathway as a consequence of negative regulatory feedback loops to limit outraged WNT signaling. A study by Le Grand

et al. discovered that FZD7 together with its ligand WNT7A also activates the non-canonical PCP pathway to control the homeostatic level of satellite stem cells for the regulation of the regenerative potential of muscle through symmetric cell division [340]. This pathway has for example also been implicated in the migration of neuronal cells [342]. Moreover, it has been shown that FZD7/WNT7A signaling also directly activates the non-canonical Akt/mTOR anabolic growth pathway in skeletal muscle [341, 343]. This has been already linked to mechanisms such as cell survival, proliferation, and metabolism [341, 343]. So these conditions might explain increased migration and cell survival in FZD7 overexpressed ESCs despite decreased WNT activity that potentially comes from negative auto-regulatory feedback loops. However, this has to be further investigated.

Since WNT7A and WNT2B are both ligands of the receptor FZD7 and therefore may also activate canonical and non-canonical WNT signaling, similar effects could be expected for them *in vitro*. Indeed, they were not observed. Recombinant WNT7A did not alter WNT activity, cell death rate and caspase and migration activity accordingly (figures 46 and 47). However, the viability of both WNT3A-treated and non-treated cells significantly dropped by WNT7A compared to the appropriate BSA controls (figure 46). Obviously, in this experiment decreased cell viability was WNT–independent. So eventually, this was unspecific and/or somehow regulated through the non-canonical Akt/mTOR anabolic growth pathway, which influences cell survival independent from β-catenin signaling. Potentially, this non-canonical WNT pathway also has auto-regulatory feedback loops that cause aberrantly increased levels of WNT7A to downregulate the signaling in order to maintain cell integrity. However, this was not analysed in this study. Concerning canonical WNT activity, possibly ESCs were not suitable to study this pathway in regard to WNT7A. This ligand, as well as WNT2B, is not expressed in ESCs and therefore e.g. potential interaction partners are underrepresented, so that for these ligands the pathway is not well represented. Other cell lines, which express all or at least the remaining WNT candidate genes, were screened but none exhibited desirable WNT7A or WNT2B mRNA expression levels or behaviour in the functional assays.

WNT2B did affect WNT signaling and cellular functions. The recombinant protein decreased WNT signaling and viability and migration activity consequently (figures 44 and 45). Reduced WNT activity might be a result of counter-regulation of outraged WNT signaling provoked by too high concentrations of WNT2B. In this study also a higher concentration of 5 µg/ml recombinant protein was used in the WNT activity assay and exhibited further downregulated WNT signaling by ~ 10 % (data not shown). This would support the theory of counter-regulation. This process might be mediated through squelching. This process has been mainly described for transcription activators who bind other transcription activators in order to inhbit the gene expression of their target genes [344]. Possibly, WNT2B also binds

transcription factors of its own pathway to restrict disproportionately activation. Since WNT2B has been also described as a ligand of FZD7, it is also possible that these effects may be mediated through the non-canonical PCP or Akt/mTOR anabolic growth pathway. However, no study has directly linked WNT2B to non-canonical WNT signaling so far.

Up to date, only WNT7A has been associated with endometriosis previously. Cooke et al. performed Wnt7a knockout experiments in mice and observed uterine adenogenesis dysfunction of endometrial glandular cells in infertile adult females underlining the importance of Wnt7a in uterine development [298]. In accordance with our study, Gaetje et al. also described WNT7A upregulation in lesions compared to diseased eutopic endometrium mainly in epithelial cells (figure 20) [345]. For the *in vitro* experiments ESCs were used for the *in vitro* experiments. Because they are of stromal origin, potentially increased protein levels of WNT7A could not affect cellular functions. Gaetje et al. postulated the theory of lesion formation through coelomic metaplasia, since patients with endometriosis expressed higher levels of WNT7A in the peritoneum than healthy women [346]. Possibly, they also included endometriotic cells in the peritoneal samples explaining the elevated WNT7A expression. Another study by Santamaria et al. observed that cells that migrated from endometriotic implants back to the eutopic endometrium in a mouse model exhibited increased Wnt7a expression not only in the epithelium but also in the stroma [347]. However, our study only revealed significantly increased WNT7A mRNA expression in epithelial ectopic cells (figure 20). Possibly, the species difference can explain the difference between our and Santamaria's study. However, the mouse experiment performed in our study did also not exhibit effects on Wnt7a mRNA expression in lesions or uteri upon WNT inhibition. In human endometrial carcinoma, WNT7A plays definitely an essential role, since WNT7A inhibition through SFRP4 reduced proliferation in endometrial cancer cells and its expression is of prognostic significance and [348, 349]. In terms of uterine function, only one study included WNT2B and none referred to FZD7 so far [350]. Downregulation of WNT2B has been described to cause estrogen-induced disruption of endometrial adenogenesis in the neonatal ewe [350].

Altogether, the results from the clinical study suggest a potential role of FZD7, WNT7A, and WNT2B in the pathogenesis of endometriosis. Immunohistochemical stainigs could partly confirm these findings. Results from the *in vitro* experiments were inconsistent, whereby it is uncertain, whether observed effects were mediated through canonical or non-canonical WNT signaling to some extent. WNT7A has been already connected to the pathogenesis of endometriosis in another study, whereas WNT2B and FZD7 were found to be potentially associated with the disease for the first time. So overall, the role of these WNT candidate genes in the disease remains uncertain and needs to be further investigated.

Finally, in comparison to the other WNT candidate genes, pharmaceutical intervention through targeting of FZD7, WNT72B, and WNT7A would even cause worse side effects since apart from canonical WNT signaling they are also able to activate non-canonical WNT siganling.

5.4 Progesterone resistance through PGR downregulation is only partially involved in endometriosis but is directly linked to aberrant WNT signaling.

Progesterone resistance in endometriosis is defined by reduced PGR expression causing elevated E2 levels (see chapter 1.2.2) [56]. In the present clinical study, a downregulation of the PGR was not observed. To the contrary, in secretory phase epithelial cells of ectopic lesions, mRNA expression of PGR was even significantly elevated (figure 23 and table 25). About 9 % of women with endometriosis do not respond to therapeutic progestins due to unknown reasons and the relief of pain though progestin therapy appears to be relatively short-termed [57, 351, 352]. Consequently, progesterone resistance might have played a limited role in our patient cohort.

But in the mouse experiment progesterone resistance was noticed suggesting that this process might be implicated. Pgr mRNA expression was significantly downregulated in lesions compared to matching uteri of both groups after 7 days of inoculation (figures 59-60 and tables 33-34). Additionally, Esr2 was significantly increased in lesions of the vehicle group after 7 and 14 days of endometrium challenge contributing to progesterone resistance (figure 59 and table 33). For the treatment group, mRNA expression of Esr2 was also significantly upregulated in lesions after 14 days (figure 60 and table 34). However, after 14 days of endometrium challenge, Pgr was downregulated in lesions originating from the treatment group compared to the vehicle group. An explanation would be that the amount of endometrial cells in lesions of the compound group decreased through WNT inhibition. Therefore, less endometrial cells are present causing significantly less abundant Pgr mRNA expression.

Generally, hormonal changes during the normal menstrual cycle are directly connected to the WNT pathway. E2 enhances Wnt/β-catenin signaling in the proliferative phase, while progesterone inhibits Wnt/β-catenin signaling, thus reducing E2 proliferative actions during the secretory phase resulting in counter-balanced estrogen-induced proliferation and enhanced differentiation (figure 61) [201, 353, 354]. Moreover, a mouse study discovered that stabilization of β-catenin in the uterus caused endometrial glandular hyperplasia and a

lack of decidual response [201, 303]. These mice exhibited increased levels of Esr1 in the epithelium [303]. In case of enhanced or unopposed E2 signaling, constitutive activation of Wnt/β-catenin signaling might trigger endometrial hyperplasia, which possibly develops further into endometrial cancer and might also be involved in endometriosis [353]. So progesterone resistance in endometriosis might fail to inhibit WNT activation and additionally elevated levels of E2 might cause the persistence of the proliferative phenotype with impaired decidualization in the endometrium of infertile patients [201]. Also migration activity of endometrial cells, WNT signaling, and increased E2 levels are associated to each other. A study from Zhang et al. demonstrated that the association of MMP9 and WNT signaling might be regulated by E2 in proliferative phase endometrial stromal cells from patients with endometriosis [355]. After E2 treatment, protein levels of MMP9 and β-catenin increased concurrently in a time- and dose-dependent manner [355]. Since MMP9 is a direct target gene of the WNT pathway, which can be increased through elevated E2 levels, these results are consistent. In the our study Mmp9 was also significantly increased in lesions of both groups after 7 days of inoculation. So the high hormonal levels of E2 in the endometrium of patients directly regulate the WNT pathway and therefore lead to increased gene expression of genes promoting cell migration. Finally, these results are in accordance with the implantation theory [3].
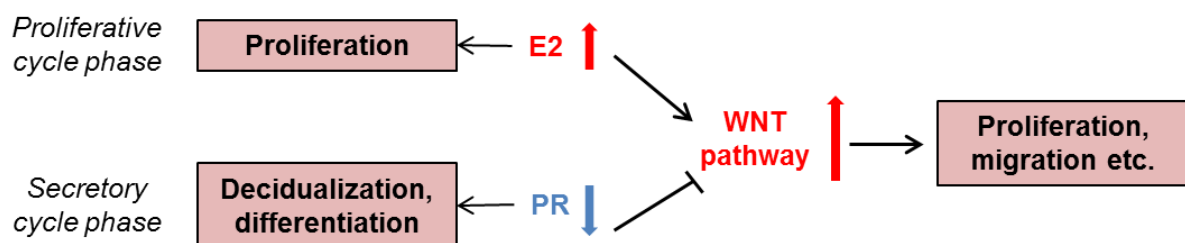
Figure 61: Connection between progesterone resistance and WNT signaling in endometriosis. Proteins/pathway marked in red are higher and in blue are lower expressed in endometriosis. In healthy endometrium, estrogen (E2) enhances WNT signaling and proliferation of the eutopic endometrium in the proliferative cycle phase. In the secretory cycle phase progesterone (PR) reduces WNT signaling and causes decidualization and differentiation of eutopic endometrial cells. Progesterone resistance in endometriosis disrupts this counter-balance especially in lesions.

Although progesterone resistance through reduced PGR expression was not seen in all endometriosis patients of our clinical study, it has been observed in the mouse experiments. Moreover, it is obviously directly linked to WNT signaling. Both processes potentially enhance each other and facilitate mechanisms such as migration, proliferation, or vascularization that may contribute to the pathogenesis of endometriosis.

6 References

1. Studio, S.T., *Our menstrual cycle.* Angea Acupuncture & Yoga 2013.
2. Foods, A., *Maca and Women: Effects on Thyroid, HRT, Menstrual Periods, and Fatigue.* Asana Foods, 2013 - 2016.
3. Giudice, L.C. and L.C. Kao, *Endometriosis.* Lancet, 2004. **364**(9447): p. 1789-99.
4. Macer, M.L. and H.S. Taylor, *Endometriosis and infertility: a review of the pathogenesis and treatment of endometriosis-associated infertility.* Obstet Gynecol Clin North Am, 2012. **39**(4): p. 535-49.
5. Borghese, B., et al., *Identification of susceptibility genes for peritoneal, ovarian, and deep infiltrating endometriosis using a pooled sample-based genome-wide association study.* Biomed Res Int, 2015. **2015**: p. 461024.
6. Koninckx, P.R., et al., *Deep endometriosis: definition, diagnosis, and treatment.* Fertil Steril, 2012. **98**(3): p. 564-71.
7. Matsuzaki, S., et al., *Fibrogenesis in peritoneal endometriosis. A semi-quantitative analysis of type-I collagen.* Gynecol Obstet Invest, 1999. **47**(3): p. 197-9.
8. Olive, D.L. and E.A. Pritts, *Treatment of endometriosis.* N Engl J Med, 2001. **345**(4): p. 266-75.
9. Verkauf, B.S., *Incidence, symptoms, and signs of endometriosis in fertile and infertile women.* J Fla Med Assoc, 1987. **74**(9): p. 671-5.
10. Practice Committee of the American Society for Reproductive, M., *Endometriosis and infertility: a committee opinion.* Fertil Steril, 2012. **98**(3): p. 591-8.
11. Hughes, E.G., D.M. Fedorkow, and J.A. Collins, *A quantitative overview of controlled trials in endometriosis-associated infertility.* Fertil Steril, 1993. **59**(5): p. 963-70.
12. Medicine, A.S.f.R., *Endometriosis.* A guide for Patients Revised 2012, 2012.
13. Greaves, E., *Endometriosis Symptoms, Causes, Treatments and Fertility.* Ovulation Calculator, 2016.
14. Sampson, J.A., *Metastatic or Embolic Endometriosis, due to the Menstrual Dissemination of Endometrial Tissue into the Venous Circulation.* Am J Pathol, 1927. **3**(2): p. 93-110 43.
15. Halme, J., et al., *Retrograde menstruation in healthy women and in patients with endometriosis.* Obstet Gynecol, 1984. **64**(2): p. 151-4.
16. D'Hooghe, T.M., *Clinical relevance of the baboon as a model for the study of endometriosis.* Fertil Steril, 1997. **68**(4): p. 613-25.
17. Nunley, W.C., Jr. and J.D. Kitchin, 3rd, *Congenital atresia of the uterine cervix with pelvic endometriosis.* Arch Surg, 1980. **115**(6): p. 757-8.
18. Ferguson, B.R., J.L. Bennington, and S.L. Haber, *Histochemistry of mucosubstances and histology of mixed mullerian pelvic lymph node glandular inclusions. Evidence for histogenesis by mullerian metaplasia of coelomic epithelium.* Obstet Gynecol, 1969. **33**(5): p. 617-25.
19. Gruenwald, P., *Origin of endometriosis from the mesenchyme of the celomic walls.* American Journal of Obstetrics and Gynecology, 1942. **44**(3): p. 470-474.
20. Nap, A.W., et al., *Pathogenesis of endometriosis.* Best Pract Res Clin Obstet Gynaecol, 2004. **18**(2): p. 233-44.

21. Grunewald, R.A. and J. Wiggins, *Pulmonary endometriosis mimicking an acute abdomen.* Postgrad Med J, 1988. **64**(757): p. 865-6.

22. Sarma, D., et al., *Cerebellar endometriosis.* AJR Am J Roentgenol, 2004. **182**(6): p. 1543-6.

23. Steele, R.W., W.P. Dmowski, and D.J. Marmer, *Immunologic aspects of human endometriosis.* Am J Reprod Immunol, 1984. **6**(1): p. 33-6.

24. Oosterlynck, D.J., et al., *Women with endometriosis show a defect in natural killer activity resulting in a decreased cytotoxicity to autologous endometrium.* Fertil Steril, 1991. **56**(1): p. 45-51.

25. Harada, T., T. Iwabe, and N. Terakawa, *Role of cytokines in endometriosis.* Fertil Steril, 2001. **76**(1): p. 1-10.

26. Lebovic, D.I., M.D. Mueller, and R.N. Taylor, *Immunobiology of endometriosis.* Fertil Steril, 2001. **75**(1): p. 1-10.

27. Witz, C.A., *Interleukin-6: another piece of the endometriosis-cytokine puzzle.* Fertil Steril, 2000. **73**(2): p. 212-4.

28. McAllister, S.L., N. Dmitrieva, and K.J. Berkley, *Sprouted innervation into uterine transplants contributes to the development of hyperalgesia in a rat model of endometriosis.* PLoS One, 2012. **7**(2): p. e31758.

29. Laux-Biehlmann, A., T. d'Hooghe, and T.M. Zollner, *Menstruation pulls the trigger for inflammation and pain in endometriosis.* Trends Pharmacol Sci, 2015. **36**(5): p. 270-276.

30. Gruen, M., et al., *Use of dynamic weight bearing as a novel end-point for the assessment of abdominal pain in the LPS-induced peritonitis model in the rat.* J Neurosci Methods, 2014. **232**: p. 118-24.

31. Laux-Biehlmann, A., et al., *Dynamic weight bearing as a non-reflexive method for the measurement of abdominal pain in mice.* Eur J Pain, 2016. **20**(5): p. 742-52.

32. Stratton, P. and K.J. Berkley, *Chronic pelvic pain and endometriosis: translational evidence of the relationship and implications.* Hum Reprod Update, 2011. **17**(3): p. 327-46.

33. Gargett, C.E., et al., *Isolation and culture of epithelial progenitors and mesenchymal stem cells from human endometrium.* Biol Reprod, 2009. **80**(6): p. 1136-45.

34. Verdi, J., et al., *Endometrial stem cells in regenerative medicine.* J Biol Eng, 2014. **8**: p. 20.

35. Sasson, I.E. and H.S. Taylor, *Stem cells and the pathogenesis of endometriosis.* Ann N Y Acad Sci, 2008. **1127**: p. 106-15.

36. Figueira, P.G., et al., *Stem cells in endometrium and their role in the pathogenesis of endometriosis.* Ann N Y Acad Sci, 2011. **1221**: p. 10-7.

37. Chan, R.W., K.E. Schwab, and C.E. Gargett, *Clonogenicity of human endometrial epithelial and stromal cells.* Biol Reprod, 2004. **70**(6): p. 1738-50.

38. Du, H. and H.S. Taylor, *Contribution of bone marrow-derived stem cells to endometrium and endometriosis.* Stem Cells, 2007. **25**(8): p. 2082-6.

39. Taylor, H.S., *Endometrial cells derived from donor stem cells in bone marrow transplant recipients.* JAMA, 2004. **292**(1): p. 81-5.

40. Simpson, J.L., et al., *Heritable aspects of endometriosis. I. Genetic studies.* Am J Obstet Gynecol, 1980. **137**(3): p. 327-31.

41. Hadfield, R.M., et al., *Endometriosis in monozygotic twins.* Fertil Steril, 1997. **68**(5): p. 941-2.

42. Hadfield, R.M., et al., *Risk factors for endometriosis in the rhesus monkey (Macaca mulatta): a case-control study.* Hum Reprod Update, 1997. **3**(2): p. 109-15.

43. Kennedy, S., H. Mardon, and D. Barlow, *Familial endometriosis.* J Assist Reprod Genet, 1995. **12**(1): p. 32-4.

44. Moen, M.H., *Endometriosis in monozygotic twins.* Acta Obstet Gynecol Scand, 1994. **73**(1): p. 59-62.

45. Bedaiwy, M.A., et al., *Genetic polymorphism in the fibrinolytic system and endometriosis.* Obstet Gynecol, 2006. **108**(1): p. 162-8.

46. Taylor, H.S., et al., *HOX gene expression is altered in the endometrium of women with endometriosis.* Hum Reprod, 1999. **14**(5): p. 1328-31.

47. Zanatta, A., et al., *The role of the Hoxa10/HOXA10 gene in the etiology of endometriosis and its related infertility: a review.* J Assist Reprod Genet, 2010. **27**(12): p. 701-10.

48. Zeitoun, K.M. and S.E. Bulun, *Aromatase: a key molecule in the pathophysiology of endometriosis and a therapeutic target.* Fertil Steril, 1999. **72**(6): p. 961-9.

49. Zeitoun, K., et al., *Deficient 17beta-hydroxysteroid dehydrogenase type 2 expression in endometriosis: failure to metabolize 17beta-estradiol.* J Clin Endocrinol Metab, 1998. **83**(12): p. 4474-80.

50. Bulun, S.E., *Endometriosis.* N Engl J Med, 2009. **360**(3): p. 268-79.

51. Bulun, S.E., et al., *Regulation of aromatase expression in estrogen-responsive breast and uterine disease: from bench to treatment.* Pharmacol Rev, 2005. **57**(3): p. 359-83.

52. Xue, Q., et al., *Promoter methylation regulates estrogen receptor 2 in human endometrium and endometriosis.* Biol Reprod, 2007. **77**(4): p. 681-7.

53. Igarashi, T.M., et al., *Reduced expression of progesterone receptor-B in the endometrium of women with endometriosis and in cocultures of endometrial cells exposed to 2,3,7,8-tetrachlorodibenzo-p-dioxin.* Fertil Steril, 2005. **84**(1): p. 67-74.

54. Attia, G.R., et al., *Progesterone receptor isoform A but not B is expressed in endometriosis.* J Clin Endocrinol Metab, 2000. **85**(8): p. 2897-902.

55. Vierikko, P., et al., *Steroidal regulation of endometriosis tissue: lack of induction of 17 beta-hydroxysteroid dehydrogenase activity by progesterone, medroxyprogesterone acetate, or danazol.* Fertil Steril, 1985. **43**(2): p. 218-24.

56. Bulun, S.E., et al., *Progesterone resistance in endometriosis: link to failure to metabolize estradiol.* Mol Cell Endocrinol, 2006. **248**(1-2): p. 94-103.

57. Wu, Y., et al., *Promoter hypermethylation of progesterone receptor isoform B (PR-B) in endometriosis.* Epigenetics, 2006. **1**(2): p. 106-11.

58. Xue, Q., et al., *Transcriptional activation of steroidogenic factor-1 by hypomethylation of the 5' CpG island in endometriosis.* J Clin Endocrinol Metab, 2007. **92**(8): p. 3261-7.

59. Fanton, J.W. and J.G. Golden, *Radiation-induced endometriosis in Macaca mulatta.* Radiat Res, 1991. **126**(2): p. 141-6.

60. Rier, S.E., et al., *Endometriosis in rhesus monkeys (Macaca mulatta) following chronic exposure to 2,3,7,8-tetrachlorodibenzo-p-dioxin.* Fundam Appl Toxicol, 1993. **21**(4): p. 433-41.

61. Koninckx, P.R., et al., *Dioxin pollution and endometriosis in Belgium.* Hum Reprod, 1994. **9**(6): p. 1001-2.

62. Pauwels, A., et al., *The risk of endometriosis and exposure to dioxins and polychlorinated biphenyls: a case-control study of infertile women.* Hum Reprod, 2001. **16**(10): p. 2050-5.

63. Eskenazi, B., et al., *Serum dioxin concentrations and endometriosis: a cohort study in Seveso, Italy.* Environ Health Perspect, 2002. **110**(7): p. 629-34.

64. P., M.J., et al., *The emerging science of endocrine disruption.* Centenary of the Foundation of the First Academy of Sciences: "Academia Lynceorum", 2004. **4**.

65. Ozkan, S., W. Murk, and A. Arici, *Endometriosis and infertility: epidemiology and evidence-based treatments.* Ann N Y Acad Sci, 2008. **1127**: p. 92-100.

66. Olive, D.L. and L.B. Schwartz, *Endometriosis.* N Engl J Med, 1993. **328**(24): p. 1759-69.

67. Chwalisz, K., et al., *Selective progesterone receptor modulators (SPRMs): a novel therapeutic concept in endometriosis.* Ann N Y Acad Sci, 2002. **955**: p. 373-88; discussion 389-93, 396-406.

68. Candiani, G.B., et al., *Repetitive conservative surgery for recurrence of endometriosis.* Obstet Gynecol, 1991. **77**(3): p. 421-4.

69. Kuohung, W., et al., *Characteristics of patients with endometriosis in the United States and the United Kingdom.* Fertil Steril, 2002. **78**(4): p. 767-72.

70. L., O.D., *Endometriosis: does surgery make a difference?* OB/GYN Management, 2002. **14**(2).

71. Hughes, E., et al., *Ovulation suppression for endometriosis.* Cochrane Database Syst Rev, 2000(2): p. CD000155.

72. Gibbons, W.E., *Management of endometriosis in fertility patients.* Fertil Steril, 2004. **81**(5): p. 1204-5.

73. Devroey, P., *[Ovarian stimulation regimens in women with endometriosis].* J Gynecol Obstet Biol Reprod (Paris), 2003. **32**(8 Pt 2): p. S42-4.

74. Fedele, L., et al., *Superovulation with human menopausal gonadotropins in the treatment of infertility associated with minimal or mild endometriosis: a controlled randomized study.* Fertil Steril, 1992. **58**(1): p. 28-31.

75. Deaton, J.L., et al., *A randomized, controlled trial of clomiphene citrate and intrauterine insemination in couples with unexplained infertility or surgically corrected endometriosis.* Fertil Steril, 1990. **54**(6): p. 1083-8.

76. Tummon, I.S., et al., *Randomized controlled trial of superovulation and insemination for infertility associated with minimal or mild endometriosis.* Fertil Steril, 1997. **68**(1): p. 8-12.

77. Clevers, H. and R. Nusse, *Wnt/beta-catenin signaling and disease.* Cell, 2012. **149**(6): p. 1192-205.

78. Logan, C.Y. and R. Nusse, *The Wnt signaling pathway in development and disease.* Annu Rev Cell Dev Biol, 2004. **20**: p. 781-810.

79. Nusse, R. and H.E. Varmus, *Many tumors induced by the mouse mammary tumor virus contain a provirus integrated in the same region of the host genome.* Cell, 1982. **31**(1): p. 99-109.

80. Nusslein-Volhard, C. and E. Wieschaus, *Mutations affecting segment number and polarity in Drosophila.* Nature, 1980. **287**(5785): p. 795-801.

81. Rijsewijk, F., et al., *The Drosophila homolog of the mouse mammary oncogene int-1 is identical to the segment polarity gene wingless.* Cell, 1987. **50**(4): p. 649-57.

82. Noordermeer, J., et al., *dishevelled and armadillo act in the wingless signalling pathway in Drosophila.* Nature, 1994. **367**(6458): p. 80-3.

83. Manoukian, A.S., et al., *The porcupine gene is required for wingless autoregulation in Drosophila.* Development, 1995. **121**(12): p. 4037-44.

84. McMahon, A.P. and R.T. Moon, *Ectopic expression of the proto-oncogene int-1 in Xenopus embryos leads to duplication of the embryonic axis.* Cell, 1989. **58**(6): p. 1075-84.

85. Behrens, J., et al., *Functional interaction of beta-catenin with the transcription factor LEF-1.* Nature, 1996. **382**(6592): p. 638-42.

86. Molenaar, M., et al., *XTcf-3 transcription factor mediates beta-catenin-induced axis formation in Xenopus embryos.* Cell, 1996. **86**(3): p. 391-9.

87. Bhanot, P., et al., *A new member of the frizzled family from Drosophila functions as a Wingless receptor.* Nature, 1996. **382**(6588): p. 225-30.

88. Wehrli, M., et al., *arrow encodes an LDL-receptor-related protein essential for Wingless signalling.* Nature, 2000. **407**(6803): p. 527-30.

89. Kinzler, K.W., et al., *Identification of FAP locus genes from chromosome 5q21.* Science, 1991. **253**(5020): p. 661-5.

90. Nishisho, I., et al., *Mutations of chromosome 5q21 genes in FAP and colorectal cancer patients.* Science, 1991. **253**(5020): p. 665-9.

91. Rubinfeld, B., et al., *Association of the APC gene product with beta-catenin.* Science, 1993. **262**(5140): p. 1731-4.

92. Su, L.K., B. Vogelstein, and K.W. Kinzler, *Association of the APC tumor suppressor protein with catenins.* Science, 1993. **262**(5140): p. 1734-7.

93. Tanaka, K., Y. Kitagawa, and T. Kadowaki, *Drosophila segment polarity gene product porcupine stimulates the posttranslational N-glycosylation of wingless in the endoplasmic reticulum.* J Biol Chem, 2002. **277**(15): p. 12816-23.

94. Willert, K., et al., *Wnt proteins are lipid-modified and can act as stem cell growth factors.* Nature, 2003. **423**(6938): p. 448-52.

95. Franch-Marro, X., et al., *In vivo role of lipid adducts on Wingless.* J Cell Sci, 2008. **121**(Pt 10): p. 1587-92.

96. Kurayoshi, M., et al., *Post-translational palmitoylation and glycosylation of Wnt-5a are necessary for its signalling.* Biochem J, 2007. **402**(3): p. 515-23.

97. Hofmann, K., *A superfamily of membrane-bound O-acyltransferases with implications for wnt signaling.* Trends Biochem Sci, 2000. **25**(3): p. 111-2.

98. Kadowaki, T., et al., *The segment polarity gene porcupine encodes a putative multitransmembrane protein involved in Wingless processing.* Genes Dev, 1996. **10**(24): p. 3116-28.

99. Takada, R., et al., *Monounsaturated fatty acid modification of Wnt protein: its role in Wnt secretion.* Dev Cell, 2006. **11**(6): p. 791-801.

100. Banziger, C., et al., *Wntless, a conserved membrane protein dedicated to the secretion of Wnt proteins from signaling cells.* Cell, 2006. **125**(3): p. 509-22.

101. Bartscherer, K., et al., *Secretion of Wnt ligands requires Evi, a conserved transmembrane protein.* Cell, 2006. **125**(3): p. 523-33.

102. Goodman, R.M., et al., *Sprinter: a novel transmembrane protein required for Wg secretion and signaling.* Development, 2006. **133**(24): p. 4901-11.

103. Coudreuse, D.Y., et al., *Wnt gradient formation requires retromer function in Wnt-producing cells.* Science, 2006. **312**(5775): p. 921-4.

104. Prasad, B.C. and S.G. Clark, *Wnt signaling establishes anteroposterior neuronal polarity and requires retromer in C. elegans.* Development, 2006. **133**(9): p. 1757-66.

105. Dann, C.E., et al., *Insights into Wnt binding and signalling from the structures of two Frizzled cysteine-rich domains.* Nature, 2001. **412**(6842): p. 86-90.

106. Janda, C.Y., et al., *Structural basis of Wnt recognition by Frizzled.* Science, 2012. **337**(6090): p. 59-64.

107. Pinson, K.I., et al., *An LDL-receptor-related protein mediates Wnt signalling in mice.* Nature, 2000. **407**(6803): p. 535-8.

108. Tamai, K., et al., *LDL-receptor-related proteins in Wnt signal transduction.* Nature, 2000. **407**(6803): p. 530-5.

109. Mao, J., et al., *Low-density lipoprotein receptor-related protein-5 binds to Axin and regulates the canonical Wnt signaling pathway.* Mol Cell, 2001. **7**(4): p. 801-9.

110. He, X., et al., *LDL receptor-related proteins 5 and 6 in Wnt/beta-catenin signaling: arrows point the way.* Development, 2004. **131**(8): p. 1663-77.

111. Tamai, K., et al., *A mechanism for Wnt coreceptor activation.* Mol Cell, 2004. **13**(1): p. 149-56.

112. Zeng, X., et al., *A dual-kinase mechanism for Wnt co-receptor phosphorylation and activation.* Nature, 2005. **438**(7069): p. 873-7.

113. Chen, W., et al., *Dishevelled 2 recruits beta-arrestin 2 to mediate Wnt5A-stimulated endocytosis of Frizzled 4.* Science, 2003. **301**(5638): p. 1391-4.

114. Fiedler, M., et al., *Dishevelled interacts with the DIX domain polymerization interface of Axin to interfere with its function in down-regulating beta-catenin.* Proc Natl Acad Sci U S A, 2011. **108**(5): p. 1937-42.

115. Schwarz-Romond, T., et al., *The DIX domain of Dishevelled confers Wnt signaling by dynamic polymerization.* Nat Struct Mol Biol, 2007. **14**(6): p. 484-92.

116. Carmon, K.S., et al., *R-spondins function as ligands of the orphan receptors LGR4 and LGR5 to regulate Wnt/beta-catenin signaling.* Proc Natl Acad Sci U S A, 2011. **108**(28): p. 11452-7.

117. de Lau, W., et al., *Lgr5 homologues associate with Wnt receptors and mediate R-spondin signalling.* Nature, 2011. **476**(7360): p. 293-7.

118. Glinka, A., et al., *LGR4 and LGR5 are R-spondin receptors mediating Wnt/beta-catenin and Wnt/PCP signalling.* EMBO Rep, 2011. **12**(10): p. 1055-61.

119. Xu, J.G., et al., *Crystal structure of LGR4-Rspo1 complex: insights into the divergent mechanisms of ligand recognition by leucine-rich repeat G-protein-coupled receptors (LGRs).* J Biol Chem, 2015. **290**(4): p. 2455-65.

120. Hsu, S.Y., et al., *The three subfamilies of leucine-rich repeat-containing G protein-coupled receptors (LGR): identification of LGR6 and LGR7 and the signaling mechanism for LGR7.* Mol Endocrinol, 2000. **14**(8): p. 1257-71.

121. Bovolenta, P., et al., *Beyond Wnt inhibition: new functions of secreted Frizzled-related proteins in development and disease.* J Cell Sci, 2008. **121**(Pt 6): p. 737-46.

122. Glinka, A., et al., *Dickkopf-1 is a member of a new family of secreted proteins and functions in head induction.* Nature, 1998. **391**(6665): p. 357-62.

123. Ellwanger, K., et al., *Targeted disruption of the Wnt regulator Kremen induces limb defects and high bone density.* Mol Cell Biol, 2008. **28**(15): p. 4875-82.

124. Semenov, M.V., X. Zhang, and X. He, *DKK1 antagonizes Wnt signaling without promotion of LRP6 internalization and degradation.* J Biol Chem, 2008. **283**(31): p. 21427-32.

125. Aberle, H., et al., *beta-catenin is a target for the ubiquitin-proteasome pathway.* EMBO J, 1997. **16**(13): p. 3797-804.

126. Li, V.S., et al., *Wnt signaling through inhibition of beta-catenin degradation in an intact Axin1 complex.* Cell, 2012. **149**(6): p. 1245-56.

127. Zhang, W., et al., *PR55 alpha, a regulatory subunit of PP2A, specifically regulates PP2A-mediated beta-catenin dephosphorylation.* J Biol Chem, 2009. **284**(34): p. 22649-56.

128. Huang, S.M., et al., *Tankyrase inhibition stabilizes axin and antagonizes Wnt signalling.* Nature, 2009. **461**(7264): p. 614-20.

129. van de Wetering, M., et al., *Armadillo coactivates transcription driven by the product of the Drosophila segment polarity gene dTCF.* Cell, 1997. **88**(6): p. 789-99.

130. Roose, J., et al., *The Xenopus Wnt effector XTcf-3 interacts with Groucho-related transcriptional repressors.* Nature, 1998. **395**(6702): p. 608-12.

131. Cavallo, R.A., et al., *Drosophila Tcf and Groucho interact to repress Wingless signalling activity.* Nature, 1998. **395**(6702): p. 604-8.

132. Hikasa, H., et al., *Regulation of TCF3 by Wnt-dependent phosphorylation during vertebrate axis specification.* Dev Cell, 2010. **19**(4): p. 521-32.

133. Lee, W., et al., *Homeodomain-interacting protein kinases (Hipks) promote Wnt/Wg signaling through stabilization of beta-catenin/Arm and stimulation of target gene expression.* Development, 2009. **136**(2): p. 241-51.

134. Lustig, B., et al., *Negative feedback loop of Wnt signaling through upregulation of conductin/axin2 in colorectal and liver tumors.* Mol Cell Biol, 2002. **22**(4): p. 1184-93.

135. Stadeli, R., R. Hoffmans, and K. Basler, *Transcription under the control of nuclear Arm/beta-catenin.* Curr Biol, 2006. **16**(10): p. R378-85.

136. Mosimann, C., G. Hausmann, and K. Basler, *Parafibromin/Hyrax activates Wnt/Wg target gene transcription by direct association with beta-catenin/Armadillo.* Cell, 2006. **125**(2): p. 327-41.

137. Tetsu, O. and F. McCormick, *Beta-catenin regulates expression of cyclin D1 in colon carcinoma cells.* Nature, 1999. **398**(6726): p. 422-6.

138. Jamora, C., et al., *Links between signal transduction, transcription and adhesion in epithelial bud development.* Nature, 2003. **422**(6929): p. 317-22.

139. ten Berge, D., et al., *Wnt signaling mediates self-organization and axis formation in embryoid bodies.* Cell Stem Cell, 2008. **3**(5): p. 508-18.

140. Brabletz, T., et al., *beta-catenin regulates the expression of the matrix metalloproteinase-7 in human colorectal cancer.* Am J Pathol, 1999. **155**(4): p. 1033-8.

141. Crawford, H.C., et al., *The metalloproteinase matrilysin is a target of beta-catenin transactivation in intestinal tumors.* Oncogene, 1999. **18**(18): p. 2883-91.

142. Wu, B., S.P. Crampton, and C.C. Hughes, *Wnt signaling induces matrix metalloproteinase expression and regulates T cell transmigration.* Immunity, 2007. **26**(2): p. 227-39.

143. Zhang, T., et al., *Evidence that APC regulates survivin expression: a possible mechanism contributing to the stem cell origin of colon cancer.* Cancer Res, 2001. **61**(24): p. 8664-7.

144. Zhang, X., J.P. Gaspard, and D.C. Chung, *Regulation of vascular endothelial growth factor by the Wnt and K-ras pathways in colonic neoplasia.* Cancer Res, 2001. **61**(16): p. 6050-4.

145. Cole, M.F., et al., *Tcf3 is an integral component of the core regulatory circuitry of embryonic stem cells.* Genes Dev, 2008. **22**(6): p. 746-55.

146. Zhang, Z., et al., *Secreted frizzled related protein 2 protects cells from apoptosis by blocking the effect of canonical Wnt3a.* J Mol Cell Cardiol, 2009. **46**(3): p. 370-7.

147. Kazanskaya, O., et al., *R-Spondin2 is a secreted activator of Wnt/beta-catenin signaling and is required for Xenopus myogenesis.* Dev Cell, 2004. **7**(4): p. 525-34.

148. Khan, Z., et al., *Analysis of endogenous LRP6 function reveals a novel feedback mechanism by which Wnt negatively regulates its receptor.* Mol Cell Biol, 2007. **27**(20): p. 7291-301.

149. Willert, J., et al., *A transcriptional response to Wnt protein in human embryonic carcinoma cells.* BMC Dev Biol, 2002. **2**: p. 8.

150. Barker, N., et al., *Identification of stem cells in small intestine and colon by marker gene Lgr5.* Nature, 2007. **449**(7165): p. 1003-7.

151. Lescher, B., B. Haenig, and A. Kispert, *sFRP-2 is a target of the Wnt-4 signaling pathway in the developing metanephric kidney.* Dev Dyn, 1998. **213**(4): p. 440-51.

152. Chamorro, M.N., et al., *FGF-20 and DKK1 are transcriptional targets of beta-catenin and FGF-20 is implicated in cancer and development.* EMBO J, 2005. **24**(1): p. 73-84.

153. Niida, A., et al., *DKK1, a negative regulator of Wnt signaling, is a target of the beta-catenin/TCF pathway.* Oncogene, 2004. **23**(52): p. 8520-6.

154. Gonzalez-Sancho, J.M., et al., *The Wnt antagonist DICKKOPF-1 gene is a downstream target of beta-catenin/TCF and is downregulated in human colon cancer.* Oncogene, 2005. **24**(6): p. 1098-103.

155. Yan, D., et al., *Elevated expression of axin2 and hnkd mRNA provides evidence that Wnt/beta -catenin signaling is activated in human colon tumors.* Proc Natl Acad Sci U S A, 2001. **98**(26): p. 14973-8.

156. Jho, E.H., et al., *Wnt/beta-catenin/Tcf signaling induces the transcription of Axin2, a negative regulator of the signaling pathway.* Mol Cell Biol, 2002. **22**(4): p. 1172-83.

157. MacDonald, B.T., K. Tamai, and X. He, *Wnt/beta-catenin signaling: components, mechanisms, and diseases.* Dev Cell, 2009. **17**(1): p. 9-26.

158. von Maltzahn, J., et al., *Wnt signaling in myogenesis.* Trends Cell Biol, 2012. **22**(11): p. 602-9.

159. Moverare-Skrtic, S., et al., *Osteoblast-derived WNT16 represses osteoclastogenesis and prevents cortical bone fragility fractures.* Nat Med, 2014. **20**(11): p. 1279-88.

160. Sugimura, R. and L. Li, *Noncanonical Wnt signaling in vertebrate development, stem cells, and diseases.* Birth Defects Res C Embryo Today, 2010. **90**(4): p. 243-56.

161. Stewart, D.J., *Wnt signaling pathway in non-small cell lung cancer.* J Natl Cancer Inst, 2014. **106**(1): p. djt356.

162. Kikuchi, A., et al., *Wnt5a: its signalling, functions and implication in diseases.* Acta Physiol (Oxf), 2012. **204**(1): p. 17-33.

163. Endo, M., et al., *Insight into the role of Wnt5a-induced signaling in normal and cancer cells.* Int Rev Cell Mol Biol, 2015. **314**: p. 117-48.

164. Mikels, A.J. and R. Nusse, *Purified Wnt5a protein activates or inhibits beta-catenin-TCF signaling depending on receptor context.* PLoS Biol, 2006. **4**(4): p. e115.

165. van Amerongen, R., et al., *Wnt5a can both activate and repress Wnt/beta-catenin signaling during mouse embryonic development.* Dev Biol, 2012. **369**(1): p. 101-14.

166. Okamoto, M., et al., *Noncanonical Wnt5a enhances Wnt/beta-catenin signaling during osteoblastogenesis.* Sci Rep, 2014. **4**: p. 4493.

167. Li, C., et al., *Non-canonical WNT signalling in the lung.* J Biochem, 2015. **158**(5): p. 355-65.

168. Pez, F., et al., *Wnt signaling and hepatocarcinogenesis: molecular targets for the development of innovative anticancer drugs.* J Hepatol, 2013. **59**(5): p. 1107-17.

169. Jones, C. and P. Chen, *Planar cell polarity signaling in vertebrates.* Bioessays, 2007. **29**(2): p. 120-32.

170. Oishi, I., et al., *The receptor tyrosine kinase Ror2 is involved in non-canonical Wnt5a/JNK signalling pathway.* Genes Cells, 2003. **8**(7): p. 645-54.

171. Ishitani, T., et al., *The TAK1-NLK mitogen-activated protein kinase cascade functions in the Wnt-5a/Ca(2+) pathway to antagonize Wnt/beta-catenin signaling.* Mol Cell Biol, 2003. **23**(1): p. 131-9.

172. Monroe, D.G., et al., *Update on Wnt signaling in bone cell biology and bone disease.* Gene, 2012. **492**(1): p. 1-18.

173. Gong, Y., et al., *LDL receptor-related protein 5 (LRP5) affects bone accrual and eye development.* Cell, 2001. **107**(4): p. 513-23.

174. Mani, A., et al., *LRP6 mutation in a family with early coronary disease and metabolic risk factors.* Science, 2007. **315**(5816): p. 1278-82.

175. Wang, Y.K., et al., *Characterization and expression pattern of the frizzled gene Fzd9, the mouse homolog of FZD9 which is deleted in Williams-Beuren syndrome.* Genomics, 1999. **57**(2): p. 235-48.

176. Niemann, S., et al., *Homozygous WNT3 mutation causes tetra-amelia in a large consanguineous family.* Am J Hum Genet, 2004. **74**(3): p. 558-63.

177. Woods, C.G., et al., *Mutations in WNT7A cause a range of limb malformations, including Fuhrmann syndrome and Al-Awadi/Raas-Rothschild/Schinzel phocomelia syndrome.* Am J Hum Genet, 2006. **79**(2): p. 402-8.

178. Parma, P., et al., *R-spondin1 is essential in sex determination, skin differentiation and malignancy.* Nat Genet, 2006. **38**(11): p. 1304-9.

179. Blaydon, D.C., et al., *The gene encoding R-spondin 4 (RSPO4), a secreted protein implicated in Wnt signaling, is mutated in inherited anonychia.* Nat Genet, 2006. **38**(11): p. 1245-7.

180. Nam, J.S., et al., *Mouse R-spondin2 is required for apical ectodermal ridge maintenance in the hindlimb.* Dev Biol, 2007. **311**(1): p. 124-35.

181. Bell, S.M., et al., *R-spondin 2 is required for normal laryngeal-tracheal, lung and limb morphogenesis.* Development, 2008. **135**(6): p. 1049-58.

182. Yamada, W., et al., *Craniofacial malformation in R-spondin2 knockout mice.* Biochem Biophys Res Commun, 2009. **381**(3): p. 453-8.

183. Grzeschik, K.H., et al., *Deficiency of PORCN, a regulator of Wnt signaling, is associated with focal dermal hypoplasia.* Nat Genet, 2007. **39**(7): p. 833-5.

184. Wang, X., et al., *Mutations in X-linked PORCN, a putative regulator of Wnt signaling, cause focal dermal hypoplasia.* Nat Genet, 2007. **39**(7): p. 836-8.

185. Barrott, J.J., et al., *Deletion of mouse Porcn blocks Wnt ligand secretion and reveals an ectodermal etiology of human focal dermal hypoplasia/Goltz syndrome.* Proc Natl Acad Sci U S A, 2011. **108**(31): p. 12752-7.

186. Biechele, S., B.J. Cox, and J. Rossant, *Porcupine homolog is required for canonical Wnt signaling and gastrulation in mouse embryos.* Dev Biol, 2011. **355**(2): p. 275-85.

187. Barker, N. and H. Clevers, *Leucine-rich repeat-containing G-protein-coupled receptors as markers of adult stem cells.* Gastroenterology, 2010. **138**(5): p. 1681-96.

188. Mustata, R.C., et al., *Lgr4 is required for Paneth cell differentiation and maintenance of intestinal stem cells ex vivo.* EMBO Rep, 2011. **12**(6): p. 558-64.

189. Barker, N., et al., *Lgr5(+ve) stem cells drive self-renewal in the stomach and build long-lived gastric units in vitro.* Cell Stem Cell, 2010. **6**(1): p. 25-36.

190. Jaks, V., et al., *Lgr5 marks cycling, yet long-lived, hair follicle stem cells.* Nat Genet, 2008. **40**(11): p. 1291-9.

191. Barker, N., et al., *Crypt stem cells as the cells-of-origin of intestinal cancer.* Nature, 2009. **457**(7229): p. 608-11.

192. Wood, L.D., et al., *The genomic landscapes of human breast and colorectal cancers.* Science, 2007. **318**(5853): p. 1108-13.

193. Bass, A.J., et al., *Genomic sequencing of colorectal adenocarcinomas identifies a recurrent VTI1A-TCF7L2 fusion.* Nat Genet, 2011. **43**(10): p. 964-8.

194. Liu, W., et al., *Mutations in AXIN2 cause colorectal cancer with defective mismatch repair by activating beta-catenin/TCF signalling.* Nat Genet, 2000. **26**(2): p. 146-7.

195. Morin, P.J., et al., *Activation of beta-catenin-Tcf signaling in colon cancer by mutations in beta-catenin or APC.* Science, 1997. **275**(5307): p. 1787-90.

196. Reya, T. and H. Clevers, *Wnt signalling in stem cells and cancer.* Nature, 2005. **434**(7035): p. 843-50.

197. Kanazawa, A., et al., *Association of the gene encoding wingless-type mammary tumor virus integration-site family member 5B (WNT5B) with type 2 diabetes.* Am J Hum Genet, 2004. **75**(5): p. 832-43.

198. Christodoulides, C., et al., *WNT10B mutations in human obesity.* Diabetologia, 2006. **49**(4): p. 678-84.

199. Grant, S.F., et al., *Variant of transcription factor 7-like 2 (TCF7L2) gene confers risk of type 2 diabetes.* Nat Genet, 2006. **38**(3): p. 320-3.

200. Moon, R.T., et al., *WNT and beta-catenin signalling: diseases and therapies.* Nat Rev Genet, 2004. **5**(9): p. 691-701.

201. Matsuzaki, S., et al., *Targeting the Wnt/beta-catenin pathway in endometriosis: a potentially effective approach for treatment and prevention.* Mol Cell Ther, 2014. **2**: p. 36.

202. Matsuzaki, S. and C. Darcha, *Involvement of the Wnt/beta-catenin signaling pathway in the cellular and molecular mechanisms of fibrosis in endometriosis.* PLoS One, 2013. **8**(10): p. e76808.

203. Huber, A.H., W.J. Nelson, and W.I. Weis, *Three-dimensional structure of the armadillo repeat region of beta-catenin.* Cell, 1997. **90**(5): p. 871-82.

204. Lepourcelet, M., et al., *Small-molecule antagonists of the oncogenic Tcf/beta-catenin protein complex.* Cancer Cell, 2004. **5**(1): p. 91-102.

205. Chen, B., et al., *Small molecule-mediated disruption of Wnt-dependent signaling in tissue regeneration and cancer.* Nat Chem Biol, 2009. **5**(2): p. 100-7.

206. Proffitt, K.D., et al., *Pharmacological inhibition of the Wnt acyltransferase PORCN prevents growth of WNT-driven mammary cancer.* Cancer Res, 2013. **73**(2): p. 502-7.

207. Liu, J., et al., *Targeting Wnt-driven cancer through the inhibition of Porcupine by LGK974.* Proc Natl Acad Sci U S A, 2013. **110**(50): p. 20224-9.

208. Bodine, P.V., et al., *A small molecule inhibitor of the Wnt antagonist secreted frizzled-related protein-1 stimulates bone formation.* Bone, 2009. **44**(6): p. 1063-8.

209. Shultz, M.D., et al., *Identification of NVP-TNKS656: the use of structure-efficiency relationships to generate a highly potent, selective, and orally active tankyrase inhibitor.* J Med Chem, 2013. **56**(16): p. 6495-511.

210. Schoumacher, M., et al., *Inhibiting Tankyrases sensitizes KRAS-mutant cancer cells to MEK inhibitors via FGFR2 feedback signaling.* Cancer Res, 2014. **74**(12): p. 3294-305.

211. Miyabayashi, T., et al., *Wnt/beta-catenin/CBP signaling maintains long-term murine embryonic stem cell pluripotency.* Proc Natl Acad Sci U S A, 2007. **104**(13): p. 5668-73.

212. Zhang, Q., et al., *Small-molecule synergist of the Wnt/beta-catenin signaling pathway.* Proc Natl Acad Sci U S A, 2007. **104**(18): p. 7444-8.

213. Emami, K.H., et al., *A small molecule inhibitor of beta-catenin/CREB-binding protein transcription [corrected].* Proc Natl Acad Sci U S A, 2004. **101**(34): p. 12682-7.

214. Coghlan, M.P., et al., *Selective small molecule inhibitors of glycogen synthase kinase-3 modulate glycogen metabolism and gene transcription.* Chem Biol, 2000. **7**(10): p. 793-803.

215. Simon, E., et al., *The spatial distribution of LGR5+ cells correlates with gastric cancer progression.* PLoS One, 2012. **7**(4): p. e35486.

216. Holland, P.M., et al., *Detection of specific polymerase chain reaction product by utilizing the 5'----3' exonuclease activity of Thermus aquaticus DNA polymerase.* Proc Natl Acad Sci U S A, 1991. **88**(16): p. 7276-80.

217. Livak, K.J. and T.D. Schmittgen, *Analysis of relative gene expression data using real-time quantitative PCR and the 2(-Delta Delta C(T)) Method.* Methods, 2001. **25**(4): p. 402-8.

218. Nguyen, U., et al., *The Simple Western[trade]: a gel-free, blot-free, hands-free Western blotting reinvention.* Nat Meth, 2011. **8**(11).

219. Dawe, C.J., et al., *Growth in Continuous Culture, and in Hamsters, of Cells from a Neoplasm Associated with Acanthosis Nigricans.* J Natl Cancer Inst, 1964. **33**: p. 441-56.

220. Satyaswaroop, P.G. and S.S. Tabibzadeh, *Extracellular matrix and the patterns of differentiation of human endometrial carcinomas in vitro and in vivo.* Cancer Res, 1991. **51**(20): p. 5661-6.

221. Desai, N.N., et al., *Novel human endometrial cell line promotes blastocyst development.* Fertil Steril, 1994. **61**(4): p. 760-6.

222. Kuramoto, H., S. Tamura, and Y. Notake, *Establishment of a cell line of human endometrial adenocarcinoma in vitro.* Am J Obstet Gynecol, 1972. **114**(8): p. 1012-9.

223. Nishida, M., et al., *[Establishment of a new human endometrial adenocarcinoma cell line, Ishikawa cells, containing estrogen and progesterone receptors].* Nihon Sanka Fujinka Gakkai Zasshi, 1985. **37**(7): p. 1103-11.

224. Richardson, G.S., et al., *KLE: a cell line with defective estrogen receptor derived from undifferentiated endometrial cancer.* Gynecol Oncol, 1984. **17**(2): p. 213-30.

225. Way, D.L., et al., *Characterization of a new human endometrial carcinoma (RL95-2) established in tissue culture.* In Vitro, 1983. **19**(3 Pt 1): p. 147-58.

226. Zeitvogel, A., R. Baumann, and A. Starzinski-Powitz, *Identification of an invasive, N-cadherin-expressing epithelial cell type in endometriosis using a new cell culture model.* Am J Pathol, 2001. **159**(5): p. 1839-52.

227. Harker, W.G., F.R. MacKintosh, and B.I. Sikic, *Development and characterization of a human sarcoma cell line, MES-SA, sensitive to multiple drugs.* Cancer Res, 1983. **43**(10): p. 4943-50.

228. Felgner, P.L., et al., *Lipofection: a highly efficient, lipid-mediated DNA-transfection procedure.* Proc Natl Acad Sci U S A, 1987. **84**(21): p. 7413-7.

229. *Classification and staging of malignant tumours in the female pelvis.* Acta Obstet Gynecol Scand, 1971. **50**(1): p. 1-7.

230. Qiagen, *TCF/LEF Reporter.* Cignal Reporter Home, 2010.

231. Promega, *ApoTox-Glo(TM) Triplex Assay.* Technical Manual, 2015.

232. Promega, *CellTiter-Glo(R) Luminescent Cell Viability Assay.* Technical Bulletin - Instructions for Use of Products, 2015.

233. Boyden, S., *The chemotactic effect of mixtures of antibody and antigen on polymorphonuclear leucocytes.* J Exp Med, 1962. **115**: p. 453-66.

234. Somigliana, E., et al., *Endometrial ability to implant in ectopic sites can be prevented by interleukin-12 in a murine model of endometriosis.* Hum Reprod, 1999. **14**(12): p. 2944-50.

235. Jiang, X., et al., *Inactivating mutations of RNF43 confer Wnt dependency in pancreatic ductal adenocarcinoma.* Proc Natl Acad Sci U S A, 2013. **110**(31): p. 12649-54.

236. Oltvai, Z.N., C.L. Milliman, and S.J. Korsmeyer, *Bcl-2 heterodimerizes in vivo with a conserved homolog, Bax, that accelerates programmed cell death.* Cell, 1993. **74**(4): p. 609-19.

237. Vaux, D.L., S. Cory, and J.M. Adams, *Bcl-2 gene promotes haemopoietic cell survival and cooperates with c-myc to immortalize pre-B cells.* Nature, 1988. **335**(6189): p. 440-2.

238. Halim, H., S. Luanpitpong, and P. Chanvorachote, *Acquisition of anoikis resistance up-regulates caveolin-1 expression in human non-small cell lung cancer cells.* Anticancer Res, 2012. **32**(5): p. 1649-58.

239. Hoang, B.H., et al., *Dickkopf 3 inhibits invasion and motility of Saos-2 osteosarcoma cells by modulating the Wnt-beta-catenin pathway.* Cancer Res, 2004. **64**(8): p. 2734-9.

240. Colvin, J.S., et al., *Lung hypoplasia and neonatal death in Fgf9-null mice identify this gene as an essential regulator of lung mesenchyme.* Development, 2001. **128**(11): p. 2095-106.

241. Yu, H., et al., *Frizzled 2 and frizzled 7 function redundantly in convergent extension and closure of the ventricular septum and palate: evidence for a network of interacting genes.* Development, 2012. **139**(23): p. 4383-94.

242. Carmon, K.S., et al., *LGR5 interacts and cointernalizes with Wnt receptors to modulate Wnt/beta-catenin signaling.* Mol Cell Biol, 2012. **32**(11): p. 2054-64.

243. Zilberberg, A., A. Yaniv, and A. Gazit, *The low density lipoprotein receptor-1, LRP1, interacts with the human frizzled-1 (HFz1) and down-regulates the canonical Wnt signaling pathway.* J Biol Chem, 2004. **279**(17): p. 17535-42.

244. Lillis, A.P., I. Mikhailenko, and D.K. Strickland, *Beyond endocytosis: LRP function in cell migration, proliferation and vascular permeability.* J Thromb Haemost, 2005. **3**(8): p. 1884-93.

245. Song, H., et al., *Low-density lipoprotein receptor-related protein 1 promotes cancer cell migration and invasion by inducing the expression of matrix metalloproteinases 2 and 9.* Cancer Res, 2009. **69**(3): p. 879-86.

246. Robinson, M.J. and M.H. Cobb, *Mitogen-activated protein kinase pathways.* Curr Opin Cell Biol, 1997. **9**(2): p. 180-6.

247. Gerdes, J., et al., *Production of a mouse monoclonal antibody reactive with a human nuclear antigen associated with cell proliferation.* Int J Cancer, 1983. **31**(1): p. 13-20.

248. Xu, X., et al., *Matrix metalloproteinase-2 contributes to cancer cell migration on collagen.* Cancer Res, 2005. **65**(1): p. 130-6.

249. Mason, D.P., et al., *Matrix metalloproteinase-9 overexpression enhances vascular smooth muscle cell migration and alters remodeling in the injured rat carotid artery.* Circ Res, 1999. **85**(12): p. 1179-85.

250. Binnerts, M.E., et al., *R-Spondin1 regulates Wnt signaling by inhibiting internalization of LRP6.* Proc Natl Acad Sci U S A, 2007. **104**(37): p. 14700-5.

251. Cruciat, C.M. and C. Niehrs, *Secreted and transmembrane wnt inhibitors and activators.* Cold Spring Harb Perspect Biol, 2013. **5**(3): p. a015081.

252. Yanagita, M., *BMP antagonists: their roles in development and involvement in pathophysiology.* Cytokine Growth Factor Rev, 2005. **16**(3): p. 309-17.

253. Airik, R., et al., *Tbx18 regulates the development of the ureteral mesenchyme.* J Clin Invest, 2006. **116**(3): p. 663-74.

254. Smolich, B.D., et al., *Wnt family proteins are secreted and associated with the cell surface.* Mol Biol Cell, 1993. **4**(12): p. 1267-75.

255. Morita, H., et al., *Neonatal lethality of LGR5 null mice is associated with ankyloglossia and gastrointestinal distension.* Mol Cell Biol, 2004. **24**(22): p. 9736-43.

256. Sun, X., et al., *Ovarian LGR5 is critical for successful pregnancy.* FASEB J, 2014. **28**(5): p. 2380-9.

257. Gandhirajan, R.K., et al., *Small molecule inhibitors of Wnt/beta-catenin/lef-1 signaling induces apoptosis in chronic lymphocytic leukemia cells in vitro and in vivo.* Neoplasia, 2010. **12**(4): p. 326-35.

258. Semb, H. and G. Christofori, *The tumor-suppressor function of E-cadherin.* Am J Hum Genet, 1998. **63**(6): p. 1588-93.

259. Resnitzky, D. and S.I. Reed, *Different roles for cyclins D1 and E in regulation of the G1-to-S transition.* Mol Cell Biol, 1995. **15**(7): p. 3463-9.

260. Zagzag, D., et al., *Expression of hypoxia-inducible factor 1alpha in brain tumors: association with angiogenesis, invasion, and progression.* Cancer, 2000. **88**(11): p. 2606-18.

261. Niwa, H., J. Miyazaki, and A.G. Smith, *Quantitative expression of Oct-3/4 defines differentiation, dedifferentiation or self-renewal of ES cells.* Nat Genet, 2000. **24**(4): p. 372-6.

262. Li, J., J. Li, and B. Chen, *Oct4 was a novel target of Wnt signaling pathway.* Mol Cell Biochem, 2012. **362**(1-2): p. 233-40.

263. Cano, A., et al., *The transcription factor snail controls epithelial-mesenchymal transitions by repressing E-cadherin expression.* Nat Cell Biol, 2000. **2**(2): p. 76-83.

264. Pepinsky, B., et al., *Structure/function studies on vascular cell adhesion molecule-1.* J Biol Chem, 1992. **267**(25): p. 17820-6.

265. Yla-Herttuala, S., et al., *Vascular endothelial growth factors: biology and current status of clinical applications in cardiovascular medicine.* J Am Coll Cardiol, 2007. **49**(10): p. 1015-26.

266. de Mattos, R.M., et al., *Aberrant levels of Wnt/beta-catenin pathway components in a rat model of endometriosis.* Histol Histopathol, 2016: p. 11730.

267. Cheng, C.W., S.K. Smith, and D.S. Charnock-Jones, *Transcript profile and localization of Wnt signaling-related molecules in human endometrium.* Fertil Steril, 2008. **90**(1): p. 201-4.

268. Brosens, I., J.J. Brosens, and G. Benagiano, *The eutopic endometrium in endometriosis: are the changes of clinical significance?* Reprod Biomed Online, 2012. **24**(5): p. 496-502.

269. Liu, H. and J.H. Lang, *Is abnormal eutopic endometrium the cause of endometriosis? The role of eutopic endometrium in pathogenesis of endometriosis.* Med Sci Monit, 2011. **17**(4): p. RA92-9.

270. Meola, J., et al., *Differentially expressed genes in eutopic and ectopic endometrium of women with endometriosis.* Fertil Steril, 2010. **93**(6): p. 1750-73.

271. Sohler, F., et al., *Tissue remodeling and nonendometrium-like menstrual cycling are hallmarks of peritoneal endometriosis lesions.* Reprod Sci, 2013. **20**(1): p. 85-102.

272. Diaz-Valdivia, N., et al., *Enhanced caveolin-1 expression increases migration, anchorage-independent growth and invasion of endometrial adenocarcinoma cells.* BMC Cancer, 2015. **15**: p. 463.

273. Catasus, L., et al., *Low-density lipoprotein receptor-related protein 1 (LRP-1) is associated with highgrade, advanced stage and p53 and p16 alterations in endometrial carcinomas.* Histopathology, 2011. **59**(3): p. 567-71.

274. Weigel, M.T., et al., *Differential expression of MMP-2, MMP-9 and PCNA in endometriosis and endometrial carcinoma.* Eur J Obstet Gynecol Reprod Biol, 2012. **160**(1): p. 74-8.

275. Matsuzaki, S. and C. Darcha, *In vitro effects of a small-molecule antagonist of the Tcf/ss-catenin complex on endometrial and endometriotic cells of patients with endometriosis.* PLoS One, 2013. **8**(4): p. e61690.

276. Gaetje, R., et al., *Invasiveness of endometriotic cells in vitro.* Lancet, 1995. **346**(8988): p. 1463-4.

277. Steelman, L.S., et al., *JAK/STAT, Raf/MEK/ERK, PI3K/Akt and BCR-ABL in cell cycle progression and leukemogenesis.* Leukemia, 2004. **18**(2): p. 189-218.

278. Yotova, I.Y., et al., *Abnormal activation of Ras/Raf/MAPK and RhoA/ROCKII signalling pathways in eutopic endometrial stromal cells of patients with endometriosis.* Hum Reprod, 2011. **26**(4): p. 885-97.

279. Wing, L.Y., et al., *Expression and mitogenic effect of fibroblast growth factor-9 in human endometriotic implant is regulated by aberrant production of estrogen.* J Clin Endocrinol Metab, 2003. **88**(11): p. 5547-54.

280. Hendrix, N.D., et al., *Fibroblast growth factor 9 has oncogenic activity and is a downstream target of Wnt signaling in ovarian endometrioid adenocarcinomas.* Cancer Res, 2006. **66**(3): p. 1354-62.

281. Tsai, S.J., et al., *Fibroblast growth factor-9 is an endometrial stromal growth factor.* Endocrinology, 2002. **143**(7): p. 2715-21.

282. Li, S.F., et al., *The number of proliferating cell nuclear antigen positive cells in endometriotic lesions differs from that in the endometrium. Analysis of PCNA positive cells during the menstrual cycle and in post-menopause.* Virchows Arch A Pathol Anat Histopathol, 1993. **423**(4): p. 257-63.

283. Jones, R.K., J.N. Bulmer, and R.F. Searle, *Immunohistochemical characterization of proliferation, oestrogen receptor and progesterone receptor expression in endometriosis: comparison of eutopic and ectopic endometrium with normal cycling endometrium.* Hum Reprod, 1995. **10**(12): p. 3272-9.

284. Scotti, S., et al., *Reduced proliferation and cell adhesion in endometriosis.* Mol Hum Reprod, 2000. **6**(7): p. 610-7.

285. Itasaki, N., et al., *Wise, a context-dependent activator and inhibitor of Wnt signalling.* Development, 2003. **130**(18): p. 4295-305.

286. Wingfield, M., et al., *Cell proliferation is increased in the endometrium of women with endometriosis.* Fertil Steril, 1995. **64**(2): p. 340-6.

287. Matsuzaki, S., et al., *Impaired down-regulation of E-cadherin and beta-catenin protein expression in endometrial epithelial cells in the mid-secretory endometrium of infertile patients with endometriosis.* J Clin Endocrinol Metab, 2010. **95**(7): p. 3437-45.

288. Pabona, J.M., et al., *Kruppel-like factor 9 and progesterone receptor coregulation of decidualizing endometrial stromal cells: implications for the pathogenesis of endometriosis.* J Clin Endocrinol Metab, 2012. **97**(3): p. E376-92.

289. Aghajanova, L., et al., *The protein kinase A pathway-regulated transcriptome of endometrial stromal fibroblasts reveals compromised differentiation and persistent proliferative potential in endometriosis.* Endocrinology, 2010. **151**(3): p. 1341-55.

290. Velarde, M.C., et al., *Increased mitogen-activated protein kinase kinase/extracellularly regulated kinase activity in human endometrial stromal fibroblasts of women with endometriosis reduces 3',5'-cyclic adenosine 5'-monophosphate inhibition of cyclin D1.* Endocrinology, 2009. **150**(10): p. 4701-12.

291. Otto, H., et al., *In silico characterization of the family of PARP-like poly(ADP-ribosyl)transferases (pARTs).* BMC Genomics, 2005. **6**: p. 139.

292. Kleine, H., et al., *Substrate-assisted catalysis by PARP10 limits its activity to mono-ADP-ribosylation.* Mol Cell, 2008. **32**(1): p. 57-69.

293. Smith, S., et al., *Tankyrase, a poly(ADP-ribose) polymerase at human telomeres.* Science, 1998. **282**(5393): p. 1484-7.

294. Lyons, R.J., et al., *Identification of a novel human tankyrase through its interaction with the adaptor protein Grb14.* J Biol Chem, 2001. **276**(20): p. 17172-80.

295. Chang, W., J.N. Dynek, and S. Smith, *NuMA is a major acceptor of poly(ADP-ribosyl)ation by tankyrase 1 in mitosis.* Biochem J, 2005. **391**(Pt 2): p. 177-84.

296. Cho-Park, P.F. and H. Steller, *Proteasome regulation by ADP-ribosylation.* Cell, 2013. **153**(3): p. 614-27.

297. Leung, A., et al., *Poly(ADP-ribose) regulates post-transcriptional gene regulation in the cytoplasm.* RNA Biol, 2012. **9**(5): p. 542-8.

298. Cooke, P.S., et al., *Uterine glands: development, function and experimental model systems.* Mol Hum Reprod, 2013. **19**(9): p. 547-58.

299. Miller, C. and D.A. Sassoon, *Wnt-7a maintains appropriate uterine patterning during the development of the mouse female reproductive tract.* Development, 1998. **125**(16): p. 3201-11.

300. Dunlap, K.A., et al., *Postnatal deletion of Wnt7a inhibits uterine gland morphogenesis and compromises adult fertility in mice.* Biol Reprod, 2011. **85**(2): p. 386-96.

301. Mericskay, M., J. Kitajewski, and D. Sassoon, *Wnt5a is required for proper epithelial-mesenchymal interactions in the uterus.* Development, 2004. **131**(9): p. 2061-72.

302. Franco, H.L., et al., *WNT4 is a key regulator of normal postnatal uterine development and progesterone signaling during embryo implantation and decidualization in the mouse.* FASEB J, 2011. **25**(4): p. 1176-87.

303. Jeong, J.W., et al., *beta-catenin mediates glandular formation and dysregulation of beta-catenin induces hyperplasia formation in the murine uterus.* Oncogene, 2009. **28**(1): p. 31-40.

304. Shelton, D.N., et al., *The role of LEF1 in endometrial gland formation and carcinogenesis.* PLoS One, 2012. **7**(7): p. e40312.

305. Villacorte, M., et al., *beta-Catenin signaling regulates Foxa2 expression during endometrial hyperplasia formation.* Oncogene, 2013. **32**(29): p. 3477-82.

306. Mohri, Y., et al., *Reduced fertility with impairment of early-stage embryos observed in mice lacking Lgr4 in epithelial tissues.* Fertil Steril, 2010. **94**(7): p. 2878-81.

307. Sone, M., et al., *LGR4 expressed in uterine epithelium is necessary for uterine gland development and contributes to decidualization in mice.* FASEB J, 2013. **27**(12): p. 4917-28.

308. Chen, Q., et al., *Embryo-uterine cross-talk during implantation: the role of Wnt signaling.* Mol Hum Reprod, 2009. **15**(4): p. 215-21.

309. Fujino, H., K.A. West, and J.W. Regan, *Phosphorylation of glycogen synthase kinase-3 and stimulation of T-cell factor signaling following activation of EP2 and EP4 prostanoid receptors by prostaglandin E2.* J Biol Chem, 2002. **277**(4): p. 2614-9.

310. Hino, S., et al., *Phosphorylation of beta-catenin by cyclic AMP-dependent protein kinase stabilizes beta-catenin through inhibition of its ubiquitination.* Mol Cell Biol, 2005. **25**(20): p. 9063-72.

311. Rocha, A.L., F.M. Reis, and R.N. Taylor, *Angiogenesis and endometriosis.* Obstet Gynecol Int, 2013. **2013**: p. 859619.

312. Donnez, J., et al., *Vascular endothelial growth factor (VEGF) in endometriosis.* Hum Reprod, 1998. **13**(6): p. 1686-90.

313. McLaren, J., et al., *Vascular endothelial growth factor is produced by peritoneal fluid macrophages in endometriosis and is regulated by ovarian steroids.* J Clin Invest, 1996. **98**(2): p. 482-9.

314. Mueller, M.D., et al., *Neutrophils infiltrating the endometrium express vascular endothelial growth factor: potential role in endometrial angiogenesis.* Fertil Steril, 2000. **74**(1): p. 107-12.

315. Ris, H.W., *The integration of a comprehensive medical program in a juvenile correctional institution.* J Am Med Womens Assoc, 1975. **30**(9): p. 367-78.

316. Sakuragi, N., et al., *Decreased E-cadherin expression in endometrial carcinoma is associated with tumor dedifferentiation and deep myometrial invasion.* Gynecol Oncol, 1994. **53**(2): p. 183-9.

317. Beliard, A., et al., *Localization of laminin, fibronectin, E-cadherin, and integrins in endometrium and endometriosis.* Fertil Steril, 1997. **67**(2): p. 266-72.

318. Shaco-Levy, R., et al., *Matrix metalloproteinases 2 and 9, E-cadherin, and beta-catenin expression in endometriosis, low-grade endometrial carcinoma and non-neoplastic eutopic endometrium.* Eur J Obstet Gynecol Reprod Biol, 2008. **139**(2): p. 226-32.

319. Gaetje, R., et al., *Nonmalignant epithelial cells, potentially invasive in human endometriosis, lack the tumor suppressor molecule E-cadherin.* Am J Pathol, 1997. **150**(2): p. 461-7.

320. Ewan, K.B. and T.C. Dale, *The potential for targeting oncogenic WNT/beta-catenin signaling in therapy.* Curr Drug Targets, 2008. **9**(7): p. 532-47.

321. Kahn, M., *Can we safely target the WNT pathway?* Nat Rev Drug Discov, 2014. **13**(7): p. 513-32.

322. Sun, X., et al., *In pursuit of leucine-rich repeat-containing G protein-coupled receptor-5 regulation and function in the uterus.* Endocrinology, 2009. **150**(11): p. 5065-73.

323. Gargett, C.E., *Uterine stem cells: what is the evidence?* Hum Reprod Update, 2007. **13**(1): p. 87-101.

324. Du, H. and H.S. Taylor, *Stem cells and female reproduction.* Reprod Sci, 2009. **16**(2): p. 126-39.

325. Maruyama, T., et al., *Human uterine stem/progenitor cells: their possible role in uterine physiology and pathology.* Reproduction, 2010. **140**(1): p. 11-22.

326. Gargett, C.E. and H. Masuda, *Adult stem cells in the endometrium.* Mol Hum Reprod, 2010. **16**(11): p. 818-34.

327. Gil-Sanchis, C., et al., *Leucine-rich repeat-containing G-protein-coupled receptor 5 (Lgr5) as a putative human endometrial stem cell marker.* Mol Hum Reprod, 2013. **19**(7): p. 407-14.

328. Valentijn, A.J., et al., *SSEA-1 isolates human endometrial basal glandular epithelial cells: phenotypic and functional characterization and implications in the pathogenesis of endometriosis.* Hum Reprod, 2013. **28**(10): p. 2695-708.

329. Liu, Z., et al., *Over-expression of LGR5 correlates with poor survival of colon cancer in mice as well as in patients.* Neoplasma, 2014. **61**(2): p. 177-85.

330. Szkandera, J., et al., *LGR5 rs17109924 is a predictive genetic biomarker for time to recurrence in patients with colon cancer treated with 5-fluorouracil-based adjuvant chemotherapy.* Pharmacogenomics J, 2015. **15**(5): p. 391-6.

331. Bu, Z., et al., *LGR5 is a promising biomarker for patients with stage I and II gastric cancer.* Chin J Cancer Res, 2013. **25**(1): p. 79-89.

332. Fassbender, A., et al., *Biomarkers of endometriosis.* Fertil Steril, 2013. **99**(4): p. 1135-45.

333. Fassbender, A., et al., *Update on Biomarkers for the Detection of Endometriosis.* Biomed Res Int, 2015. **2015**: p. 130854.

334. Wilhelm, D., S. Palmer, and P. Koopman, *Sex determination and gonadal development in mammals.* Physiol Rev, 2007. **87**(1): p. 1-28.

335. Capel, B., *R-spondin1 tips the balance in sex determination.* Nat Genet, 2006. **38**(11): p. 1233-4.

336. Matzuk, M.M. and D.J. Lamb, *The biology of infertility: research advances and clinical challenges.* Nat Med, 2008. **14**(11): p. 1197-213.

337. Jordan, B.K., et al., *Up-regulation of WNT-4 signaling and dosage-sensitive sex reversal in humans.* Am J Hum Genet, 2001. **68**(5): p. 1102-9.

338. Choi, E.J., et al., *Prognostic significance of RSPO1, WNT1, P16, WT1, and SDC1 expressions in invasive ductal carcinoma of the breast.* World J Surg Oncol, 2013. **11**: p. 314.

339. Flanagan, D.J., et al., *Frizzled7 functions as a wnt receptor in intestinal epithelial lgr5(+) stem cells.* Stem Cell Reports, 2015. **4**(5): p. 759-67.

340. Le Grand, F., et al., *Wnt7a activates the planar cell polarity pathway to drive the symmetric expansion of satellite stem cells.* Cell Stem Cell, 2009. **4**(6): p. 535-47.

341. von Maltzahn, J., C.F. Bentzinger, and M.A. Rudnicki, *Wnt7a-Fzd7 signalling directly activates the Akt/mTOR anabolic growth pathway in skeletal muscle.* Nat Cell Biol, 2012. **14**(2): p. 186-91.

342. Mayor, R. and E. Theveneau, *The role of the non-canonical Wnt-planar cell polarity pathway in neural crest migration.* Biochem J, 2014. **457**(1): p. 19-26.

343. Manning, B.D. and L.C. Cantley, *AKT/PKB signaling: navigating downstream.* Cell, 2007. **129**(7): p. 1261-74.

344. Ptashne, M., *How eukaryotic transcriptional activators work.* Nature, 1988. **335**(6192): p. 683-9.

345. Gaetje, R., et al., *Characterization of WNT7A expression in human endometrium and endometriotic lesions.* Fertil Steril, 2007. **88**(6): p. 1534-40.

346. Gaetje, R., et al., *Endometriosis may be generated by mimicking the ontogenetic development of the female genital tract.* Fertil Steril, 2007. **87**(3): p. 651-6.

347. Santamaria, X., E.E. Massasa, and H.S. Taylor, *Migration of cells from experimental endometriosis to the uterine endometrium.* Endocrinology, 2012. **153**(11): p. 5566-74.

348. Peng, C., et al., *Expression and prognostic significance of wnt7a in human endometrial carcinoma.* Obstet Gynecol Int, 2012. **2012**: p. 134962.

349. Carmon, K.S. and D.S. Loose, *Secreted frizzled-related protein 4 regulates two Wnt7a signaling pathways and inhibits proliferation in endometrial cancer cells.* Mol Cancer Res, 2008. **6**(6): p. 1017-28.

350. Hayashi, K. and T.E. Spencer, *WNT pathways in the neonatal ovine uterus: potential specification of endometrial gland morphogenesis by SFRP2.* Biol Reprod, 2006. **74**(4): p. 721-33.

351. Waller, K.G. and R.W. Shaw, *Gonadotropin-releasing hormone analogues for the treatment of endometriosis: long-term follow-up.* Fertil Steril, 1993. **59**(3): p. 511-5.

352. Vercellini, P., I. Cortesi, and P.G. Crosignani, *Progestins for symptomatic endometriosis: a critical analysis of the evidence.* Fertil Steril, 1997. **68**(3): p. 393-401.

353. Wang, Y., et al., *Wnt/Beta-catenin and sex hormone signaling in endometrial homeostasis and cancer.* Oncotarget, 2010. **1**(7): p. 674-84.

354. Wang, Y., et al., *Progesterone inhibition of Wnt/beta-catenin signaling in normal endometrium and endometrial cancer.* Clin Cancer Res, 2009. **15**(18): p. 5784-93.

355. Zhang, L., et al., *Intracellular Wnt/Beta-Catenin Signaling Underlying 17beta-Estradiol-Induced Matrix Metalloproteinase 9 Expression in Human Endometriosis.* Biol Reprod, 2016.

7   LIST OF FIGURES

8 LIST OF TABLES

9 LIST OF ABBREVIATIONS

µg	Microgramm
µl	Microliter
µm	Micrometer
µM	Micromolar
7TM	Seven-transmebrane
ACE	Angiotensin I converting enzyme
ADP	Adenosine diphosphate
ADPr	ADP-ribose
AKT	also known as protein kinase B (PKB)
AP	Alkaline phosphatase
APC	Adenomatous polyposis coli
ARFGAP1	GTPase activating protein of ADP-ribosylation factor 1
ASRM	American Society for Reproductive Medicine
ATP	Adenosine triphosphate
BAX	Bcl-2-like protein 4
BCA	Bicinchoinic acid
BCL2	B-cell lymphoma 2
BRAF	B-Raf proto-oncogene, serine/threonine kinas
Brg-1	ATP-dependent helicase SMARCA4
BSA	Bovine serum albumin
Ca²⁺	Calcium
CACNA1A	Calcium channel, voltage-dependent
CAMKII	Ca^{2+}-calmodulin dependent kinase II
CAV1	Caveolin-1
CBP	CREB-binding protein
CD	Cluster of differentiation
CD10	Neprilysin
CD13	Alanyl aminopeptidase
CD133	Prominin 1
CD140B	Platelet-derived growth factor receptor
CD166	Activated leukocyte cell adhesion molecule
CD248	Endosialin
CD34	Hematopoietic progenitor cell antigen CD34
CD36	Thrombospondin receptor
CD74	HLA class II histocompatibility antigen gamma chain
CD9	Cell growth-inhibiting gene 2 protein or Tetraspanin-29
CD90	Thymus cell antigen 1
Cdc73	Cell division cycle 73
CDH1	E-cadherin
CDK1	Cyclin D1
cDNA_	Complementary DNA_
CK1γ	Casein kinase 1-gamma
CLDN3	Claudin-3

CLL	Chronic lymphatic leukaemia
CN	Calcineurin
CO₂	Carbon dioxide
COX-2	Cyclooxygenase 2
CRD	Cysteine-rich domain
d	Day
DAB	3,3'-Diaminobenzidine
DAG	Diacylglycerol
DAPI	4′,6-Diamidin-2-phenylindol
DIE	Deeply infiltrating endometriosis
DKK	Dickkopf
DMSO	Dimethyl sulfoxide
DNA_	Deoxyribonucleic acid
Dvl	Dishevelled
e.g.	*exempli gratia* - for example
E2	Estrogen or 17β-estradiol
E-Cad	E-Cadherin
Em	Emission
EMMA	Endometriosis Marker Austria
EpCAM	Epithelial cell adhesion molecule
ER	Endoplasmic reticulum
ERK	extracellular signal-regulated kinases - today named MAPK
ESC	Endometrial stromal cell
ESR1	Estrogen receptor 1
ESR2	Estrogen receptor 2
et al.	*et alii*
EtOH	Ethanol
Ex	Excitation
FACS	Fluorescence-activated cell sorting
FAP	Familial adenomatous polyposis
FAP	Fibroblast activation protein
FC	Fold change
FCS	Fetal calf serum
FGF9	Fibroblast growth factor 9
FITC	Fluorescein isothiocyanate
FSC	Forward scatter
FSC-H	FSC-Height
FSC-W	FSC-Width
FSH	Follicle stimulating hormone
FZD	Frizzled
g	Gramm
GAPDH	Glyderaldehyde-3-phosphate dehydrogenase
GnRH	Gonatropin-releasing hormone
GOI	Gene of interest
GPCR	G-protein coupled receptor
GSK3	Glycogen synthase kinase 3
h	Hours

HCG	Chrionic gonadotropin
HIF1A	Hypoxia-inducible factor 1-alpha
HKG	House keeping genes
HLA	Human leukocyte antigen
HRP	Horseradish peroxidase
HSD17B2	17-beta hydroxysteroid dehydrogenase 2
IC	Isotype control
IC$_{50}$	Half maximal inhibitory concentration
IgG	Immunglobulin G
IgK	Immunglobulin GK
IHC_	Immunohistochemistry
IL	Interleukin
IP3	Inositol 1,4,5-triphosphate
JNK	c-Jun N-terminal kinase
kDa	Kilodalton
kg	Kilogramm
Ki-67	Antigen identified by monoclonal antibody Ki-67
KRT	Keratin
l	Liter
LAGESO	Landesamt für Gesundheit und Soziales Berlin
LCM	Laser capture microdissection
LEF	Lymphoid enhancer factor
LGR	Leucine-rich repeat-containing G-protein coupled receptor
LH	Lutenizing hormone
LiCl	Lithiumchlorid
LRP	Lipoprotein receptor-related protein
m	Meter
M	Molar
MAPK10	Mitogen-activated protein kinase 10
Max	Maximum
mCMV	Minimal promoter of the cytomegalovirus
MEK	Member MAPK/ERK signaling
mg	Milligramm
Mg^{2+}	Magnesium
Min	Minutes
Min	Minimum
MKI67	Marker of proliferation Ki-67
ml	Milliliter
mm	Millimeter
mM	Millimolar
mmol	Millimol
MMP	Matrix metallopeptidase
MMTV	Mouse mammary tumor virus
mRNA	Messenger RNA
mTOR_	Mechanistic target of Rapamycin
MUC1	Mucin 1

n	Number
NAD	Nicotinamide adenine dinucleotide
Neg	Negative control
NFAT	Nuclear factor of activated T-cells
ng	Nanogramm
NK Calls	Natural ciller cells
NLK	Nemo like kinase
nm	Nanometer
nM	Nanomolar
nmol	Nanomol
NSAIDs	Non-steroidal anti-inflammatory drugs
nt	Tme in seconds
NT	Non-targeting
O_2	Oxygen
OMA	Endometrioma
p	p-value
P	Sorting gate
PCP	Planar cell polarity
PCR	Polymerase chain reaction
PE	Phycoerythrin
PGE2	Prostaglandin E2
PGR	Progesterone receptor
PGR-A	Progesterone receptor isoform B
PGR-B	Progesterone receptor isoform A
PI3K	Posphatidylinositol 3-kinase
PIP2	Phosphatidyl inositol 4,5 biphosphate
PKA	Protein kinase A
PKC	Protein kinase C
PLC	Phosphor lipase C
pmol	Pikomol
PORCN	Procupine
Pou5f1/Oct4	Octamer-binding transcription factor 4
PP2A	Protein phosphatase 2A
PR	Progesterone
qRT-PCR	Quantitative real time PCR
Rac	Ras-related C3 botulinum toxin substrate
Raf	Rapidly accelerated fibrosarcoma protein
RANTES	Regulated on activation, normal T cell expressed and secreted
Ras	Rat sarcoma G-protein
RIN	RNA integry number
RIPA	Radioimmunoprecipitation assay
RISC	RNA-induced silencing complex
RLT	RNeasy lysis buffer
RNA	Ribonucleic acid
ROCK	Rho-associated protein kinase
rpm	Rounds per minute
rRNA	Ribosomal RNA

RSPO	R-spondin
RT	Room temperature
s	Svedberg units
Sec	Seconds
SF1	Steroidogenic factor 1
SFRP	Secreted frizzled-related protein
siRNA	Small interfering RNA
SNAI2	Snail family zinc finger 1
SNP	Single-nucleotide polymorphisms
SOSTDC1	Sclerostin domain containing 1
SSC	Sideward scatter
SSC-H	SSC-Hight
SSC-W	SSC-Width
SUP	Peritoneal superficial endometriosis
TBST	Tris-buffered saline with Tween20
TBX18	T-Box 18
TCF	T-cell factor
TCF7L2	gene coding TCF4
TICAM2	Toll-like receptor adaptor molecule 2
TMEM87A	Transmembrane protein 87A
TMEM97	Transmembrane protein 97
TMEM9B	Transmembrane protein 9B
TNF	Tumor necrosis factor
TNKS	Tankyrase
TRE	TCF/LEF transcriptional response element
TSH	Thyroid-stimulating hormone
VCAM1	Vascular cell adhesion protein 1
VEGF	Vascular endothelial growth factor
VEGFA	Vascular endothelial growth factor A
vs.	Versus
VTI1A	Vesicle transport through interaction with t-SNAREs 1A
W	Watt
WIF	WNT inhibitory protein
WLS	Wntless
WNT	Wingless-type MMTV integration site family
x g	Centrifugal acceleration
βcat	β-catetin
β-TrCP	F box/WD repeat protein